

# NEURONAL DYSFUNCTION IN THE 15Q13.3 MICRODELETION DISORDER

CHARACTERIZATION OF NEURAL TISSUE FROM 15Q13.3 MICRODELETION  
FAMILIES REVEALS NOVEL MECHANISTIC FEATURES UNDERLYING  
NEURODEVELOPMENTAL DISEASE

By LEON CHALIL, BHSC

A Thesis Submitted to the School of Graduate Studies in Partial Fulfilment of the  
Requirements for the Degree Doctor of Philosophy

McMaster University © Copyright by Leon Chalil, March 2023

McMaster University DOCTOR OF PHILOSOPHY (2023) Hamilton, Ontario  
(Biochemistry)

TITLE: Characterization of 15q13.3 Microdeletion Families Reveals Novel  
Mechanistic Features Underlying Neurodevelopmental Disease

AUTHOR: Leon Chalil, B.H.Sc. (Honours) (McMaster University)

SUPERVISOR: Dr. Karun K. Singh

NUMBER OF PAGES: xvii, 207

**Lay abstract**

Using a genetic disorder and patient samples, the work in this thesis provides novel insights into the underlying causes of brain and nerve disorders. Patients with this disorder are missing a large amount of genetic material, and can develop disorders such as seizures, autism spectrum disorders, and ADHD and may also fail to achieve general milestones in socialization, growth, learning, and motor development. Because it is dangerous and invasive to access patient brain and nerve samples directly, this project converted patient blood or skin samples into neurons which were then studied. This thesis aimed to achieve three broad objectives. The first was to characterize an excitatory neuron subtype from three different families to identify changes in shape, connectivity, and function. The second objective involved identifying how these neurons might express different gene profiles, and what this means for the mechanisms involved in disease development. The third objective was to investigate a possible mechanism at the molecular level, which might offer insights into future therapies. The totality of the work in this thesis provides new insights into the cellular and molecular bases for disease in the 15q13.3 microdeletion disorder and offers future perspectives on how this disorder and others like it might be investigated and treated in the future.

**Abstract**

The 15q13.3 microdeletion disorder is a clinically delineated set of neuropsychiatric phenotypes associated with the loss of genetic material from the 15q13.3 BP4-5 locus. To functionally characterize cellular features of the 15q13.3 microdeletion disorder and identify genetic and molecular elements contributing to disease pathophysiology, we assayed excitatory glutamatergic pyramidal neurons derived by the expression of the neurogenin-2 transcription factor in induced pluripotent stem cells (iPSCs) of 15q13.3 microdeletion patients and family members. Day 28 (DIV28) neurons were first functionally and morphologically assayed, revealing family-specific changes to population-level activity, individual action potential changes, and dendritic complexity with axon projection being decreased in all families. We followed up these experiments with RNA sequencing at an earlier timepoint (DIV14), identifying early changes in gene expression and pathway enrichment which varied appreciably between two families, potentially due to underlying clinical variations. Finally, we treated a proband and control with a potent, selective GSK3 inhibitor and found that the proband was comparatively insensitive to its effects on action potential properties. Taken together, these findings underscore the multi-layered heterogeneity in this disorder at the clinical, cellular and molecular level, and offer new insights into disease pathobiology and potential mechanisms.

## Acknowledgments

*“Dull repetition is the rust of sacred verses”* – The Dhammapada, verse 241

During the past seven years, I have spent more time thinking of these words than almost any others. The great intellectual and humanitarian edifices of our time are no longer being built up around the classically sacred, but the idea is as relevant as ever. My own training intersected the realms of scientific inquiry and medical practice, which follow old traditions that are always trying to update themselves to the modern world. As much as they are complex and demanding, they are equally meaningful and worthwhile pursuits. I feel fortunate to have had the opportunity to pursue them in these years. I feel even more fortunate to the people that made it possible in big ways and small. The easiest thing in the world is to slip into dull repetition, to lose sight of the path, and to forget what is most real and important in your life and work. I am eternally grateful to everyone who helped keep the sacred alive and fresh for me during these past few years.

None of the work contained herein would have been possible without the support and mentorship of my supervisor, Dr. Karun Singh. What first drew me to the lab was Karun’s enthusiasm for the frontiers of research and the open learning environment he enabled, and I’m proud of the work we did during these years. His support and mentorship made me a better thinker, and for that I am grateful.

I would also like to acknowledge Dr. Matthew Miller and Dr. Bradley Doble, who comprised my PhD supervisory committee. Their sharp minds, deep funds of

knowledge, and commitment to my development as a researcher were invaluable.

I am grateful to the 15q13.3 team, Dr. Brianna Unda and Savannah Kilpatrick. Always ready to lend their time and thoughts, I am lucky to have had the opportunity to work with them. Dr. Sean White taught me patch clamp electrophysiology and played a formative role in my early training.

Thanks also to Dylan and Steve for the fishing trips that kept me sane. Biren Dave and Dr. William Gwynne were constant sources of interesting ideas and great friends besides. This thesis is also dedicated to the memory of Eric Lovinger (1994 – 2019), whose absence is felt every day.

Thank you to Annie, for everything.

I am luckiest of all to have had the unwavering support and encouragement of my parents and siblings. Anything I have made of myself I owe to them.

## Table of Contents

Lay abstract .....	iii
Abstract.....	iv
Acknowledgments .....	v
Table of Contents .....	vii
List of Figures .....	x
List of Tables .....	xii
List of abbreviations and symbols.....	xiii
Declaration of academic achievement.....	xvii
Chapter 1: Introduction.....	1
1.1 Neurodevelopmental disorders (NDDs) .....	1
1.1.1 Background .....	1
1.1.2 Etiology.....	2
1.1.3 NDD-associated CNVs.....	8
1.1.4 Summary .....	28
1.2 The 15q13.3 microdeletion disorder.....	30
1.2.1 Background .....	30
1.2.2 Pathophysiology.....	37
1.2.3 Advantages as a model disorder .....	37
1.3 Experimental approach.....	40
1.3.1 Conceptualizing disease pathogenesis in NDDs .....	41
1.3.2 Induced pluripotent stem cells (iPSCs) .....	43
1.3.3 Induced glutamatergic neurons .....	43
1.3.4 Functional and morphological profiling.....	45
1.3.5 Transcriptomics.....	45
1.4 Thesis Aims.....	46
1.5 Summary .....	49
Chapter 2: Cellular phenotyping of 15q13.3 microdeletion family neurons reveals characteristic functional and morphologic deficits .....	51
2.1 Abstract .....	51
2.2 Introduction.....	52
2.3 Methods.....	58
2.3.1 iPSC reprogramming.....	58
2.3.2 iPSC thawing and passaging.....	59
2.3.3 iPSC NGN2/rtTA infection.....	60
2.3.4 iN induction protocol.....	60
2.3.5 NGN2 iN RT-qPCR .....	61
2.3.6 Multi-Electrode Arrays.....	62
2.3.7 Electrophysiology .....	63
2.3.8 Morphologic analysis.....	64
2.3.9 Culturing neurons from E16-17 mouse cortices.....	66
2.3.10 Genotyping E16-17 mice .....	66
2.4 Results.....	68

2.4.1	A novel cohort of 15q13.3 microdeletion patient families reveals previously unreported clinical and structural findings .....	68
2.4.2	15q13.3 microdeletion patient iNs show altered population-level spiking activity.....	69
2.4.3	Action potential properties are altered in three 15q13.3 microdeletion families without changes in sEPSCs.....	70
2.4.4	Dendritic complexity variation in 15q13.3 microdeletion families and controls	71
2.4.5	Miniature excitatory postsynaptic current frequency is increased in Df(h15q13)/+ cortical pyramidal neurons compared to wildtype littermates..	71
2.4.6	Impaired axon projection is a consistent feature in 15q13.3 microdeletion patient iNs .....	72
2.5	Figures and Tables .....	73
2.6	Discussion .....	98
2.6.1	A previously unreported index of 15q13.3 microdeletion families reveals novel characteristics potentially linked to disease .....	99
2.6.2	Using iNs to generate novel functional and morphological insights into the 15q13.3 microdeletion disorder.....	102
2.6.3	Insights from cellular phenotyping of 15q13.3 microdeletion families	103
2.6.4	Limitations and future directions.....	104
Chapter 3: Co-culture transcriptomic analysis of early iNs from two 15q13.3 microdeletion families reveal disease-relevant pathways .....		106
3.1	Abstract .....	106
3.2	Introduction.....	107
3.3	Methods.....	111
3.3.1	iN induction and plating.....	111
3.3.2	RNA sequencing and analysis.....	111
3.4	Results.....	113
3.4.1	Improvement of alignment rates by separation of mouse and human transcripts from a co-culture system .....	113
3.4.2	Distinct clustering of 15q13.3 microdeletion probands and familial control.....	113
3.4.3	Differences in functional enrichment analysis underlying variation in 15q13.3 microdeletion families.....	115
3.4.4	Differentially expressed genes in 15q13.3 microdeletion probands at DIV14 .....	116
3.4.5	Gene set enrichment analysis of 15q13.3 microdeletion reveals novel and known developmentally relevant gene sets.....	117
3.5	Figures.....	119
3.6	Discussion .....	133
3.6.1	Separation of mouse and human reads in a co-culture system .....	133
3.6.2	Transcriptome variation in neurodevelopmentally relevant genes between two 15q13.3 microdeletion families .....	134

3.6.3	GSEA and functional analysis reveals pathways implicated in neurodevelopment.....	138
3.6.4	Limitations .....	140
3.6.5	Future Directions.....	141
Chapter 4:	GSK3 specific inhibition is associated with altered currents in control but not 15q13.3 microdeletion patient iNs .....	143
4.1	Abstract .....	143
4.2	Introduction.....	144
	Evidence for mechanistic convergence in NDDs.....	144
4.3	Methods.....	147
	Electrophysiology recordings .....	147
	Multi-electrode array recordings.....	147
	Morphological analysis .....	148
	Antibodies .....	148
	Western blot.....	149
	LDH assay.....	149
4.4	Results.....	150
	4.4.1 Chronic ChIR99021 treatment alters spiking in both a control and 15q13.3 microdeletion proband iN .....	150
	4.4.2 Acute ChIR99021 treatment alters intrinsic action potential parameters in control but not proband iNs.....	150
	4.4.3 15q13.3 microdeletion iNs manifest disruptions in the axon initial segment .....	151
	4.4.4 Molecular consequences of ChIR99021 administration in iNs .....	152
4.5	Figures.....	153
4.6	Discussion .....	171
	4.6.1 Disruption of the axon initial segment in a 15q13.3 microdeletion disorder proband.....	171
	4.6.2 Paradoxical impacts of GSK3 inhibition in a 15q13.3 microdeletion proband.....	172
	4.6.3 Altered proband response to GSK3 inhibition is not explained by cytotoxicity.....	173
	4.6.4 Limitations .....	174
	4.6.5 Future directions.....	176
Chapter 5:	Discussion .....	178
	Insights into disease pathogenesis in the 15q13.3 microdeletion disorder.....	178
	A platform for the investigation of rare genetic disorders underlying neurodevelopmental disorders .....	182
	Future directions.....	183
	Concluding remarks .....	187
References.....		189

## List of Figures

Figure 1.3.1: Heritability and penetrance of NDD-predisposing mutations .....	4
Figure 1.3.2: 15q13.3 microdeletion BP4-BP5 region.....	34
Figure 1.3.1: Excitation/inhibition as a conceptual schema underlying neuropsychiatric disorder pathogenesis .....	42
Figure 1.3.2: Induction and management protocol for induced neurons .....	44
Figure 2.5.1: visual abstract and workflow schematic.....	73
Figure 2.5.2: Pedigree and breakpoint alignment map for the three patient families profiled in this study .....	75
Figure 2.5.3: Population-level spiking differences vary by 15q13.3 microdeletion families.....	78
Figure 2.5.4: Differences in action potential characteristics in 15q13.3 microdeletion iNs .....	81
Figure 2.5.5: Spontaneous synaptic transmission in 15q13.3 microdeletion iNs.	84
Figure 2.5.6: Axon projection capacity in 15q13.3 microdeletion iNs .....	86
Figure 2.5.7: Sholl analysis of three 15q13.3 microdeletion families.....	88
Figure 2.5.8: Validation of iPSCs used in this study .....	90
Figure 2.5.9: Extended electrophysiologic parameters .....	92
Figure 2.5.10: Extended MEA parameters .....	94
Figure 2.5.11: Df(h15q13)/+ mouse cortical pyramidal neuron mEPSCs .....	96
Figure 3.5.1: Visual abstract and workflow schematic .....	119
Figure 3.5.2: Principal coordinate analysis of 15q13.3 microdeletion families...	121
Figure 3.5.3: Functional enrichment analysis of highly correlated Principal Coordinate Genes .....	124
Figure 3.5.4: Volcano plots showing DEGs in 15q13.3 microdeletion families ..	125
Figure 3.5.5: Clustering of DEGs at the 6p21.1-22.1 locus .....	128
Figure 3.5.6: Gene set enrichment analysis .....	130
Figure 3.5.7: FPKM expression of 15q13.3 BP4-5 region and flanking genes ..	132
Figure 4.5.1: ChIR99021 administration alters population-level spiking activity in both proband and control iNs .....	153
Figure 4.5.2: Acute treatment (3d) with 2uM ChIR99021 fails to alter action potential properties 15q13.3 microdeletion proband .....	155
Figure 4.5.3: Paradoxical response of ChIR99021 administration on inward current.....	158
Figure 4.5.4: Spontaneous synaptic transmission in ChIR99021 treated iNs ....	160
Figure 4.5.5: Western blot of GSK3 $\beta$ and pGSK3 $\beta$ in response to ChIR99021 administration .....	162
Figure 4.5.6: Disruption of the axon initial segment in a 15q13.3 microdeletion proband.....	164
Figure 4.5.7: Arborization complexity of control and proband lines is decreased by ChIR99021 administration.....	166
Figure 4.5.8: LDH levels are not significantly altered by short-term (3d) ChIR99021 administration.....	168

Figure 4.5.9: Homozygous L233F mutation in OTUD7A catalytic region in a patient with seizures and developmental delay..... 170

## List of Tables

Table 2.5.1: Index of patient families .....	74
Table 3.5.1: Mapping rates for split and unsplit mouse and human reads.....	120
Table 3.5.2: Top genes contributing to principal coordinates .....	123
Table 3.5.3: Chromosomal clustering of DEGs by patient family .....	127

**List of abbreviations and symbols**

aCSF	<i>Artificial cerebrospinal fluid</i>
ADHD	<i>Attention-deficit hyperactivity disorder</i>
AIS	<i>Axon initial segment</i>
	<p>The AIS refers to the structural arrangement in the early portion of the axon which is responsible for the arrangement of elements required for the initiation of action potentials. The AIS is rich in voltage-gated sodium channels, and is typically identified by the presence of the scaffolding protein ankyrin-G.</p>
AMPA	<i><math>\alpha</math>-amino-3-hydroxy-5-methyl-4-isoxazolepropionic acid</i>
AP	<i>Action potential</i>
ARHGAP11B	<i>Rho GTPase-activating protein 11B</i>
ASD	<i>Autism spectrum disorder</i>
BDNF	<i>Brain-derived neurotrophic factor</i>
bFGF	<i>Basic fibroblast growth factor</i>
BP	<i>Biological process</i>
CC	<i>Cellular component</i>
CD	<i>Cluster of differentiation</i>
CHRFAM7A	<i>CHRNA7-FAM7A fusion protein</i>
CHRNA7	<i>Cholinergic receptor nicotinic alpha 7 subunit</i>
DAPI	<i>4',6-diamidino-2-phenylindole</i>
DEG	<i>Differentially expressed gene</i>
DIV	<i>Day in vitro</i>

DMSO	<i>Dimethyl sulfoxide</i>
DOX	<i>Doxycycline</i>
DSM-5	<i>Diagnostic and Statistical Manual, Fifth Edition</i>
EEG	<i>Electroencephalogram</i>
FAN1	<i>FANCD2/FANCI-associated nuclease 1</i>
FBS	<i>Fetal bovine serum</i>
GDD	<i>Generalized developmental delay</i>
GDNF	<i>Glial cell-derived neurotrophic factor</i>
GO	<i>Gene ontology</i>
GOLGA8	<i>Golgin A8</i>
GSEA	<i>Gene set enrichment analysis</i>
GSK3	<i>Glycogen synthase kinase 3</i>
HET	<i>Heterozygous</i>
iN	<i>Induced neuron</i>
	<p>Though iNs may refer to any neuron whose differentiation was induced by defined factors, in this report they refer to neurons generated by inducing iPSC differentiation by the transcription factor neurogenin-2. This protocol generates a highly pure (&gt;99%) population of excitatory glutamatergic cortical pyramidal neurons.</p>
iNI	<i>Induced neuron media</i>
iPSC	<i>Induced pluripotent stem cell</i>
	<p>iPSCs are derived from somatic tissues (typically fibroblasts or CD34+ white blood cells) by transcription factor reprogramming. Differentiated iPSCs are a</p>

versatile model to study patient-specific tissues, particularly sensitive or scarce ones.

IQ	<i>Intelligence quotient</i>
KEGG	<i>Kyoto Encyclopedia of Genes and Genomes</i>
Lam	<i>laminin</i>
MAP2	<i>Microtubule-associated protein 2</i>
MEA	<i>Multi-electrode array</i>
	An MEA uses a matrix of evenly spaced electrodes to record extracellular electrical activity from a cell or tissue layer placed in direct contact. MEA recordings can produce a variety of parameters, resolved at either single- or multi-electrode resolution, to ascertain the dynamics of a neural population.
mEPSC	<i>Miniature excitatory postsynaptic currents</i>
MF	<i>Molecular function</i>
MTMR10	<i>Myotubularin related protein 10</i>
NDD	<i>Neurodevelopmental disorder</i>
Ngn2	<i>Neurogenin 2</i>
NMDA	<i>N-methyl-D-aspartate</i>
NPC	<i>Neural progenitor cell</i>
NRXN1	<i>Neurexin-1</i>
OTUD7A	<i>OTU Deubiquitinase 7A</i>
PCA	<i>Principal Component Analysis</i>
PCR	<i>Polymerase chain reaction</i>
PDL	<i>Poly-D lysine</i>

PEI	<i>Polyethylenimine</i>
pLI	<i>Probability of loss-of-function intolerance</i>
PTX	<i>Picrotoxin</i>
Puro	<i>Puromycin</i>
rtTA	<i>Reverse tetracycline-controlled transactivator</i>
sEPSC	<i>Spontaneous excitatory postsynaptic current</i>
SHANK	<i>SH3 and multiple ankyrin repeat domains 3</i>
TJP1	<i>Tight junction protein 1</i>
TRPM1	<i>Transient receptor potential cation channel subfamily M member 1</i>
TTX	<i>Tetrodotoxin</i>
WT	<i>Wild type</i>

## **Declaration of academic achievement**

The work presented herein was carried out by myself, except as specified below:

### **Chapter 2:**

Savannah Kilpatrick assisted with iN transfection, axon length quantification, and qPCR of deleted genes from Families 1–3.

Dr. Brianna Unda assisted with MEA plating and recordings for one experiment.

Dr. Sehyoun Yoon performed the Sholl analysis for Families 1 and 2.

### **Chapter 4:**

Dr. Brianna Unda assisted with the running of the Western blot in Figure 4.5.5.

Dr. Sehyoun Yoon provided AIS quantification and analysis.

## **Chapter 1: Introduction**

### **1.1 Neurodevelopmental disorders (NDDs)**

#### **1.1.1 Background**

Neurodevelopmental disorders (NDDs) encompass a variety of conditions which impair childhood development in a variety of social, motor, language and cognitive domains (APA, 2013). Though many disorders may fall under this description, the most common ones include autism spectrum disorder (ASD), attention-deficit hyperactivity disorder (ADHD), seizure disorders, and more generalized intellectual disability/developmental delay (ID/DD). At present, NDD diagnostic criteria are set by the Diagnostic and Statistical Manual, Fifth Edition (DSM-V) (APA, 2013), and diagnosis is principally based on clinical evaluation for relevant symptomatology. While efforts to find biomarkers for these disorders are ongoing, these have proven largely elusive.

Investigations into the causes of NDDs have identified certain features of interest. NDDs are highly heritable, suggesting a genetic underpinning. Twin studies have additionally revealed that these disorders are highly sensitive to specific genome-level arrangements of genetic factors, evidenced by the large concordance gap between monozygotic and dizygotic twins for disorders such as ASD (Figure 1.3.2) (Colvert et al., 2015; Tick et al., 2016). Because of the age of onset and severity of many of these disorders, there is a strong negative selection pressure on underlying mutations. As a result, highly penetrant mutations are comparatively infrequent (often only arising *de novo*), while lower penetrance or

necessary-but-insufficient mutations will be more frequent but their role in the disorder will be more difficult to discern (see Figure 1.3.1).

In recent years, a class of these mutations termed copy number variants (CNVs) has increasingly gained prominence for their role in NDDs. CNVs are gains or losses of continuous tracts of chromosomal material, typically on the order of kilo- or megabases. CNVs can encompass dozens of genes, and many are highly penetrant for the development of NDDs. Several of these CNVs occur at chromosomal “hotspots”, meaning that they are highly recurrent with defined breakpoints (Fu et al., 2010). This recurrence is largely explained by the copy number expansion of genetic elements flanking these regions in recent human evolution. The ostensible reason for this expansion is that these elements played an important role in driving the rapid increase in human brain size (Antonacci et al., 2014). This is reflected in dosage-linked macrocephaly/microcephaly with gains or losses (respectively) in many of these elements (Bernier et al., 2016; I. T. Fiddes et al., 2018; Golzio et al., 2012). This trade-off between rapid brain expansion and regional chromosomal instability is reflected in CNV hotspots associated with nervous system disorders. At present, the Simons Foundation Autism Research Initiative (SFARI) (Basu et al., 2009) indexes 17 CNV loci, though more continue to be discovered.

### **1.1.2 Etiology**

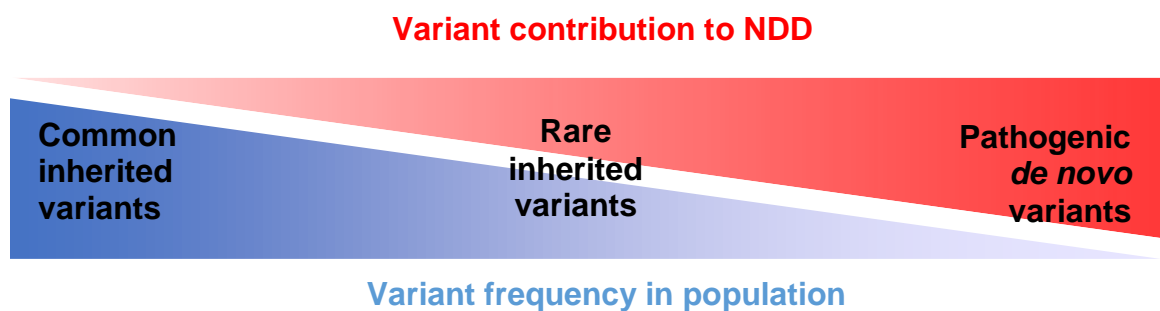
There are several features of NDDs which provide clues to their mechanistic investigation. With few exceptions, NDDs represent very uniquely human

disorders, and animals cannot recapitulate the entirety of the clinical phenotype. As a consequence, the pathologic locus in the human disorder must be located in the uniquely human structures. For neuropsychiatric diseases, many of these will be related to the area of greatest differentiation in the human brain, the neocortex. Both the neocortex and the genetics underlying its recent evolutionary history are, therefore, high-yield candidates for the investigation of these disorders.

The genetic factors associated with neurodevelopmental disorders are numerous and have been extensively indexed in various large-scale studies and repositories such as SFARI, MSSNG, and ENCODE. A variety of studies have analyzed many mutations of these genes and offered insights into the manifestations of neurodevelopmental disorders at the molecular, cellular, tissue, and clinical levels. Much like the diseases they result in, the genetic disorders themselves vary greatly. Because these disorders are often under negative selection pressures (due to decreased fecundity in patient populations), their penetrance is negatively correlated with their frequency in the population. Indeed, very few of these mutations are fully penetrant for neuropsychiatric disease, and of these most are confined to *de novo* mutations. Because these are not inherited, they are under no multigenerational selection pressures and can manifest in serious diseases. These particularly serious mutations offer valuable tools for the study of extremal neurodevelopmental outcomes, though they have correspondingly rare representation in the population. In contrast, common

variants will be more represented in the population but are generally less penetrant. While their contribution to disease might prove more prevalent, the effect size will be considerably smaller (Figure 1.3.1) (Bourgeron, 2015).

**Figure 1.3.1: Heritability and penetrance of NDD-predisposing mutations**



Adapted from Bourgeron (2015)

**Figure 1.3.1:** Representation of different types of variants, and their contribution to NDDs. While a pathogenic *de novo* mutation might produce an NDD on its own, it might take the chance presence of several common inherited variants to do the same. A chromosomal microdeletion might be an example of several common variants (deletions, in this case) coalescing into a clinical phenotype. Adapted from (Bourgeron, 2015).

Because a unified theory of neurodevelopmental dysfunction is the goal of these studies, it is difficult to anticipate in advance what a satisfactory answer might look like. The overarching goal of these studies is to understand the mechanisms of these disorders and to ultimately identify possible points of intervention for both individual genetic causes and the clinical disorders they cause.

There are other features of a genetic disorder which make it more desirable for further study. One compelling line of evidence is the evolutionary history of the genetic elements involved in the disorder. Tautologically, precursors to human genetic elements follow a gradual decrease in homology from our closest relative species to more distant ones. If a gene or genetic element is unique to humans and associated with neuropsychiatric disease, its importance is typically simpler to appreciate: it is a human-specific gene and its dysfunction results in human-specific disorders. However, it may also be of considerable interest if genetic elements with evolutionary histories extending across multiple species are also associated with what appears to be a human-specific disorder. In scenarios such as this, both model organisms and human studies can yield complementary data and illustrate the different levels at which these disorders might manifest.

Despite cross-species homology in genes and genomic regions related to this disorder, neurodevelopmental disorders themselves are largely centred on human neural and cognitive dysfunction, they may have correlates in model organisms which are conducive to study. For example, while autism spectrum disorders are highly human-specific, comparisons may be drawn to socialization behaviours in rodents. For functional disorders with much more objective presentations, (such as movement or seizure disorders) this task is much more straightforward.

In recent years, a large body of evidence has accumulated implicating a multitude of genetic elements in the development of these disorders. Many of these

disorders have a high heritability, and twin studies have revealed that specific genetic makeup plays an important role in determining the proclivity to develop these disorders (Gottesman, 1991).

The conceptual schemata which describe the ways in which genome-wide mutation burden may collectively produce these disorders are reviewed elsewhere. In short, the relevant mutations can be considered to be either spontaneously arising (*de novo*) or inherited, and comprise either single-nucleotide polymorphisms (SNPs) or duplications/deletions of contiguous tracts of genomic DNA. In this review, we are interested in a subclass of this latter group known as copy number variants (CNVs), and in particular microdeletions and microduplications. CNVs represent both normal and pathological variations in the copy numbers of different genomic elements. CNVs are typically on the order of kilo- or mega basepairs and can involve dozens of genes.

Certain CNVs have features which make them suitable for the study of NDDs. A higher-level consideration of CNVs in neurodevelopmental disorders has previously been reviewed (Fu et al., 2010). Located at chromosomal “hotspots” (Fu et al., 2010; Lupski & Stankiewicz, 2005) (which are flanked by homologous repeats segments, increasing susceptibility to inversions, rearrangements, and duplications/deletions), these CNVs are highly recurrent and can be very penetrant for select NDDs. Consequently, these CNVs can represent a comparatively severe genetic cause of NDDs, while remaining comparatively

frequent at the population level. However, it is frequently nonobvious how these CNVs are causative for the associated NDDs. An improved understanding of the ways in which CNVs underlie NDD pathobiology will inform care for patients with the respective CNV, and expand understanding of the common mechanisms underlying these disorders more broadly.

There is good reason to believe that select genes may be driving NDD phenotypes in many of these disorders. For example, in the case of the 2q23.1 CNV, MBD5 was identified as the driver gene by the study of nested deletions in patients with clinically similar presentations, which isolated MBD5 as the only gene in the minimal deletion region (Talkowski et al., 2011). However, this is atypical, in that for most CNVs there will be insufficient patient cases to make this determination. This is due both to the rarity of these CNVs in general, as well as the recurrence of their breakpoints, such that rearrangements involving single genes are extremely rare, and certainly unlikely to provide definitive evidence in most cases. However, these CNVs still serve to highlight local genetic elements potentially underlying the disorder, which can be studied using a combination of animal models, mutations in individual genes, and the associated cellular and molecular pathways. A variety of such studies have revealed potential roles for genes within these disorders. Given the high rate of co-occurrence between various NDDs (Rosen et al., 2018), and their association with these highly recurrent CNVs, the following sections will review a selection of several of various genes within them.

*Note that this is a lengthy section, and the discussion of the main CNV investigated in this thesis (the 15q13.3 microdeletion) begins on page 31.*

### **1.1.3 NDD-associated CNVs**

#### **1q21.1**

The 1q21.1 region is highly complex, involving over 30 genes in the two major regions associated with clinical disorders. Deletions of the proximal region are most notably associated with the thrombocytopenia absent radius (TAR syndrome). Duplications and deletions of both the proximal and distal regions are reported in patients with neuropsychiatric abnormalities, including developmental delay (DD), intellectual disability (ID), hypotonia, seizures, autistic features, brain abnormalities, and other behavioural problems (Rosenfeld et al., 2012). CNVs in the distal region have been estimated to have a penetrance of 29.1% and 36.9% for duplications and deletions (respectively) (Rosenfeld et al., 2013). Deletions of the distal region (~1.35 Mb) (Velinov & Dolzhanskaya 2010) are associated strongly with microcephaly, while duplications of this region are more strongly linked to macrocephaly autistic features (Rosenfeld et al., 2012) and schizophrenia later in life (Dolcetti et al., 2013). Segmental duplications in the region delineate four breakpoints among which CNVs are most commonly observed, though other rearrangements in the region are also possible. Though associated with many neurodevelopmental phenotypes, the 1q21.1 CNVs have considerable variation in their clinical presentation (Aldinger, 2009), and many carriers are largely asymptomatic.

To date, little remains known about the contribution of specific genes to the neuropsychiatric phenotypes in this disorder. The distal microdeletion can vary in size by up to 2 Mb due to the spread in the segmental duplications within the breakpoint region. However, the most conservative region enclosed by the breakpoints encompasses the protein-coding genes *PRKAB2*, *FMO5*, *CHD1L*, *BLC9*, *ACP6*, *GJA5*, *GJA8*, *GPRB89B*, *GPRB89C*, *PDZK1*, *HYDIN2*, *NBPF11*, and *NBPF24* (Rosenfeld et al., 2012). Several pseudogenes are also present in the region. The majority of work on these genes has focused on their role in cancer biology. To date, little is known about the role of any genes in this CNV region on outcomes involving the nervous system. Mutations in *GJA8*, which encodes a gap junction lens protein of the eye lens, are an identified cause of congenital cataracts and other eye disorders (Arora et al., 2008; Ge et al., 2014; Huang et al., 2015), but not an apparent cause of any neurodevelopmental phenotypes. Mutations in the other gap junction protein in the region, *GJA5*, are associated with atrial fibrillation (Shi et al., 2012) and congenital heart disease (Soemedi et al., 2012).

In a case study of a 1q21.1 distal microdeletion patient, *CHD1L* and *BCL9* were proposed to be candidate genes underlying the language disorder phenotype. *CHD1L* is part of the chromodomain helicase DNA-binding protein family, of which several members (*CHD2*, *CHD7*, and *CHD8*) are linked to neuropsychiatric outcomes such as epileptic encephalopathy and ASD (Gabriele et al., 2018). While this study showed expression level changes of 1q21.1 genes (notably

*CHD1L* and *BCL9*) and potential interacting partners suspected to be involved in language disorders, the connection to neurodevelopment remains largely speculative (Benítez-Burraco et al., 2018).

One promising candidate is *NOTCH2NL*, which is highly duplicated in the breakpoint regions flanking the enclosed recurrent 1q21.1 CNV regions. Like other segmentally duplicated genes in CNV hotspots, *NOTCH2NL* duplications are thought to underlie the rapid enlargement of the human neocortex in recent evolution (Ian T. Fiddes et al., 2018). *NOTCH2NL* has been shown to positively modulate Notch signalling in radial glia neural stem cells, which is proposed to directly influence the number of cortical neurons (Ian T. Fiddes et al., 2018). This has been suggested as the likely mechanism for macrocephaly/microcephaly, which are observed in 1q21.1 microduplications/microdeletions (respectively) (Ian T. Fiddes et al., 2018). Studies of the therapeutic potential of modifying Notch signalling have been thus far limited to cancer biology (Andersson & Lendahl, 2014; Wang et al., 2010; Yuan et al., 2015). However, given the direct relevance of neuronal progenitor functionality to neurodevelopment, this might prove to be a promising avenue for early intervention.

While other genes (*PRKAB2* and *PDZK1*) are also thought to be involved in the neurodevelopmental phenotype of the disorder based on tissue expression data, they remain largely unstudied in this context. While some candidates have emerged as plausible contributors to 1q21.1 CNV disorders, no clear drivers are evident at present.

**2p16.3 – NRXN1**

Recurrent CNVs of the 2p16.3 region span an approximately 330 kb length and are overwhelmingly represented by microdeletions (the reported ratio of deletions to duplications based on indexed cases in the SFARI database is roughly 21.5).

The CNVs in this region map to the *NRXN1* gene, which is the singularly identified driver of neuropsychiatric phenotypes associated with this disorder.

Neurexins are presynaptic adhesion proteins and play an important role in synaptic organization and transmission (Pak et al., 2015; Trotter et al., 2019).

*NRXN1* expression profiles link high isoform-specific expression to the dorsolateral prefrontal cortex early in neurodevelopment and suggest an altered expression profile in schizophrenia and bipolar disorder (Jenkins et al., 2016).

The core phenotype of the 2p16.3 microdeletion involves severe intellectual disability, language delay, ASD, seizures, and hypotonia (Béna et al., 2013; Ching et al., 2010; Dabell et al., 2013; Gauthier et al., 2011; Schaaf et al., 2012).

*NRXN1* deletions are also linked to the development of schizophrenia later in life (Kirov et al., 2009; Todarello et al., 2014). Because the implicated gene is known, subsequent research has focused on identifying the relevance of other factors in the variability of disease presentation. Exonic deletions are known to be more important than intronic ones for the development of NDDs (Lowther et al., 2017).

Studies of variable exon deletions in *NRXN1* show that patients with a C-terminus deletion have a greater risk of developing epilepsy (Béna et al., 2013; Schaaf et al., 2012). It was initially thought that C-terminus deletions were also associated

with macrocephaly (Béna et al., 2013), though a subsequent larger cohort study did not replicate this finding (Schaaf et al., 2012).

Disruptions in *NRXN1* exhibit incomplete penetrance, and it is not uncommon for probands to have inherited the deletion from asymptomatic parents (though compound heterozygotes have a more penetrant and severe phenotype)(Béna et al., 2013). The variability in this penetrance is thought to result from differences in genetic background. Studies have identified high rates of additional rare CNVs in 2p16.3 microdeletion patient cohorts (Béna et al., 2013).

### **7q11.23**

CNVs of the 7q11.23 region typically span 1.5–1.8 Mb and can contain up to 28 genes (Pober, 2010). The 7q11.23 region is best known for deletions, which result in the Williams-Beuren syndrome (WBS). WBS is characterized by characteristic facial dysmorphia, social behaviour, and delay in growth and mental faculties. However, duplications in this region have also been associated with neuropsychiatric outcomes, including epilepsy, learning disorders, behavioural problems, and ASD. No gene has been definitively identified as the cause of the neuropsychiatric phenotypes in this disorder. However, several genes have been linked to neuronal phenotypes, and are considered possible candidates.

*LIMK1* encodes a LIM domain-containing kinase which is highly expressed in the brain(Frangiskakis et al., 1996). *LIMK1* was first implicated in patients with partial-WBS phenotypes, and a minimal deletion region implicating *LIMK1* and

*ELN* (elastin)(Frangiskakis et al., 1996). *LIMK1* was considered to be the driver of visuospatial constructive cognition in these patients, due to the identified role of elastin outside of neuronal phenotypes (Frangiskakis et al., 1996). LIM kinases have been implicated in neurodevelopment through actin remodelling (Cuberos et al., 2015; Frendo et al., 2019), particularly as facilitators of synaptic spine development and stability (George et al., 2015; Hoogenraad et al., 2004). A study of *LIMK1* knockout mice showed decreased numbers of upper-layer cortical pyramidal neurons, attributable to fewer neural progenitor cells in these animals, and defects in neuronal migration(Mao et al., 2019).

*GTF2I* (general transcription factor II-I) and *GTF2RD1* (GTF2I repeat domain containing 1) are two related genes in this CNV region which have been associated with both craniofacial and neuropsychiatric outcomes in 7q11.23 CNVs. Studies of deletion breakpoints in WBS and partial-WBS patients have identified an absence of mental retardation when *GTF2I* and *GTF2RD1* are not also deleted, providing an interesting inferential result for the involvement of these genes (Antonell et al., 2009; Ferrero et al., 2010; Hirota et al., 2003; Morris et al., 2003). Additionally, SNPs identified in *GTF2I* have been linked to sociability, suggesting that GTF2I might drive this aspect of the broader phenotype (Crespi & Hurd, 2014). Interestingly, *Gtf2i* heterozygous mice (homozygosity is fatal *in utero* due to severe neural tube defects) show increased social behaviour, reminiscent of the hypersociability characteristic of WBS patients (Sakurai et al., 2010). In one study which selectively deleted *GTF2I* in

excitatory forebrain neurons of mice, it was found that the resulting WS-like neurocognitive abnormalities were associated with decreases in myelin thickness, oligodendrocyte numbers, and axonal conductivity and that the behavioural abnormalities could be rescued by clemastine or improved axonal conductivity (Barak et al., 2019). Reduced myelin thickness and reduced numbers of mature oligodendrocytes were also identified in the frontal cortices of WS patients (Barak et al., 2019). Interestingly, *GTF2I* dosage is directionally important to the presenting neurocognitive profile, with copy number losses tending towards a hypersocial phenotype, including mental retardation and impaired visuospatial ability, and copy number gains manifesting in an autistic phenotype, with severe language impairments and repetitive behaviour (Shirai et al., 2017). *GTF2RD1* loss is thought to drive the craniofacial abnormalities seen in WBS patients. This has been supported by the identification of a patient with an atypical deletion involving *GTF2RD1* (among other genes) but not *GTF2I* (Dai et al., 2009). The patient demonstrated characteristic WBS facial dysmorphism but tested far above expectation in cognition (Dai et al., 2009). This has been further corroborated in *Gtf2ird1*-null mice, which manifest craniofacial abnormalities (Tassabehji et al., 2005). In general, however, *GTF2I* and *GTF2RD1* are thought to synergistically influence the craniofacial and visuospatial cognitive deficits in this disorder.

Other suspected genes in this region include *STX1A* (syntaxin-1) and *CLIP2*. *STX1A* is a SNARE protein involved in synaptic vesicle exocytosis and shows

strong expression in the brain. However, *Stx1a* knockout mice are grossly normal, though they do show deficits in hippocampal LTP and conditioned fear memory extinction, suggesting a role for *STX1A* in synaptic plasticity (Fujiwara et al., 2006), but demoting its candidacy as the driver of this disorder. In human studies, *STX1A* SNPs are associated with high-functioning autism (Nakamura et al., 2008) and are thought to play a role in the intelligence of patients with WBS (Gao et al., 2010), supporting a secondary role for *STX1A* in neuropsychiatric phenotypes. While *CLIP2* was initially given strong credibility as a main driver of this disorder, the identification of *CLIP2* hemizygous deletion patients with no clinical abnormalities has largely excluded it from consideration as a main driver in this disorder (Vandeweyer et al., 2012).

### **8p23.1**

The 8p23.1 region is susceptible to rearrangements, with the typical CNV region spanning 3.4–3.7 Mb and including up to 31 genes and microRNAs (Barber et al., 2013). Both the microdeletion and microduplication syndromes are significant for learning disabilities, congenital heart defects, and microcephaly/macrocephaly (respectively). Most research on driver gene candidates in this disorder has focused on cardiac defects, highlighting the main role of the transcription factors *GATA4* and *SOX7*. Two candidates with identified neurophysiological consequences are *MCPH1* (microcephalin) and miR124-1.

*MCPH1* mutations are an identified cause of primary microcephaly, which suggests a primary role for this gene in the head size abnormalities of the 8p23.1

CNV. *MCPH1* is a DNA-damage response protein, and is also implicated in premature chromosome condensation syndrome (Trimborn et al., 2004). The various functions carried out by *MCPH1* are reviewed elsewhere (Liu et al., 2016). Known to be under positive selection pressure in the human evolutionary lineage, *MCPH1* has attracted considerable interest as a potential driver of the neurocognitive phenotypes in this disorder.

miR-124-1 is the most highly expressed microRNA in neuronal tissue, and is a known modifier of neuronal progenitor fate. miR-124-1 is particularly implicated in the development of neural lineage cancers. Despite its evident involvement in neurodevelopment, the relationship of miR-124-1 to specific phenotypes in the 8p23.1 CNVs remain incompletely understood.

### **15q11-13**

The 15q11-13 region has two distinguishing features which are relevant to the clinical presentation of its accompanying CNVs. The most common CNV in this region is a deletion, which may occur between breakpoints 1 and 3 (class I deletions), or between BP2 and 3 (class II deletions) (Sahoo et al., 2006). While both deletions result in the development of an NDD, the inheritance (maternal vs. paternal) will determine if the disorder is Angelman syndrome (AS) or Prader–Willi syndrome (PWS), respectively. Because the class I deletion encompasses the class II region, the phenotypes in these patients are more severe (Sahoo et al., 2006). Though the BP1-2 region alone was largely considered to have little pathologic relevance, further refinements have identified specific roles for

encompassed genes in promoting NDD development, and associated disorders are grouped under 15q11.2 CNVs.

### *Angelman syndrome*

Angelman syndrome presents with the core findings of developmental delay, ataxia/tremors, severely impaired speech acquisition, and may develop seizures with highly characteristic EEG abnormalities (Kalsner & Chamberlain, 2015). This disorder results from maternal deletions of the PWS/AS critical region.

Perturbations to the *Ube3A* gene, which encodes ubiquitin-protein ligase E3A, were identified as sufficient for the development of AS, thus implicating it as the driver of this disorder (Kishino et al., 1997). Subsequent work would identify UBE3A imprinting as brain-specific (Rougeulle et al., 1997; Vu & Hoffman, 1997), offering further clues to its potential role in neuropsychiatric disease.

Much of the insights into the role of UBE3A in driving neurodevelopmental phenotypes have come from mouse studies. Mice deficient in the maternal copy of *Ube3A* (*Ube3A<sup>m-/p+</sup>*) demonstrate impairments in recovery from long-term potentiation (LTP), but no evidence of synaptic transmission deficits at baseline, nor any neuroanatomical abnormalities (Jiang et al., 1998). In the same mouse model, Greer et al. identified the plasticity “master regulator” protein *Arc* as a target of *Ube3A*-mediated ubiquitination, which was associated with a selective decrease in AMPA receptors at excitatory synapses (Greer et al., 2010).

Further insights into the putative role of *Ube3A* at the synapse have come from studies of *Ube3A* duplication. While distinct from AS, duplications of the 15q11-

13 region are highly recurrent and penetrant for many neuropsychiatric phenotypes, particularly autism spectrum disorder. Ube3A duplication/triplication mice show impaired social behaviours which are proportional to Ube3A copy number and consistent with an autism paradigm. Interestingly, the gain of Ube3A impaired excitatory synaptic transmission, impacting both pre- and postsynaptic sites (Smith et al., 2011). Subsequent work further identified that disrupted regulation of the autism-linked gene Cerebellin-1 (Cbln1) by loss of Ube3a might underlie sociability deficits (Vaishnav Krishnan et al., 2017). Cbln1 is a binding partner of neurexins 1–3 (NRXN1–3) presynaptically, and delta-1 ionotropic glutamate receptor subunits (GRID1–2) postsynaptically, providing a plausible rationale for the trans-synaptic deficits observed with Ube3a deletions. Consistent with its role in LTP recovery, the gain of Ube3a acts synergistically with seizure activity in the development of impaired sociability (V. Krishnan et al., 2017). Attempts to study the mechanistic role of Ube3a in human models have been difficult. Several groups have derived iPSCs from patients with Ube3a disruptions (Fink et al., 2017; Germain et al., 2014; Lee et al., 2018; Niki et al., 2019; Pólvora-Brandão et al., 2018; Stanurova et al., 2016). These models have provided important clues to the potential role of Ube3a in driving the pathologies of this disorder. These models have identified similarities in differentially expressed genes in both deletion and duplication (Germain et al., 2014)g, and dysregulated electrophysiologic maturation in membrane and synaptic properties of iPSC-derived neurons. One important caveat is that due to unreliable

imprinting of the PWS/AS critical region in iPSCs and iPSC-derived neurons, these models remain an important impediment to accurate disease modelling (Pólvora-Brandão et al., 2018; Stanurova et al., 2016).

Though the mechanistic features of Ube3a CNVs remain largely unresolved, early proof-of-concept targeted treatments have been attempted. As the paternal Ube3a allele is retained in most cases of AS, efforts to re-express it aim to bypass the question of mechanism by addressing the fundamental insult. However, extensive off-target effects preclude the immediate translation of this intervention.

Ube3a is among the best-established single-driver genes from a CNV implicated in NDDs. Although the disruption of this gene faithfully recreates the core symptomatology of AS, the mechanisms by which this occurs remain largely unknown. While both synaptic phenotypes and GABAergic neurons are, at present, the principally implicated points of mechanistic convergence in driving the clinical phenotype, a more refined understanding of the implicated pathways remains outstanding.

### ***Prader–Willi Syndrome/Schaaf–Yang Syndrome***

Prader–Willi Syndrome (PWS) is a complementary disorder to AS, in that the deletion of the paternal copy of the 15q11-13 critical region causes a complete loss of expression for maternally imprinted genes. PWS presents with a more generalized developmental delay phenotype than AS, though there is a neurodevelopmental component to the disorder, including intellectual disability

(Kalsner & Chamberlain, 2015), behavioural problems, and in some cases autism (Butler & Thompson, 2000; Dykens et al., 2011). To date, no clear genes have unilaterally emerged as drivers of these disorders. Deleterious mutations affecting *MAGEL2* (melanoma antigen like 2), which is one of the affected genes in the PWS, have been shown to recapitulate several cardinal features of the disorder as part of Schaaf–Yang syndrome (SHFYNG), and to be particularly penetrant for neurodevelopmental phenotypes including autism spectrum disorders (Schaaf et al., 2013), behavioural abnormalities, and developmental delay/intellectual disability ("Correction: Corrigendum: The phenotypic spectrum of Schaaf-Yang syndrome: 18 new affected individuals from 14 families," 2016). In mouse brains, *Mage12* is highly expressed during mid-to-late gestation (particularly the hypothalamus), and decreases to a low expression level in the adult mouse brain, suggesting a potential developmental role (Lee, 2000). *Mage12* is predicted to facilitate the action of E3-ubiquitin ligases (Doyle et al., 2010; Tacer & Potts, 2017), the action of which has been shown to indirectly regulate Retromer-mediated transport (Hao et al., 2013). Hypothalamic oxytocin neurons in *Mage12* deficient mice have a decreased firing rate, reduced spontaneous excitatory postsynaptic currents (sEPSCs), and a decrease in AMPA-R-dependent currents (Ates et al., 2019). Studies in *Mage12* deficient mice demonstrate leptin-insensitivity of pro-opiomelanocortin (POMC) expressing neurons of the hypothalamus, which develops in an age-onset manner (Mercer et al., 2013; Pravdivyi et al., 2015). Interestingly, this is accompanied by decreased

hypothalamic oxytocin, and early postnatal oxytocin administration can rescue poor suckling (Schaller et al., 2010) and behavioural deficits in adult mice (Meziane et al., 2015).

While MAGEL2 is a clear contributor to NDD phenotypes, its mechanistic role remains to be determined. Contradictory evidence suggests that deletion of MAGEL2 (as well as MKRN3 and NDN) is not sufficient to cause PWS (Kanber et al., 2009). Further, while preliminary functional data strongly support its role in oxytocin neurons of the hypothalamus, human studies remain to be conducted in support of the molecular underpinnings, and to inform targets for potential interventions.

### **16p11.2**

CNVs in the 16p11.2 region are associated with several NDDs, including ASD (Fernandez et al., 2009; Hanson et al., 2010; Kumar et al., 2007; Kumar et al., 2009), developmental delay, and dysmorphic features (Fernandez et al., 2009). The typical CNV region encompasses a 600 kb segment and 29 genes (Zufferey et al., 2012). Microdeletions of this region are phenotypically more severe than microduplications (Fernandez et al., 2009). Studies of the implicated genes in this region do not favour an interpretation of a singular gene as the driver of the neurodevelopmental phenotypes in this CNV. Studies have been unsuccessful in identifying a single-driver gene behind the NDD phenotypes of the 16p11.2 CNV, likely due to the complexity and size of the region. Several genes in this region (KCTD13, TAOK2, MAPK3, and SEZ6L2) have been implicated as potential NDD

risk loci and evidence from animal and human models has established a putative role for their contribution to neuropsychiatric phenotypes.

KCTD13 (potassium channel tetramerization domain containing 13) rare variants have been identified as schizophrenia risk loci (Degenhardt et al., 2016).

KCTD13 demonstrates a dose-dependent ability to induce micro/macrocephaly in cases of deletion/overexpression (respectively), in a zebrafish model of the disorder (Golzio et al., 2012). Neural precursor cells derived from KCTD13 knockout iPSCs demonstrate impaired DNA synthesis and impaired proliferation, and cortical neurons derived from the same iPSCs had impaired neurite formation which was rescued by ERBB signalling activation (Kizner et al., 2019).

Interestingly, the ERBB was identified as a potential target by RNA-sequencing-based pathway determination (Kizner et al., 2019). Human protein developmental network analyses highlight an important role for the KCTD13 pathway in late mid-fetal brain development, potentially underlying brain size/connectivity phenotypes (Lin et al., 2015). A mouse study of KCTD13 deletion demonstrated decreased synaptic transmission which was rescued by RhoA inhibition (Escamilla et al., 2017). Interestingly, this study did not identify any changes in brain size or cellular proliferation associated with KCTD13 deficiency (Escamilla et al., 2017).

MAPK3 (mitogen-activated protein kinase 3) is a serine/threonine kinase which is involved in various cellular growth and maintenance function (Roskoski, 2012). It was identified as a potential driver in a cohort of ASD patients with missense mutations (Schaaf et al., 2011). Deleterious mutations of functionally related

proteins identified by a proteomics analysis (Friedman et al., 2011) identified a similar (though less severe phenotype), highlighting an important corroborative role for proteomic analyses in driver gene mechanistic discovery (Park et al., 2017).

TAOK2 (thousand and one amino-acid kinase 2) is a MAP kinase pathway activator (Chen & Cobb, 2001) and is known to be involved in the DNA-damage stress response (Raman et al., 2007). In cultured mouse cortical neurons, TAOK2 downregulation impaired neurite formation and branching complexity (de Anda et al., 2012). *In vivo*, TAOK2 downregulation was associated with decreased basal dendritic arborization, and impaired axonal elongation (de Anda et al., 2012). Subsequent work would identify the loss of TAOK2 as compromising dendritic stability, and demonstrate the role of TAOK2 in stabilizing the postsynaptic density scaffolding protein *PSD95* by phosphorylation of Septin7 (Yadav et al., 2017). Richter et al. found that TAOK2 deletion was implicated to affect brain size in a dosage-dependent manner, and also contribute to behavioural abnormalities related to cognition, anxiety, and social interaction (Richter et al., 2019). This was accompanied by decreased basal dendrite density in prefrontal cortical (PFC) neurons, reduced dendritic spine density, and altered distribution of spine morphology (Richter et al., 2019). It was further shown that TAOK2 and RhoA exist in the same protein complex and that the observed phenotypes are mediated by RhoA signalling (Richter et al., 2019).

SEZ6L2 (seizure-related 6 homolog-like 2) variants have been associated with autism (Kumar et al., 2009). Triple knockout mice for the SEZ homolog proteins BSRP (A-C) (*brain-specific receptor-like proteins*) develop motor coordination defects and have impaired cerebellar synaptic maturation (Miyazaki et al., 2006). However, a clear mechanistic link has yet to be established between SEZ6L2 and the pathobiology of NDDs.

At present, mechanistic and associative evidence suggests that there is no clear single-driver gene underlying NDDs in the 16p11.2 CNV disorder. Despite this, some evidence suggests a potential overlap of signalling pathways for three of the candidate drivers in this region (TAOK2, MAPK3, and KCTD13) through RhoA and MAPK signalling. Interestingly, in two mouse models of the 16p11.2 hemizygous mice, both cognitive and social phenotypes are rescued by the GABA<sub>B</sub> agonist R-Baclofen (Stoppel et al., 2018), though the mechanisms of this remain unknown. While the cause of the 16p11.2 CNV does not appear to be attributable to one genetic element, identifying convergent signalling pathways between these elements might offer insights into common disease pathways for associated NDDs, and highlight novel downstream targets for intervention.

### **17p11.2**

Microdeletions and microduplications of the 17q11.2 region are associated with Smith–Magenis syndrome (SMS) and Potocki–Lupski syndrome (PTLS), respectively, and associated CNVs can span 0.9–3.7 Mb. The SMS core phenotype consists of distinctive craniofacial abnormalities, sleep disturbances,

DD/ID, behavioural problems, and otolaryngologic deficits. The PTLS presents with DD/ID, and behavioural issues, and are more likely to be diagnosed with ASD. The *RAI1* (retinoic acid-induced 1) gene was isolated as causative by studies of patients with deletions or missense mutations in *RAI1* who recapitulate the SMS phenotype (Girirajan et al., 2006), and by identifying it as the only gene in the minimal region of duplication overlap in cohorts of PTLS patients (Zhang et al., 2010). While *RAI1* is the accepted driver of disorder phenotypes, there is clear evidence that other genes in the region are responsible for other phenotypic features of this disorder, including severity (Girirajan et al., 2006).

### **22q11.2**

Microdeletions of the 22q11.2 region were originally identified as the underlying cause in most cases of DiGeorge/velocardiofacial syndrome (VCFS) (Driscoll et al., 1993; Driscoll et al., 1992; Scambler et al., 1992). More recently, CNVs of the 22q11.2 region have been associated with disorders such as schizophrenia (Bassett et al., 2008; Karayiorgou et al., 1995), ASD (Fine et al., 2005; Vorstman et al., 2006), and early onset psychosis (Vorstman et al., 2006). For a comprehensive review, see Hiroi et al. (Hiroi et al., 2013). The most common CNV region spans 3 Mb, though a rarer nested deletion (~1.5Mb) can produce the very same phenotypes observed in this disorder (Carlson et al., 1997; Gong, 1996). Several genes in this region are identified as potential drivers of the associated neurodevelopmental phenotypes, including *Tbx1*, *Zdhhc8*, and *Dgcr8*.

Dgcr8 (DiGeorge syndrome chromosomal 8) encodes a subunit of a microprocessor complex involved in microRNA processing. Complete Dgcr8 knockout is lethal in mice, underscoring the importance of its function (Fénelon et al., 2011). Fénelon et al. discovered that Dgcr8 heterozygous mice have mild structural changes in layer 5 basal dendritic spines (Fénelon et al., 2011). They further identified that these mice have synaptic plasticity deficits, manifesting in greater long-term depression in layer 5 neurons (Fénelon et al., 2011).

Unsurprisingly, the mechanisms underlying Dgcr8 dysregulation are thought to be microRNA mediated. Interestingly, these phenotypes worsened over time as miR-338-3p levels decreased, could be recreated by acute knockdown of miR-338-3p, and were rescued by its re-expression (164). Dcgr8 is also thought to partially regulate a microRNA encoded in the 22q11.2 region (miR-185), which represses the expression of *Mirta22*, responsible for regulating dendritic and spine development (Xu et al., 2013).

Zdhhc8 encodes a palmitoyltransferase with high expression levels in the brain, both in humans and mice (Liu et al., 2002). Mukai et al. first identified Zdhhc8 as a potential schizophrenia risk gene by identifying a high-risk SNP (rs175174) (Mukai et al., 2004). It has also recently been implicated as a potential regulator of epileptic seizure susceptibility (Yang et al., 2018). Surprisingly, Zdhhc8<sup>-/-</sup> mice show sexually dimorphic deficits in exploratory behaviour and prepulse inhibition, which are more pronounced in female mice (Mukai et al., 2004). Mechanistic evidence for the potential role of Zdhhc8 was first highlighted by its ability to

regulate PSD-95 by palmitoylation (Ho et al., 2011; Mukai et al., 2008), a finding which potentially underlies deficits in dendritic spine morphology and density, as well as decreased dendritic complexity, in *Zdhhc8<sup>+/-</sup>* and *Zdhhc8<sup>-/-</sup>* mice (Mukai et al., 2008). Interestingly, GSK3 $\beta$  inhibition during early development has been shown to rescue behavioural phenotypes in a 22q11.2 microdeletion mouse model (Tamura et al., 2016), and axonal branching phenotypes in a *Zdhhc8<sup>-/-</sup>* mouse (Mukai et al., 2015)). While this approach is preliminary and relatively high-level with respect to disease pathobiology, it importantly highlights the developmental aspect of these disorders and the potential for early intervention in modifying the disease trajectory.

### **22q13.3**

CNVs of the 22q13.3 region are almost always microdeletions, which are responsible for Phelan–McDermid syndrome (PMS). This condition presents principally with global developmental delay, intellectual disability, severe speech deficits, hypotonia, and motor deficits. Interestingly, it is among the most penetrant conditions for ASD, for which it has attracted considerable interest as a research target.

The 22q13.3 CNV region can vary widely in size, with the recurrent region extending up to 9 Mb, and potentially extending to a terminal deletion. These CNVs can involve ~30–190 genes, though the majority of interest has been focused on the *SHANK3* (SH3 and multiple ankyrin repeat domains 3) gene which is thought to be principally responsible for the major neuropsychiatric

phenotypes in this disorder. *SHANK* proteins encode postsynaptic scaffolds, and defects in their functionality are accordingly associated with synaptic defects that are clinically linked to neuropsychiatric disorders. *SHANK3* is deleted in nearly all CNV cases, and individual pathological variants have been identified in patients with the core phenotype of the PMS.

Given the size of the CNV and the number of genes that are potentially involved, it is unsurprising that other genes in this region have also been linked to neuropsychiatric outcomes. A review by Mitz et al. systematically profiled genes found in this region and identified five groupings associated with the purported phenotypic correlates (Mitz et al., 2018). This analysis considered several parameters in determining disease-relevant genes, including genes which are known independent risk factors for specific neuropsychiatric disorders, the probability of loss-of-function intolerance (pLI score) of the genes, and an estimated population impact factor (PIF). The groups consider potentially diverse roles for genes in neurodevelopment, synaptic organization, and mitochondrial function. However, *SHANK3* retains its central role as the purported driver of the PMS, and these genes are largely considered in the context of how they might act in concert with *SHANK3* to modify disease outcomes.

#### **1.1.4 Summary**

As previously stated, the fact of NDD development overlap between and co-occurrence within various genetic aberrations is suggestive of mechanistic overlap. The correct level of abstraction for identifying these shared features is

nonobvious, and this section has highlighted some of the possible ways that these may be characterized and leveraged for actionable insights.

While innumerable clinical states and genetic mechanisms for disease can be theorized, only a fairly limited number of highly recurrent ones are observed. This is for two reasons. Clinically, only a narrow band of early life developmental abnormalities are compatible with life, and it is within this band that pathology is observed. Genetically, specific loci are similarly susceptible to rearrangement and mutation due to (1) the non-fatality of these mutations, and (2) genetic elements which increase the likelihood of specific changes (duplicated flanking regions). Taken together, this group of highly recurrent NDD-associated CNVs have a heterogenous presentation, and in many cases (even where the “driver” gene is purportedly known) have features linked to multiple genes in the region.

## 1.2 The 15q13.3 microdeletion disorder

### 1.2.1 Background

The 15q13.3 microdeletion is a rare chromosomal abnormality, with a population prevalence estimated between 1 in 5525 (Gillentine et al., 2018) and 1 in ~40,000 (Sharp et al., 2008). Patients with this deletion are at an increased risk for the development of ASD, ADHD, epilepsy (particularly absence seizures), and learning disabilities (Lowther et al., 2015; Ziats et al., 2016). The microdeletion is named for its location on the q arm of chromosome 15, in region 1, band 3, sub-band 3. In the case of the 15q13.3 microdeletion, the minimally deleted region is approximately 1.5 Mb and contains seven genes (*CHRNA7*, *OTUD7A*, *MTMR10*, *KLF13*, *FAN1*, *TPRM1*, and *ARHGAP11B*). For a map of the region, see Figure 1.3.2. Other phenotypic manifestations include an increased incidence of cardiovascular structural abnormalities, and increased cancer risk. Evidence suggests that three genes potentially contribute to neuropsychiatric outcomes in this disorder: *CHRNA7*, *OTUD7A*, and *FAN1*.

*CHRNA7* (encoding the  $\alpha 7$  nicotinic acetylcholine receptor) has historically been seen as the most likely driver gene in 15q13.3 CNVs. Evidence for this view comes from minimal breakpoint analyses, which show *CHRNA7* to be the only fully deleted gene in sub-deletions (Endris et al., 2010; Hoppman-Chaney et al., 2013; Shinawi et al., 2009; Szafranski et al., 2010). Mutations in *CHRNA7* are also enriched in autism spectrum disorder (Bacchelli et al., 2015), and generalized epilepsy (Damiano et al., 2015). Losses of *Chrna7* copy number are

associated with more severe clinical outcomes than gains (Gillentine & Schaaf, 2015). *CHRNA7* deletion has been proposed as a disruptor of mouse hippocampal inhibitory circuitry (Adams et al., 2012), resulting in altered hippocampal GABA<sub>A</sub> receptor subunit expression (Adams et al., 2012; Bates et al., 2014), increased *GAD67* and parvalbumin (Bates et al., 2014), and decreased *GAD65* levels (Adams et al., 2012; Bates et al., 2014). Interestingly, however, *Chrna7* deficient mice do not consistently recapitulate core features of the 15q13.3 microdeletion syndrome (Yin et al., 2017). *Chrna7* overexpression is capable of rescuing dendritic spine phenotypes observed in 15q13.3 heterozygous mice (Uddin et al., 2018). While *Chrna7* clearly plays an important role in this disorder, the variability of its phenotypic consequences in both mice (Yin et al., 2017) and humans suggests that it may not be sufficient to drive the phenotypes underlying this disorder (Gillentine et al., 2017). Most of the original research into the affected genes in the 15q13.3 microdeletion focused on the role of *CHRNA7* which encodes the  $\alpha 7$ -nicotinic acetylcholine receptor subunit. Several patients with *CHRNA7* deletions were shown to manifest core phenotypes of the 15q13.3 microdeletion disorder (Hoppman-Chaney et al., 2013; Shinawi et al., 2009; Spielmann et al., 2011). In addition, case reports have indicated that aggression can be ameliorated in these patients by the administration of nicotinic agonists (Cubells et al., 2011). Because *CHRNA7* is a neuronally expressed receptor, the plausibility of its role in an NDD disorder lead

to its adoption as the leading candidate for the 15q13.3 microdeletion for several years.

In recent years, data published by our group (Uddin et al., 2018) and others (Yin et al., 2018) have revealed novel roles for *OTUD7A* as a candidate for the driver gene underlying phenotypes in the 15q13.3 microdeletion. *OTUD7A* encodes ovarian tumour (OTU) deubiquitinase 7A, which is a subfamily of deubiquitinating enzymes. Though *OTUD7A* is known to target lysine-11 linkages for deubiquitination with a high degree of specificity (Mevisen et al., 2013; Mevisen et al., 2016), its role in cellular function remains largely unknown. *OTUD7A* null mice recapitulate core features of the 15q13.3 microdeletion (Yin et al., 2018) better than *CHRNA7* null mice (Yin et al., 2017), and manifest dendritic spine abnormalities including decreased density (Uddin et al., 2018; Yin et al., 2018) and altered morphologic characteristics (Uddin et al., 2018). Additionally, the previously reported deletions of *CHRNA7* were shown to also encompass the first exon of *OTUD7A* (Uddin et al., 2018). Subsequent genomic analysis revealed that of the genes in the 15q13.3 microdeletion region, *OTUD7A* is the most intolerant to loss-of-function (LoF) mutations, underscoring its importance to normal development (Uddin et al., 2018). A recent clinical report in the European Journal of Human Genetics described a child born to consanguineous parents with an extremely rare homozygous mutation (leucine-233 → phenylalanine) in the catalytic domain of *OTUD7A* (Garret et al., 2020). This patient had early

onset, severe epileptic seizures with learning and speech difficulties (Garret et al., 2020).

Other implicated genes in the region include *FAN1*, which encodes the Fanconi-associated nuclease 1. Exome sequencing identifies *FAN1* mutations as associated with both ASD and schizophrenia (Ionita-Laza et al., 2014). *FAN1* has also been identified as a significant modifier of disease trajectory for trinucleotide expansion repeat disorders such as Huntington's (Goold et al., 2019), fragile X syndrome (Zhao & Usdin, 2018), and spinocerebellar ataxia type 3 (Mergener et al., 2019). However, *FAN1* does not appear to be a primary driver of these or other neurodevelopmental phenotypes.

*KLF13* (Kruppel-like factor 13) is typically identified as a transcription factor playing an important role in the proliferation capacity of various cancers and a determinant of congenital cardiac defects (Chen et al., 2022; Ding et al., 2022; Lavalley et al., 2006; Liang et al., 2023; Wang et al., 2020). While it has not been a highly implicated gene in neuropsychiatric disease, recent work has shown a role for it in protecting against excitotoxicity in neurons (Avila-Mendoza et al., 2020). While KLF family proteins have been implicated in neurite outgrowth (Moore et al., 2009), they remain largely understudied and the role of this gene in the 15q13.3 microdeletion disorder is poorly understood.

*TRPM1* encodes the transient receptor potential cation channel subfamily M member 1. It was previously thought to be confined to the retina for expression, but no consistent ophthalmologic phenotype is present in patients with a deletion

in this gene. *Trpm1*<sup>-/-</sup> mice do have functional abnormalities resembling ADHD (Hori et al., 2021). There are reports of visual impairments (Spielmann et al., 2011) and congenital retinal defects (Lepichon et al., 2010) in patients with a homozygous 15q13.3 deletion, but *TRPM1* remains a low-confidence gene in this disorder.

### Figure 1.3.2: 15q13.3 microdeletion BP4-BP5 region

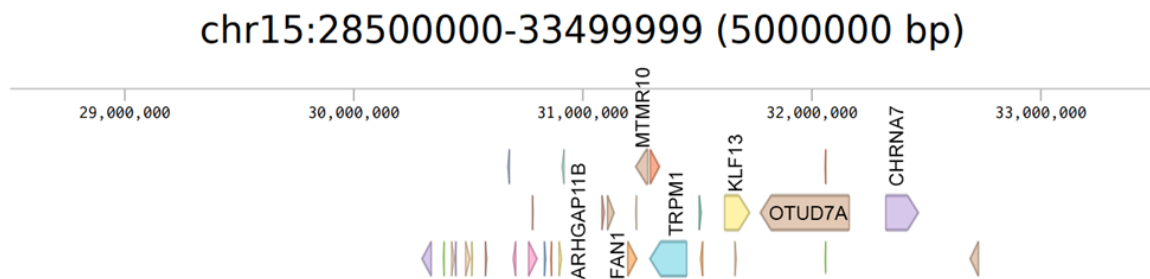


**Figure 1.3.2:** Alignment map of the human 15q13.3 chromosome region, highlighting the “classic” ~1.5Mb deletion region and regionally located genes (schematic created with Benchling.com software).

### ***Structural features of the 15q13.3 microdeletion region***

In recent hominid evolution, many genomic regions underwent rapid expansion under selection pressures to increase cortical size. This resulted in many highly homologous regions comprised of these repeat elements. During homologous recombination, these regions have a comparatively high propensity to misalign and produce inverted chromosomal segments. Subsequent rearrangements represent a high risk of either gains or losses of these inverted regions, which become duplications and deletions. Because these regions originally expanded as an adaptation to augment nervous system (principally cortical) development,

the altered dosage of genes resulting from deletion or duplication will often increase the propensity for neuropsychiatric disease. In some cases, reciprocal CNVs can have surprisingly linear effects on developmental abnormalities, such as micro- and macrocephaly in a matched deletion and duplication disorder (respectively) (Bernier et al., 2016; Ian T. Fiddes et al., 2018; Golzio et al., 2012). The major susceptibility elements in the 15q13 region are the *GOLGA8* repeats. *GOLGA8* encodes the golgin subfamily A member 8, is part of the larger family of similar golgin “coiled-coil” proteins. Despite the apparent presence of golgins in nearly all eukaryotic life and their role in Golgi membrane trafficking, their loss does not appear to cause fatal cellular injury (Munro, 2011). *GOLGA8* does not appear to play a functional role in the pathophysiology of the 15q13.3 microdeletion disorder (Bekpen & Tautz, 2019). Importantly, however, many copies of *GOLGA8* are present along chromosome 15 (Bekpen & Tautz, 2019). This segmental duplication predisposes many regions of the chromosome to rearrangements, including inversions and subsequent deletions and/or duplications (Antonacci et al., 2014). These are the so-called breakpoints of the chromosome, and the recurrent 15q13.3 deletions will align with them. The expansion of this element (along with *ARHGAP11B*) in recent hominid evolution is the possible consequence of a selection pressure towards neocortex expansion, at the cost of chromosomal stability (Antonacci et al., 2014). *ARHGAP11B* encodes Rho GTPase-Activating Protein 11B, which was formed through the partial duplication of the *ARHGAP11A* gene in recent hominid

evolution (Dennis et al., 2017; Florio et al., 2015; Hevner, 2020). *ARHGAP11B* is noteworthy as a key protein involved in the neocortical expansion which differentiates modern humans from their closest primate relatives. *ARHGAP11B* expression variably increases both cortical size and folding in mouse, ferret, and marmoset models (Heide et al., 2020; Kalebic et al., 2018; Xing et al., 2021). This effect is thought to be partially mediated by increased proliferation of basal progenitor cell populations, particularly radial glial cells (Florio et al., 2015; Florio et al., 2016; Penisson et al., 2019). Recent evidence suggests that *ARGHAP11B* may act to alter the metabolic state of these progenitors through the modulation of mitochondrial membrane proteins including the mitochondrial permeability transition pore (mPTP) and the adenine nucleotide translocase (ANT) (Namba et al., 2020). It has been suggested that both deletions and mutations impacting this gene have been overlooked due to its high sequence homology to *ARHGAP11A* (Heide & Huttner, 2021). However, heterozygous 15q13.3 microdeletion patients may manifest with either micro- or macrocephaly and many deletions will not encompass *ARHGAP11B* (Lowther et al., 2015). In addition, while the clinical evidence for a direct role of *ARHGAP11B* in neuropsychiatric disease is suggestive of a role in schizophrenia and bipolar disorder (Chen et al., 2016; Gregoric Kumperscak et al., 2021; Vadgama et al., 2019), the evidence remains largely suggestive, and there remains considerable uncertainty concerning the role of this gene in the classic 15q13.3 microdeletion syndrome.

## **Overview**

### **1.2.2 Pathophysiology**

The most distinctive feature of the clinical 15q13.3 microdeletion is the propensity to absence seizures (Lowther et al., 2015). Interestingly, a seizure phenotype is recapitulated by the Df(h15q13)/+ mouse (Fejgin et al., 2014; Forsingdal et al., 2016; S. R. O. Nilsson et al., 2016), which is important for several reasons.

Firstly, cortical seizures are facilitated by the overexcitation of pyramidal neurons. Typically, this is prevented (or contained) by inhibitory interneuron populations which insulate the seizure activity until the tissue can recover. If the excitation of the pyramidal neuron population exceeds the capacity of the inhibitory neurons to contain it, a seizure results. If this persists, brain tissue becomes damaged due to excitotoxicity, and significant circuit remodelling may result (Kandel, 2013). This early propensity to seizure activity may direct circuit development in early life and underlie many of the other phenotype presentations in the 15q13.3 microdeletion. However, the mechanisms driving these absence seizures are unclear, and beyond this speculative mechanism, very little remains known.

### **1.2.3 Advantages as a model disorder**

It is estimated that approximately 80% of individuals with the 15q13.3 microdeletion will manifest some neuropsychiatric phenotype (Lowther et al., 2015). Interestingly, a recent analysis of neurons derived from 15q13.3 patient lines revealed that there were no significant differences in methylation or chromatin accessibility, suggesting that the loss of genes was directly responsible

for the phenotype (Zhang et al., 2021). This same study further identified global transcriptional and epigenetic changes associated with the 15q13.3 microdeletion, including several which were significant for NDD pathobiology (Zhang et al., 2021). Because of its penetrance and the comparatively limited number of genetic factors involved, the 15q13.3 microdeletion is a promising candidate for the discernment of a well-defined etiology in an NDD-associated disorder.

The 15q13.3 microdeletion satisfies many of these characteristics, which makes it a promising candidate for studying a genetic condition associated with neurodevelopmental disorders. Clinically, it can be thought of as intermediate in both population prevalence and penetrance for NDDs. It is mostly maternally inherited (Lowther et al., 2015) and manifests in a combination of functional disorders (such as absence seizures), and psychiatric disorders (such as ASD, ADHD, ID/DD). Importantly, the 15q13.3 region itself has a relevant recent and ancient evolutionary history. Copy number of genetic elements in the region appears to have rapidly expanded during a period of human-specific brain expansion and development (Antonacci et al., 2014), while homologous versions of the region's core region are maintained in the 7qC region of the mouse genome (Fejgin et al., 2014). Mouse models of this deletion recapitulate both seizure propensity and behavioural dysfunctions of the human disorder (Fejgin et al., 2014; Simon R. O. Nilsson et al., 2016).

The 15q13.3 region is one of several genomic hotspots that are highly implicated in neurodevelopmental disease. Interestingly, the 15q13.3 deletion is associated with neuropsychiatric diseases such as autism and ADHD (with an onset in early development), and schizophrenia (with an onset in early adulthood). These two peaks of disease mark two important transition points for the developing brain. In early life, the brain has the most synapses that it will ever have. These are successively reduced, and it is believed to be in this period and process that the early conditions for autism are laid down (Bourgeron, 2015). The symptomatic manifestations of schizophrenia coincides with the completion of neocortical development in the early to mid-twenties. It is likely not coincidental that these regions which expanded under selection pressures in humans are associated with the especially human neocortex expansion. However, it is also noteworthy that very few of these diseases can be diagnosed from a clinical examination alone. The fact of the genetic aberration is not perfectly coincident with some set of behavioural or physical features, and there is often considerable overlap between these genetic disorders and the associated clinical conditions. A possible explanation for this is that these mutations are convergent upon a limited set of mechanisms.

Taken together, the 15q13.3 microdeletion disorder represents a highly penetrant, recurrent CNV that has both human-specific and cross-species dysfunctions represented with respect to neuropsychiatric pathology. While many of these features are shared by other comparator CNVs (for example 16p11.2 or

1q21.1), the 15q13.3 region has some advantages. Chief among these is the comparatively limited number of genetic elements involved, which may be as few as six genes in the most conservative form of the traditional deletion. In addition, the 15q13.3 microdeletion very characteristically manifests in an absence seizure disorder. This combination of limited genetic elements and uncommon but objective clinical findings make the 15q13.3 microdeletion a strong candidate for studying concrete manifestations of neuropsychiatric disease and their genetic correlates.

### **1.3 Experimental approach**

To address this in our study, we pursued cellular phenotyping of induced neurons from three different 15q13.3 microdeletion families. There are three salient points when considering the experimental path pursued herein (1) the heterogeneity of the disorder (for descriptions of our own cohort see the Family/iPSC index, Table 2.5.1), incomplete penetrance, and absence of robust biomarkers for NDDs are suggestive of a subtle and likely variable cellular phenotype; (2) in the absence of an isogenic control (especially difficult for a chromosomal rearrangement of this size), familial controls offer the best proxy for the genetic background in which disease occurs; (3) reductive models of neural systems are best suited to identifying cell-autonomous deficits.

Because the inherent heterogeneity of this disorder was a feature we were interested in disentangling, we opted not to group samples, but rather to analyze the families independently and draw comparisons thereafter.

### **1.3.1 Conceptualizing disease pathogenesis in NDDs**

While many approaches and schema have been proposed to explain the pathophysiologic underpinnings of these disorders, a definitive explanation remains elusive. NDDs (and neuropsychiatric diseases more broadly) are often described spectrally, with disease severity existing along a continuum. This distinction has had considerable clinical utility, allowing for the triaging of patients for various treatment purposes. A natural consequence of this framing has been to investigate the level at which these spectra may be represented (see Figure 1.3.1). For example, it has been postulated that these disorders are the results of imbalances in excitation-inhibition balance (i.e. too much excitation results in seizures, too little results in absence of brain function in some form), or connectivity between neurons. Similar explanations of imbalances between two extremes exist at all levels of analysis (molecular, cellular, tissue, organism). These are simplistic, low dimensional explanations and we should not ultimately expect them to have significant explanatory power. However, at any given level of analysis they may have utility in offering a useful comparative paradigm for the comparison of selected features. A highly reductive model was used in this thesis, and various forms of these comparisons are made to highlight select properties of the neurons.

**Figure 1.3.1: Excitation/inhibition as a conceptual schema underlying neuropsychiatric disorder pathogenesis**

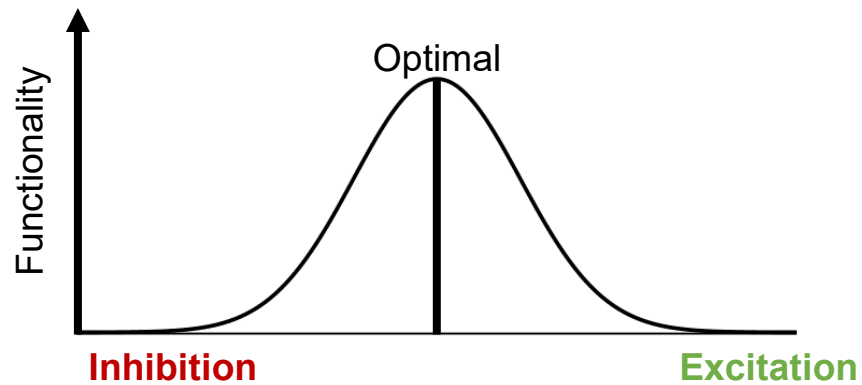


**Figure 1.1.2:** The bottom panel shows the common form of a bell curve schematic with disease at extrema of some functional or structural construct, in this case labelled for functionality as a consequence of “level” of excitation. Another example might include neuronal connectivity. In general, the form of this idea is to suggest that disease occurs at extrema of neuronal properties with a spectrum of possible outcomes, mirroring clinical disease.

### **1.3.2 Induced pluripotent stem cells (iPSCs)**

iPSCs are derived from somatic tissues (typically fibroblasts or CD34+ white blood cells) by transcription factor reprogramming (Takahashi et al., 2007). iPSCs are multipotent, renewable, patient-derived, and can be generated noninvasively. Further differentiation of iPSCs into cells/tissues of interest are a versatile model to study patient-specific tissues, particularly inaccessible or scarce ones. iPSCs have become a mainstay of human-disease research for their differentiation capacity and manipulability (for example in gene editing). Many different models can be derived from iPSC populations, ranging from pure 2-dimensional cultures (similar to the model used in this thesis) to complex 3-dimensional arrangements (as in the case of organoids). Models derivable from iPSCs are outlined in a review by Sanders et al (Sanders et al., 2019). While many options exist for differentiating iPSCs into neural tissue (Hong & Do, 2019), we currently use a single-step induction protocol which generates a population of pure excitatory glutamatergic neurons (Y. Zhang et al., 2013). This protocol allows for the rapid generation of a robust, highly replicable neuron population.

### **1.3.3 Induced glutamatergic neurons**

Induced neurons (iNs) are generated by forced expression of the transcription factor neurogenin-2 (Ngn2) (Y. Zhang et al., 2013). This protocol allows for the conversion of non-neural tissue (iPSCs, in the case of this study) into a highly homogenous population of cortical-like glutamatergic neurons. These gain functional and morphological maturity rapidly and are readily co-plated with

mouse glia which extends culture viability significantly. This model has been used extensively for the characterization of patient lines and offers a highly manipulable platform for the investigation of neuronal properties.

**Figure 1.3.2: Induction and management protocol for induced neurons**

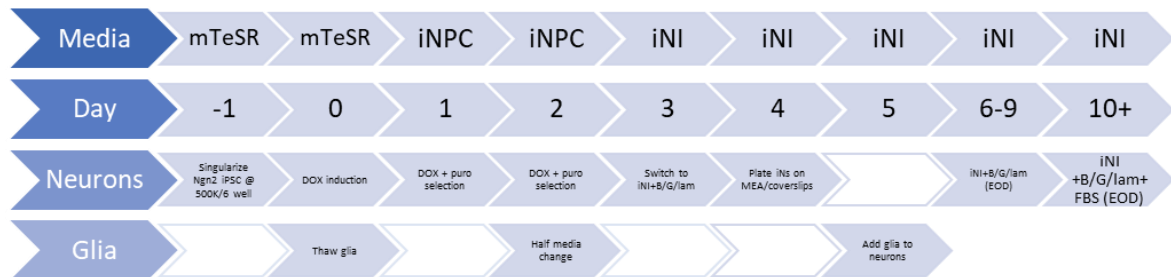


**Figure 1.3.2:** Timeline schematic showing induction timeline and media/drug administration requirements. Prior to induction iPSCs are infected with a construct containing a doxycycline-inducible element rtTA activating Ngn2 expression alongside the reporter (EGFP) and puromycin resistance gene used for positive selection.

Consequently, this aim sought to identify consistent (though likely subtle) cell-autonomous differences between induced neurons from 15q13.3 microdeletion probands and their familial controls. Rather than attempt to reproduce the composition of a functional nervous system, the Ngn2 induction model aims to provide a variance-minimized neuronal platform to amplify disease-relevant differences. While this system trades off real-world validity, it offers the possibility of producing concrete, cell-autonomous results in a neuronal model.

For many of these disorders, different models may be used which each carry their own advantages and drawbacks.

#### **1.3.4 Functional and morphological profiling**

Functional phenotyping was pursued at both the individual cell level by whole-cell patch clamp electrometry and at a cell population level by multi-electrode array (MEA) recordings. Whole-cell patch clamp allows for high-resolution recordings of intracellular currents from individual neurons, allowing for precise quantification of their membrane and functional properties. It is largely limited due to being an experimental endpoint, and low-throughput due to the technical difficulty involved (Hill & Stephens, 2021). Multi-electrode arrays (MEA) use a grid of electrodes upon which cells are plated to record field potentials which can be filtered to identify action potential firing (“spiking”). MEAs allow for repeat recordings of neurons across time in their native media, and allow for the correlation of activity across electrodes to quantify population-level activity and connectivity (Obien et al., 2014).

Morphological quantification of iNs aimed to characterize their degree of neurite outgrowth as a proxy of their developmental capacity. Neurite outgrowth is characterized by the degree of arbour complexity, determined by the number of intersections recorded at concentric rings at fixed distances from the soma (Sholl analysis). To more fully characterize neurons we also pursued quantification of axon projection capacity, and excitatory presynaptic connections were quantified.

#### **1.3.5 Transcriptomics**

RNA sequencing has become an affordable method by which to assess the transcriptome of various tissues. Transcriptome analysis broadly involves the

sequencing of mRNA and calculation of relative abundance of these transcripts alongside mapping to known genes. These data are then used for subsequent downstream analysis which may include the analysis of differentially expressed genes, determination of shared pathways for altered gene sets, and assessment of sample clustering through principal coordinate analysis. RNA sequencing offers a high throughput, high fidelity, and comparatively inexpensive modality by which to assess the transcriptional state of a tissue of interest. This can be a powerful method for novel pathway and mechanism discovery, and several studies have leveraged RNA sequencing to elucidate core features of NDDs (Blumenthal et al., 2014; Breen et al., 2023; Saw et al., 2020).

#### **1.4 Thesis Aims**

This thesis is split into three broad aims, which comprise the three chapters contained herein. The common model system used by all chapters involved the generation of iPSCs by Yamanaka factor reprogramming (Takahashi et al., 2007), followed by differentiation into induced neurons (iNs) by expression of neurogenin-2 (Y. Zhang et al., 2013).

##### ***Aim 1: Functional and morphological characterization of iNs from 15q13.3 microdeletion families.***

In this study, we report a clinical set of six 15q13.3 microdeletion families with associated clinical findings, collected with our collaborators from Europe, SickKids in Toronto, and Hamilton Health Sciences. The clinical 15q13.3 microdeletion disorder has pronounced functional (and often structural)

abnormalities, though incomplete penetrance. By using a cohort of patients with proven disease, we aimed to correlate the functional and morphological characteristics of these patient neurons. As mentioned previously, this aim used patch clamp electrophysiology and multi-electrode arrays characterize functional changes in these neurons, and investigated neurite projection capacity. The findings from this work highlighted cellular variability in both functional and morphological metrics, but did find a consistent decrease in axon projection capacity at an early time point in these neurons. These findings were included in a publication on which I was second author in *Molecular Psychiatry* (Unda et al., 2023). This represented a novel contribution to the research literature around this disorder, by performing the first in-depth phenotyping of patient neurons from unassembled cohort of 15q13.3 microdeletion patients, and highlights the inherent variability of this disorder at multiple levels.

***Aim 2: Transcriptomic analysis of 15q13.3 microdeletion families.***

As Aim 1 identified considerable heterogeneity in both functional and morphological deficits, we were interested in pursuing transcriptomics to discover potential common mechanisms across these patients at a molecular level. While several previous studies had attempted to characterize the transcriptomic impacts of this deletion, our approach was distinct in two ways. First, the iNs used for RNA sequencing were co-cultured with mouse glia which enabled them to mature in a way more concordant with the neurons used in Aim 1 and to be extended to a later time point. This did require splitting the mouse and human

reads computationally, which was achieved successfully. Second, our analysis attempted to match our earlier phenotyping work by performing comparisons between controls and probands within patient families. This differs from most studies in the research literature which use non-familial controls and pool control and proband samples, respectively. Using this approach, we were able to identify differential gene expression patterns between 2 patient families, highlighting the inherent variability in this disorder. However, we were also able to identify common differentially expressed genes and pathways of neurodevelopmental relevance.

***Aim 3: Validation of altered signalling pathways in the 15q13.3 microdeletion disorder.***

Extending on both our own work and that of others, we were interested in investigating the role of GSK3 in the 15q13.3 microdeletion disorder. This line of investigation is built on previous work from our group and findings from Aims 1 and 2. Previous work related to the overlap between the OTUD7A gene from the 15q13.3 microdeletion, and the ankyrin-G protein localized at the axon initial segment. given the action potential abnormalities and acts on projection impairment identified in Chapter 1, we were interested in identifying whether GSK3 might be a convergent signalling pathway underlying disease pathogenesis across multiple neuropsychiatric disorders. Interestingly, we were able to demonstrate that the proband line was comparatively insensitive to the effects of GSK 3 inhibition and, unlike the control, did not manifest the expected

disruptions in action potential properties. While several previous analyses (and my own work from Aim 2) implicated Wnt signalling in this deletion, the cellular and molecular phenotyping provided in this aim highlight a novel and previously unknown abnormality in GSK3 signalling in a 15q13.3 microdeletion proband.

## **1.5 Summary**

Stated briefly, this project aims to characterize cultured neurons derived from heterozygous 15q13.3 microdeletion (15q13.3 microdeletion) patients and their familial controls. The principal interest in the clinical 15q13.3 microdeletion syndrome has been the neuropsychiatric manifestations. These include both general developmental delays, as well as more specific diseases such as autism, ADHD, and epilepsy (Lowther et al., 2015; Ziats et al., 2016). In this project, peripheral tissue samples (blood and fibroblasts) from these families were used to derive induced pluripotent stem cells (iPSCs). This results in a renewable, manipulable, and highly differentiable cell line from patients with proven clinical disease. These iPSCs are differentiated into a homogenous population of excitatory, cortical-like neurons (iN) by the forced expression of the neurogenin-2 (Ngn2) transcription factor (Yingsha Zhang et al., 2013).

For three separate 15q13.3 microdeletion families, iNs were assayed for functional and morphological differences. Of these, the two most promising families were subject to RNA sequencing to identify early transcriptomic changes underlying differential growth trajectories. Finally, based on converging lines of evidence from mouse 15q13.3 microdeletion studies, we pursued a drug-based

intervention to identify differential responses to GSK3 inhibition between a 15q13.3 microdeletion and their familial control.

## **Chapter 2: Cellular phenotyping of 15q13.3 microdeletion family neurons reveals characteristic functional and morphologic deficits**

### **2.1 Abstract**

The 15q13.3 microdeletion disorder is understood to correspond to a clinical phenotype which typically includes absence seizures, intellectual disability, and developmental delay. In addition to these, it is also a risk factor for the development of various other neuropsychiatric disorders such as autism spectrum disorder, attention-deficit hyperactivity disorder, and schizophrenia. However, little remains known about the cellular phenotypes of patients with these disorders. In this chapter, a novel cohort of 15q13.3 microdeletion families is described, which describe previously unreported structural defects of the brain. Functional and morphological studies of neurons derived from three of these patient families identified consistent deficits in action potential properties and axon projection capacity. We further profile the electrical activity of these neuron populations across time and identify heterogeneity in the clinical presentations. Collectively, these data suggest that iNs derived from 15q13.3 microdeletion patients do demonstrate heterogenous cell-autonomous findings at a structural and functional level.

## 2.2 Introduction

As mentioned in the introductory chapter of this thesis, the 15q13.3 microdeletion disorder has considerable clinical heterogeneity. Due to the embryologic impacts of the disorder, it is typical for multiple organ systems to be affected. However, even if consideration is limited to neuropsychiatric phenotypes, there remain considerable differences in the clinical presentation of these patients, the specific configuration of NDDs they will develop, and the severity of this presentation. The question of why some patients are grossly asymptomatic while others go on to develop severe disease given this same mutation remains of primary interest across this entire class of disorders. Indeed, many interesting questions might be posed of these disorders. Is a patient's disease status strongly determined by their specific genetic makeup, or is it highly path dependent? Are NDD-associated CNVs best thought of as driver or passenger mutations? At what level of abstraction is the impact of these disorders best understood?

In the literature to date, a great deal of focus has been placed on clinical characterizations of these disorders. Where work has been dedicated to more mechanistic efforts, several approaches may be taken. Animal models can often be used, particularly in the case where there is high homology in the implicated genetic factors for a disorder. The 15q13.3 microdeletion disorder is such a case, as the human 15q13.3 region is syntenic to the mouse 7qC region. This has been extended to the generation of the Df(h15q13)/+ mouse model, which is shown to recapitulate several cardinal features of the human disorder (Fejgin et al., 2014;

S. R. O. Nilsson et al., 2016). As mentioned above, animal models are typically conceptualized as carrying the advantages of highly controlled genetic backgrounds, high manipulability, ease of neural tissue access, and the potential for behavioural studies, with the typical drawback being that they are not able to faithfully recapitulate the biology of uniquely human disorders. Our group has previously published several key findings from this mouse model, identifying dendritic spine defects in cortical pyramidal neurons which could be rescued by the re-expression of key genes from the microdeletion region (Uddin et al., 2018). Human models of these disorders may also be employed in the study of CNV-associated NDDs. These models are conceptually closer to recapitulating the human-disease-relevant portion of the disorders, though they harbour several limitations. Even in disease-proven individuals, neural tissue (particularly of the brain and central nervous system) is not readily accessible for research purposes. There are two ways in which this issue is typically circumvented. The first method involves the comparatively rare situation where brain tissue may become available, for example in post-mortem cases or in a particularly unusual biopsy scenario. While these may give direct access to the tissue of interest from a patient with a proven clinical phenotype, this tissue will be non-renewable (as neurons are postmitotic), fragile, and will importantly not be matched to familial controls whose tissues are almost certainly unlikely to be available at the same time. The second method involves the reprogramming of peripheral tissues (such as fibroblasts or blood) into induced pluripotent stem cells (iPSCs). This

population of cells is renewable, derived from a patient with proven clinical disease, has multipotent differentiation capacity, and can easily and justifiably be collected from unaffected patients to serve as controls.

The optionality afforded by this approach does require additional consideration for experimental design. The operative questions here are:

(1) What is the most appropriate cell population to differentiate the patient iPSCs into for a particular set of experimental questions?

(2) What is the best available control for the patient line?

For question (1), many options now exist for the directed differentiation of iPSCs to various neural populations. These vary in their structural and cellular composition but can be loosely categorized on the (respective) axes of 2-dimensional vs. 3-dimensional cultures, and highly homogenous vs. highly heterogenous populations. For our purposes, it will suffice to point out the general reasons why one approach might be pursued over another, and the reasons for the specific approach used in this study.

As discussed above, organoids represent the most complex of these model systems, as determined by both their structural arrangements and cellular compositions. They develop into three-dimensional spheroid configurations and can be directed to represent structural and population-level arrangements intended to model various brain regions (for example cerebral, dorsal-ventral, etc). While they are slower to maturation (it is not atypical for experimental endpoints to be in excess of 6 months), they offer significant advantages where

spatiotemporal ascertainment of neuronal development is desired. In the domain of reprogramming peripheral tissues to model disease, organoids offer the strongest face validity. Apart from the technical challenges associated with the culturing and experimental endpoints, the dimensionality (both spatial and population levels) requires correspondingly complex analytic approaches to produce meaningful insights. In many instances, however, these analyses may be more revelatory of the organoid itself rather than the underlying disease process it is aiming to model.

In this thesis we opted to pursue phenotyping of Ngn2 induced neurons, which for a highly homogeneous population of cortical pyramidal-like neurons which rapidly reach functional maturity. While this approach does trade spatiotemporal and population complexity, the reductive nature and model-level homogeneity can potentially amplify otherwise subtle differences while maintaining a human neuronal aspect. Because the findings in the disorders are typically expected to be subtle at the neuronal level, we, therefore, sought to characterize these iNs on functional and morphological metrics.

With respect to question (2) above, the choice of a suitable control depends on the optimization of factors along several axes. Two of the axes along which these lines are often chosen are the desired degree of (A) genetic background control, and (B) clinically proven disease. These tend to be difficult to co-optimize. For example, the scenario that comes closest to optimizing for both is likely to resemble identical twins where only one twin acquired a mutation at the two-cell

stage while the other twin did not, and the clinical status of both could be known. Short of this vanishingly rare scenario, various trade-offs need to be made in the choice of control lines. Where genetic background control is most desired, the use of isogenic lines may be preferred. These can be difficult to generate (though made easier by the advent of CRISPR-Cas9 gene editing), and correlation to clinical disease is often unclear (whether the isogenic line was generated by repairing a patient line, or introducing a mutation to a patient line). If an isogenic control line is used to introduce mutations, this has the advantage of allowing the comparison of many mutations to a reference baseline (for an example of this approach see (Deneault et al., 2019). Particularly if the reference line and its derivatives are readily available (for example, as part of a biobank), this approach offers a scalable method by which to study a variety of genetic mutations and retain some degree of translatability to findings. (Miller et al., 2009)

There is considerable clinical heterogeneity in the 15q13.3 microdeletion disorder, both in presentation, NDD co-occurrence, and penetrance. The source of this heterogeneity remains unclear, partly because of an incomplete understanding of the pathophysiologic underpinnings of the clinical phenotypes themselves. Consequently, this aim sought to identify consistent (though likely subtle), cell-autonomous differences between induced neurons from 15q13.3 microdeletion probands and their familial controls. Rather than attempt to reproduce the composition of a functional nervous system, the Ngn2 induction model (see Figure 2.5.1 for project workflow and induction timeline) aims to

provide a variance-minimized neuronal platform to amplify disease-relevant differences. While this system trades off real-world validity, it offers the possibility of producing concrete, cell-autonomous results in a neuronal model which may be built upon to identify translatable mechanistic features and pathways. Taken together, these parameters describe both general and specific measures of neuronal maturity. To the extent that patient iNs differ from matched controls (including trends both within and between patient families), these differences will be suggestive of a core phenotype whose cumulative effect increases the proclivity of patients to develop clinical disease.

## **2.3 Methods**

*The methods presented here are generally adapted to the specific experiments carried out for the purposes of this thesis. However, there is inevitable similarity to methods presented in several papers that I co-authored during this PhD. Effort has been taken to modify them as appropriate, though similarity in phrasing necessarily remains.*

### **2.3.1 iPSC reprogramming**

All pluripotent stem cell work was approved by the Canadian Institutes of Health Research Stem Cell Oversight Committee. Blood was collected from individuals with approval from SickKids Research Ethics Board after informed consent was obtained, REB approval file 1000050639. This study was also approved by the Hamilton Integrated Research Ethics Board, under project #2707. iPSCs were generated by Sendai virus reprogramming and clonal expansion using the CytoTune – iPSC 2.0 kit (ThermoFisher) to deliver the reprogramming factors. Briefly, patient blood was collected and centrifuged in Ficoll, with the PBMC layer manually extracted. An enriching formula was used to preferentially enhance CD34+ PBMC specific survival. PBMCs from Families 1 and 2 were reprogrammed by CCRM (MaRS centre, Toronto, ON) and iPSCs from Family 3 were generated in-house. Once colonies were large enough (approximately 15–17 days post Sendai transduction), each colony was transferred to 1 well of a 12-well plate coated with irradiated MEFs and plated in iPSC media (DMEM/F12 supplemented with 10% KO serum, 1x non-essential amino acids, 1x GlutaMAX,

1 mM  $\beta$ -mercaptoethanol, and 16 ng/mL basic fibroblast growth factor (bFGF)). Once iPSCs were expanded and established, they were transferred to Matrigel-coated plates and grown in mTeSR1 (STEMCELL Technologies). ReLeSR (STEMCELL Technologies) was used for subsequent passaging. iPSC lines were validated through flow cytometry of pluripotency markers and IHC, and G-banding analysis to confirm a normal karyotype.

### **2.3.2 iPSC thawing and passaging**

iPSCs were thawed by warming in a 37 °C waterbath until a small ice pellet remains. A total of 9 mL of DMEM/F12 is added dropwise, and the cells are mixed, then spun at 200 x g for 3 minutes. Aspirate supernatant and gently re-suspend cell pellet in 3 mL of mTeSR + Y-27632 (10 $\mu$ M) + penicillin/streptomycin (1%). Care is taken to ensure that the pellet lifts in small colonies, without singularizing the cells themselves. Cells are plated at one vial per well in a 6-well flat bottom tissue culture plate, precoated with Matrigel. Replace with fresh mTeSR media without Y-27632 the day after thaw. Maintain cells by daily medium exchange.

iPSCs are passaged once they achieve ~80–85% confluency (typically 3–4 days). To passage, remove spent medium from culture and wash with DPBS. Add 1 mL/well of ReLeSR, and split 1:3 to 1:6 into a 6-well plate precoated with Matrigel.

### **2.3.3 iPSC NGN2/rtTA infection**

Singularized iPSCs were plated on Matrigel-coated 6-well plates at a density of  $2.50 \times 10^5$  cells per well, in 2 mL of mTeSR containing 10  $\mu$ M Y-27632. The following day, they were changed into 2 mL of fresh mTeSR containing 10  $\mu$ M Y-27632, 1  $\mu$ g/mL polybrene, Ngn2 and rtTA lentiviruses which had been titred to target an MOI of 1 for all transductions. The virus-containing media was replaced with fresh mTeSR at 24 hours post-infection. The cells were allowed to recover to approximately 70–80% confluency before being passaged into 6-well Matrigel-coated plates. At their next 70–80% confluency, cells were either frozen (in media containing 50% knockout serum, 40% mTeSR, and 10% DMSO) or singularized for induction into iN. All infected iPSCS were used within 5 passages of infection to maintain induction efficiency.

### **2.3.4 iN induction protocol**

At day -1 of induction, singularized Ngn2/rtTA infected iPSCs were plated at a density of  $5.0 \times 10^5$  cells per well onto Matrigel-coated 6 well plates, in 2 mL of mTeSR containing 10  $\mu$ M Y-27632. At day 0 of induction, cells were changed into fresh mTeSR containing 1  $\mu$ g/mL of doxycycline hyclate. On days 1 and 2 of induction, cells received fresh iNPC media (DMEM/F12 containing 1% N-2 supplement, 1% Penicillin/Streptomycin, 1% NEAA, 1% Sodium Pyruvate and 1% GlutaMAX) containing 1  $\mu$ g/mL of doxycycline hyclate and 1–2  $\mu$ g/mL puromycin. On day 3, cells were changed into fresh iNI media (Neurobasal with SM1 supplement, 1% Penicillin/Streptomycin, and 1% GlutaMAX) containing BDNF

(10 ng/ $\mu$ L; Peprotech), GDNF (10 ng/ $\mu$ L; Peprotech), and laminin (1 $\mu$ g/mL). On day 4, cells were replated onto polyornithine/laminin-coated 12 mm coverslips, or polyethylenimine coated 48-well multi-electrode array plates. On day 5, mouse glia were added to the wells. All wells received half media changes every other day with iNI media containing with BDNF, GDNF and laminin (with 2.5% FBS added after day 10) for the duration of the experiment. iNs used for RNA/protein extraction were maintained in their induction wells until day 7 with no glia, and received a fresh media change on day 5.

### **2.3.5 NGN2 iN RT-qPCR**

iPSC-derived NGN2 iNs were plated without glia on 12-well plates at a density of  $5 \times 10^5$  cells per well. Total RNA was extracted at DIV day 7 using a commercial kit (Norgen, Cat. #17200), and 1  $\mu$ g of RNA was used for cDNA synthesis using the qScript cDNA synthesis kit according to manufacturer instructions (Quanta Biosciences). Primers were designed using the Universal Probe Library (UPL) Profinder software for human (Roche, version 2.53, see table) or using previously published sequences and adjusted to be intron-spanning. Quantitative PCR was performed using SYBR Green super mix (FroggoBio) and the QuantStudio 3 thermocycler (Applied Biosystems). Data were analyzed using the Thermo Cloud™ to generate relative expressions normalized to the housekeeper EIF3L.

### 2.3.6 Multi-Electrode Arrays

The 48-well Cytoview MEA plates (Axion Biosystems, M768-tMEA-48B) were coated with 0.1% Polyethylenimine (PEI) 24 hours prior to plating. Primary mouse cortical cultures were dissected at E16 and plated onto PEI-coated 48-well Cytoview MEA plates at a density of  $3 \times 10^4$  cells/well in plating media containing Neurobasal medium, 10% fetal bovine serum, 1% penicillin/streptomycin, and 2 mM GIBCO Glutamax supplement. After 1.5 hr, media was changed to serum-free feeding media containing Neurobasal medium, 2% B27 supplement, 1% penicillin/streptomycin, and 2 mM L-glutamine. Half of the culture media was replaced every 2 days.

For human iNs, 40,000 cells were plated on each well of 48-well MEA plates on day 4 post-induction, and allowed to attach for 1.5 hours in a 37-degree Celsius incubator. On day 5 post-induction, 20,000 CD1 mouse glia were added to each well. The plates received half media changes every other day (iNI+BDNF+GDNF+laminin, with 2.5% FBS added after day 10 post-induction).

MEA recordings were taken approximately twice per week using the Axion Maestro Pro.

To record extracellular spontaneous activity, MEA plates were placed in the MaestroPro MEA system (Axion Biosystems) at 37 °C for 5 minutes to acclimate, followed by a 10-minute recording period. Spike data were analyzed with the AxIS Navigator software (Axion Biosystems) at a sampling rate of 12.5 kHz with a 4 kHz Kaiser Window low pass filter and a 200 Hz IIR High Pass filter. Analyzed

data were exported to CSV files and statistical analysis was performed in GraphPad Prism 6 software. Wells that had zero active electrodes throughout the duration of the experiment were excluded for statistical analysis. Raster plots were generated with the Neural Metric Tool (Axion Biosystems).

### **2.3.7 Electrophysiology**

On day 4 post-induction, iNs were added to 24-well plates (Corning) at 100,000 cells/well on polyornithine/laminin-coated 12 mm coverslips, in iNI media containing BDNF, GDNF and laminin (as above). On day 5 post-induction, 50,000 previously cultured CD1 mouse glia were plated onto these coverslips. The cells were maintained until for 4 weeks post-induction, receiving half media changes every other day. At day 10, 2.5% FBS was added to the media and maintained for the duration of the experiment.

Whole-cell recordings (Olympus BX51 WI) were performed at room temperature using an Axoclamp 700B Amplifier (Molecular Devices). Trace recordings were managed using Clampex 10.7 and analyzed in Clampfit 10.7. Borosilicate glass pipettes (WPI; 1B150F-4) were used to prepare patch electrodes (P-97 or P1000; Sutter Instruments) and used for recordings with an intracellular solution containing (in mM): 123 K-gluconate, 10 KCl, 10 HEPES, 1 EGTA, 2 MgCl<sub>2</sub>, 0.1 CaCl<sub>2</sub>, 1 MgATP, 0.2 Na<sub>4</sub>GTP (pH 7.2 by KOH), with or without 0.06% (m/v) sulpharhodamine B to aid in visual identification of neuron morphology post-recording. Standard HEPES aCSF was used for all recordings, containing (in mM): 140 NaCl, 2.5 KCl, 1.25 NaH<sub>2</sub>PO<sub>4</sub>, 1 MgCl<sub>2</sub>, 10 glucose, 2CaCl<sub>2</sub> (pH 7.4 by

NaOH). Recordings were sampled at 10–20kHz and low pass filtered at 1 kHz. The membrane potential was clamped at -70mV adjusted for a junction potential of -10mV, and action potentials were elicited with step currents of 10 pA (beginning at -40pA). Recordings were excluded if the series resistance exceeded 25 M $\Omega$ .

For mouse recordings, whole-cell recordings (BX51WI; Olympus) from cultured DIV12-16 mouse cortical neurons were generated using an Axoclamp 700B Amplifier (Molecular Devices) with borosilicate electrodes (P-97 puller; Sutter Instruments) containing a cesium-based intracellular solution (in mM): 125 CsCl; 5 NaCl; 1 MgCl<sub>2</sub>; 10 HEPES; 10 EGTA; 3 MgATP; and 0.3 NaGTP (pH 7.2). Cells were bathed in HEPES aCSF for the duration of recording. The composition of the aCSF was (in mM): 140 NaCl; 5 KCl; 2 MgCl<sub>2</sub> (anhydrous); 2 CaCl<sub>2</sub>; 10 HEPES; 10 glucose (pH 7.4). A total of 1  $\mu$ M TTX and 100  $\mu$ M picrotoxin were added to the bathing medium to block Na-dependent action potentials and GABA currents, respectively. Recordings were performed at -65 mV using Clampex 10.7 (Molecular Devices), corrected for a calculated -5 mV junction potential and analyzed using the Template Search function from Clampfit 10.7 (Molecular Devices).

### **2.3.8 Morphologic analysis**

For axonal morphology analyses on transfected human iNs, morphometric analyses were performed on randomly sampled transfected neurons. Images of neurons were acquired using the Zeiss-880 confocal with AIRYSCAN at 20x

magnification with 0.6 zoom. Imaging conditions such as laser gain, pinhole, and stack increments were kept constant between images. Images were processed using NIH image software (ImageJ) as a maximum projection of a single or tiled image. All images were processed under the same brightness and contrast conditions. Individual VENUS positive neurons were identified, and SMI-312 positive axons were traced from the base of the soma along the entire projection using the NeuronJ extension. A branch point was defined as a process that extended orthogonal along the axon that exceeded 20  $\mu\text{m}$  in length (Dent and Kalil, 2001).

Confocal images of immunostained iNs were obtained with a Nikon C2+ confocal microscope. To analyze ankyrin-G intensities in the axons, we took confocal images using the 60x oil-immersion objective (NA = 1.40) as z-series of 8 images (2 x 2 stitched; 392.57  $\mu\text{m}$  x 392.57  $\mu\text{m}$ ), taken at 0.4  $\mu\text{m}$  intervals, with 1895  $\times$  1895 pixel resolution. Detector gain and offset were adjusted in the channel of cell fill (Venus) to enhance edge detection. Intensity plot profiles for ankyrin-G in the axon were measured by ImageJ with a single plane which was shown as the strongest signal in the AIS. Every 5  $\mu\text{m}$  of ankyrin-G intensity was measured and averaged across neurons to produce average intensity plot profiles  $\pm$  SEM.

Confocal images were taken using the 20x objective (NA = 0.75) as z-series of 8–11 images (2 x 2 stitched; 1185.43  $\mu\text{m}$  x 1185.43  $\mu\text{m}$ ), taken at 0.4  $\mu\text{m}$  intervals, with 1895  $\times$  1895 pixel resolution. MAP2 stained images were obtained, and traces of dendrites were drawn and analyzed with Sholl analysis by ImageJ.

### **2.3.9 Culturing neurons from E16-17 mouse cortices**

Cortical neuron cultures were prepared as previously described<sup>27</sup> from C57BL/6 E16-17 embryonic mice with Df(h15q13)/+ fathers and WT mothers. Cells were plated in 24-well plates at a density of  $1.75 \times 10^5$  cells per well onto 12 mm coverslips coated with poly-D-lysine and laminin in plating media (Neurobasal media + 10% fetal bovine serum + penicillin/streptomycin, L-glutamine). After 1.5 hr, media was changed to culturing media (NB + B27 + penicillin/streptomycin, L-glutamine). Culturing media were rotated every 3–4 days for the duration of the experiment.

### **2.3.10 Genotyping E16-17 mice**

Tail segments of mice were collected at the time of culturing, and stored at -30 °C if they could not be used immediately. DNA was extracted and PCR amplified from these samples using the Extract-N-Amp XNAT2 kit (Sigma). Primers for the Df(h15q13) deletion and wildtype regions were provided by Taconic (the company that created the mouse). The primers for the Df(h15q13) deletion (302 bp product) are 5'-TCACAGAGAATGTAAGTAGCAGAGG-3' (Forward) and 5'-GAAGTCTGACATCGAAATTGTCC-3' (Reverse). For the wildtype region (271 bp product), the primers are 5'-GCTTTCTGGCTTTCATCTCC-3' (Forward) and 5'-GAAGTCTGACATCGAAATTGTCC-3' (Reverse). PCR products were visualized on a 2% Agarose gel stained using RedSafe dye. Genotypes were interpreted by another graduate student in the lab to maintain blinding to the genotype group during experiments and analysis.



## **2.4 Results**

### **2.4.1 A novel cohort of 15q13.3 microdeletion patient families reveals previously unreported clinical and structural findings**

Pertinent clinical characteristics from six 15q13.3 microdeletion families are reported in this study (Table 2.5.1). For five of the families (Families 2–6), complete or condensed clinical notes were provided regarding the patients' treatments and investigations. Family one was reported in the MSSNG database, and only had limited psychometric testing available. With the exception of Family 5 (and Family 1, for which clinical information was unavailable), all the probands in this cohort had absence seizure epilepsy disorders, in line with the reported core finding of this disorder. Of additional note, with the exception of Family 1, all probands had varying degrees of intellectual impairment as determined by IQ testing. Additionally, clinical notes from Family 2 and 3 do confirm learning difficulties.

Family 2 has several features of interest. The proband in this family has an absence seizure phenotype, but interestingly the mother (the carrier from whom the proband is believed to have inherited the deletion) does not. Indeed, while the mother is reported to have a learning disorder she has no other neuropsychiatric phenotypes. The family history reveals that this proband has two paternal aunts with seizure disorders. While the etiology of the neuropsychiatric phenotype in this patient cannot be ascertained ambiguously, there is clinical evidence to suggest possible contribution from both the maternal side (by way of inheritance

of the 15q13.3 microdeletion), and the paternal side through the possible inheritance of a proclivity to seizure disorder. While the subtype of seizure in the paternal aunts is not known, this family offers potential insight into the interacting factors which differentiate carriers of the 15q13.3 microdeletion from clinically affected probands.

Interestingly, probands from Families 4 and 5 had thickened a thickened corpus callosum detected on MRI. This is a highly unusual finding in the 15q13.3 microdeletion disorder, which may present in some cases with the opposite finding of corpus callosum agenesis (Whitney et al., 2021). However, this finding did lead us to investigate axon projection in these neurons as a possible source of abnormal projection fibre formation underlying corpus callosum abnormalities in these patients.

We pursued reprogramming of three patient lines in this study due to time constraints, but plan to expand this profiling to our entire patient cohort.

#### **2.4.2 15q13.3 microdeletion patient iNs show altered population-level spiking activity**

Longitudinal recordings of iNs from all three patient families revealed significant differences in spiking activity in proband iNs in Family 1 and 2, though at different timepoints. For both patients in these families, WMFR was decreased at later timepoints (Figure 2.5.3 panels A and E). Interestingly, network burst frequency was also decreased at later timepoints in both families, though it was increased in Family 1 previous to DIV 53 and delayed in its increase for Family 2 (Figure 2.5.3

C and G). For Family 2 both the proband and carrier showed decreased network burst frequency at later timepoints, though the carrier did not show a difference in WMFR. Within Family 2, both the proband and carrier showed an increase network burst duration which increased gradually throughout the experiment, though the carrier showed a more pronounced increase than the proband (2.5.3G). Family 3 showed minor changes throughout the recording window but had no pronounced phenotype which was comparable to the other families (Figure 3.5.3 pane I-K).

### **2.4.3 Action potential properties are altered in three 15q13.3 microdeletion families without changes in sEPSCs**

Across the three families characterized in this study, we detected subtle differences in action potential properties recorded between DIV26-28. The probands from Family 2 and Family 3 required increased amounts of injected currents to fire the first action potential (Figure 2.5.4E and 2.5.4I). The proband from Family 3 additionally demonstrates an increased action potential threshold (Figure 2.5.4F). While the proband from Family 1 did not show any significant differences in intrinsic electrophysiologic parameters, there was a trend towards decreased action potential amplitude (Figure 2.5.4G) and increased membrane resistance (Figure 2.5.4J). There was a varied response to action potential train firing in response to injected current (Figure 2.5.4M-O), with the asymptomatic 15q13.3 microdeletion carrier from Family 2 (86S) showing the most pronounced decrease. While there was a detected effect in Family 3 as well, there were

ultimately minimal differences in action potential train firing capacity between probands and controls. Notably, the least appreciable difference in action potential among these families was Family 1, for which the clinical phenotype is unknown but the full-scale IQ is in the normal range at 101. At a cell-autonomous level, this finding could point towards compensation at the neuronal level as reflected in our system.

Proband iNs from all three families did not show differences in either frequency or amplitude of sEPSCs (Figure 2.5.5). There were no differences identified in any other intrinsic membrane properties of these neurons (Figure 2.5.9).

#### **2.4.4 Dendritic complexity variation in 15q13.3 microdeletion families and controls**

Sholl analysis of all three patient families is shown in Figure 2.5.7. Only the proband in Family 1 had decreased arborization demonstrated. Note also that Family 2 had appreciably lower peak arborization. Family 3 is shown but statistics are not performed as there were only 2 biological replicates present.

#### **2.4.5 Miniature excitatory postsynaptic current frequency is increased in Df(h15q13)/+ cortical pyramidal neurons compared to wildtype littermates**

Recordings of miniature excitatory postsynaptic currents (mEPSCs) from cortical pyramidal neurons of the Df(h15q13)/+ mouse, and found that mEPSC frequency was increased compared to wildtype littermates. Our group did previously report a finding of unchanged mEPSCs in Df(h15q13)/+ mouse brain slices (Uddin et al., 2018). The finding of increase mEPSC frequency in 2-dimensional culture

from embryonic day 16–17 cortices of these mice is particularly interesting given the previous finding of decreased dendritic spine density in the same mouse model (Uddin et al., 2018).

#### **2.4.6 Impaired axon projection is a consistent feature in 15q13.3**

##### **microdeletion patient iNs**

Axon outgrowth was quantified by tracing transfected neurons expressing the Venus construct. Within each family, probands had consistently decreased axon length compared to the familial controls. Axon quantification was performed at DIV10 due to the rapid outgrowth of axons in the early period which would otherwise limit quantification due to the convolution of the processes and difficulty of imaging secondary to microscope field of view limitations. One additional interesting feature of note is the appreciable variation in axon length between families, potentially underscoring intrinsic differences in the capacity of these lines to reach maturity dependent on their genetic background. As in the case of the electrometry findings reported in this chapter, this variation in the achieved axon length by an identical time point does underscore the benefit of our approach to stratify by patient family rather than pooling probands and controls.

## 2.5 Figures and Tables

Figure 2.5.1: visual abstract and workflow schematic

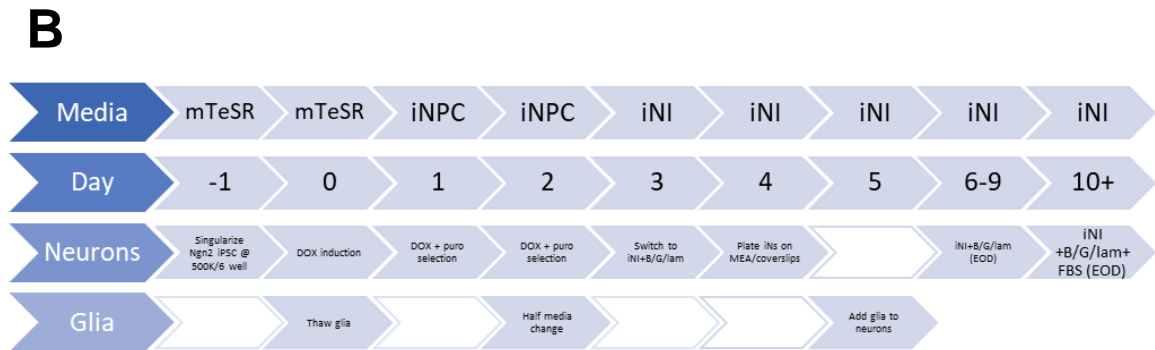
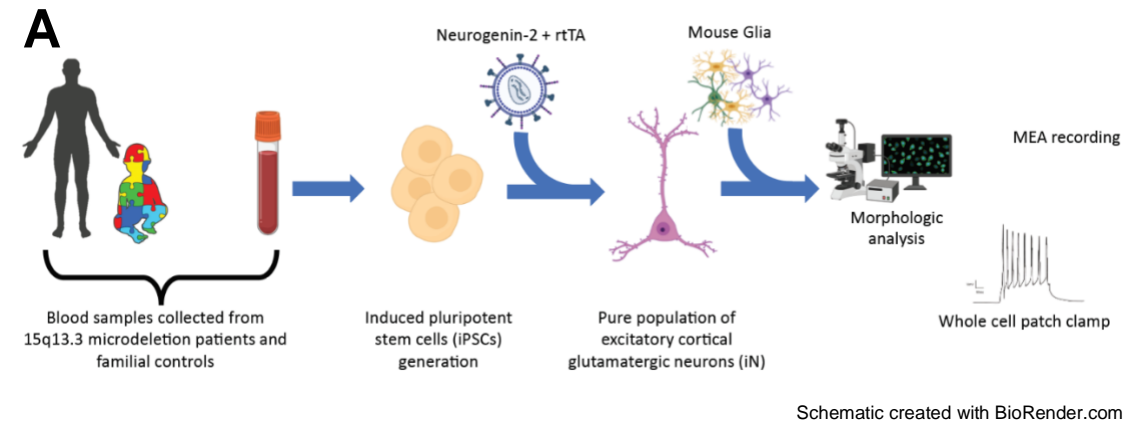


Figure 2.5.1: visual abstract and workflow schematic

(A) project workflow demonstrating sample collection, reprogramming to iPSCs, induction of iNs, and subsequent analyses (created with BioRender.com)

(B) iN induction timeline showing inducible constructs (above) and timeline/media below

**Table 2.5.1: Index of patient families**

	LINE ID	SEX	PROBAND RELATION	CNV status	NEUROPSYCHIATRIC PROFILE	OTHER PERTINENT CLINICAL DATA	STATUS
Family 1	89E	F	MOTHER	-	-	-	CONTROL
	90N	F	-	15q13.2-q13.3del	ASD*	IQ = 101*	PROBAND
Family 2	86S	F	MOTHER	15q13.2-q13.3del			CARRIER
	88T	M	BROTHER	-			CONTROL
	87V	F	-	15q13.2-q13.3del	Absence epilepsy	IQ range = 54–65, height/weight 97 <sup>th</sup> percentile for age; two paternal aunts with seizure disorders	PROBAND
	0205-002	M	FATHER	-			CONTROL
Family 3	0205-003	F	-	15q13.2-q13.3del	Learning difficulties, ASD, ADHD, severe absence epilepsy		PROBAND
	1004-001	F	MOTHER	-	-	-	CONTROL
Family 4	1004-002	M	FATHER	15q13.2-q13.3del	Healthy	Healthy	CARRIER
	1004-003	F	-	15q13.2-q13.3del	ID (moderate), single absence seizure episode	IQ = 71, thickened corpus callosum, craniofacial abnormalities, born at 28 weeks gestation due to PROM	PROBAND
	1005-001	F	MOTHER	-	-	-	CONTROL
Family 5	1005-002	M	FATHER	15q13.1-q13.3del	Language delay	Congenital strabismus	CARRIER
	1005-003	F	-	15q13.1-q13.3del	Severe language delay, GDD, motor delay	IQ = 56, thickened corpus callosum	PROBAND
Family 6	1212-001	F	MOTHER	-	-	-	CONTROL
	1212-002	M	FATHER	15q13.2-q13.3del	Learning difficulties, unspecified psychiatric problems, myoclonic absence seizures		AFFECTED
	1212-003	F	-	15q13.2-q13.3del	Learning difficulties, myoclonic absence seizures	IQ = 63, MRI shows arachnoid cyst of the posterior fossa and left hippocampal malrotation	PROBAND

ID = intellectual disability, GDD = global developmental delay, ASD = autism spectrum disorder, ADHD = attention-deficit hyperactivity disorder, PROM = premature rupture of membranes

\*Limited clinical notes available

**Figure 2.5.2: Pedigree and breakpoint alignment map for the three patient families profiled in this study**

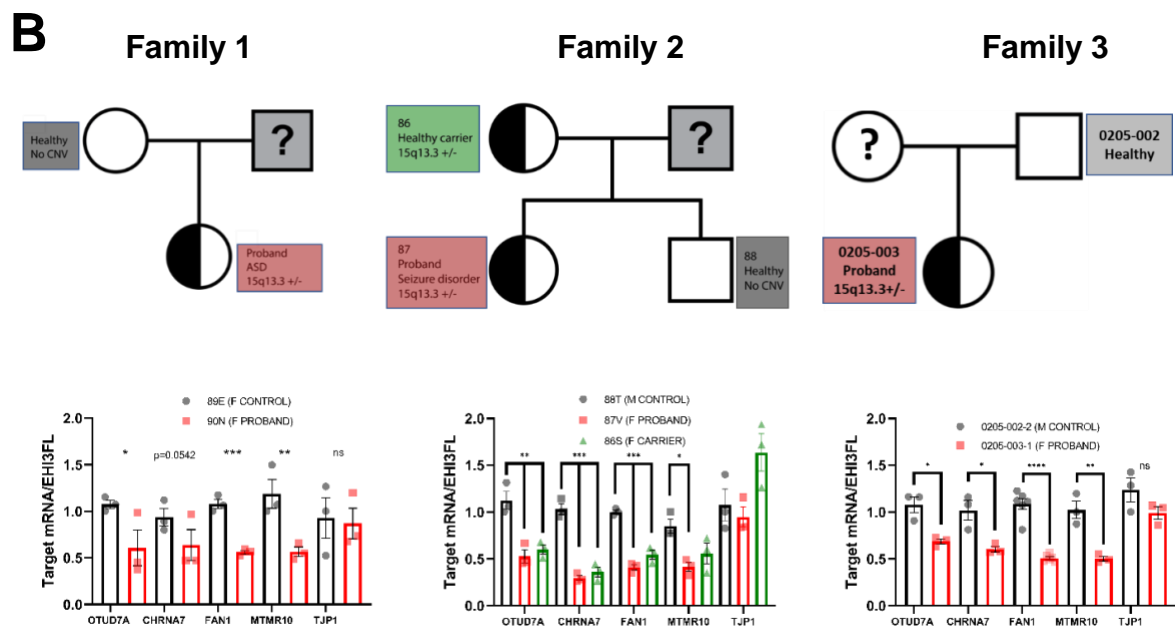
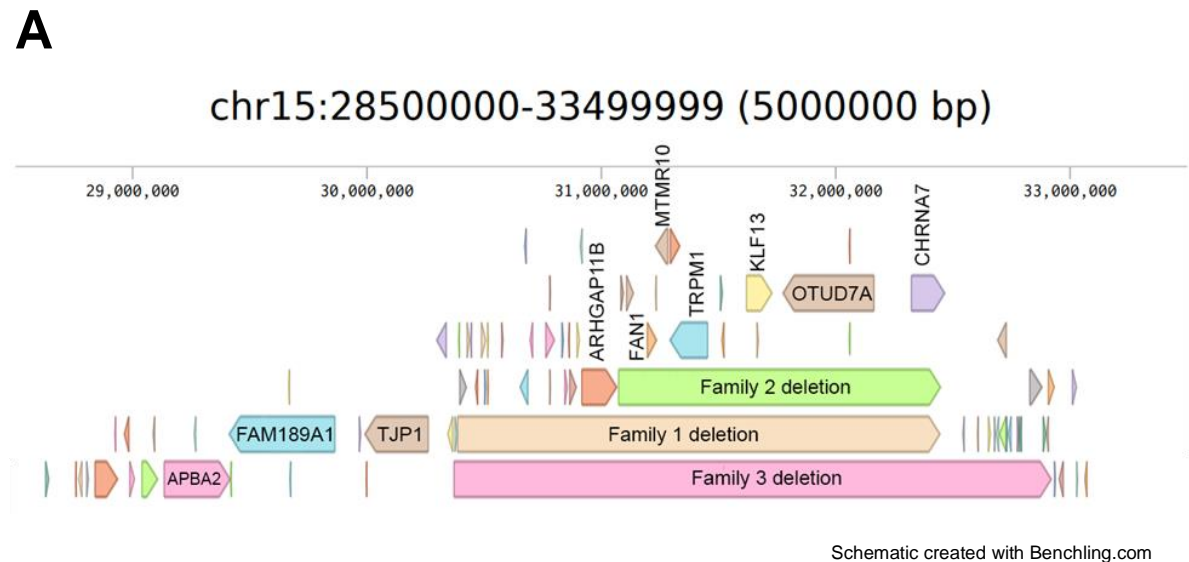


**Figure 2.5.2: Pedigree and breakpoint alignment map for the three patient families profiled in this study**

- (A) The breakpoint alignment map for the three families investigated is characterized in this chapter, adapted from the alignment map generated in Benchling. Breakpoints were determined through clinical microarrays reported alongside the patient clinical vignette provided by the care team, and the base pair positions are given as follows: Family 1 (30386399–32444273), Family 2 (31073735–32446830), and Family 3 (30386398–32914240). Note also that despite the significant variation in deletion size listed above, these all fit the descriptor of 15q13.2-13.3 microdeletions. Schematic created with Benchling.com (Benchling, 2023).
- (B) Pedigrees of the three families characterized in this chapter with associated RT-PCR validation of deleted genes. Validations were performed on DIV7 iNs, and mRNA expression of target (OTUD7A, CHRNA7, MTMR10, FAN1) and flanking (TJP1) genes were normalized to EIF3L levels. For Families 1 and 3, levels for each gene were compared by unpaired two-tailed t-test, with significance levels \* $p < 0.05$ , \*\* $p < 0.01$ , \*\*\* $p < 0.001$ , \*\*\*\* $p < 0.0001$ . Family 2 gene levels were compared by one-way ANOVA, OTUD7A  $F(2, 6) = 19.30$   $P = 0.0024$ , CHRNA7  $F(2, 6) = 74.63$ ,  $P < 0.0001$ , FAN1  $F(2, 6) = 82.81$   $P < 0.0001$ , MTMR10  $F(2, 6) = 7.564$   $P = 0.0229$ , TJP1  $F(2, 6) = 5.089$   $P = 0.0510$  with Dunnett's posthoc test.  $N = 3$  biological replicates per gene were used.

Breakpoint map adapted from schematic in Benchling ([www.benchling.com](http://www.benchling.com))

Figure 2.5.3: Population-level spiking differences vary by 15q13.3

microdeletion families

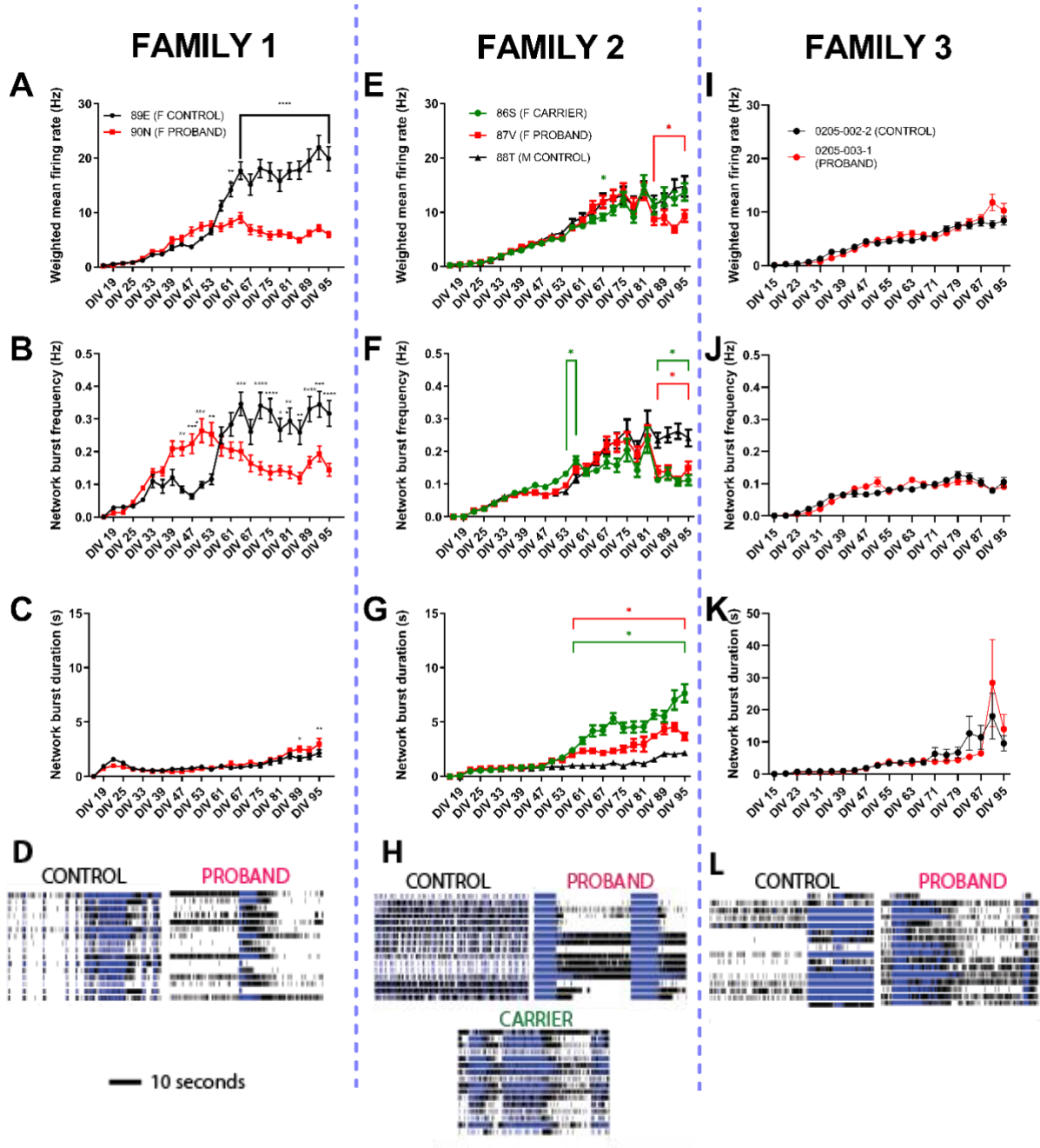


**Figure 2.5.3: Population-level spiking differences vary by 15q13.3del families**

Multi-electrode array recordings for three 15q13.3 microdeletion families, showing weighted mean firing rate (WMFR; panels A, E, I), network burst frequency (panels B, F, J), and network burst duration (panels C, G, K), and representative raster plots taken from DIV 87 (D, H, L). All data were analyzed by repeated measures two-way ANOVA with Dunnett's post hoc test, with \* $p < 0.05$ , \*\* $p < 0.01$ , \*\*\* $p < 0.001$ , \*\*\*\* $p < 0.0001$ .

Family 1: (A) WMFR (Interaction,  $F(23, 1329) = 19.13$   $P < 0.0001$ ; Timepoint,  $F(23, 1329) = 43.82$   $P < 0.0001$ ; Genotype,  $F(1, 1329) = 255.8$   $P < 0.0001$ ), (B) Network Burst Frequency (Interaction,  $F(23, 1386) = 11.20$   $P < 0.0001$ ; Timepoint,  $F(23, 1386) = 20.30$   $P < 0.0001$ ; Genotype,  $F(1, 1386) = 25.00$   $P < 0.0001$ ), (C) Network Burst Duration (Interaction,  $F(23, 1386) = 1.928$   $P = 0.0053$ ; Timepoint,  $F(23, 1386) = 26.14$   $P < 0.0001$ ; Genotype,  $F(1, 1386) = 2.334$   $P = 0.1268$ ).

Family 2: (E) WMFR (Interaction,  $F(46, 3017) = 1.901$   $P = 0.0003$ ; Timepoint,  $F(23, 3017) = 83.65$   $P < 0.0001$ ; Genotype,  $F(2, 3017) = 5.644$   $P = 0.0036$ ), (F) Network Burst Frequency (Interaction,  $F(46, 3017) = 4.111$   $P < 0.0001$ ; Timepoint,  $F(23, 3017) = 66.56$   $P < 0.0001$ ; Genotype,  $F(2, 3017) = 19.30$   $P < 0.0001$ ), (G) Network Burst Duration (Interaction,  $F(46, 3005) = 12.29$   $P < 0.0001$ ; Timepoint,  $F(23, 3005) = 74.37$   $P < 0.0001$ ; Genotype,  $F(2, 3005) = 251.1$   $P < 0.0001$ ).

Family 3: (I) WMFR (Interaction,  $F(20, 1680) = 2.827$   $P < 0.0001$ ; Timepoint,  $F(3.212, 269.8) = 78.03$   $P < 0.0001$ ; Genotype,  $F(1, 84) = 0.4475$   $P = 0.5053$ ), (J) Network Burst Frequency (Interaction,  $F(20, 1680) = 2.047$   $P = 0.0041$ ; Timepoint,  $F(7.443, 625.2) = 49.21$   $P < 0.0001$ ; Genotype,  $F(1, 84) = 0.02359$   $P = 0.8783$ ), (K) Network Burst Duration (Interaction,  $F(20, 1680) = 2.982$   $P < 0.0001$ ; Timepoint,  $F(3.975, 333.9) = 52.98$   $P < 0.0001$ ; Genotype,  $F(1, 84) = 1.326$   $P = 0.2528$ ).

Figure 2.5.4: Differences in action potential characteristics in 15q13.3

microdeletion iNs

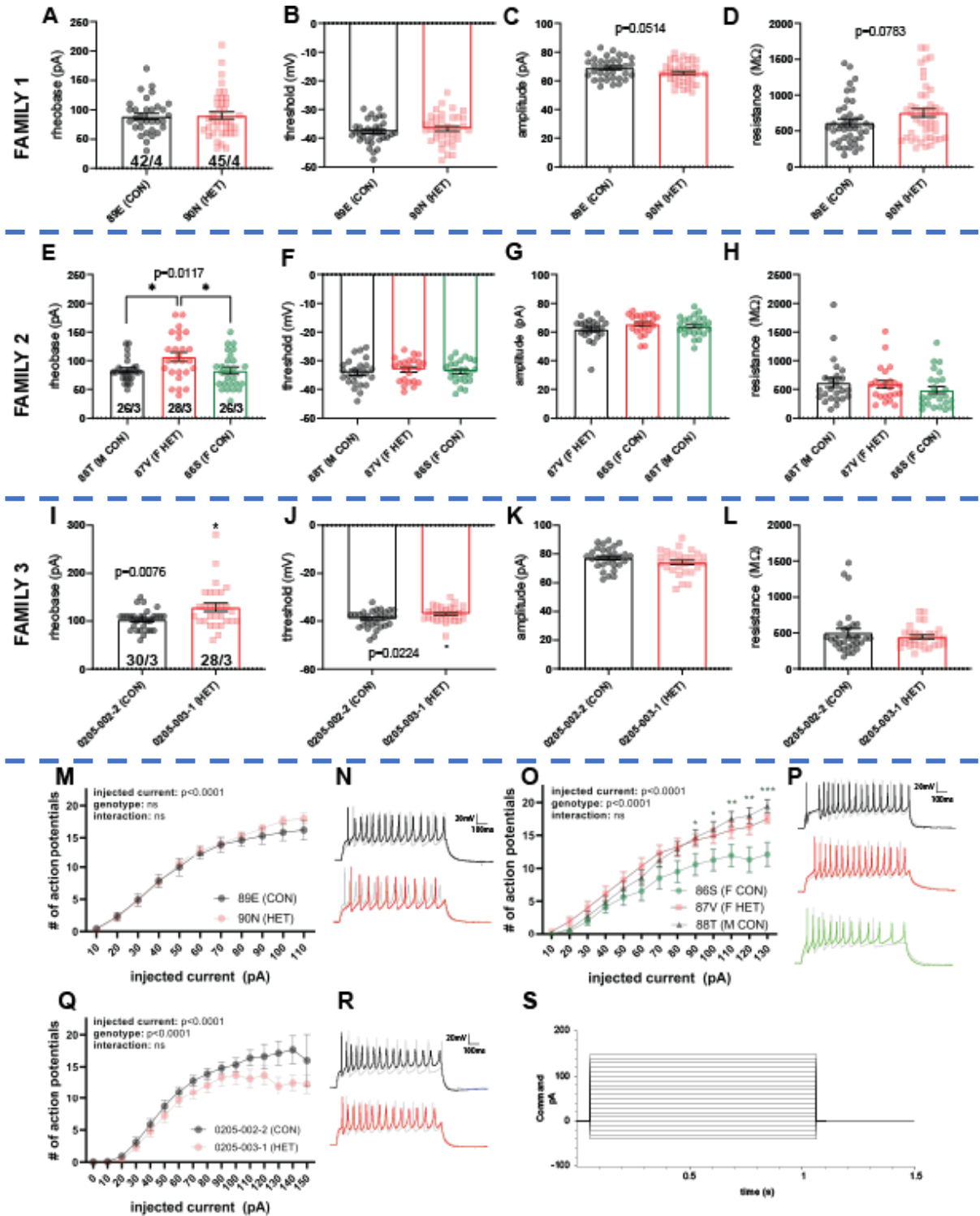


### Figure 2.5.4: Differences in action potential characteristics in 15q13.3

#### microdeletion iNs

Selected intrinsic electrophysiologic properties of the three 15q13.3 microdeletion families are reported, including *rheobase* (A, E, I), *AP threshold* (B, F, J), *AP amplitude* (C, G, K), and *membrane resistance* (D, H, L). For Families 1 and 3, these metrics were analyzed by unpaired two-tailed t-test or Mann–Whitney test, with significance levels \* $p < 0.05$ , \*\* $p < 0.01$ , \*\*\* $p < 0.001$ , \*\*\*\* $p < 0.0001$ . Family 2 metrics were analyzed by one-way ANOVA (Rheobase  $F(2, 73) = 4.730$   $P = 0.0117$ ; Threshold  $F(2, 68) = 0.3923$   $P = 0.6770$ ; Amplitude  $F(2, 68) = 1.482$   $P = 0.2345$ ; Membrane resistance  $F(2, 68) = 0.8926$   $P = 0.4144$ ) with Dunnett's post hoc test. Biological/technical replicates are indicated on the rheobase graphs.

*Intrinsic excitability* is reported in figures M, O and Q, with associated representative traces at N, P, and R (respectively) shown for 60 pA (gray) and 110 pA (colour). (S) trace showing step command levels for the current injection. Analysis by mixed-effect model or two-way ANOVA with Tukey's post hoc test. Significance levels indicated on graphs correspond to \* $p < 0.05$ , \*\* $p < 0.01$ , \*\*\* $p < 0.001$ , \*\*\*\* $p < 0.0001$ . N=biological replicates, n=technical replicates. (M) 89E (N=3, n=22), 90N (N=3; n=25); Injected current,  $F(1.374, 111.2) = 433.7$   $P < 0.0001$ ; Condition,  $F(3, 139) = 0.5424$   $P = 0.6541$ ; Interaction,  $F(42, 1133) = 0.2940$   $P > 0.9999$  (O) 86S (N=3, n=26), 87V (N=3, n=28), 88T (N=3, n=26) Injected current,  $F(2.394, 119.1) = 211.0$   $P < 0.0001$ ; Condition,  $F(2, 69) =$

5.094  $P=0.0086$ ; Interaction,  $F(24, 597) = 2.047$   $P=0.0025$ ); (Q) 0205-002-2 (N=3, n=29), 0205-003-1 (N=3, n=29); Injected current,  $F(15, 603) = 0.7090$   $P=0.7766$ ; Condition,  $F(15, 603) = 78.61$   $P<0.0001$ ; Interaction,  $F(1, 603) = 21.41$   $P<0.0001$ ).

**Figure 2.5.5: Spontaneous synaptic transmission in 15q13.3 microdeletion**

iNs

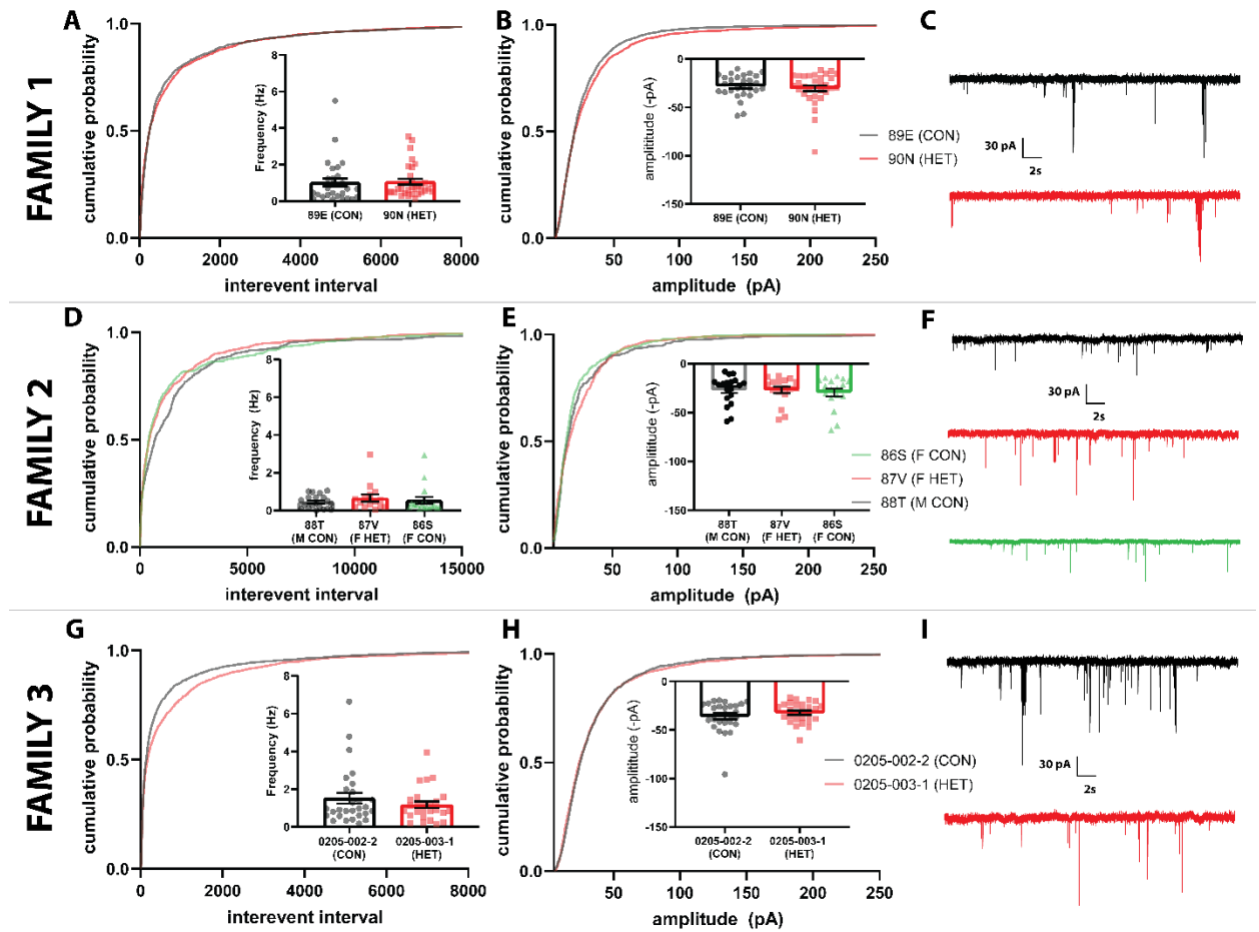


**Figure 2.5.5: Spontaneous synaptic transmission in 15q13.3 microdeletion****iNs**

No changes were detected in spontaneous excitatory postsynaptic current (sEPSC) frequency (A, D, and G) or amplitude (B, E, and H) for three 15q13.3 microdeletion families. Frequency histograms of current properties are shown in the respective panel. Associated representative traces are also shown (C, F, I). For Families 1 and 3, these metrics were analyzed by unpaired two-tailed t-test or Mann–Whitney test. Family 2 metrics were analyzed by one-way ANOVA (Frequency  $F(2, 49) = 0.5076$   $P=0.6051$ ; Amplitude  $F(2, 50) = 0.1960$   $P=0.8226$ ) with Dunnett's posthoc test. Family 1 (89E CON (N=4, n=28), 90N HET (N=4, n=31)); Family 2 (86S CARRIER (N=3, n=17), 87V HET (N=3, n=17)), 88T CON (N=3, n=19); Family 3 (0205-002-2 CON (N=3, n=28), 0205-003-1 HET (N=3, n=26)). Significance levels shown correspond to \* $p<0.05$ , \*\* $p<0.01$ , \*\*\* $p<0.001$ , \*\*\*\* $p<0.0001$ .

Figure 2.5.6: Axon projection capacity in 15q13.3 microdeletion iNs

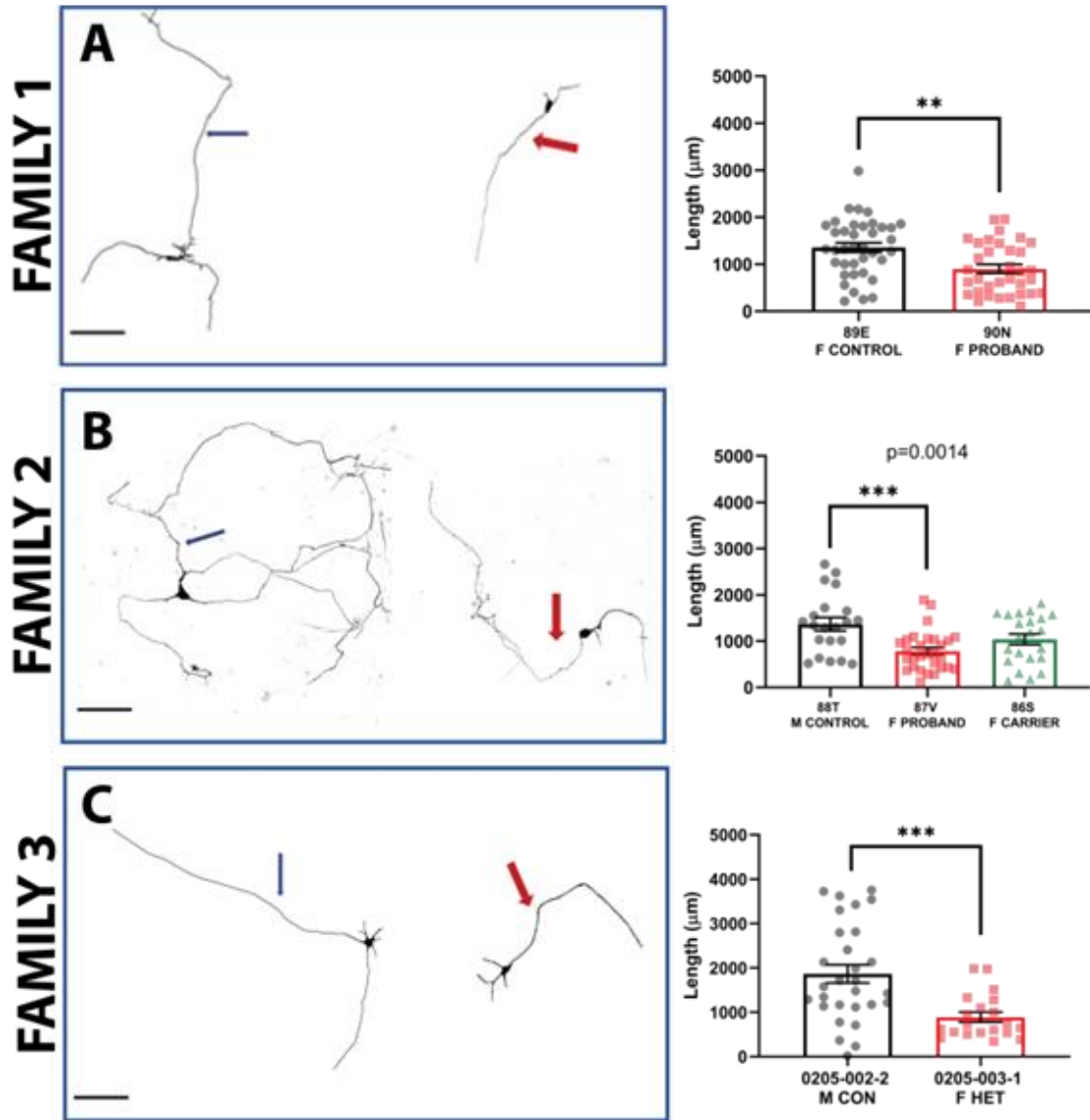


**Figure 2.5.6: Axon projection capacity in 15q13.3 microdeletion iNs**

DIV10 iNs from three 15q13.3 microdeletion families show a consistent decrease in axon projection capacity in probands comparative familial controls.

Representative traces are shown on the left side of the respective panel. Note that no difference was detected for the carrier in Family 2 (Panel B, right). For Families 1 and 3, axon length differences were analyzed by unpaired two-tailed t-test. Family 2 metrics were analyzed by one-way ANOVA (Axon Length F (2, 69) = 7.230 P=0.0014) with Tukey's posthoc test. Family 1 (89E CON (N=4, n=38), 90N HET (N=4, n=34)); Family 2 (86S CARRIER (N=3, n=22), 87V HET (N=3, n=29), 88T CON (N=3, n=21); Family 3 (0205-002-2 CON (N=3, n=29), 0205-003-1 HET (N=3, n=21)). Significance levels shown correspond to \*p<0.05, \*\*p<0.01, \*\*\*p<0.001, \*\*\*\*p<0.0001. Axon indicated by arrows, with blue arrow pointing to control iN and red arrow to proband iN. Scale bar 100µm.

**Figure 2.5.7: Sholl analysis of three 15q13.3 microdeletion families**

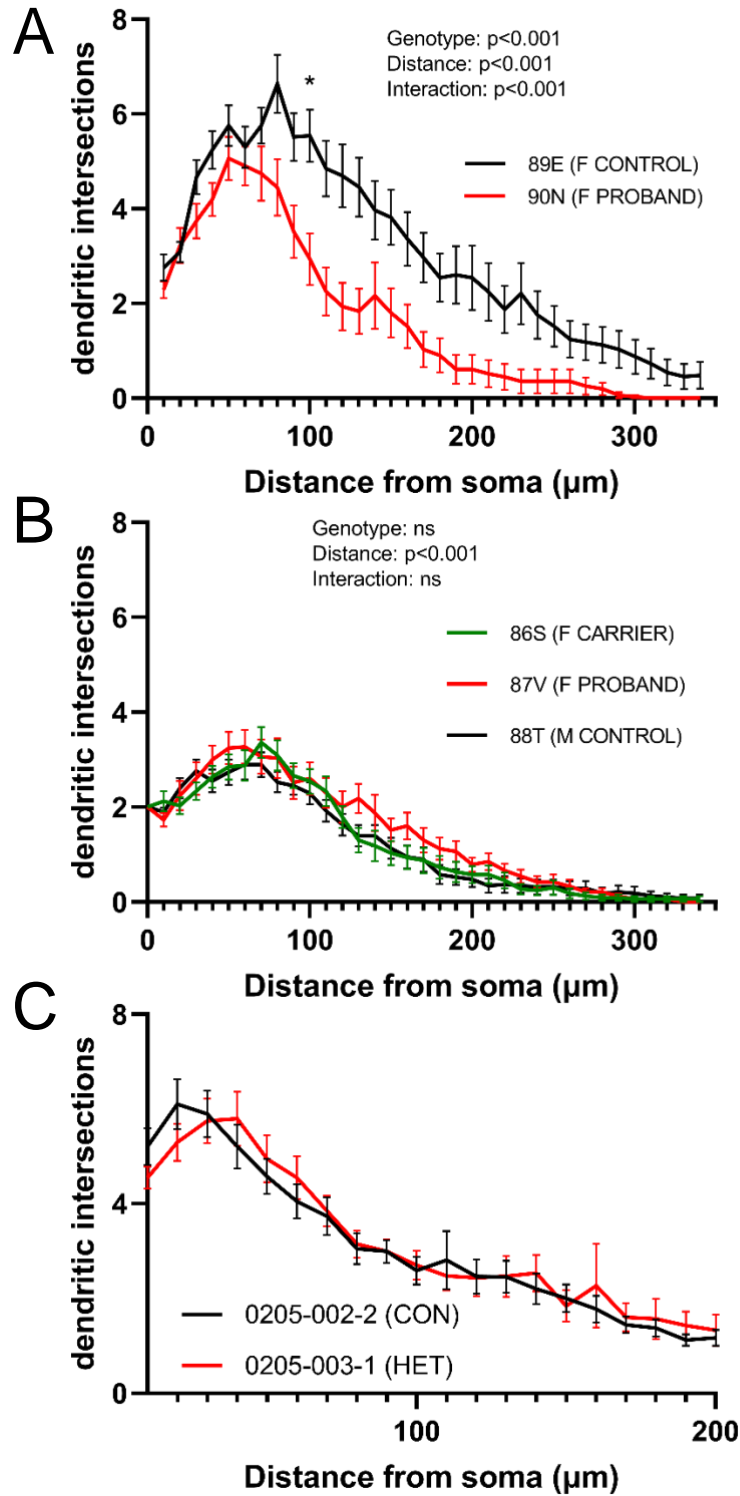


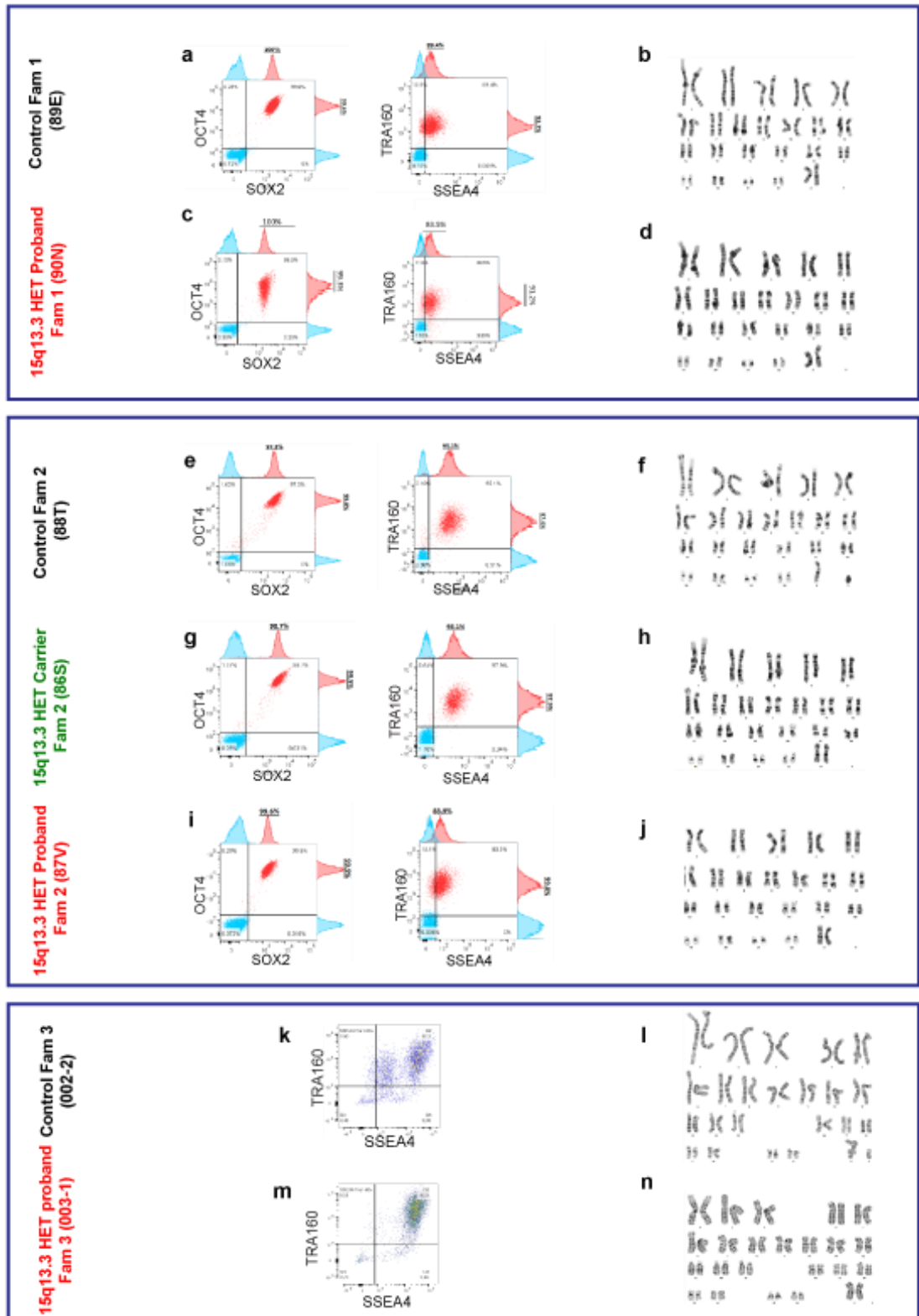
**Figure 2.5.7: Sholl analysis of three 15q13.3 microdeletion families**

Sholl analysis of DIV 28 iNs from three patient families (Families 1, 2 and 3 are shown in panels A, B, and C respectively). Number of dendritic intersections (y-axis) are plotted against the distance they occur from the cell soma (x-axis).

Two-Way Repeated Measures ANOVA: Family 1 N=3 infections, 89E n=34, 90N n=34 (Interaction  $F(33,2046) = 2.290$   $P < 0.001$ ; Distance  $F(5.299, 328.5) = 48.30$   $P < 0.001$ ; Genotype  $F(1,62) = 13.25$   $P < 0.001$ ); Family 2, N=3 infection, 86S n=35, 87V n=35, 88T n=35 (Interaction  $F(68,3434) = 0.8120$   $P = 0.866$ ; Distance  $F(6.274, 633.6) = 48.30$   $P < 0.001$ ; Genotype  $F(2,101) = 1.620$   $P = 0.203$ ). Plots are Mean  $\pm$  SEM.

Significance levels \* $p < 0.05$ . No statistics were performed on Family 3. N=2 infections, 0205-002-2 n=19, 0205-003-1 n=20. Plot is Mean  $\pm$  SD.

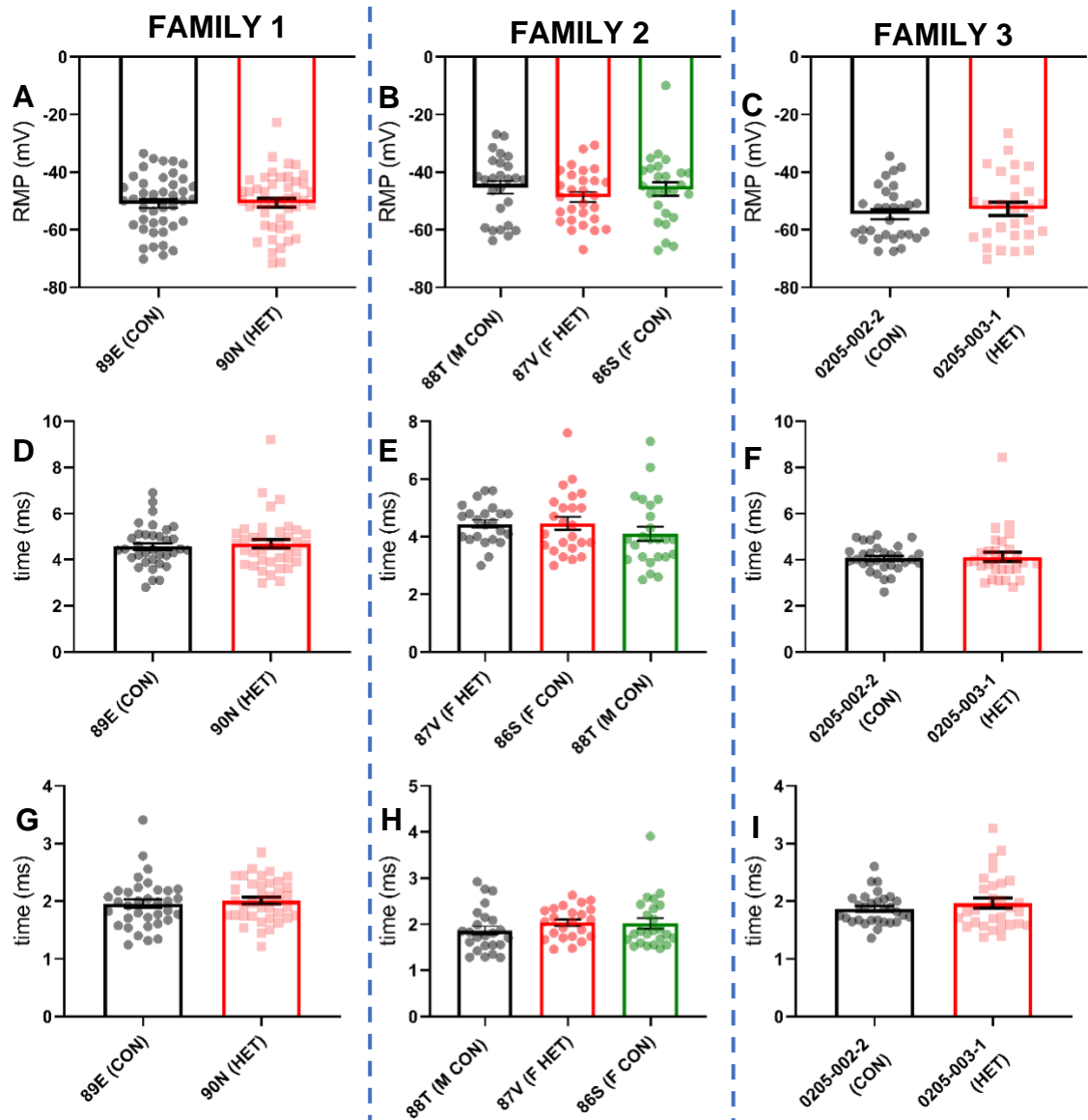
Figure 2.5.8: Validation of iPSCs used in this study



**Supplementary Figure 2.5.1: validation of iPSCs used in this study**

Validation of pluripotency markers and karyotyping of reprogrammed lines used in this study. For all three families flow cytometry was used to confirm the presence of the pluripotency markers TRA160 and SSEA4 (panels K and M, and the right side of panels A, C, E, G, I). Families 1 and 2 were reprogrammed by CCRM, and also include flow cytometry confirmation of OCT4 and SOX2 (panels A, C, E, G, I, left). Representative karyotypes from G-banding analysis are presented in panels B, D, F, H, J, L, and N. Only included for subsequent use if they demonstrated the pluripotency markers and had a normal karyotype.

Figure 2.5.9: Extended electrophysiologic parameters



**2.5.9: Extended electrophysiologic parameters**

Selected intrinsic electrophysiologic properties of the three 15q13.3 microdeletion families are reported, including rheobase (A, E, I), AP threshold (B, F, J), AP amplitude (C, G, K), and membrane resistance (D, H, L). For families 1 and 3, these metrics were analyzed by unpaired two-tailed t-test or Mann–Whitney test. Family 2 metrics were analyzed by one-way ANOVA (RMP  $F(2, 77) = 0.7219$   $P=0.4891$ ; Action Potential Width  $F(2, 68) = 0.9540$   $P=0.3903$ ; Action Potential Half-Width  $F(2, 68) = 0.9596$   $P=0.3882$ ). Biological/technical replicates for all conditions Family 1 89E CONTROL (N=4, n=42), 90N PROBAND (N=4, n=45); Family 2 86S CARRIER (N=3, n=26), 87V PROBAND (N=3, n=28), 88T CONTROL (N=3, n=26); Family 3 0205-002-2 CONTROL (N=3, n=30), 0205-003-1 PROBAND (N=3, n=28).

Figure 2.5.10: Extended MEA parameters

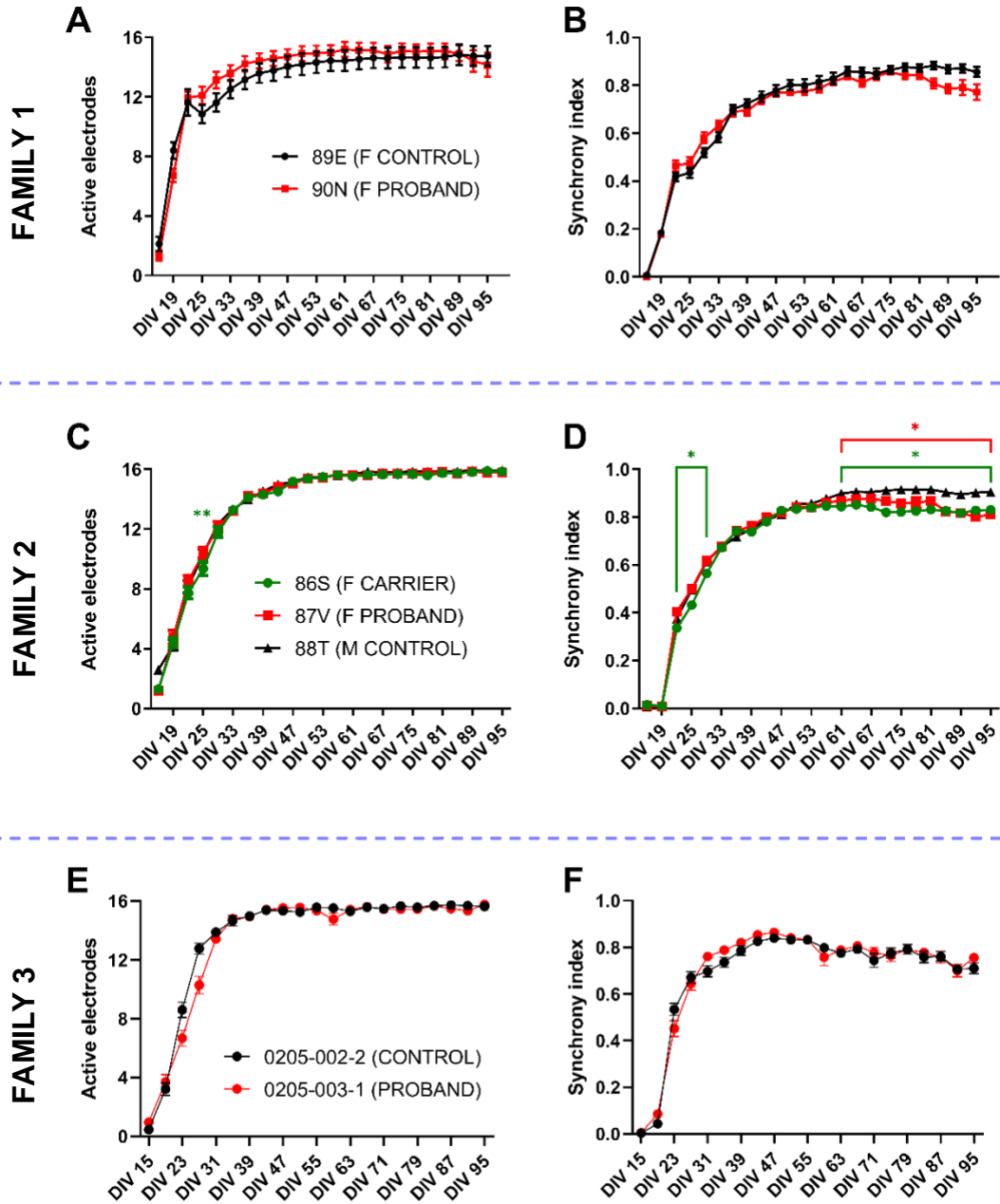


**Figure 2.5.10: Extended MEA parameters**

Extended multi-electrode array metrics for three 15q13.3 microdeletion families, showing active electrodes (panels A, C, E), and synchrony index (panels B, D, F). Family 2 had a subtle decrease in active electrodes in the carrier (86S) line at DIV 25, and a brief decrease in synchrony between DIV 21 and 29. There was thereafter a persistent decrease in synchrony in the proband (87V) and carrier (86S) lines from Family 2 from DIV 61 onwards. No other changes were detected across the other families and lines. All data were analyzed by repeated measures two-way ANOVA with Dunnett's post hoc test, with \* $p < 0.05$ , \*\* $p < 0.01$ .

Family 1: (A) Active electrodes (Interaction,  $F(23, 1424) = 0.6091$   $P = 0.9257$ ; Timepoint,  $F(23, 1424) = 31.91$   $P < 0.0001$ ; Genotype,  $F(1, 1424) = 5.039$   $P = 0.0249$ ), (B) Synchrony Index (Interaction,  $F(23, 1356) = 1.959$   $P = 0.0044$ ; Timepoint,  $F(23, 1356) = 201.9$   $P < 0.0001$ ; Genotype,  $F(1, 1356) = 10.19$   $P = 0.0014$ ). Family 2: (C) Active Electrodes (Interaction,  $F(46, 3017) = 1.113$   $P = 0.2793$ ; Timepoint,  $F(23, 3017) = 983.6$   $P < 0.0001$ ; Genotype,  $F(2, 3017) = 6.455$   $P = 0.0016$ ), (D) Synchrony Index (Interaction,  $F(46, 3017) = 3.431$   $P < 0.0001$ ; Timepoint,  $F(23, 3017) = 1183$   $P < 0.0001$ ; Genotype,  $F(2, 3017) = 65.02$   $P < 0.0001$ ). Family 3: (E) Active Electrodes (Interaction,  $F(20, 1680) = 4.508$   $P < 0.0001$ ; Timepoint,  $F(5.108, 429.1) = 619.1$   $P < 0.0001$ ; Genotype,  $F(1, 84) = 1.863$   $P = 0.1759$ ), (F) Synchrony Index (Interaction,  $F(20, 1680) = 1.735$   $P = 0.0227$ ; Timepoint,  $F(6.472, 543.6) = 339.7$   $P < 0.0001$ ; Genotype,  $F(1, 84) = 0.4943$   $P = 0.4839$ )

Figure 2.5.11: Df(h15q13)+ mouse cortical pyramidal neuron mEPSCs

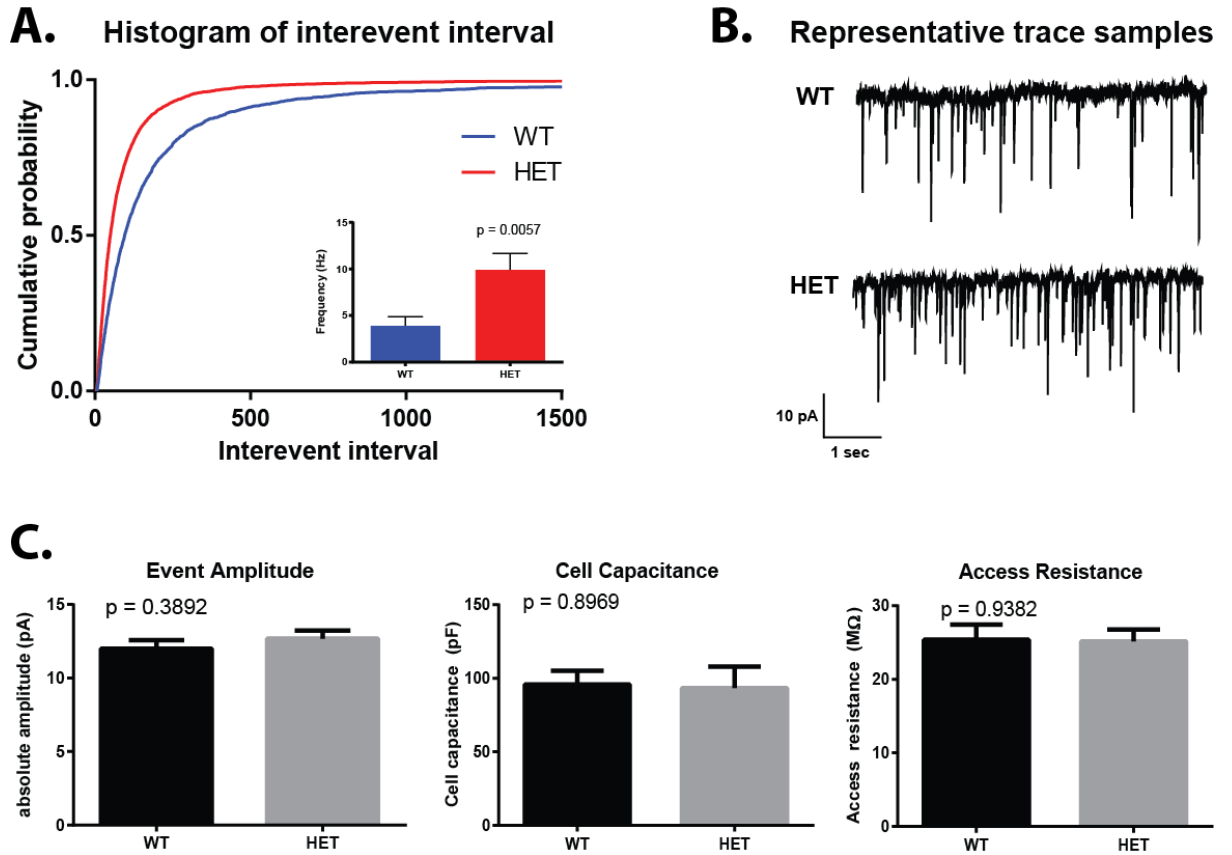


**Figure 2.5.11: Df(h15q13)/+ mouse cortical pyramidal neuron mEPSCs**

Cultured cortical pyramidal neurons from E16-17 mice show increased miniature excitatory postsynaptic current (mEPSCs) frequency in Df(h15q13)/+ HET animals compared to their wildtype (WT) littermates. (A) There is an increased frequency of mEPSC events in HET Df(h15q13) neurons compared to WT. (B) Sample traces showing representative segments of recordings. (C) No differences were observed between groups in the amplitude of recorded events, cell capacitance, or the resistance of the system. WT (N=3, n=18); HET (N=3, n=18). All samples analyzed by unpaired t-test, with significance levels indicated as \* $p < 0.05$ , \*\* $p < 0.01$ , \*\*\* $p < 0.001$ , and \*\*\*\* $p < 0.0001$ .

## 2.6 Discussion

In this chapter I have described a new index of 15q13.3 microdeletion patients and familial control with samples presently banked by our group. These patients demonstrated many of the cardinal features of the 15q13.3 microdeletion disorder, though there were abnormal corpus callosum findings on MRI in two patients which lead us to pursue axon projection experiments. We characterized functional and morphological properties of three patient families, using familial controls and stratifying analysis by family. We did identify novel functional properties of patient iNs from three families, which revealed heterogeneity between families by MEA recording, and subtle disturbances to action potential properties across families. We further identified decreased dendritic arborization in the Family 1 proband, and axon projection deficits in all three families which represents the most consistent finding. Cellular characterization did not appear to correlate clearly with clinical severity of this disorder, possibly secondary to the multi-layered heterogeneity in these patients. This study extends upon the research literature in both CNV-associated NDDs generally, and the 15q13.3 microdeletion specifically, by providing a series of phenotyping case studies of 15q13.3 microdeletion families. While this highlighted several findings of interest, there was significant variability between families which was not readily explained or correlated to clinical presentation.

### **2.6.1 A previously unreported index of 15q13.3 microdeletion families reveals novel characteristics potentially linked to disease**

In this study, we have reported a novel cohort of 15q13.3 microdeletion families collected both locally and through collaborators. There are several notable features of these probands and their associated family members. One feature of note is that all of the probands in the study are female. Based on the published research literature, there does not appear to be a sex-based preference for the development of this disorder. While the reported number of families is comparatively small, the consistency in the sex of the proband is potentially interesting for several reasons. It is also noteworthy that in the majority of at least half of the probands in our cohort (Families 4–6), the 15q13.3 microdeletion appears to have been inherited from their father. Indeed, the only confirmed maternal inheritance is in the proband from Family 2. This is a considerable deviation from the published inheritance patterns in the research literature, though it is not anticipated to have had any significant impact on this study as the present phenotyping has focused on Families 1–3. Furthermore, this region is not known to be imprinted and to date, there is no definitive evidence that a specific parent of origin is related to important differences in disease pathogenesis. From an experimental standpoint, having the probands be the same sex between different families provides an improved basis for the comparison of specific cellular and molecular findings. It is also noteworthy that in general females are comparatively protected against the development of various neuropsychiatric

conditions. This is best identified in the case of autism spectrum disorder, where the ratio of male to female cases is roughly 3:1 (Loomes et al., 2017). While the potential reasons for this are numerous, one of the prominent explanations is the difference in the presentation of these disorders between males and females. In the case of the 15q13.3 microdeletion, the fact of an objective genetic marker partially circumvents this difficulty by allowing the assembly of similar cohorts, and the study of important differences between them at the clinical, functional, and morphological levels.

There are several additional features of interest in the patient cohort assembled in the study. While the timeframe under which the work included in this thesis did not permit the reprogramming and phenotyping of the samples, the patients from Families 4 and 5 (see Table 2.5.1) both had a thickened corpus callosum. These findings had previously been reported in the research literature as associated with this disorder. However, this finding did call into question possible axon projection defects and was an important determinant of pursuing the axon projection experiments in this thesis. Indeed, even in families where this was not reported as an MRI finding (possibly because MRIs are not the standard of care for these patients in Canada, and the ones for which we have the finding are reported in Europe), we were able to demonstrate what is likely the most durable, finding across probands, compared to familial controls in the study, which is the axon projection deficits. This demonstrates the utility of the Neurogenin-2 system to extend findings from clinical reports of these complex patients into concrete

findings at the cellular level. Notably, one patient had an arachnoid cyst which is a known finding in 15q13.3 microdeletion patients (Whitney et al., 2021). As expected, the patients had significant intellectual impairments, with the exception of the proband from Family 1. The probands from four out of six Families (Families 2, 3, 4, and 6) had significant absence seizures, in line with the published clinical phenotype for this disorder. Interestingly, clinical phenotype did not appear to closely correspond with functional or morphological characterizations. For example, the patient with the most pronounced seizure disorder (0205-003) had grossly unremarkable cellular findings. Note also that the microdeletion size did not clearly correspond to clinical severity in our patient cohort. While the microarray did provide deletion coordinates, the overall breakpoint regions were the same in the assayed families. While larger CNVs are expected to have a greater impact on phenotype, this has not been studied in great detail to date. It is plausible that larger CNVs might have consequences related to genomic architecture and which are not trivially anticipated from sequence alone. While certain models have been proposed to link CNV size with neuropsychological parameters (Huguet et al., 2018), in the absence of a clear theory of disease pathogenesis for specific disorders, the exact impact of this is difficult to ascertain.

### **2.6.2 Using iNs to generate novel functional and morphological insights into the 15q13.3 microdeletion disorder**

The 15q13.3 microdeletion encompasses a clinical spectrum for which few mechanistic features have been elucidated to date. However, these mechanistic features can often be suggestive of underlying defects at the cellular level. For example, there is a characteristic absence seizure phenotype in this disorder, though the etiology is not evident from the clinical investigations alone. However, as highlighted in Figure 1.3.1, one of the preeminent models for understanding the causative features of neurodevelopmental disorders involves the imbalance of excitatory and inhibitory signals in the central nervous system. While this paradigm is not fully capable of encompassing the complexities of these disorders, it does provide a useful framework for mechanistic investigation. As the dominant excitatory cell type in the neocortex—and the most populous—pyramidal glutamatergic neurons are a natural cell type to investigate for intrinsic deficits which may underlie an excitation/inhibition imbalance.

Note that while the population firing characteristics as determined by MEA (Figure 2.5.3) were most exaggerated for family one, this was not reflected in action potential properties (Figure 2.5.4). This might be for several reasons. While attempts were made to choose cells for electrophysiological recordings in an unbiased manner, it is necessarily the case that this is a more sensitive modality and will have a bias towards cells which tolerate the invasiveness of the recording procedure. While this does have the benefit of isolating for cells of a

known set of characteristics, it does introduce selection bias which would not be reflected in MEA recordings of entire populations. It is also the case that the patch clamp recordings were taken at an earlier time point when the MEA recordings remain grossly unrevealing. This could potentially underlie important changes in population characteristics which would not be adequately captured by the early timepoint electrophysiology.

### **2.6.3 Insights from cellular phenotyping of 15q13.3 microdeletion families**

In the case of patch clamp electrophysiology, many of the recorded parameters are close in value to one another. While it is possible that this reflects a true lack of change between the control and 15q13.3Het, another consideration is that because the Ngn2 protocol produces a highly uniform population of iNs, (especially compared to other methods of neuron generation, see (36)), it is expected that the range of possible variation for these parameters will be limited, especially in early timepoints. Some studies have pursued later phenotyping of Ngn2 neurons (Meijer et al., 2019; Rhee et al., 2019), and given the timeline of findings in the MEA experiments we are intending to pursue this as well.

The differences we have found, where they exist, are not “snapshots” of neuronal properties. Rather, they are often subtle changes that emerge through the range of some variable. For example, though no single distance from the soma shows a difference in dendritic intersections, the aggregate finding is that there are fewer intersections overall. This is likewise true for the intrinsic excitability, which is not different at any one current injection, but rather through all of the steps used.

While the MEA findings are more pronounced, they are largely later onset. One possibility suggested by this is that these cells are functioning in a mostly normal manner, but can have an impaired ability to adapt to stressors, both pathologic and in the normal course of development. We will be probing this adaptability by investigating the ability of synaptic architecture to “scale” (plasticity) in 15q13.3 microdeletion lines.

#### **2.6.4 Limitations and future directions**

While the work in this chapter outlines novel functional and morphological characteristics of neurons derived from a cohort of 15q13.3 microdeletion families, there are several potential shortcomings of the model system and experimental design utilized.

With respect to the principal model system, the neurogenin-2 induction system has several limitations. The main limitation is related to the composition of the population of neurons generated by this method. While these are cortical pyramidal-like excitatory glutamatergic neurons as verified by their functional and morphological characteristics, these neurons take a highly artificial developmental trajectory towards maturation. As a consequence, the model will be unable to capture many potentially salient features of neurodevelopment. For example, while these neurons start out in the iPSC stage, after induction they have an extremely shortened “neural progenitor cell” phase. This limits the capacity of the system to assess dysfunctions in neurogenesis, and the potential impacts of the microdeletion in this window. Particularly for NDDs where this

period may be an especially sensitive period, this potentially represents a significant shortcoming of the system in addressing certain classes of questions. Another drawback of the approach used is the characterization of one iPSC clone per line. While this did allow for the analysis of additional families, it is certainly the case that this has the potential to skew the results if a non-representative clone is used. While we took precautions with iPSC quality control (Figure 2.5.8), there remains the possibility of clone-specific abnormalities which iPSCs are known to occasionally exhibit. Future work will improve on this by incorporating multiple clones per line in phenotyping and analysis.

## **Chapter 3: Co-culture transcriptomic analysis of early iNs from two 15q13.3 microdeletion families reveal disease-relevant pathways**

### **3.1 Abstract**

In this chapter, iNs from two 15q13.3 microdeletion probands and familial controls were assayed by RNA sequencing. We aimed to extend findings from Chapter 1 to identify new disease-relevant insights into the transcriptomic profile of these patients using a co-culture system using human iNs and CD1 mouse glia with computational splitting of reads. This system significantly improves the health and extends the viability of these cultures, allowing analysis of a pure population of patient-derived neurons at a more functionally and morphologically mature date than has been previously assayed in the literature. We conducted DEG analysis, PCA, and identified enriched pathways differentiating proband from controls. We also identified pathways driving opposing transcriptional responses between families, potentially underlying clinical heterogeneity. We find that there is significant variation between the two families with respect to differentially expressed genes and altered pathways, including those with implications for neurodevelopment. This work extends on previous transcriptomic analyses and offers a later timepoint analysis

### 3.2 Introduction

Despite its well-bounded breakpoints, implicated genes, and known association to NDDs, the 15q13.3 microdeletion disorder is clinically heterogeneous, and little remains known about the underlying mechanisms. In Chapter 2, we used the highly homogeneous Ngn2 system to characterize 15q13.3 microdeletion patient-derived neurons on functional and morphological metrics aiming to identify possible commonalities at these levels and found consistent changes in axon projection defects with a high degree of variability among other morphological and functional properties. However, the clinical and genetic background heterogeneity present in these samples continued to preclude a clear mapping to the cellular phenotyping. We were therefore interested in identifying molecular correlates of disease states, particularly those with developmental implications. To pursue this, we prioritized Families 1 and 3 for RNA sequencing based on a combination a combination of functional and clinical phenotype severity. RNA sequencing is a high throughput, comparatively inexpensive modality to assess transcriptional changes and identify potentially altered genes and pathways underlying disease. Several previous attempts have been made to provide transcriptomic insights into 15q13.3 microdeletion patients. A recently published analysis of DIV 6 neurogenin-2 neurons derived from 15q13.3 patient lines which were not plated with glia (Zhang et al., 2021). While this study revealed that there were no significant differences in methylation or chromatin accessibility, suggesting that loss of genes was directly responsible for the

phenotype (Zhang et al., 2021), the early timepoint (DIV 6) and lack of glial support are impediments to the development of neuronal structures in these cells, which decreases the likelihood of transcriptional discovery for disease-relevant pathways. Another recent study by Körner et al. attempted to bridge transcriptomic changes between 15q13.3 microdeletion patients and Df(h15q13)/+ mice, finding that there was enrichment of GO terms related to nervous system development and DNA binding in patient samples (Korner et al., 2022). This study was limited by the use of unrelated control samples and the analysis of patient blood for the comparison to mouse cortical tissue.

We sought to improve on this previous work by performing RNAseq on a modified version of the co-culture model from Chapter 2 and extracted RNA at DIV14 for transcriptomic analysis. The choice of timepoint leverages the fact that at DIV14, iNs are comparatively immature, showing early electrophysiologic function and active growth of neuronal structures (Meijer et al., 2019). As a result, this timepoint strikes a balance between the development of neuronal features and the early developmental period which might underlie later aberrant growth trajectories. This timepoint is also between the detected axon projection defects (DIV10), and the remainder of the functional and morphological assays (DIV28). To minimize the impact of mouse transcriptomic contamination, human iNs are CD1 mouse glia were co-plated at the minimal ratio (10:1, respectively) which would allow extended viability. Mouse and human reads were separated using

the *bbsplit* tool (Bushnell, 2018) and aligned to both the mouse and human reference transcriptomes.

In addition to the continuity this affords for the comparison of this transcriptomic and functional/morphological data, this approach has several advantages over previous work. The use of supportive glia allows the extension of these cultures to later timepoints and facilitates neuronal maturation. Other methods for the generation and analysis of human neurons (e.g., EB, organoid) have longer maturation timelines, as well as more complex populations from which the disambiguation of specific cell-type-specific samples can be technically challenging. In contrast to these models, the use of supplementary mouse glia provides a platform that is readily available, sourced from widely used animals with controlled genetic backgrounds, and is considerably less expensive. With respect to transcriptomic analysis, while a more complex all-human platform (such as the EB or organoid methods, or in a rarer example co-plating with human glia) might require single-cell RNA sequencing to disentangle the cellular subtypes, species-specific transcript variation allows for effective separation of mouse and human reads with the species additionally acting a proxy for the desired cell type. Additionally, iNs in the co-culture system reach maturity sooner, allowing more rapid iteration and manipulability of the model. For a discussion of selecting appropriate models and controls, please see Section 2.2 above.

In this chapter, we aimed to leverage the advantages of a human-iN/mouse-glia platform to analyze neuronal transcriptomic differences which might underlie

functional and morphological deficits in our patient cohort and the 15q13.3 microdeletion more generally. We identified significant inter-familial variability in differentially expressed genes and altered pathways, potentially offering further insight into the heterogeneity of this disorder in early development.

### **3.3 Methods**

*The methods presented here are generally adapted to the specific experiments carried out for the purposes of this thesis. However, there is inevitable similarity to methods presented in several papers that I co-authored during this PhD. Effort has been taken to modify them as appropriate, though similarity in phrasing necessarily remains.*

#### **3.3.1 iN induction and plating**

iN plating was performed as described in Section 2.3.3, with the following changes:

iNs were plated directly onto polyornithine/laminin directly 12 well culture plates at a density of  $1 \times 10^6$  cells per well. CD1 mouse glia were added at a concentration of  $1.0 \times 10^5$  glia per well. Co-cultures were collected at DIV14 for subsequent processing.

#### **3.3.2 RNA sequencing and analysis**

RNA extraction was performed using the Norgen Plus RNA Extraction Kit (Cat. 48300). Library preparation was performed using the NEB Ultra II Directional mRNA library prep kit, and paired-end sequencing (2 x 150 bp) was performed on 1 lane of a Novaseq S1 flowcell. Separation of fasta files into separate mouse and human reads was conducted using the bbsplit tools (Bushnell, 2018), with the reference mapping assembly constructed against the most up to date GRCm39 and GRCh38 reference genomes as of October 2021. Ambiguous

reads (<0.1%) were discarded. Reads were aligned to the GRCh38 reference transcriptome v104 using Salmon, and further analysis was performed using the DESeq2 workflow in R as previously described (Huber et al., 2015; Love et al., 2015; Love et al., 2014). Hallmark gene sets were obtained from the MSigDB (Broad Institute, STATE) and enrichments were determined using FKPM-transformed read counts from each subject using GSEA version 4.2.1.(Subramanian et al., 2005). The g:Profiler g:GOS tool was used for functional enrichment analysis of GO terms (for MF, BP, and CC), and KEGG pathways, with the significance threshold set at <0.05 as determined by the g:SCS ranking algorithm (Raudvere et al., 2019).

## **3.4 Results**

### **3.4.1 Improvement of alignment rates by separation of mouse and human transcripts from a co-culture system**

As per Table 3.5.1, the alignment of unsplit samples to the GRCh38 reference transcriptome yielded a mapping rate between 74 and 82% which was improved to >93% for human to GRCh38 mapping after splitting mouse and human reads. Note that the unsplit reads do not necessarily allow an inference regarding the neuron-to-glia ratio in samples as the pure CD1 mouse glia samples aligned at approximately 19%, which is comparable to the split mouse to GRCh38 alignment rates. While the split “human” reads from these CD1 glia had slightly improved mapping rates, the interpretation of this is difficult as the absolute read abundances were very low (data not shown). This does, however, suggest a lower burden of contamination. For both split and unsplit samples, overlap in mapping is evident as the summed totals of alignment to both genomes exceed 100%. However, the purified mouse and human reads map to their respective transcriptome at published levels.

### **3.4.2 Distinct clustering of 15q13.3 microdeletion probands and familial control**

Principal coordinate analysis revealed distinct clustering of 15q13.3 microdeletion probands and familial controls from both families. It is noteworthy that the control and proband from Family 1 were more closely clustered, likely related to a lower number of DEGs in this family. Interestingly, the PCA plot combining both families

(Figure 3.5.1A) shows a large majority of variability as explained by two principal coordinates. These appear to grossly align with the replicate/line (PC1), and control/proband status (PC2). While both control lines vary minimally on PC2, the proband lines are distributed opposingly along this PC axis with respect to the control lines.

For the subdivided PCA plots in Figure 3.5.1B and 3.5.1C (Families 1 and 3, respectively), there was a greater comparative separation of the control and proband lines along the putative PC1 and PC2 axis (which most closely constitutes an inversion of PC1 and PC2 from Panel A). The top 20 such genes are shown in Table 3.5.2, with comparisons for shared genes between positive and negative correlations bolded. As expected based on the combined plot, there is minimal overlap in these top-ranked genes which account for the majority of variation between the control and proband lines. Interestingly, KLF13 was the only negatively correlated gene along PC1 for both families and was the only 15q13.3 microdeletion region gene detected in the DEG analysis.

For positively correlated genes, only NLRP2 (NLR Family Pyrin Domain Containing 2) and HSA1P (heat shock protein family A (Hsp70) member 1B) were identified among the top 20 genes between both families. Only GABBR1 (GABA type B receptor subunit 1) was detected as a negatively correlated gene along PC2 of both families. There were no positively correlated genes identified between families along PC2.

### **3.4.3 Differences in functional enrichment analysis underlying variation in 15q13.3 microdeletion families**

To extend this work, we performed g:Profiler g:GOST analysis of the top 50 most positively correlated (positive and negative) genes from PC1 for each individual family (corresponding to Figure 3.5.2 Panels B and C) to identify possible pathways which drove these differences (Raudvere et al., 2019). The results of this analysis are shown in Figure 3.5.4. Note that in most cases, the enrichment of GO and KEGG processes was driven by a fairly limited number of genes. For example, for negatively correlated genes in Family 1, both HSPA1B (Heat Shock Protein Family A Member 1B) and HSPA1A (Heat Shock Protein Family A Member 1A) are represented in 9 out of 11 categories and as a consequence, the enrichment is weighted towards categories such as misfolded protein binding and cellular response to heat. Likewise, for negatively correlated genes in Family 3, among 95 enriched pathways, 90 had two or more collagen-chain peptides represented (with the most highly ranked ones being COL1A1 and COL3A1 represented 71 times, and COL1A2 represented 62 times). As a consequence, the detected pathways are nearly all related to collagen assembly or extracellular matrix organization.

Interestingly, for Family 3, nervous system development was identified as an enriched process under, notably but not exclusively driven by MAPT, ATAT1, EHMT2, BAG6, NNAT, TBX20, and several PCDH genes.

Antigen presentation and presentation was identified as an enriched pathway for positively correlated genes in both Families 1 and 3, driven by HLA-A and TAP2 in Family 1, and HLA-B and HLA-C in Family 3.

#### **3.4.4 Differentially expressed genes in 15q13.3 microdeletion probands at DIV14**

As noted, Family 3 demonstrated appreciably more differentially expressed genes than Family 1 (207 vs. 95 DEGs, respectively). These genes are plotted with selected labels in Figure 3.5.3, and the difference is evident in the volcano plot. Importantly, among the most significantly altered genes, only KLF13 and HSPA1B were altered in a directionally consistent manner between families. Note that in several instances gene symbols may be duplicated, as shown for AGPAT1 and BAG6 in Figure 3.5.3 Panel A. Likewise, while AGPAT1 was altered, its symbol is duplicated in Family 1, and it is a top-ranked gene for decreased log<sub>2</sub>-fold expression in Family 3. This is an anticipated consequence of multiple Ensembl IDs mapping to a single gene symbol as part of the annotation process. The disambiguation of these symbols is not straightforward, and as they represent individually annotated transcripts no imputation or consolidation was pursued for the purposes of this work.

Reads from 15q13.3 deletion region genes were also plotted as FPKM in Figure 3.5.6. KLF13 was the only detected differentially expressed gene between both families, though FAN1 was decreased in Family 1. Note the multiple ENSG IDs for KLF13, FAN1, and MTMR10, which have varying patterns of expression. For

example, the KLF13 reads with ID ENSG00000275746 are effectively undetectable in probands but well expressed in controls, while the ENSG00000169926 transcript had significant expression in both lines in both families and was indeed increased in Family 3. This is likewise true for MTMR10, though expression levels were more even between both ENSG IDs.

While both OTUD7A and CHRNA7 had decreased absolute FPKM counts in probands vs. controls, this did not reach significance as part of the DESeq2 analysis. This may be partially due to their low abundance compared to other genes in the region, which will tend to underpower them for discovery given their expected roughly two-fold decrease in a heterozygous proband.

There was also minimal detection of TRPM1, ARHGAP11B, and GOLGA8H. TRPM1 is expected to only be expressed in retinal cells, and this is, therefore, consistent. ARHGAP11B and GOLGA8H are highly duplicated chromosomal regions with many homologous subtypes, and unambiguous identification of their transcripts may be technically challenging.

#### **3.4.5 Gene set enrichment analysis of 15q13.3 microdeletion reveals novel and known developmentally relevant gene sets**

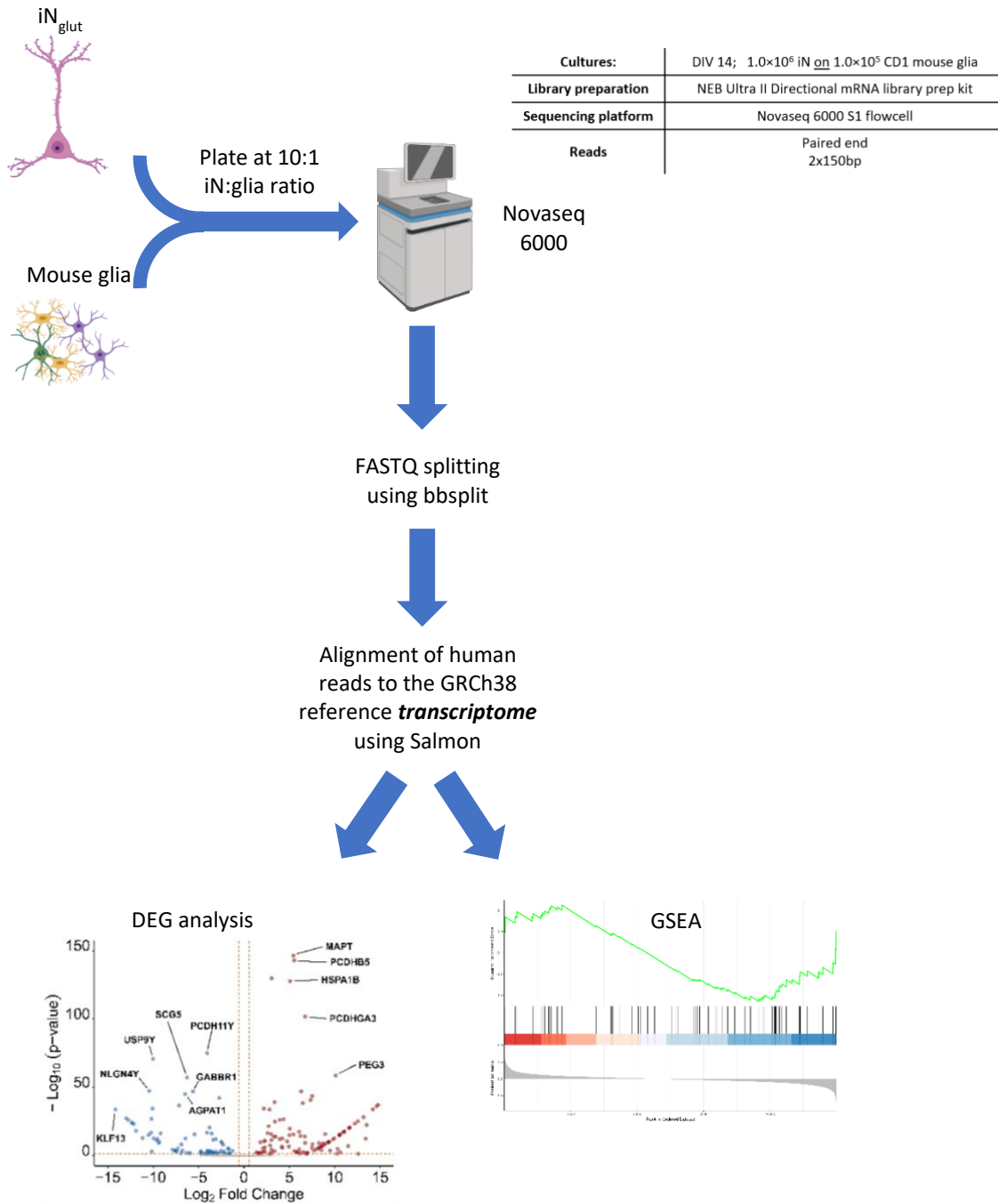
GSEA likewise identified considerably more enriched pathways in the Family 3 control line than the Family 1 control line. Note that enrichment was only detected in these lines and not either proband.

G2M Checkpoint and E2F Targets were enriched in both families. Notably, among the enriched pathways in Family 3 was Wnt beta catenin signalling and

TGF beta signalling. DNA repair was also identified, which was likewise detected by previous work (Zhang et al., 2021). Interestingly, TNFalpha signalling via NFkB was also enriched, whose noncanonical signalling pathway regulated by OTUD7B (highly homologous to OTUD7A) (Hu et al., 2013).

### 3.5 Figures

**Figure 3.5.1: Visual abstract and workflow schematic**



Schematic created with BioRender.com

**Table 3.5.1: Mapping rates for split and unsplit mouse and human reads**

	Unsplit to GRCh38	Split human to GRCh38	Split mouse to GRCh38	Unsplit to GRCm39	Split human to GRCm39	Split mouse to GRCm39
89E CONTROL	77.96%	93.74%	19.61%	34.29%	23.25%	94.66%
	74.42%	93.39%	19.41%	36.07%	22.31%	94.45%
	81.50%	93.89%	19.16%	31.28%	23.54%	94.63%
	78.47%	93.86%	19.39%	33.93%	23.42%	94.76%
90N PROBAND	77.21%	93.76%	19.90%	34.12%	22.74%	94.79%
	76.26%	93.63%	19.57%	34.86%	22.66%	94.66%
	76.44%	93.55%	19.17%	34.70%	22.66%	94.51%
	76.50%	93.43%	19.36%	34.33%	22.51%	94.50%
0205-002-2 CONTROL	71.12%	93.70%	20.07%	40.46%	22.87%	94.91%
	75.23%	93.98%	19.95%	36.88%	23.06%	95.14%
	72.73%	93.72%	19.73%	38.81%	22.80%	94.86%
	77.02%	93.79%	19.77%	34.42%	22.92%	94.91%
0205-003-1 PROBAND	73.42%	93.77%	19.95%	38.25%	22.83%	94.89%
	74.65%	93.97%	19.98%	37.39%	23.01%	95.05%
	73.34%	93.52%	19.61%	37.77%	22.57%	94.68%
	75.34%	94.09%	20.01%	36.94%	23.21%	95.18%
CD1 mouse glia	18.94%	21.26%	20.20%	92.98%	16.92%	94.88%
	18.81%	20.30%	20.08%	92.72%	14.88%	94.68%
	19.15%	20.18%	20.44%	93.15%	15.56%	95.03%

**Figure 3.5.2: Principal coordinate analysis of 15q13.3 microdeletion families**

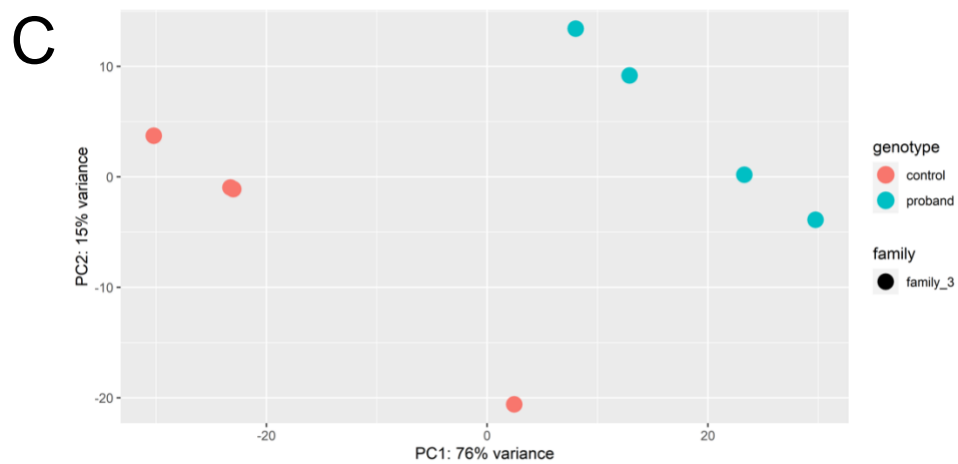
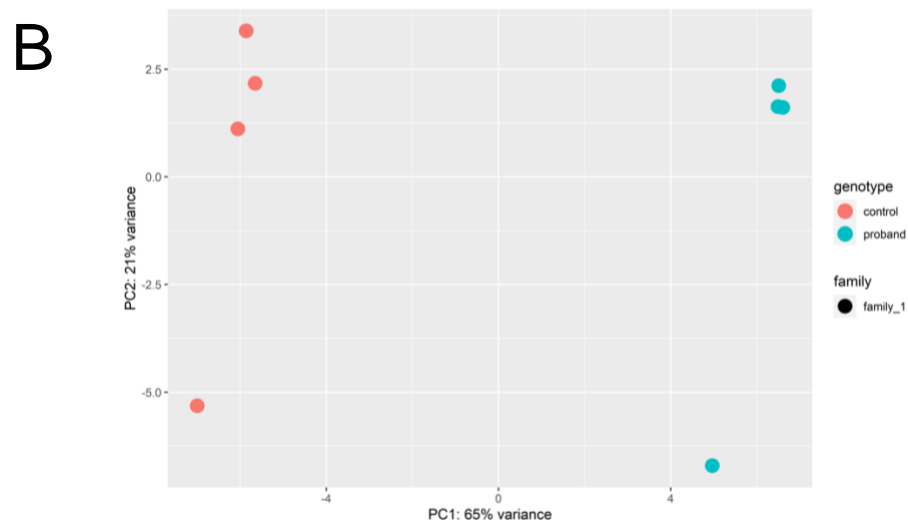
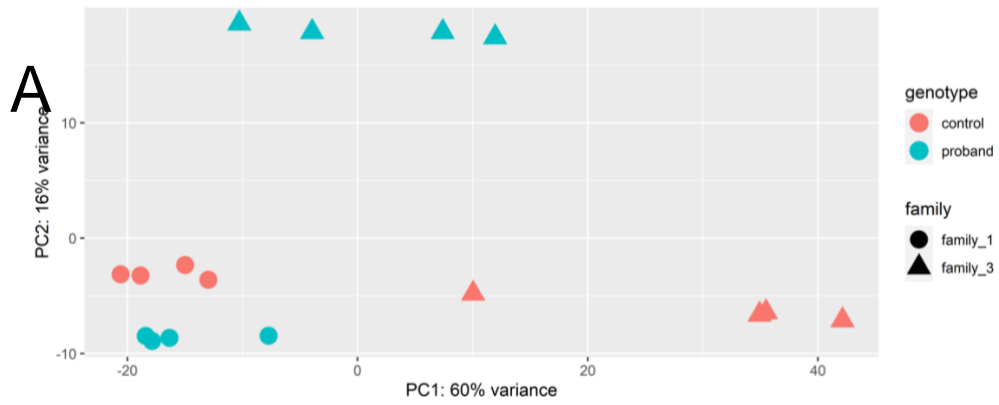


**Figure 3.5.2: Principal component (PCA) analysis plot of 15q13.3**

**microdeletion families**

(A) Combined PCA plot showing both patient families, with variance captured by

PC1 and PC2 shown on axes

(B) Split PCA plot plots showing Family 1 (Panel B), and Family 3 (Panel C)

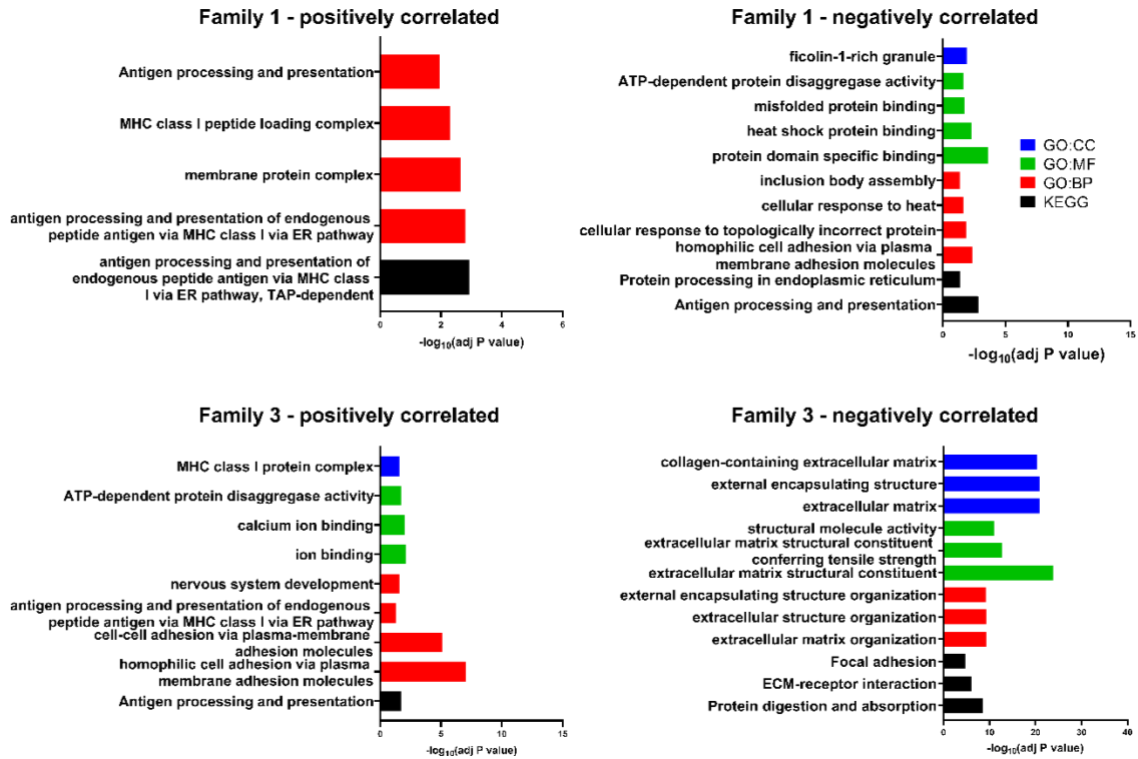
**Table 3.5.2: Top genes contributing to principal coordinates**

Family 1 PC1 top positive correlation	Family 3 PC1 top positive correlation	Family 1 PC2 top positive correlation	Family 3 PC2 top positive correlation
PRRC2A	PEG3	SRCIN1	PEG3
BAG6	NSF	SERPINE2	DDX39B
GABBR1	DDX39B	P2RX3	NSF
SCG5	AGPAT1	CRABP1	AGPAT1
BAG6	GNL1	PTP4A1	GNL1
AGPAT1	MAPT	PRPH	GABBR1
ATP6V1G2	PCDHGA3	SIX1	PCDHGA3
PCDHGB6	GABBR1	FRAS1	VAR1
TRIM27	VAR1	HTR3A	MAPT
CSNK2B	PCDHGA7	FSTL1	PCDHGA7
PPP1R11	KANSL1	OLFM3	PCDHB5
<b>HSPA1B</b>	PCDHB5	NNAT	HSPA1B
<b>NLRP2</b>	PRRC2A	KITLG	CSNK2B
HSPA1B	<b>HSPA1B</b>	LRRC3B	DAXX
MARF1	CSNK2B	RGS4	PRRC2A
HLA-A	LRRC61	INSYN2A	NLRP2
PCDHB16	<b>NLRP2</b>	ALK	ABCF1
KANSL1	INPP5F	EYA1	LRRC61
DDAH2	DAXX	CNTN2	ATAT1
GABRG3	PCDHB18P	CRLF1	FAM83H

Family 1 PC1 top negative correlation	Family 3 PC1 top negative correlation	Family 1 PC2 top negative correlation	Family 3 PC2 top negative correlation
AGPAT1	COL6A3	COL1A1	KLF13
ACACA	COL3A1	PRRC2A	USP9Y
<b>KLF13</b>	RPS4Y1	BAG6	RPS4Y1
ATP6V1G2	IGF2	FN1	CHCHD2
BAG6	COL1A2	<b>GABBR1</b>	NLGN4Y
PEG3	<b>KLF13</b>	<b>GABBR1</b>	SCG5
PRRC2A	COL1A1	WLS	NLRP2
BDP1	USP9Y	SPARC	<b>GABBR1</b>
CTSB	LUM	EBF3	DDX3Y
CANX	COL5A1	GPM6A	AGPAT1
PPP1R11	CHCHD2	LHX9	BDP1
HSPA1B	POSTN	COL18A1	DUSP8
GABBR1	DCN	PCDHGB6	KDM5D
SCG5	NLGN4Y	GRIA2	TRIM27
GABBR1	FN1	FLNA	EIF1AY
DCAF11	NID2	PCSK1	NDUFA6
PCDHGA7	NLRP2	COL4A1	SLC39A7
DAXX	IGFBP5	CACNA2D1	HLA-C
EBF3	BDP1	SSBP2	DDX39B
CHL1	DDX3Y	COL3A1	PCDH11Y

**Figure 3.5.3: Functional enrichment analysis of highly correlated Principal Coordinate Genes**



**Figure 3.5.3:** Plotting of the top 50 positively (left panels) and negatively (right panels) correlated genes from the main Principal Coordinate from Family 1 (top panels) and 3 (bottom panels). Processes were identified using the gProfiler g:GOST tool for the Gene Ontology terms Cellular Component (CC, blue), Molecular Function (MF, green), Biological Process (BP, red), or KEGG (Kyoto Encyclopedia of Genes and Genomes)

**Figure 3.5.4: Volcano plots showing DEGs in 15q13.3 microdeletion families**

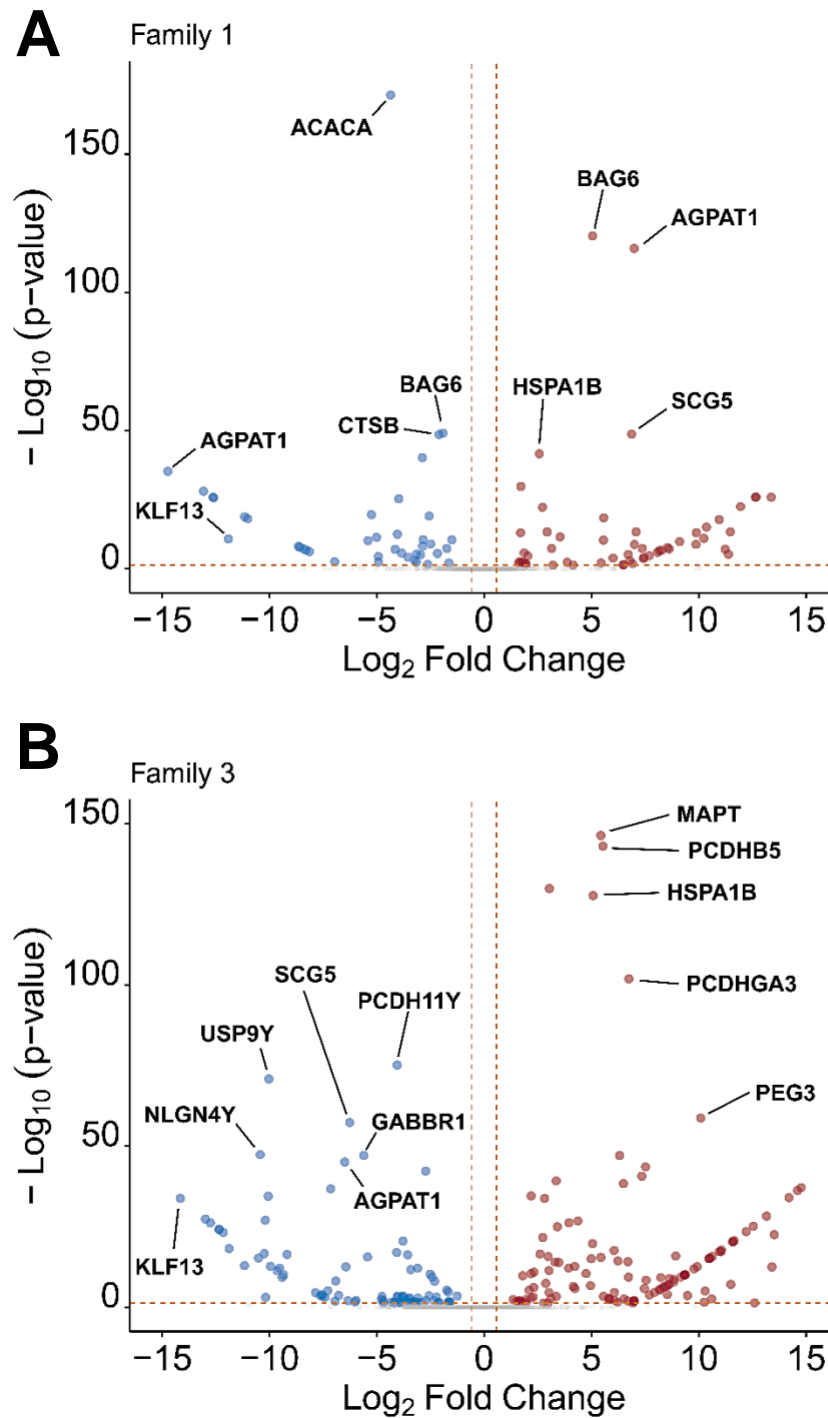


**Figure 3.5.4: Volcano plots showing DEGs in 15q13.3 microdeletion families**

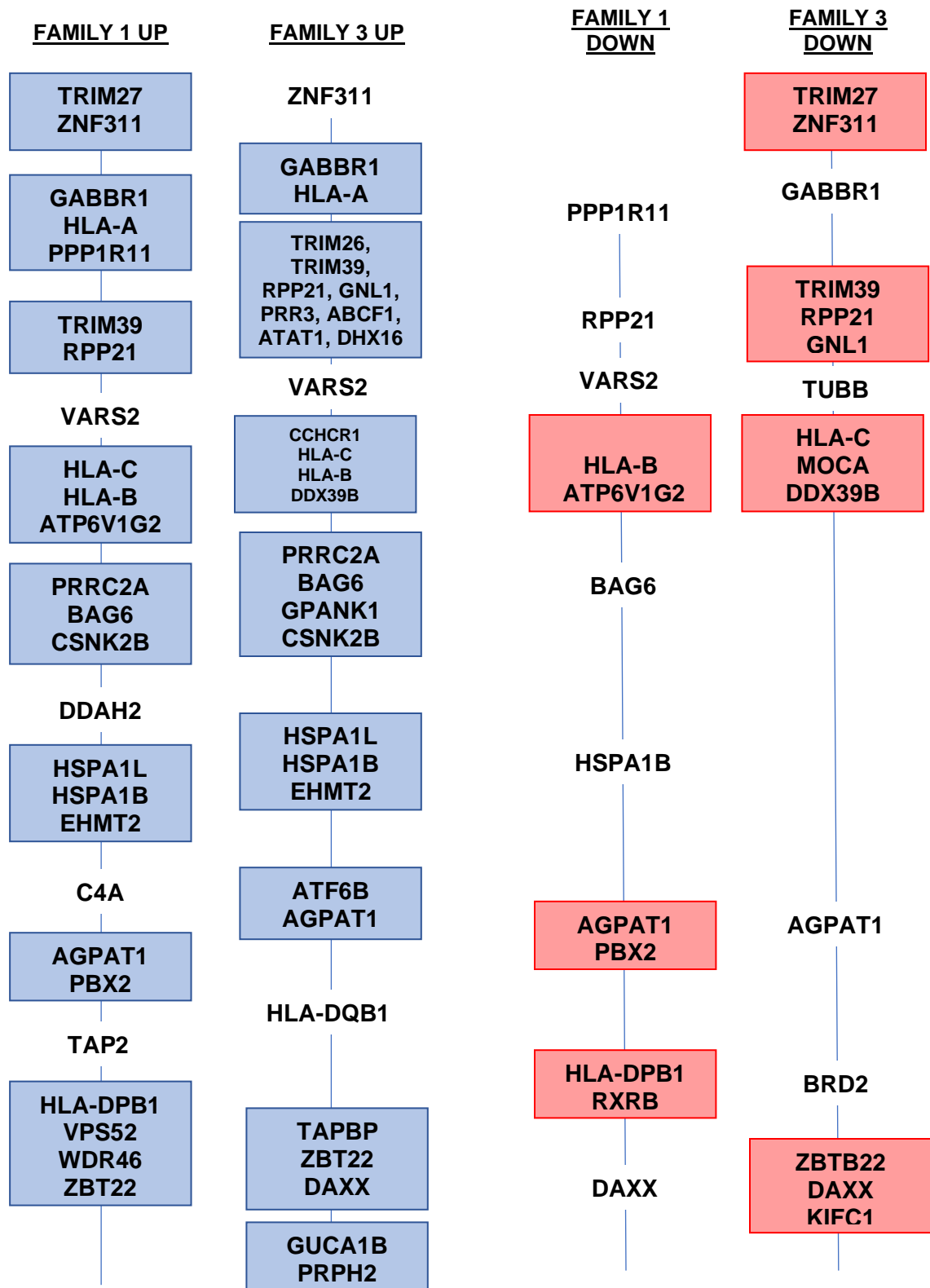
Volcano plots for Family 1 (A) and Family 3 (B) showing log transformed fold changes for genes (increased in red, and decreased in blue) and log transformed p-values. Significance cut-off lines are shown in dotted red.

**Table 3.5.3: Chromosomal clustering of DEGs by patient family**

chr	Family 1 UP		Family 3 UP		Family 1 DOWN		Family 3 DOWN	
	DEGs	C	DEGs	C	DEGs	C	DEGs	C
2p	-	-	2	1	-	-	-	-
5q	-	-	13	2	7	2	-	-
6p	26	8	31	8	12	3	15	4
7q	-	-	2	1	-	-	-	-
8q	-	-	-	-	3	1	-	-
11p	-	-	-	-	2	1	-	-
15q	-	-	-	-	3	1	5	1
16q	-	-	-	-	-	-	3	1
17q	-	-	12	2	3	1	5	1
19q	-	-	7	2	-	-	-	-
Y	-	-	-	-	-	-	10	2

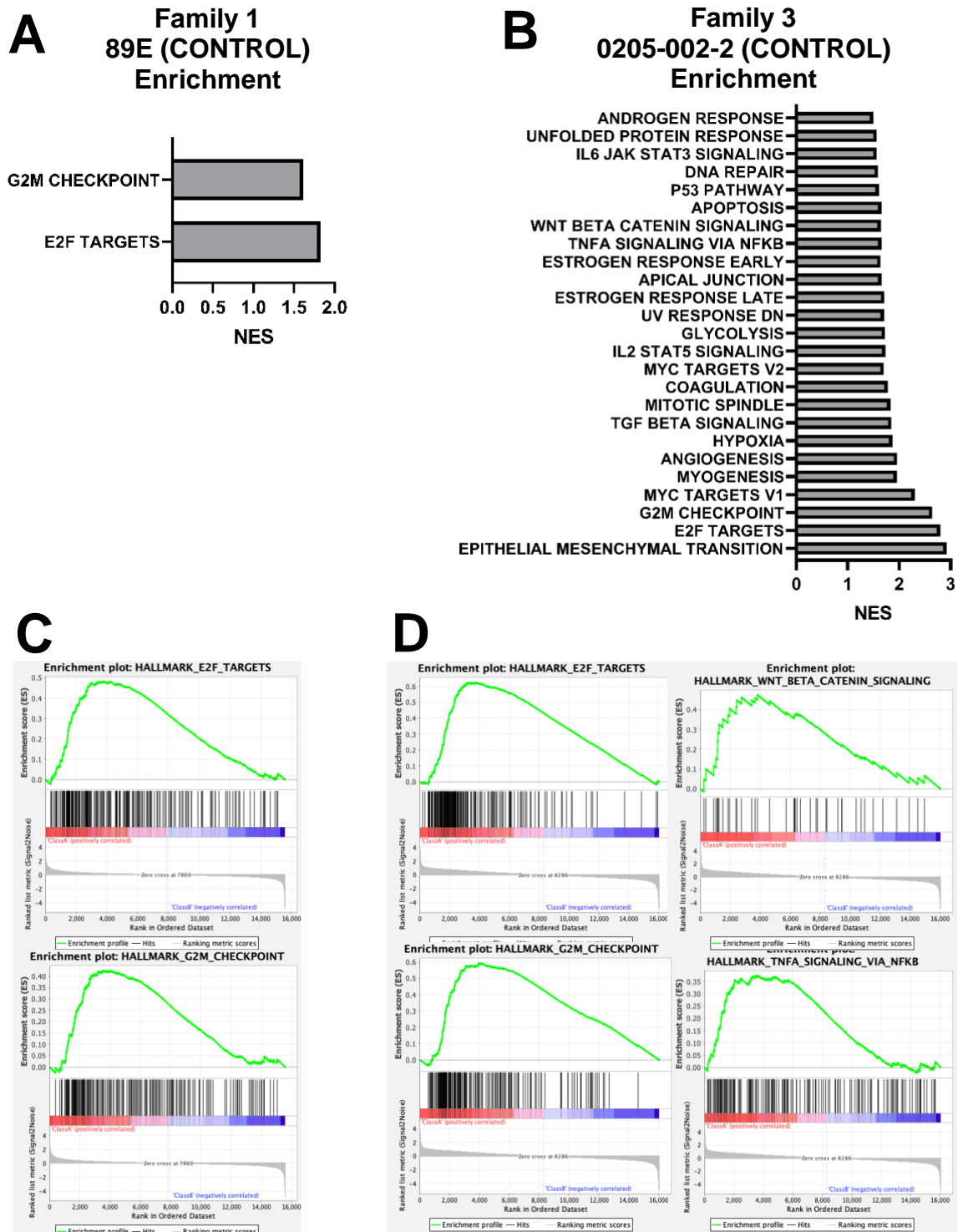
**Table 3.5.3:** Table showing the number of DEGs (differentially expressed genes) and number of clustered genes (gap of 5 or fewer genes) across all chromosomal sites where clusters were detected. Columns are divided to align DEGs which are increased (left) and decreased (right).

Figure 3.5.5: Clustering of DEGs at the 6p21.1-22.1 locus



**Figure 3.5.5:** Linear alignment map of genes detected in the 6p21-22 region from increased DEGs (Family 1 left, Family 3 centre left), and decreased DEGs (Family 1 centre right, Family 3 right). Map alignment is shown from the 6p22.1 region (top) to the 6p21.1 region (bottom). Gene distances not to scale, and is adapted to facilitate ease of comparison. Comparison list generated using Cluster Locator (<http://clusterlocator.bnd.edu.uy/>) (Pazos Obregón et al., 2018).

Figure 3.5.6: Gene set enrichment analysis



**Figure 3.5.5: Gene set enrichment analysis**

(A, B) Normalized enrichment scores for significant ( $p < 0.05$ ;  $FDR < 0.25$ ) gene sets determined by GSEA for Family 1 (Panel A) and Family 3 (Panel B).

(C, D) Enrichment plots for significantly altered pathways for Family 1 (Panel C) and Family 3 (Panel D).



### **3.6 Discussion**

The study of neurological disorders carries with it special challenges due to the sensitivity of neural tissues and the difficulty of acquiring them from patients.

Moreover, for disorders whose etiology may be subtle, there are additional difficulties in identifying the correct level of abstraction at which to investigate the related deficits. In this chapter, we aim to extend the work from Chapter 2 and build on the findings related to intrinsic neuronal deficits in iNs. We also attempted to build on efforts from other groups to provide insight into the early transcriptome and its relation to disease pathogenesis in the 15q13.3 microdeletion disorder. This chapter used a mouse-human co-culture system which allowed the extension of the system to a later time point that had been previously reported and allowed iNs to develop functionally and morphologically to a time point closer to the one in which we had reported findings previously. The principal strength of this experimental design is that it both permits maturation of the target cells (the patient iNs) and allows for more effective separation of the neuronal and glial transcripts as these are proxied by the human and mouse reads, respectively.

#### **3.6.1 Separation of mouse and human reads in a co-culture system**

The separation of mouse glial and human neuronal reads was achieved using the *bbsplit* tool (Bushnell, 2018). One of the main advantages of this program is the assembly of a novel mapping index and comparison of reads to the human and mouse transcriptome simultaneously, allowing for “best fit” mapping for each

read. Interestingly, this method was able to extract limited reads from even control mouse glia and does suggest that some degree of contamination remains inevitable.

Other tools for the separation of mouse and human reads exist (for example Xenofilter (Kluin et al., 2018)), and a comparison of read outputs against these methods can be pursued in the future. While the indication for the computational deconvolution of mouse and human reads in our study is not common (the typical use case more closely aligns with xenograft experiments in mice, for example in cancer research), this application has previously been employed in a similar system.

### **3.6.2 Transcriptome variation in neurodevelopmentally relevant genes between two 15q13.3 microdeletion families**

While many genes were differentially expressed in our patient families, select genes were chosen for consideration for their prominent significance levels (for a visualization of this see Figure 3.5.3), and potentially disease-relevant status based on the literature. These genes are grouped below based on the direction of their expression change, and which families this corresponds to.

#### Upregulated genes in Families 1 and 3

HSPA1B was upregulated in both probands, albeit to different degrees. Note that while HSPA1B is not known to be implicated in neurodevelopment, it is related to prognosis in colon cancer. Colon cancer risk is increased in the 15q13.3

microdeletion, and this finding of increased HSPA1B might relate to the oncogenic risk profile in these patients.

Downregulated genes in Families 1 and 3: KLF13 (ENSG00000275746) was downregulated in both families, which is expected for this deletion. There were multiple ENSG IDs detected mapping to KLF13, which localize to alternatively spliced variants and in the case of Family 3 this corresponded to both an increase and decrease dependent on the specific transcript. This was likewise true for FAN1. While this introduces a complication into the interpretation of this data, it also serves to highlight the complexity of the transcriptional profile.

Upregulated genes in Family 1: SCG5 (secretogranin 7B2) is a neuroendocrine regulatory protein (Mbikay et al., 2001). Its principal clinical utility has been cancer prognostication (Plesec et al., 2017; Xu et al., 2020), and it is not presently implicated in NDD pathogenesis. SCG5 is directly distal to the 15q13.3 BP5 locus, and its upregulation may be a consequence of the microdeletion altering the local genomic architecture.

AGPAT1 encodes the 1-acylglycerol-3-phosphate O-acyltransferase, which plays an important role in the conversion of lysophosphatidic acid to phosphatidic acid. Mice which are deficient in AGPAT1 have several metabolic derangements and notably develop abnormalities in hippocampal development and audiogenic seizures (Agarwal et al., 2017).

Downregulated genes in Family 1: ACACA encodes the Acetyl-coenzyme A carboxylase. Loss of this gene has been associated clinically with global

developmental delay, microcephaly and facial dysmorphia, though this is presumed to be attributable to alteration in lipid metabolism (Lou et al., 2021).

CTSB encodes the protein cathepsin B, and its inhibition is known to impede neurite outgrowth in mice through the regulation of lysosome trafficking (Jiang et al., 2020), though there is not much information on its role in neurodevelopment.

Up and down (Family 1): BAG6 and AGPAT1 had both increased and decreased transcripts detected in Family 1, suggestive of alternative splicing. The role of AGPAT1 is described above. BAG6 encodes the Bcl-2-associated athanogene 6, and while it is not neurodevelopmentally implicated it has been speculated that it might play a role in avoiding neurodegradation (Kasu et al., 2022).

Upregulated in Family 3: MAPT (Microtubule-Associated Protein Tau) is best known for its role in tauopathies underlying various neurodegenerative disorders (Ando et al., 2020; Strang et al., 2019; Young et al., 2021). Importantly, tau is an axonal marker and plays a role in distal axonal stability (Sjolin et al., 2022). While the reason for its increase in this proband is unclear, it is possibly compensatory given the axonal deficits presented in Figure 2.4.6.

PCDHB5 encodes the protocadherin beta-5 protein which is predicted to play an important role in neural connectivity. Its expression is also increased in the 16p11.2 deletion (Sundberg et al., 2021).

PEG3 is an imprinted gene containing kruppel-type zinc finger domains, and has been shown to inhibit Wnt signalling through increased  $\beta$ -catenin degradation (Thiaville et al., 2013) and to modulate TNF-NF $\kappa$ B signalling (Relaix et al., 1998).

### Downregulated in Family 3

NLGN4Y (neuroligin 4Y) is a postsynaptic scaffolding protein which plays an important role in synaptic scaffolding and has been suggested as a possible susceptibility gene partially explaining the differential rates of autism in males and females (Nguyen et al., 2020). However, this difference is likely fully attributable to the sex difference between the control (male) and proband (female), as this NLGN isoform is expressed only on the Y chromosome.

GABBR1 encodes the  $\beta$ 1 subunit of the B-subtype GABA receptor. While GABA signalling is implicated in many disease states and pathways, GABBR1 specifically is not a highly implicated NDD gene (Ma et al., 2005).

One additional note of interest is the significant clustering of DEGs (both upregulated and downregulated) in the chromosome 6p21.1-22.1 region (Table 3.5.3, Figure 3.5.5). They are proximal to a CNV locus known in cases of 6p microdeletions with DD, craniofacial malformations, cardiac defects, and in rare cases eye abnormalities (Davies et al., 1999). Cases of 6p duplication also present with a neuropsychiatric phenotype (Cornelis et al., 2015; Freire et al., 2013; Lin et al., 2005; Nakane et al., 2013). While the causality underlying this is of uncertain significance, it is possible that genomic structural changes secondary to the 15q13.3 microdeletion result in altered regulation of this 6p region, and that this may play a role in both disease pathogenesis and the induction of gene expression from the detected antigen presentation, TNF $\alpha$  and heat shock protein response pathways. The chromosome 6p locus is not typically associated

with a susceptibility to rearrangements in iPSCs, though it does remain possible that there is an unknown mutation in this region among these patients. However, given the overlap of the implicated genes at this locus across both patient families, it does raise the possibility that the microdeletion is having a transcriptional effect at this site. While there is some evidence of proximity between chromosomes 6 and 15 (Bolzer et al., 2005), this connection is not yet fully elucidated. It is also worth noting that there is a well-identified role of the immune system in autism spectrum disorder (as well as other neuropsychiatric conditions), and that both the HLA genes and other polymorphisms in the chromosome 6p region have been previously implicated as risk factors for the development of these disorders (Breen et al., 2023; Robinson-Agramonte et al., 2022; Torres et al., 2012; Voineagu & Eapen, 2013; Warren et al., 1986). Neurons are not typically considered immunologically active cells, though the role of the immune system in synaptic pruning and neuronal development is evident. It is therefore probable that further sequelae of altered chromosome 6p transcriptional activity could better be demonstrated in additional CNS cell types, particularly those with known immune functions (such as microglia). Further work will be required to identify implicated factors underlying this transcriptional shift.

### **3.6.3 GSEA and functional analysis reveals pathways implicated in neurodevelopment**

We were interested in identifying the factors underlying the differential clustering of probands from two different 15q13.3 microdeletion families. We performed

functional analysis on the top 50 positively and negatively correlated genes from the main principal component, along which the control and probands were most differentiated in each family. This identified that the “antigen processing and presentation of endogenous antigen peptides via MHC class I via ER pathway” process was enriched among the positively correlated genes along this main principle coordinate axis. One interesting point of note is that the Family 3 correlated gene set and Family 1 *negatively* correlated gene set both shared the GO:MF pathways for “ATP-dependent protein disaggregase activity” and the KEGG pathway for “antigen processing and presentation”. This may partially explain the anti-directional separation of these proband samples on the combined PCA plot. However, the origin of this differential expression is not ascertainable on the basis of this experiment alone, and subsequent investigations will be required to elucidate this.

It is also noteworthy that for Family 3, there was enrichment in the biological process category for nervous system development. While Family 3 had a greater number of differentially expressed genes and had a greater associated change in these functionally enriched pathways, particularly for downregulated pathways this appeared to be dominated by a limited number of genes. As previously stated, the Family 3 negatively correlated process is mainly driven by the differential expression of a variety of collagen subunits.

Our GSEA analysis also revealed a variety of enriched classes, though these were principally in Family 3. Compared to the DIV6 iNs from the previous study

(Zhang et al., 2021), this family had more enriched categories. Interestingly, there was minimal overlap between these analyses, although closely related terms were detected in both included nucleic acid repair and Wnt-related pathways. The 15q13.3 microdeletion region is in proximity to the 15q11-13 region known for the Prader–Willi and Angelman syndromes which are a consequence of parent-specific imprinting of genes, notably UBE3A. While the 15q13.3 region is not known to be imprinted, it is possible that genomic architecture changes induced by gains or loss of material might have downstream impacts on regions controlling imprinting and that this might be a mechanism by which extra-deletional gene expression is altered.

#### **3.6.4 Limitations**

While the work presented in this chapter aimed to improve on previous transcriptomic analysis conducted on 15q13.3 microdeletion, there are several potential limitations of the experimental method contained herein.

One of the main ways in which this work attempted to improve on previous studies was by co-culturing 15q13.3 microdeletion patient-induced neurons with mouse glia. In doing so we were able to improve neuronal viability and maturation, extend cultures to later dates, and provide a closer matching of the model system to other phenotyping work conducted in the study. The expected drawback of this is cross-species contamination due to the presence of the CD1 mouse glial RNA. We attempted to minimize the effect of this by plating the iN and glia at a 10:1 ratio (respectively), which was the minimal viable ratio to

extend the iN viability to DIV14 (data not shown). While the use of a interspecies co-culture system made the transcriptomics amenable to species-based separation (compared to, for example, the use of human glia or a system which would generate a multitude of cell types) the disadvantage of this approach is in the fact that where the fidelity of this separation cannot be absolutely verified, there will remain some contamination in the final reads. We attempted to quantify the fidelity of this approach by plating a mouse glia only condition, though the corresponding “iN only” condition was not feasible due to the nonviability of these cells at the experimental endpoint without glial support.

Importantly, the discovery of altered transcription at the chromosome 6p21.1-22.1 locus highlighted the limitations of the restricted cell types present in this model system. Particularly as the genes expressed in this region (and the subsequent pathways they represent) are immunologic in origin, the homogeneity of this system and its use of a specific subtype of excitatory glutamatergic neurons limits the functional assessment of immunological consequences on developmental trajectory,

### **3.6.5 Future Directions**

The work presented in this chapter offers a look into the early developmental period of 15q13.3 microdeletion iNs and underscores the multi-level variability which may partially underlie the clinical heterogeneity of this disorder. Future work can aim to expand on this in several ways. First, while these experiments offer transcriptomic insight at DIV14, more longitudinal studies with additional

timepoints will be essential to understanding the development of the transcriptome in early neural outgrowth and its contributions to disease. Additionally, while this analysis was aimed at identifying transcriptional variation as a source of both disease pathogenesis and clinical variability, additional lines of evidence are necessary to corroborate these findings. Importantly, to further pursue the consequences of altered transcription at the chromosome 6p21.1-22.1 locus, further work is required which will incorporate additional cell types including those with primary immunologic roles in the CNS such as microglia. While this work highlighted variation among two 15q13.3 microdeletion families, the inclusion of additional families in subsequent analyses will be required to properly contextualize these findings. For example, while proband lines did not cluster together in the PCA, the inclusion of additional patient lines might reveal multiple distinct transcriptomic states that these cells can assume and which underlie disease pathogenesis.

## **Chapter 4: GSK3 specific inhibition is associated with altered currents in control but not 15q13.3 microdeletion patient iNs**

### **4.1 Abstract**

There is suggestive evidence for mechanistic overlap in NDDs due to the high degree of co-occurrence of these disorders with one another. We were interested in extending the work from Chapters 2 and 3 to interrogate possible mechanisms in the 15q13.3 microdeletion. Recent work from our lab has shown that the 15q13.3 region gene OTUD7A plays an important role in the stabilization of Ankyrin-G and the maintenance of normal Ankyrin-G levels at the Axon Initial Segment (AIS). Interestingly, Ankyrin-G is a top implicated gene in Bipolar Disorder. We were interested in identifying possible mechanistic overlap between these disorders, and as Wnt signalling had been implicated in both this pathway and our previous transcriptomic work we decided to pursue related targets. As Bipolar Disorder is treated by Lithium which acts to inhibit GSK3, we used a highly selective and specific small molecule inhibitor of GSK3 (ChIR99021) to identify potential functional and morphologic changes in iNs of a 15q13.3 microdeletion family. We find that the 15q13.3 microdeletion proband is comparatively insensitive to GSK3 inhibition, and does not develop the expected insult to action potential properties on ChIR99021 administration. This highlights a novel and unexpected finding in the 15q13.3 microdeletion and suggests potential new avenues of mechanistic investigation.

## 4.2 Introduction

### Evidence for mechanistic convergence in NDDs

There is a high rate of co-occurrence for many NDDs and neuropsychiatric disorders, and it is known that their development is highly sensitive to specific genetic composition. The co-occurrence (especially as it is incomplete) indicates that there must be specific configurations of these genetic makeups that will result in disease, particularly co-occurring disease. Naturally, this also has to account for environmental factors, which modify the genetic background to produce this. However, it should follow that mechanisms in one neuropsychiatric disorder can (and often do) have significant translatability to others.

Our group recently identified that OTUD7A (which is a proposed driver gene of the 15q13.3 microdeletion) interacts with Ank3 at the AIS, which is an implicated pathway in bipolar disorder. While Bipolar Disorder is not a common presentation of the 15q13.3 microdeletion disorder (Lowther et al., 2015), the proximity of these apparently disparate signalling pathways underlying neuropsychiatric disease was considered noteworthy for further investigation.

A previous publication from our lab highlighted a novel role for a previously underappreciated gene in this microdeletion, OTUD7A. OTUD7A encodes a Lysine-11 (K11) specific deubiquitinase (Mevisse et al., 2013; Mevisse et al., 2016), for which few specific protein targets are presently known. A proximity-labelling proteomics screen of OTUD7A conducted by another member of the lab (Dr. Brianna Unda) identified ankyrin-G (gene name Ank3) as a top hit (Unda et

al., 2023). Ank3 is a scaffolding protein and is best known for its localization in the axon initial segment (AIS) (Rasband, 2010). The AIS is a region of the neuron which is responsible for the initiation of action potentials (Rasband, 2010).

Ankyrin-G has several isoforms, which may differentially localize to dendritic spines as well. We have previously shown a small decrease in ankyrin-G levels in the brains of 15q13.3 microdeletion mice and in 15q13.3 microdeletion proband iNs (Unda et al., 2023). We were therefore interested in identifying whether dysregulation of ankyrin-G as a key scaffold in both the AIS and dendritic spines is related to the observed deficits in this model, with respect to both the functional and morphological parameters.

Ankyrin-G is best known for its role in bipolar disorder. While the 15q13.3 microdeletion does not clearly reproduce the features of bipolar disorder, Ankyrin-G is also listed as an SFARI “high confidence” autism risk gene. It is noteworthy that bipolar disorder can often be successfully treated with Lithium, with the consensus mechanism being the inhibition of glycogen synthase kinase 3 (Harwood & Agam, 2003). This inhibition has the net effect of activating the canonical Wnt signalling pathway, as GSK3 identifies the Wnt effector  $\beta$ -catenin for ubiquitination and degradation (Doble & Woodgett, 2003). It is also noteworthy that AnkG is a known regulator of Wnt signalling, by modifying the availability of  $\beta$ -catenin (Durak et al., 2015). Interestingly,  $\beta$ -catenin has a known K11 polyubiquitination site, though whether this represents a pro- or anti-degradation signal is reported conflictingly in the literature (Dimitrova et al., 2010; Jin et al.,

2008; Li et al., 2018; Xu et al., 2009). However, recent work from our group demonstrated that OTUD7A is involved in the stabilization of both Ankyrin-B and Ankyrin-G and maintenance of normal levels at the axon initial segment (Unda et al., 2023), suggesting a possible overlap in these pathways.

For this aim, I was interested in whether the 15q13.3 microdeletion pathobiology could be linked to GSK3 signalling as described above. To this end, we used ChIR99021, a highly selective and potent GSK3 inhibitor ( $IC_{50}$  GSK3 $\alpha$  = 10nM,  $IC_{50}$  GSK3 $\beta$  = 6.7nM) to investigate potential differences in GSK3 signalling pathways between the proband and control in one family. This was supported by previous work from our group showing that ChIR99021 treatment could “rescue” select parameters in a 15q13.3 deletion mouse model (Unda et al., 2023).

ChIR99021 exerts its action by competitive inhibition of ATP binding to GSK3 (Ring et al., 2003). Previous studies with this drug have shown that it rescues microtubule dynamics in AnkG deficient mice (Garza et al., 2018), and modifies voltage-gated sodium channels in medium spiny neurons (Scala et al., 2018).

Preliminary data in our human lines has shown that proband lines respond differently than control lines to ChIR99021 administration. We are interested in characterizing the difference in this aim.

### 4.3 Methods

*The methods presented here are generally adapted to the specific experiments carried out for the purposes of this thesis. However, there is inevitable similarity to methods presented in several papers that I co-authored during this PhD. Effort has been taken to modify them as appropriate, though similarity in phrasing necessarily remains.*

#### **Electrophysiology recordings**

Essentially as described in Section 2.3.6 with the following adjustments:

Cells were treated with 2  $\mu$ M ChIR99021 (Sigma #SML0146) added during scheduled media half changes beginning 3 days before the experimental endpoint.

#### **Multi-electrode array recordings**

One day before plating, 48 well MEA plates (16 electrodes per well) were coated for 2 hours at 37°C with sterile filtered 0.1% polyethylenimine in pH 8.4 borate buffer. The wells were washed four times with ultrapure water and left to dry uncovered overnight. On day 4 post-induction, 40,000 iN cells were plated in a 20  $\mu$ L droplet on the glass portion of the well and allowed to attach for 1.5 hours in a 37°C incubator. On day 5 post-induction, 20,000 CD1 mouse glia were added to each well. The plates received half media changes every other day (iNI+BDNF+GDNF+laminin, with 2.5% FBS added after day 10 post-induction). For ChIR99021 experiments, 2  $\mu$ M ChIR99021 (Sigma #SML0146) or an

equivalent volume of vehicle (DMSO) was added to all conditions in a half media change beginning at DIV 11 and continuing for the duration of the experiment. MEA recordings were taken approximately twice a week using the Axion Maestro Pro, through the AxIS Navigator software's Spontaneous Neural activity module. Plates were allowed to acclimatize to the prewarmed recordings machine for 5 minutes, followed by 10 minutes of spike recordings. These recordings were analyzed to generate advanced metrics for the Neural Offline sorting function, using the default program parameters.

### **Morphological analysis**

iNs were plated as described above and fixed at DIV28 for puncta and Sholl analysis. For axon tracing experiments, iNs were used at DIV 10. For all other experiments, iNs were used at DIV28. Prior to staining, iNs were fixed for 20 minutes in 4% PFA, then stored in DPBS without calcium/magnesium until use. Confocal images were captured on a Zeiss LSM700 or LSM880 at 63x magnification for puncta, or 20x magnification for Sholl. All image analysis was performed in ImageJ.

### **Antibodies**

Antibodies used in this chapter include: rabbit anti-GSK3 $\beta$  (Cell Signaling Technology #9369T; Western Blot 1:1000), rabbit anti-pGSK3 $\beta$  (Cell Signaling Technology #9369T; Western Blot 1:1000), mouse anti- $\alpha$ -tubulin (Cell Signaling Technology #2144S; Western Blot 1:1000), MAP2 chicken polyclonal (1:1000; Cedarlane CLN182 or Aves labs), Synapsin-1 mouse monoclonal (1:2000;

Synaptic systems 106 011), and ankyrin-G mouse monoclonal (1:200; Neuromab 75-146). All secondary antibodies were raised in donkey and used at a concentration of 1:500.

### **Western blot**

Protein extraction and Western blotting were performed as previously described (Unda et al., 2023), with the following modifications. iNs were plated on Matrigel in 6 well plates at  $1.0 \times 10^6$  cells per well treated with 2  $\mu$ M ChIR99021 on DIV4 and DIV6. Protein was collected on DIV7. Cells were lysed in RIPA buffer and 20ug of protein per sample was loaded into 4-15% Tris-glycine gels and transferred to a PVDF membrane (Bio-Rad). Membranes were blocked for 1 h in 5% milk in 1X TBST, incubated with primary antibody overnight at 4 °C, then with secondary antibody (donkey anti-mouse or antirabbit HRP, GE Healthcare) for 1 h at room temperature before exposure using a ChemiDoc MP system (Bio-Rad).

### **LDH assay**

For the LDH cytotoxicity assay, the Thermo Fisher CyQUANT LDH cytotoxicity assay kit (#C20300) was used as described. 500  $\mu$ L of media was collected from each well of co-cultured iNs on or about DIV28 and flash frozen until the time of the assay.

## **4.4 Results**

### **4.4.1 Chronic ChIR99021 treatment alters spiking in both a control and 15q13.3 microdeletion proband iN**

In aggregate, chronic treatment with 2  $\mu$ M ChIR99021 appears to have a similar effect on both lines as determined by MEA recordings across time. Treated lines experience suppression of frequency-based metrics related to both individual electrode firing rates (weighted mean firing rate, network burst frequency; Figure 4.5.1B), and multi-electrode firing rates (network burst frequency; Figure 4.5.1D). Interestingly, there appear to be minor differences between the proband and control lines. The discordance between frequency-based spiking metrics and duration (Figure 4.5.1D, E), suggests that while most cells are impaired in autonomous firing, the active subset maintains their ability to fire long trains of action potentials. This likewise suggests that the comparative functional insensitivity of the proband to ChIR99021 as demonstrated in Figure 4.5.2 and 4.5.3 is surmountable by extended administration of the drug.

### **4.4.2 Acute ChIR99021 treatment alters intrinsic action potential parameters in control but not proband iNs**

Treatment of iNs with 2  $\mu$ M ChIR99021 for 3 days altered intrinsic electrophysiological properties related to action potential amplitude and width in the control but not the proband (Figure 4.5.2). These deformations are suggestive of impaired sodium currents (related to amplitude), for which there is precedent in the literature (Scala et al., 2018). Indeed, inward currents were decreased in the

control but not proband lines as shown in Figure 4.5.3. The increase in AP width (measured from the threshold) suggests that the early phase of the action potential is slower than normal, potentially indicating difficulty in the initiation of the action potential. The absence of any changes between treated and untreated conditions in the proband is suggestive of a comparative insensitivity to GSK3 inhibition with respect to action potential properties and their underlying determinants.

This was additionally noted on inward current recordings in Figure 4.5.3 which demonstrated diminishment in the 89E (CON) ChIR99021 treated condition but not the 90N (PROBAND) ChIR99021 treated condition.

No changes to sEPSC properties were appreciated on ChIR99021 administration in either group (Figure 4.5.4).

#### **4.4.3 15q13.3 microdeletion iNs manifest disruptions in the axon initial segment**

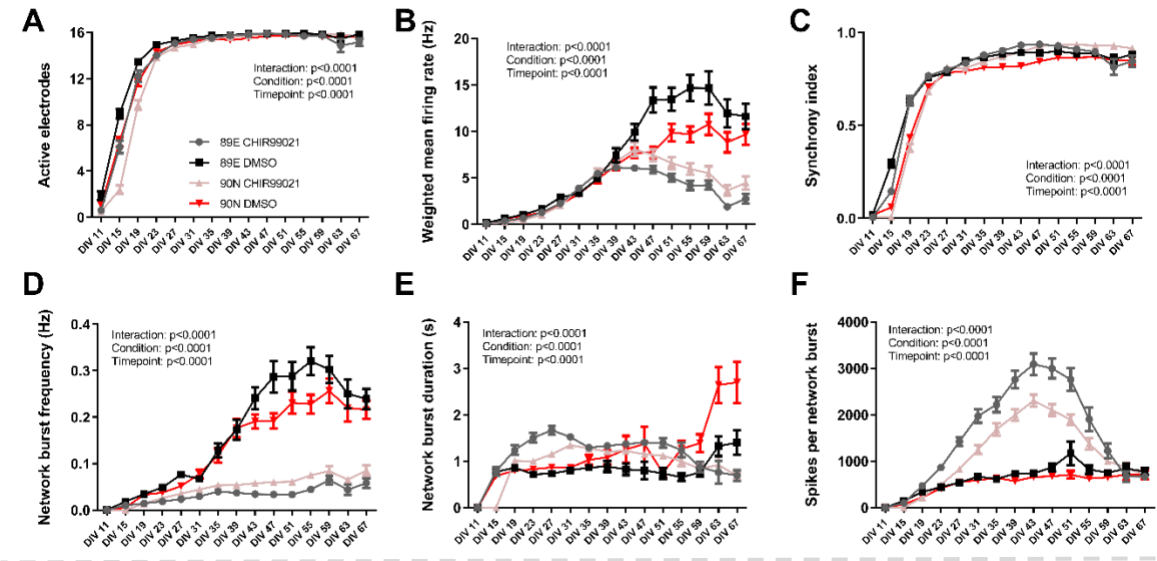
DIV 28 15q13.3 microdeletion proband iNs from Family 1 had decreased arbour complexity on ChIR99021 administration in both proband and control groups as measured by Sholl analysis of microtubule-associated protein 2 (MAP2) positive processes (Figure 4.5.7), and decreased proximal ankyrin-G intensity in the AIS (Figure 4.5.6A). However, they did not show differences in synapsin-1 puncta density (Figure 4.5.6B).

#### **4.4.4 Molecular consequences of ChIR99021 administration in iNs**

Western blotting was performed to assess for changes in GSK3 $\beta$  and pGSK3 $\beta$  (Figure 4.5.5). Levels of both GSK3 $\beta$  and pGSK3 $\beta$  were decreased with short-term ChIR99021 administration, though the ratio of pGSK3 $\beta$ /GSK3 $\beta$  was unaltered (Figure 4.5.5). Note however that the interpretation of the blot is complicated by the apparent saturation of the loading control ( $\alpha$ -tubulin). Further, while difficult to appreciate due to the diffuse nature of the bands, a doublet appears present for both GSK3 $\beta$  and pGSK3 $\beta$  which could represent a known brain-specific isoform (Liu & Klein, 2018; Soutar et al., 2010). Note also that no changes in LDH levels were appreciated between groups (Figure 4.5.8).

### 4.5 Figures

**Figure 4.5.1: ChIR99021 administration alters population-level spiking activity in both proband and control iNs**



Max significant difference	Active electrodes	WMFR	Synchrony index	Network burst frequency	Network burst duration	Spikes/network burst
<b>89E DMSO</b> vs. <b>89E ChIR99021</b>	****	****	****	****	****	****
<b>89E DMSO</b> vs. <b>90N DMSO</b>	****	****	****	****	****	*
<b>89E DMSO</b> vs. <b>90N ChIR99021</b>	****	****	****	****	***	****
<b>90N DMSO</b> vs. <b>89E ChIR99021</b>	ns	****	****	****	****	****
<b>90N DMSO</b> vs. <b>90N ChIR99021</b>	****	****	**	****	****	****
<b>89E ChIR99021</b> vs. <b>90N ChIR99021</b>	****	ns	****	ns	*	****

**Figure 4.5.2: ChIR99021 administration alters population-level spiking**

**activity** (A, C) chronic ChIR99021 administration does not decrease active electrodes or the synchrony index over time; (B) ChIR99021 differentially impacts WMFR of the control and proband lines beginning at DIV 39 in both vehicle and drug-treated groups; (D-F) Both single electrode bursting and network bursting are decreased from the point of ChIR99021 treatment in both control and proband lines, though the network burst duration and spike counts in the remaining network bursts are increased throughout, tapering off at the end of the recording window.

*N=3 infections, 89E DMSO n=36, 89E ChIR99021 n=36, 90N DMSO n=34, 90N ChIR99021 n=35 (wells per timepoint). All MEA data analyzed by two-way ANOVA with Tukey's multiple comparisons test where appropriate.*

**Figure 4.5.2: Acute treatment (3d) with 2 $\mu$ M ChIR99021 fails to alter action potential properties 15q13.3 microdeletion proband**

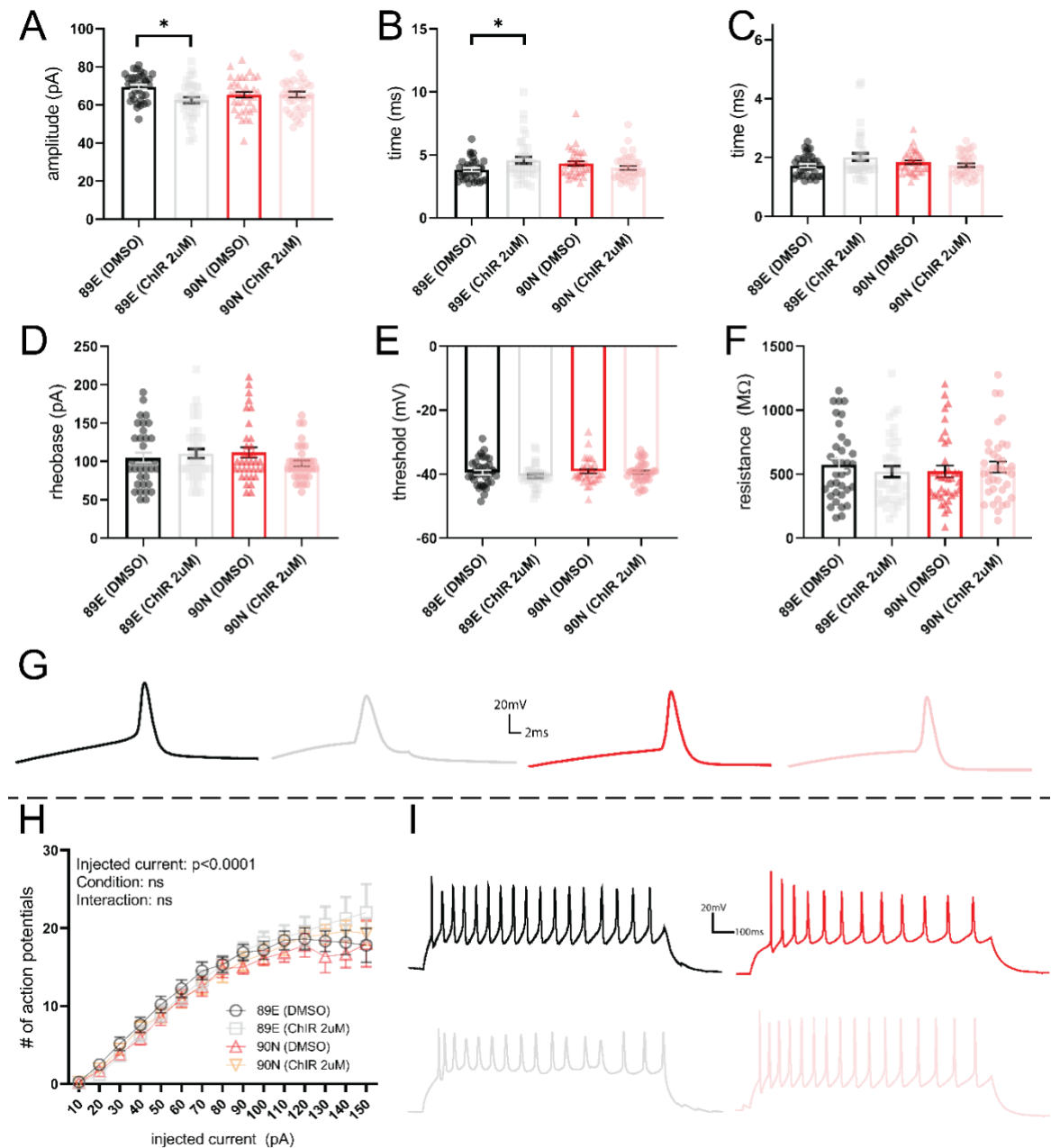


**Figure 4.5.2: Acute treatment (3d) with 2uM ChIR99021 fails to alter action potential properties 15q13.3 microdeletion proband.** (A) Representative

traces of action potentials from all conditions, showing shortening and widening only in the control. (B) AP amplitude and width are decreased only in the 89E (CON) ChIR99021 2uM group compared to 89E (CON) DMSO, with no significant changes to width, half-width, or other membrane properties. (H) Action potential train is unchanged with ChIR99021 administration across all groups,

Intrinsic properties by two-way ANOVA (Amplitude (Interaction:  $F(1, 142) = 5.910$   $P=0.0163$ , Treatment:  $F(1, 142) = 5.406$   $P=0.0215$ , Genotype:  $F(1, 142) =$

$0.1631$   $P=0.6869$ ); AP width (Interaction:  $F(1, 141) = 8.047$   $P=0.0052$ ,

Treatment:  $F(1, 141) = 1.078$   $P=0.3009$ , Genotype:  $F(1, 141) = 0.09138$

$P=0.7629$ ); AP half-width (Interaction:  $F(1, 142) = 5.780$   $P=0.0175$ , Treatment:  $F(1, 142) =$

$1.288$   $P=0.2583$ , Genotype:  $F(1, 142) = 1.002$   $P=0.3186$ ); Rheobase

(Interaction:  $F(1, 139) = 2.779$   $P=0.0978$ , Treatment:  $F(1, 139) = 0.5650$

$P=0.4535$ , Genotype:  $F(1, 139) = 0.2560$   $P=0.6137$ ); Resistance (Interaction:  $F(1, 142) =$

$0.9598$   $P=0.3289$ , Treatment:  $F(1, 142) = 0.04982$   $P=0.8237$ ,

Genotype:  $F(1, 142) = 0.03240$   $P=0.8574$ ); Capacitance (Interaction:  $F(1, 143) =$

$0.04317$   $P=0.8357$ , Treatment:  $F(1, 143) = 0.7542$   $P=0.3866$ , Genotype:  $F(1,$

$143) = 0.01289$   $P=0.9098$ ); AP Threshold (Interaction:  $F(1, 142) = 0.3735$

$P=0.5421$ , Treatment:  $F(1, 142) = 1.463$   $P=0.2284$ , Genotype:  $F(1, 142) = 1.475$

$P=0.2266$ )) with Tukey's multiple comparisons test. N=3 infections, 89E DMSO

n=35, 90N DMSO n=35, 89E ChIR99021 n=38, 90N ChIR99021 n=35. Intrinsic

excitability analyzed by mixed effects model (Injected current,  $F(1.374, 111.2) = 433.7$   $P < 0.0001$ ; Genotype,  $F(3, 139) = 0.5424$   $P = 0.6541$ ; Interaction,  $F(42, 1133) = 0.2940$   $P > 0.9999$ ). Significance levels indicated on graphs correspond to \* $p < 0.05$ , \*\* $p < 0.01$ , \*\*\* $p < 0.001$ , \*\*\*\* $p < 0.0001$ .

**Figure 4.5.3: Paradoxical response of ChIR99021 administration on inward current**

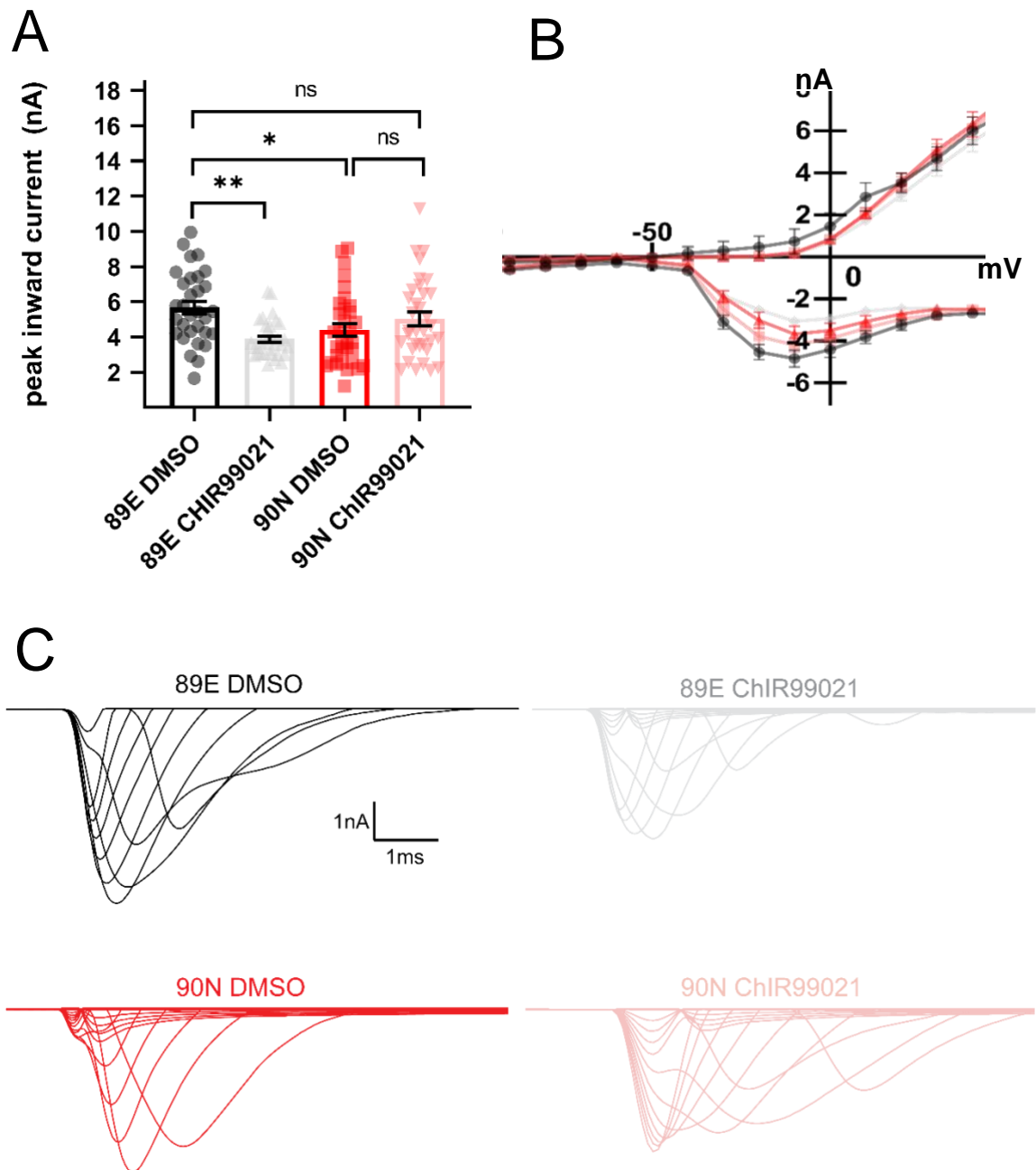


**Figure 4.5.3: currents**

(A) Peak inward current (nA) for both vehicle and drug-treated lines

(B) Current/voltage plot showing both inward and outward currents for all four lines

(C) Representative inward currents as labelled.

Analysis performed by two-way ANOVA (Interaction:  $F(1, 127) = 13.21$   $P=0.0004$ , Treatment:  $F(1, 127) = 3.053$   $P=0.0830$ , Genotype:  $F(1, 127) = 0.03759$   $P=0.8466$ ) with Tukey's multiple comparisons test. Significance levels indicated on graphs correspond to \* $p<0.05$ , \*\* $p<0.01$ , \*\*\* $p<0.001$ , \*\*\*\* $p<0.0001$ .

Figure 4.5.4: Spontaneous synaptic transmission in ChIR99021 treated iNs

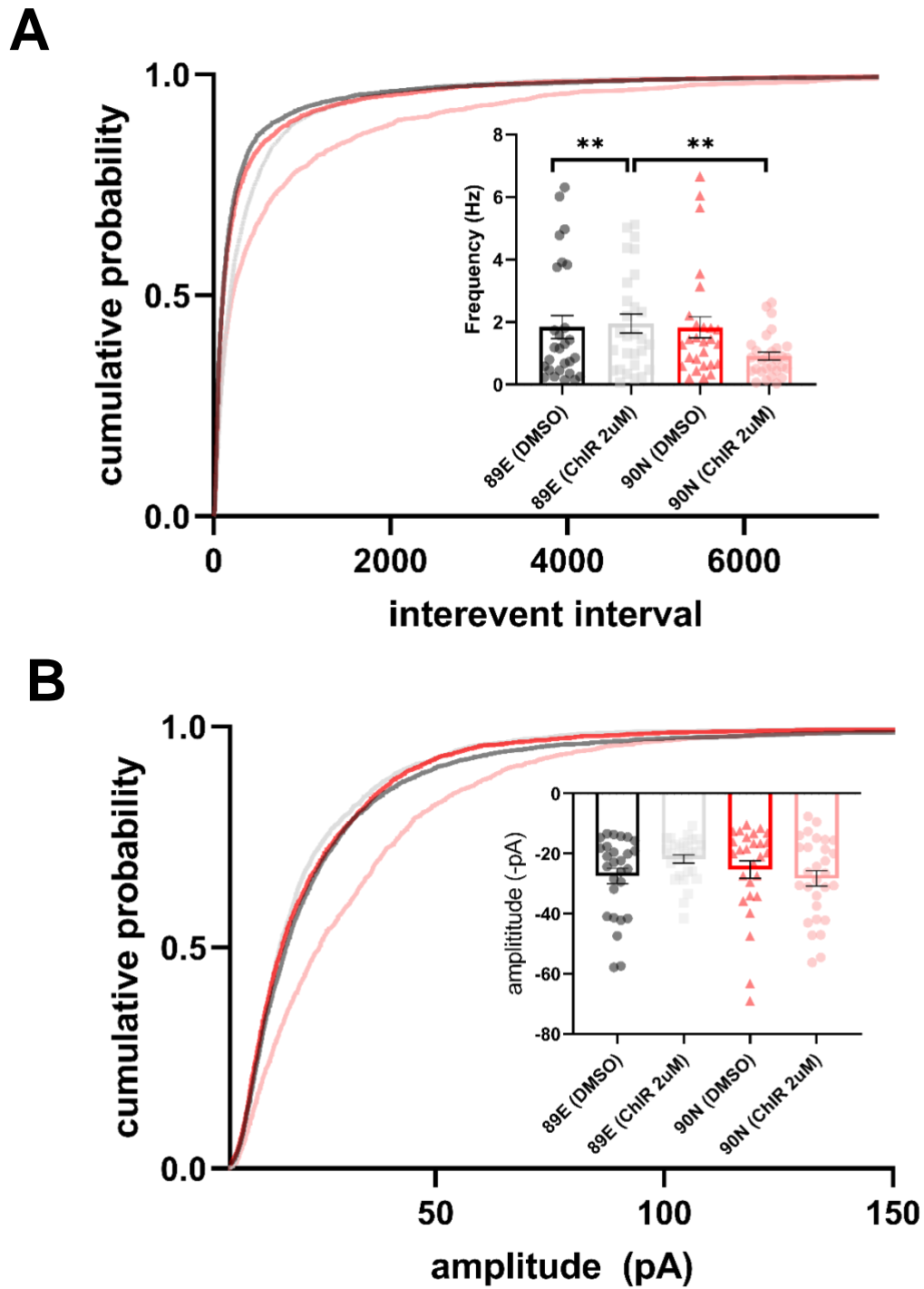
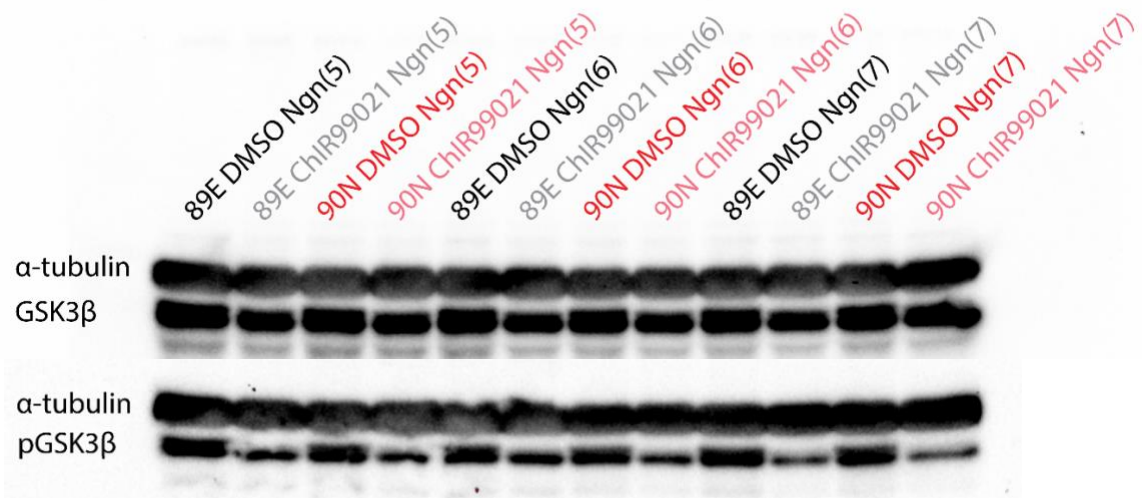


**Figure 4.5.4: Spontaneous synaptic transmission in ChIR99021 treated iNs**

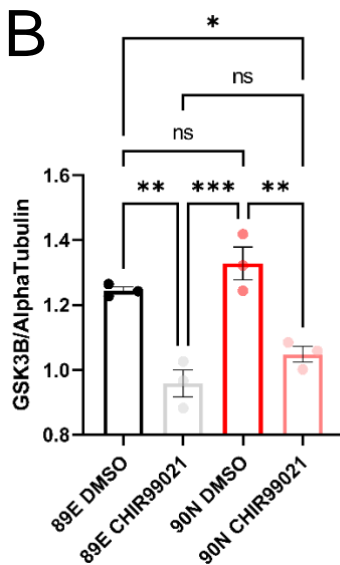
Administration of ChIR99021 does alter sEPSC frequency but not amplitude in both control and 15q13.3 microdeletion proband iNs. N=3 infections, 89E DMSO n=27, 90N DMSO n=27, 89E ChIR99021 n=28, 90N ChIR99021 n=29. One-way ANOVA: sEPSC amplitude,  $F(3, 107) = 1.475$   $P=0.2254$ ; sEPSC frequency  $F(3, 107) = 2.830$   $P=0.0419$ .

**Figure 4.5.5: Western blot of GSK3 $\beta$  and pGSK3 $\beta$  in response to ChIR99021 administration**

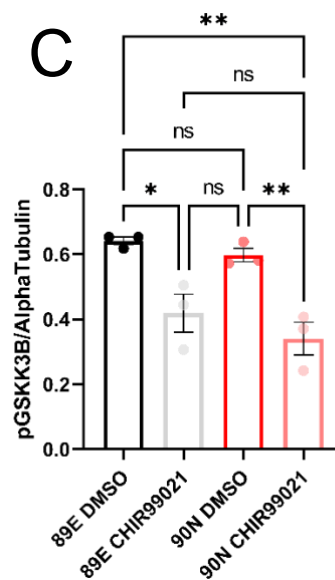
**A**



**B**



**C**



**D**

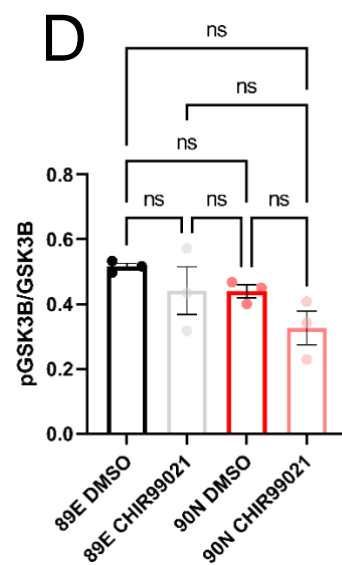


**Figure 4.5.5: Molecular validation of cellular response to ChIR99021 administration**

Analysis performed by two-way ANOVA. GSK3B (Interaction:  $F(1, 8) = 0.008592$   $P=0.9284$ , Treatment:  $F(1, 8) = 64.20$   $P<0.0001$ , Genotype:  $F(1, 8) = 5.988$   $P=0.0401$ ); pGSK3 (Interaction:  $F(1, 8) = 0.1796$   $P=0.6829$ , Treatment:  $F(1, 8) = 35.28$   $P=0.0003$ , Genotype:  $F(1, 8) = 2.307$   $P=0.1673$ ); GSK3/pGSK3 (Interaction:  $F(1, 8) = 0.1739$   $P=0.6877$ , Treatment:  $F(1, 8) = 4.057$   $P=0.0787$ , Genotype:  $F(1, 8) = 4.231$   $P=0.0737$ ) with Tukey's multiple comparisons test. Significance levels indicated on graphs correspond to \* $p<0.05$ , \*\* $p<0.01$ , \*\*\* $p<0.001$ , \*\*\*\* $p<0.0001$ .

**Figure 4.5.6: Disruption of the axon initial segment in a 15q13.3**

**microdeletion proband**

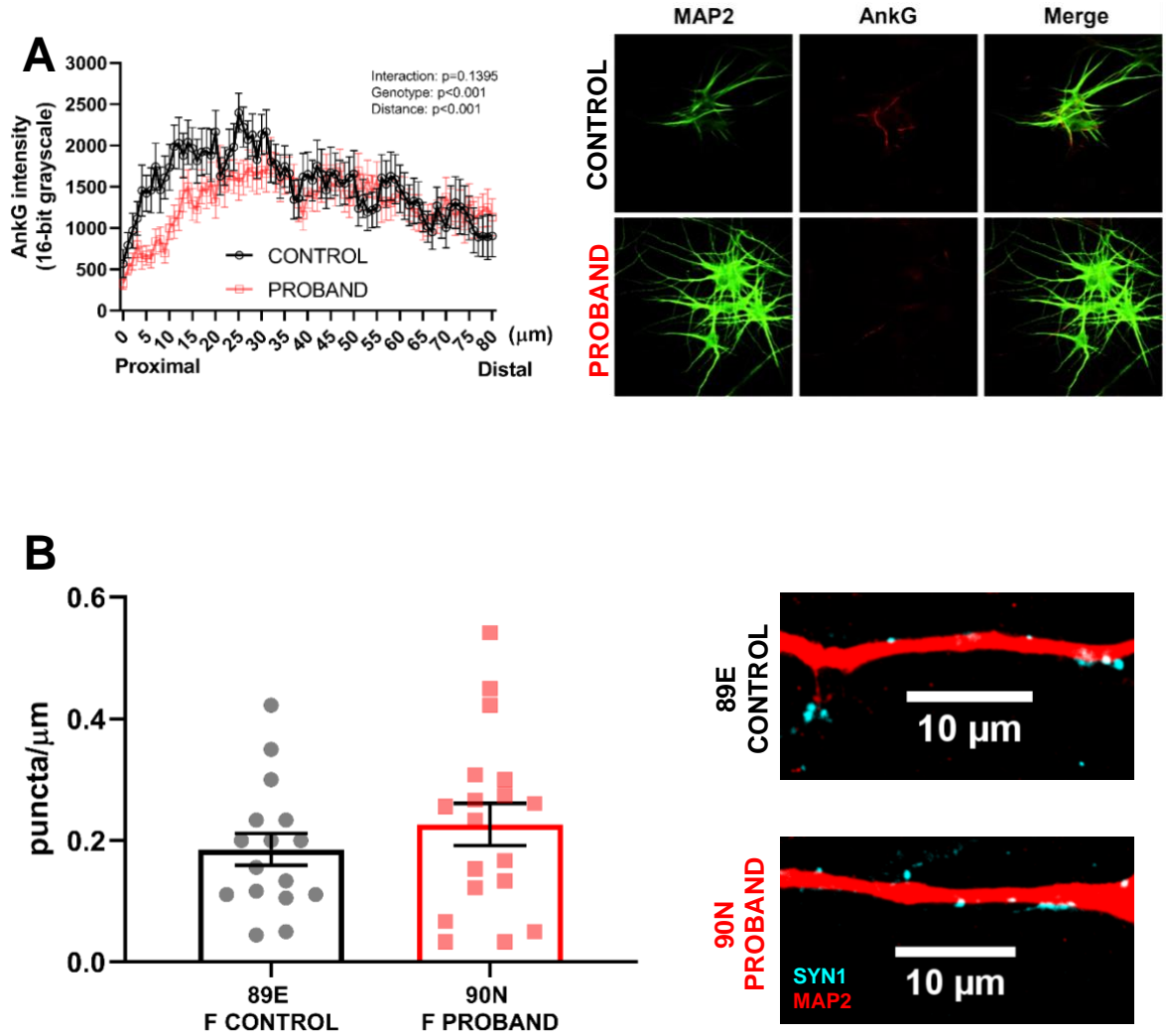


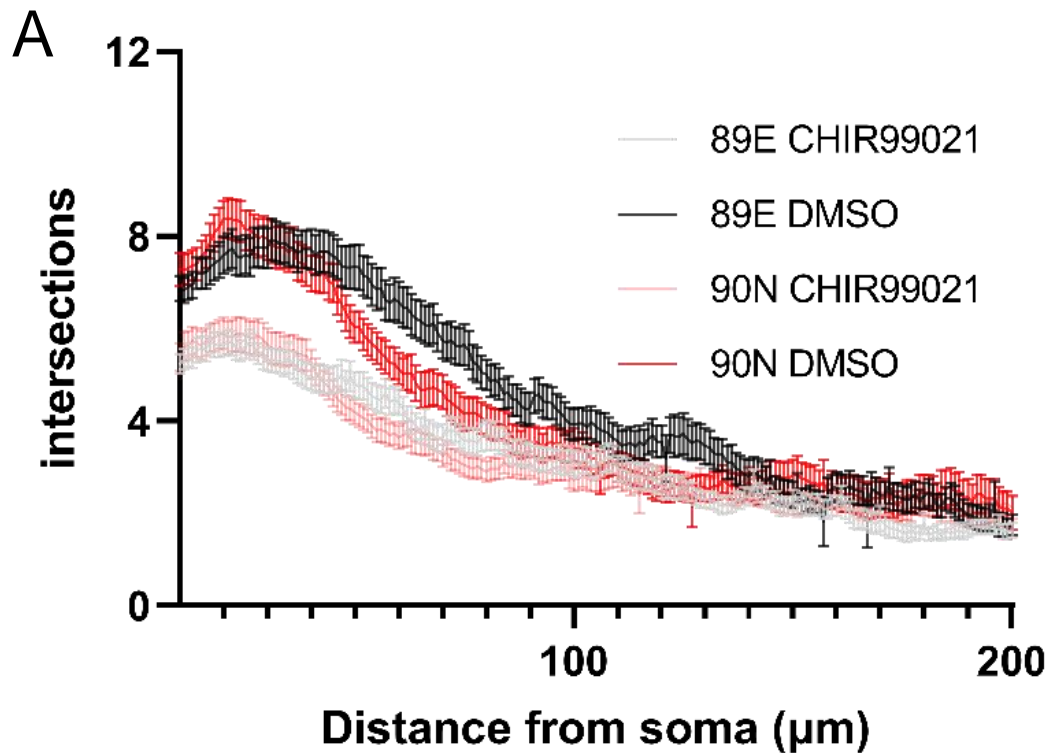
**Figure 4.5.6: Disruption of the axon initial segment in a 15q13.3**

**microdeletion proband**

(A) AIS: CONTROL n = 22, PROBAND n = 31. N=3 infections. Analyzed by Two-Way ANOVA with Dunnett's posthoc test. \*p<0.01

(B) SYNAPTIC PUNCTA: N=2 infections, Parental control n=16, 15q13.3 proband n=18. Data shown as Mean ± SD. 25,000 iN/50,000 glia per 12 mm coverslip, fixed at DIV28.

**Figure 4.5.7: Arborization complexity of control and proband lines is decreased by ChIR99021 administration**



**B**

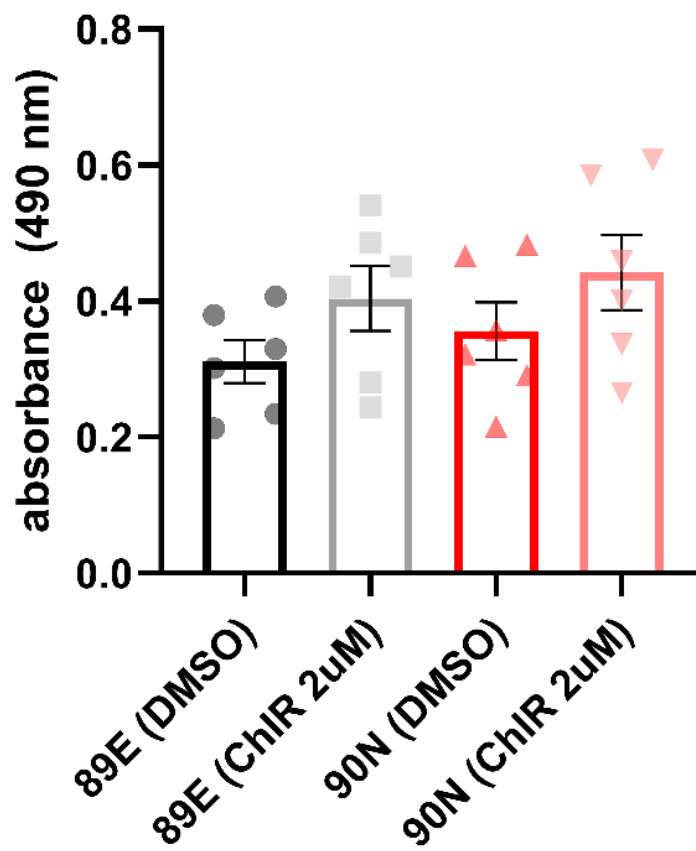
ANOVA table	SS (Type III)	DF	MS	F (DFn, DFd)	P value
Distance	105552	200	527.8	F (200, 38244) = 94.83	P<0.0001
Genotype	255.9	1	255.9	F (1, 38244) = 45.99	P<0.0001
Treatment	10040	1	10040	F (1, 38244) = 1804	P<0.0001
Distance x Genotype	2299	200	11.49	F (200, 38244) = 2.065	P<0.0001
Distance x Treatment	5846	200	29.23	F (200, 38244) = 5.252	P<0.0001
Genotype x Treatment	285.8	1	285.8	F (1, 38244) = 51.35	P<0.0001
Distance x Genotype x Treatment	526.6	200	2.633	F (200, 38244) = 0.4731	P>0.9999
Residual	212838	38244	5.565		

**Figure 4.5.7: Arborization complexity of control and proband lines is decreased by ChIR99021 administration**

Sholl analysis for both control (89E) and 15q13.3 microdeletion proband (90N), with and without 2  $\mu$ M ChIR99021 administration.

Three-way ANOVA (Distance F (200, 38244) = 94.83  $P < 0.0001$ ; Genotype F (1, 38244) = 45.99  $P < 0.0001$ ; Treatment F (1, 38244) = 1804  $P < 0.0001$ ; Distance x Genotype F (200, 38244) = 2.065  $P < 0.0001$ ; Distance x Treatment F (200, 38244) = 5.252  $P < 0.0001$ ; Genotype x Treatment F (1, 38244) = 51.35  $P < 0.0001$ ; Distance x Genotype x Treatment F (200, 38244) = 0.4731  $P > 0.9999$   
N=3 infections, 89E DMSO n=56, 89E CHIR n=60, 90N DMSO n=66, 90N ChIR99021 n=63).

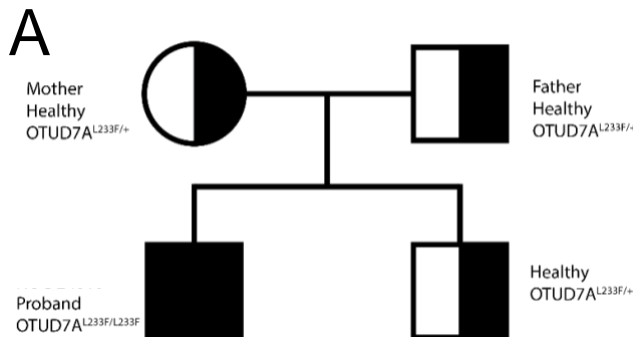
**Figure 4.5.8: LDH levels are not significantly altered by short-term (3d) ChIR99021 administration**



**Supplementary Figure 4.5.2: LDH levels are not significantly altered by short-term (3d) ChIR99021 administration**

LDH assay shows no significant effect of short-term (3-day) ChIR99021 administration. Analyzed by two-way ANOVA (Interaction:  $F(1, 20) = 0.005460$   $P=0.9418$ , Treatment:  $F(1, 20) = 3.951$   $P=0.0607$ , Genotype:  $F(1, 20) = 0.8600$   $P=0.3648$ ).  $N=3$  biological replicates, each datapoint represents three averaged technical replicates.

**Figure 4.5.9: Homozygous L233F mutation in OTUD7A catalytic region in a patient with seizures and developmental delay**



SEX	PROBAND RELATION	MUTATIONS	NEUROPSYCHIATRIC PROFILE	OTHER PERTINENT CLINICAL DATA	STATUS
F	MOTHER	OTUD7A <sup>L233F/wt</sup> 14q12del (245 kb)	-	Nonspecific learning disorder	CARRIER
M	<b>PROBAND</b>	OTUD7A <sup>L233F/L233F</sup> 14q12del (245 kb)	Epileptic encephalopathy (absence seizures), motor delay, global developmental delay	-	<b>HOMOZYGOUS</b>
M	BROTHER	OTUD7A <sup>L233F/wt</sup>	-	Nonspecific learning disorder	CARRIER
M	FATHER	OTUD7A <sup>L233F/wt</sup>	-	Nonspecific learning disorder	CARRIER

## **4.6 Discussion**

### **4.6.1 Disruption of the axon initial segment in a 15q13.3 microdeletion disorder proband**

Quantification of the AIS in a 15q13.3 microdeletion proband showed decreased proximal intensity compared to the familial control. As this experiment required specialized imaging technology and a collaborator's assistance, we were not able to pursue a ChIR99021 treatment study to assess the impacts on the AIS.

However, it is noteworthy that the AIS is disrupted at baseline in this disorder, particularly given the known actions of GSK3 signalling at this locus.

Note that while there were disturbances to action potential properties in a genotype-selected manner this was not evidently reflected in the Sholl analysis which showed similar suppression of dendritic branching complexity in both genotypes. Sholl analysis re-demonstrated the proximal dendritic complexity deficits in the proband demonstrated in Figure 2.5.7.

While axon projection was not assessed in response to GSK3 inhibition, it is noteworthy that GSK3 is known to phosphorylate tau (Gomez-Ramos et al., 2006; Kanai et al., 2009; Yang et al., 1993; Yang et al., 1994), and that GSK3 inhibition has been shown to rescue deficits in microtubule dynamics secondary to Ankyrin-G disruption (Garza et al., 2018). The significance of this in our model is unclear, but will be an important source of future investigation to further relate neurite and axonal outgrowth deficits to our findings.

#### **4.6.2 Paradoxical impacts of GSK3 inhibition in a 15q13.3 microdeletion proband**

The work in this chapter highlights the differential role of GSK3 signalling in a 15q13.3 microdeletion family. Interestingly, the proband could be described as comparatively resistant to the functional effects of this GSK3 inhibition, as it did not manifest the expected action potential or sodium current disturbances anticipated.

Interestingly, only the control line was responsive to acute 2  $\mu$ M ChIR99021 administration at approximately four weeks, showing deformations to the action potential amplitude and width. Chronic 2  $\mu$ M ChIR99021 administration was assessed by multi-electrode array recordings. In the acute phase of these treatments, there were likewise genotype-specific differences, but these were largely buried by suppression of most spiking frequency metrics thereafter. Previously published work suggests that ChIR99021 administration is capable of modulating sodium currents in a manner dependent on specific channel and neuron subtypes (Scala et al., 2018), and this is possible contributory to the observed changes presented here. There are also known effects of GSK3 at the AIS diminishing sodium current amplitude (Tapia et al., 2013), which we could reproduce in WT but not HET. Given this, there is reason to believe that there is altered GSK3 regulation of the AIS assembly in these patients (Tapia et al., 2013). Moreover, GSK3 activity is implicated in the regulation of both sodium and potassium channels (James et al., 2015; Marosi et al., 2022), and its altered

baseline function and response to inhibitory signals might underlie susceptibility to abnormal intrinsic properties in these neurons. It is doubly interesting that these findings are demonstrable in the 15q13.3del family from this study which did not show any electrophysiologic differences at baseline.

While the administered dose of ChIR99021 was below the typical dose used for the induction of Wnt signaling, as we did not assay Wnt activation directly it remains possible that some level of Wnt signaling modulation was present and contributed to the finding presented in this chapter. Further, while GSK3 is the primary target of ChIR99021, there is some evidence to suggest that off-target effects are expected at micromolar ranges of drug administration. Further studies (including both GSK3 knockdown/inhibition by other means, as well as using lower ChIR99021 concentrations) will be required to better isolate the effects of GSK3 inhibition alone on observed phenotypes.

#### **4.6.3 Altered proband response to GSK3 inhibition is not explained by cytotoxicity**

Interestingly, while the action potential properties showed a paradoxical response to GSK3 inhibition in the 15q13.3 microdeletion proband, this was not reflected in GSK3 or pGSK3 levels as determined by Western blot (Figure 4.5.5). Levels of both GSK3 and pGSK3 were decreased on ChIR99021 administration, but this was directionally consistent across both probands and controls. There were also no differences in either GSK3 or pGSK3 levels between the control and proband

lines. Additionally, there did not appear to be significantly different LDH levels, and cytotoxicity is unlikely to play a major role in the action of ChIR99021.

One possible interpretation of these findings is that while GSK3 and pGSK3 levels respond normally to ChIR99021 administration (by decreasing), the underlying “tone” of GSK3 action is different between control and proband lines. For example, if the proband line had lower GSK3 “tone” managing sodium current action and GSK3 was inhibited there would be a smaller noted effect. Future experiments to measure GSK3 $\alpha$  levels will be necessary to identify the details of this change, and the consequences on downstream signalling pathways. However, it is important to note that interpretation of GSK3 $\beta$  and pGSK3 $\beta$  levels is complicated by the apparent saturation of  $\alpha$ -tubulin. It is also unusual that GSK3 $\beta$  levels were decreased (Lee et al., 2021).

#### **4.6.4 Limitations**

While this chapter does highlight the use of a highly potent and specific GSK3 antagonist in ChIR99021, additional work would be required to increase confidence in the underlying pathway which is implicated. GSK3 signalling is a plausible explanation for the perturbations observed given evidence from previous studies regarding the expected changes to currents (Scala et al., 2018), and this is supported by several lines of evidence presented in this chapter. For example, knock-downs of GSK3 could be performed alongside ChIR99021 administration to identify if there would be any residual effects of drug administration related to genotype-specific functional impairment.

Another limitation posed by the work in this chapter is the differential timeline across which ChIR99021 was administered. It became clear from the MEA experiments that prolonged administration would result in suppression of spiking activity, and it is evident from the LDH assay that even short-duration administration of this drug is a stressor. Longer-term administration of this drug appeared to produce significant suppression in firing activity, and given the stress induced, it remains unclear the degree of contribution from alterations in GSK3 signalling compared to generalized stress.

The loading control difficulties described above also limit the interpretation of the shown Western blot in identifying the contribution, if any, of absolute GSK3 $\beta$  and pGSK3 $\beta$  levels on the observed functional differences. Note also that at the ChIR99021 concentration used there remains the possibility of both off-target effects (Lee et al., 2021) and induction of Wnt-signaling. The experiments presented herein do not assess the extent of these, and as such they cannot be ruled out as potentially contributory.

While there was not a detected significant effect of ChIR99021 administration on LDH levels, it is probable that there was a durable effect of both short-term and persistent GSK3 inhibition on cellular stress. Additionally, the media tested in this study were drawn from experimental wells with co-cultured iNs and CD1 mouse glia. Where only the iN LDH response was of interest, the effect of glial background LDH response might have a dilutive effect.

#### 4.6.5 Future directions

Given the well-characterized action of GSK3 in the AIS and in modulating sodium currents, the paradoxical reaction identified in the Family 1 15q13.3 microdeletion proband highlights a potentially new mechanism by which our previously reported AIS disruption might produce functional impairments which underlie disease pathogenesis. This finding also extends the discovery of the AIS as a novel region of overlap in NDDs and other neuropsychiatric diseases.

While GSK3 inhibition using similar doses of ChIR99021 is a possible mechanism of Wnt-signalling induction (Huang et al., 2017), the possible impact of this was not assessed in this study. However, as both work contained in this thesis (Figure 3.5.6B) and by others (Zhang et al., 2019) have highlighted Wnt signalling-related pathways as potentially implicated in this disorder, further work will be required to better identify the mechanisms involved. However, the present work does partially isolate for the effects of GSK3 in this way, and provide valuable insights related to GSK3-specific signalling.

We also described a family harbouring a leucine-to-phenylalanine substitution within the catalytic domain of OTUD7A (Figure 4.5.9). The consanguineous parents both harboured a copy of the so-named L233F mutation, and the proband of note was homozygous for this mutation (OTUD7A<sup>L233F/L233F</sup>). This family was described in a 2020 report published in *Clinical Genetics* (Garret et al., 2020). In our recent publication, the mutation harboured by this patient resulted in instability of AnkG and decreased levels at the AIS (Unda et al., 2023). This

proband presents with severe epileptic encephalopathy, in marked contrast to his brother, mother and father who are all heterozygous carriers of the same mutation. While the family members presented with intellectual impairment and learning difficulties, they were not reported to have seizure disorders. The proband also had a 14q12 deletion inherited from his mother, though this was of uncertain clinical significance. While we did characterize data from this proband, in the absence of a familial control I did opt not to include that work in this thesis.

## **Chapter 5: Discussion**

A pertinent discussion of the results presented in this thesis is presented in the corresponding section for each chapter. The discussion in this section is aimed at providing a higher-level discussion of topics related to the work contained in this thesis, and how it might be extended in the future.

### **Insights into disease pathogenesis in the 15q13.3 microdeletion disorder**

The 15q13.3 microdeletion disorder represents a highly heterogeneous disorder at both the clinical and cellular levels. In this study, we have profiled neurogenin-2-induced neurons from three 15q13.3 microdeletion patients and familial controls, finding a consistent trend of functional abnormalities related to action potential initiation and firing, as well as impaired neurite outgrowth. We followed up this work by profiling the transcriptome of two families. This revealed previously unknown clustering of DEGs at the 6p chromosomal region in both families, identified neurodevelopmentally relevant biological processes which were altered, while also highlighting differences in the overall transcriptome potentially underlying family-specific differences in clinical disease.

At a granular level, the data here present a mixed picture whereby the separate 15q13.3 microdeletion families all show variations in the cellular phenotyping as well as the clinical presentation without a straightforward way to link the two mechanistically. However, at a higher level, we are presented with general structural defects and variations on the theme of a cell population, which has narrowly compensated for a developmental insult in order to preserve core

functionality. The preliminary transcriptomic analyses are suggestive of primary clustering occurring by family, although with clear separations between control and proband lines. Indeed, the use of a potent GSK3 inhibitor revealed the existence of clear differences in the regulation of action potential dynamics between a control and proband line. Taken together, these data suggest a picture of subtle molecular dysfunction which manifests in slightly varied cellular phenotypes that in turn have the potential to accumulate and increase the proclivity towards the development of clinical disease. This is not a surprising finding and echoes the real-world manifestation of the 15q13.3 microdeletion, which is variable in penetrance and presentation. Future studies will expand the patient index to continue developing a series of clinically correlated core phenotypes, aiding understanding of both the 15q13.3 microdeletion and neurodevelopmental disorders more broadly.

One of the difficulties associated with the study of rare genetic disorders of variable penetrance is the generation of suitable controls. Solutions to this must often manage a trade-off between the proven pathogenicity of the genetic makeup in a patient line and the matching of genetic background in an isogenic line. Stated another way, correcting a mutation in a patient line to create an isogenic control leaves open the question of whether this line would be a control at the clinical phenotype level. Similarly, introducing a mutation to an established cell line leaves open the question of whether the newly edited line would have a pathological clinical phenotype. The project described in this thesis used familial

controls, aiming to strike a balance between clinical certainty over disease status and offering as close a genetic match as is feasible to obtain. The drawback to this approach is in the genetic variation between the proband and familial control. This is potentially additionally complicating for various neurodevelopmental disorders, many of which appear to result from accumulated genetic insults, where the specificity of genetic makeup may be a factor of outsized import. Many studies attempt to circumvent these issues by adopting a hybrid design. In one common example of this, patient samples may be pooled together in experiments and compared against a group of reference controls. Often, these controls will be totally unrelated to the families, and drawn either from central biobanks or volunteer donors. Studies may attempt to manage the heterogeneity introduced by this design by attempting to match these controls to the probands on factors such as age, sex, and ethnicity (among others). This approach carries many of the same advantages and caveats as using familial controls, as it orients the groups around clinical phenotype at the expense of genetic variation. However, this design also introduces an additional trade-off between the apparent increase in validity and/or power introduced by sample pooling and the possibility of differences between lines cancelling one another out when combined. This consideration is amplified in importance for disorders such as the one studied here, where a mixed clinical picture and indeterminate biomarkers require studies to dissect mechanisms more finely, rather than aim for bulk findings using conventional measures.

The stratification of analyses in this study by family attempted to address these points directly. One of the major advantages of this method can be noted by comparing within-family variation to between-family variation. Despite the highly controlled and reductive nature of the model used, there remained considerable differences in lines derived from different families. This might be the case for many reasons. Contributing factors include (but are not limited to) familial genetic background, precise nature of the microdeletion, reprogramming batch, neurogenin-2 infection, induction, and general reagent variation. While quality control benchmarks were regularly checked to minimize the impact of these factors, they were undoubtedly a source of variation in this work. Because the natural comparison was within-family, we aimed to minimize sources of variation in those comparisons. The size of this project also precluded the concurrent completion of reprogramming and inductions for all families. Therefore, simultaneous reprogramming and infection were limited to each family (replicates were frozen down from sister wells post-infection to control for this as well). The family-stratified design also accounted for as much of the background genetic variation as was feasible for this study.

The design of this study was instead able to draw out differences in other key areas. There are two specific points that demonstrate the strengths of the approach used. The first is the absolute scale of the differences in key parameters between both families. A clear example of this is the difference in magnitude of axon lengths between Family 3 and the other families (Figure

2.5.6). The second point is more subtle, and related to the possible range within which the parameters themselves might vary. The clinical disorders which are associated with the 15q13.3 microdeletion occupy a range between a healthy (or subclinical) state and a severe presentation which is either highly debilitating or incompatible with life. The disorders themselves are clinically diagnosed, and with limited exceptions (such as seizure disorders) there are no biologically diagnostic markers of disease. These presentations and prevalence of these disorders can, therefore, be thought of as under a survival bias of sorts. A parallel can be considered with respect to assayed parameters of the iNs from the different lines. In addition to the comparative homogeneity of the system, the functional parameters are themselves also constrained in the degree to which they might vary. For many parameters, only slight differences are possible.

### **A platform for the investigation of rare genetic disorders underlying neurodevelopmental disorders**

The experimental approach undertaken in this thesis was novel in several ways and may serve in whole or part as a model for future investigations of the 15q13.3 microdeletion disorder and other similar disorders.

This project contributes to the field of genetic neurodevelopmental disorder study, specifically to the study of pathogenic copy number variants (CNVs). As a part of the 15q13.3 microdeletion literature, it contributes the largest study at its depth of functional and morphological phenotyping. The transcriptomic analyses conducted within this study are comparatively rare for the model system as well,

in that the iNs used were grown on mouse glia (as were all other cultures in this study). This has two advantages. The first is that iNs are more robust when grown on glia, allowing them to be maintained to later timepoints and develop more complex neuronal structures, which increases the likelihood of disease-relevant findings (Meijer et al., 2019; Y. Zhang et al., 2013). The second is that using a mixed-species system allows for the computational separation of mouse and human transcripts. In the iN/mouse glia co-culture model, this also separates the reads between neurons and glia. The benefit of this is that bulk RNAseq read depths can be obtained on the homogenous target population of neurons (Burke et al., 2020). Finally, we pursued a drug administration study in one family to identify differential responses between the patient and control, as a way to identify differences in signalling pathways between these conditions. The use of multiple 15q13.3 microdeletion family-derived neurons for the study of functional, morphological, and molecular disturbances contributes important pathophysiologic insights to the 15q13.3 microdeletion literature and an investigational roadmap to the broader NDD literature.

### **Future directions**

While the work in this thesis has provided novel insights into the cellular phenotypes and mechanisms contributing to disease pathogenesis in 15q13.3 microdeletion disorder, much further work remains to be completed.

While the in-depth case series conducted with these patient families does comprise the core experimental approach of this paper, as mentioned previously,

there are other possible condition-control arrangements that might be pursued. Part of the work in this thesis can be thought of as contributing “qualitative” findings to the body of knowledge related to this disorder by drawing out general dysfunctions to axonal properties in structure and function. Notably, these differences would have been more difficult to detect or obfuscated with the pooling of cases and controls, respectively. It would also have been potentially more difficult to interpret these results in the context of a nonrelated control. However, given the pattern of findings across multiple families identified in this study, other experimental designs may now be tenable for the investigation of more targeted loci of neuronal dysfunction in this disorder.

While timing did not permit more extensive phenotyping of multiple families, this is a clear next step for the project. Continuing to identify the phenotypic spectrum of this disorder at multiple levels will add further insight into commonalities and differences underlying disease.

Future work on this study will also expand into more complex models with varied structural organization and/or cellular compositions (e.g., organoids). In addition to being more “valid” systems (Hong & Do, 2019; Lancaster & Knoblich, 2014; Lancaster et al., 2013; Marton & Pasca, 2020; Mayhew & Singhania, 2022), profiling other neuronal subtypes remains an essential part of any unifying theory of these disorders. As described in the introduction to this thesis, many of the models used to frame investigative questions in NDD research are related to structural or functional parameters which are considered to be disease causing at

extrema. For all these parameters however, regulation is managed by a diverse set of so populations and molecular signaling pathways. For example, under an “excitation slash inhibition” model, even a highly simplified system still requires both excitatory and inhibitory neuronal populations. Indeed, even for the 15q13.3 microdeletion studied in this thesis, not only are seizures a core phenotype, but evidence from mouse models highlights dysfunction in parvalbumin positive interneurons. The causes of these disorders are multifold even beyond this. While many models have high plausibility because of their evident relatedness to either clinical features of the disorders, or easily identifiable structural and or functional features of neural tissue, we now know that many other generalized pathways (for example those related to cellular energetics, immune function, and “cell state” level dysfunction to the transcriptome/proteome) are implicated in disease pathogenesis. With particular reference to altered immunologic pathways describing in Chapter 3, while it is possible that the regional targeting of the 6p21-22 region is secondary to 3D architectural changes associated with the microdeletion and are thus cell-type independent, the model system used in this study is not capable of fully elucidating the consequences of this on disease pathogenesis. It does provide interesting evidence in support of genetic alteration on a more likely architectural vs functional basis, and further investigation of other cell population whose function would more likely be altered by these changes (notably microglia) is required. Ultimately, however, this will require more advanced experimental designs to characterize. For example, in addition to more

complex models which organically produce complex cell populations (for example EB or organoid methods), there are additional directed differentiation protocols for the derivation of other neuronal and glial subtypes (Allen et al., 2022; Heider et al., 2021; Marton & Pasca, 2020). While we did attempt co-cultures using both the iNs described in this study and inhibitory interneuron populations following a previously described protocol (Barretto et al., 2020; Yang et al., 2017), time constraints did not allow for the inclusion of that work in this thesis. However, there are many possible experimental designs (particularly factorial ones), which could investigate co-culture of excitatory, inhibitory, and glial cells derived from both patient and family lines (Allen et al., 2022; Boecking et al., 2022). However, this project has demonstrated the clear advantages of profiling a reductive model for the purposes of minimized variance in phenotype discovery and sensitive pathway discovery.

One other area of possible future work is the investigation of patients with mutations to specific genes within this disorder. Our group has published on the contribution of OTUD7A as a driver gene underlying disease pathogenesis in the 15q13.3 microdeletion disorder (Uddin et al., 2018). We also performed early phenotyping on iNs derived from the previously mentioned OTUD7A<sup>L233F/L233F</sup> patient described above, though in the absence of a matched control line, this work was not included in the thesis. Note that this patient poses difficulty in disambiguating the known genetic factors (namely his homozygous mutation status and additional 14p12 microdeletion) from those of his family members. It

does seem probable that the incremental mutation to the OTUD7A<sup>L233F</sup> locus is responsible for the pronounced clinical presentation compared to those of his family members. However, of the available familial samples, an edited line would have to be generated for the development of a control sample and this does carry the difficulty of having uncertain clinical significance. Ultimately, either correction of this mutation in the patient line or the introduction of this mutation (in heterozygous and homozygous form) to an established reference line will likely prove to be the best approach for the cellular characterization of this mutation.

### **Concluding remarks**

The bulk of the work in this thesis has focused on presenting cellular and molecular-level data from 15q13.3 microdeletion family iNs. However, equally important has been the approach taken to interrogate this microdeletion. The work presented here followed from patient clinical data (including neuropsychiatric and structural brain findings), through cellular findings (network activity, action potential metrics, and axon projection), and identified a novel finding linked to a highly implicated NDD target pathway (paradoxical response to GSK3 inhibition in the proband). The use of comparatively unbiased pathway discovery techniques (RNA sequencing) bolstered and corroborated these findings, but did not serve as a substitute to a careful analysis of subtle findings which might otherwise have been missed in the search for clear and obvious answers. While the heterogeneity of this disorder does make it difficult to determine which findings will translate, it is my hope that as much as this thesis

has contributed novel insights at multiple layers of pathobiologic abstraction which will build towards a unified understanding and treatment of this disorder and others, it has also showcased a careful and directed interrogation through these layers as well.

## References

- Adams, C. E., Yonchek, J. C., Schulz, K. M., Graw, S. L., Stitzel, J., Teschke, P. U., & Stevens, K. E. (2012). Reduced Chrna7 expression in mice is associated with decreases in hippocampal markers of inhibitory function: implications for neuropsychiatric diseases. *Neuroscience*, *207*, 274-282.  
<https://doi.org/10.1016/j.neuroscience.2012.01.033>
- Agarwal, A. K., Tunison, K., Dalal, J. S., Nagamma, S. S., Hamra, F. K., Sankella, S., Shao, X., Auchus, R. J., & Garg, A. (2017). Metabolic, Reproductive, and Neurologic Abnormalities in Agpat1-Null Mice. *Endocrinology*, *158*(11), 3954-3973. <https://doi.org/10.1210/en.2017-00511>
- Aldinger, K. A. (2009). Copy number variation at 1q21.1 results in a spectrum of developmental abnormalities. *Clinical Genetics*, *75*(5), 425-427.  
[https://doi.org/10.1111/j.1399-0004.2009.01186\\_2.x](https://doi.org/10.1111/j.1399-0004.2009.01186_2.x)
- Allen, M., Huang, B. S., Notaras, M. J., Lodhi, A., Barrio-Alonso, E., Lituma, P. J., Wolujewicz, P., Witztum, J., Longo, F., Chen, M., Greening, D. W., Klann, E., Ross, M. E., Liston, C., & Colak, D. (2022). Astrocytes derived from ASD individuals alter behavior and destabilize neuronal activity through aberrant Ca(2+) signaling. *Mol Psychiatry*, *27*(5), 2470-2484.  
<https://doi.org/10.1038/s41380-022-01486-x>
- Andersson, E. R., & Lendahl, U. (2014). Therapeutic modulation of Notch signalling — are we there yet? *Nature Reviews Drug Discovery*, *13*(5), 357-378.  
<https://doi.org/10.1038/nrd4252>
- Ando, K., Ferlini, L., Suain, V., Yilmaz, Z., Mansour, S., Le Ber, I., Bouchard, C., Leroy, K., Durr, A., Clot, F., Sarazin, M., Bier, J. C., & Brion, J. P. (2020). de novo MAPT mutation G335A causes severe brain atrophy, 3R and 4R PHF-tau pathology and early onset frontotemporal dementia. *Acta Neuropathol Commun*, *8*(1), 94.  
<https://doi.org/10.1186/s40478-020-00977-8>
- Antonacci, F., Dennis, M. Y., Huddleston, J., Sudmant, P. H., Steinberg, K. M., Rosenfeld, J. A., Miroballo, M., Graves, T. A., Vives, L., Malig, M., Denman, L., Raja, A., Stuart, A., Tang, J., Munson, B., Shaffer, L. G., Amemiya, C. T., Wilson, R. K., & Eichler, E. E. (2014). Palindromic GOLGA8 core duplicons promote chromosome 15q13.3 microdeletion and evolutionary instability. *Nat Genet*, *46*(12), 1293-1302. <https://doi.org/10.1038/ng.3120>
- Antonell, A., Del Campo, M., Magano, L. F., Kaufmann, L., Martinez de la Iglesia, J., Gallastegui, F., Flores, R., Schweigmann, U., Fauth, C., Kotzot, D., & Perez-Jurado, L. A. (2009). Partial 7q11.23 deletions further implicate GTF2I and GTF2IRD1 as the main genes responsible for the Williams-Beuren syndrome neurocognitive profile. *Journal of Medical Genetics*, *47*(5), 312-320.  
<https://doi.org/10.1136/jmg.2009.071712>
- APA. (2013). *Diagnostic and statistical manual of mental disorders : DSM-5™* (5th edition. ed.). American Psychiatric Publishing, a division of American Psychiatric Association.
- Arora, A., Minogue, P. J., Liu, X., Addison, P. K., Russel-Eggitt, I., Webster, A. R., Hunt, D. M., Ebihara, L., Beyer, E. C., Berthoud, V. M., & Moore, A. T. (2008). A novel connexin50 mutation associated with congenital nuclear pulverulent cataracts. *Journal of Medical Genetics*, *45*(3), 155-160.  
<https://doi.org/10.1136/jmg.2007.051029>

- Ates, T., Oncul, M., Dilsiz, P., Topcu, I. C., Civas, C. C., Alp, M. I., Aklan, I., Ates Oz, E., Yavuz, Y., Yilmaz, B., Sayar Atasoy, N., & Atasoy, D. (2019). Inactivation of Magel2 suppresses oxytocin neurons through synaptic excitation-inhibition imbalance. *Neurobiology of Disease*, 121, 58-64.  
<https://doi.org/10.1016/j.nbd.2018.09.017>
- Avila-Mendoza, J., Subramani, A., Sifuentes, C. J., & Denver, R. J. (2020). Molecular Mechanisms for Kruppel-Like Factor 13 Actions in Hippocampal Neurons. *Mol Neurobiol*, 57(9), 3785-3802. <https://doi.org/10.1007/s12035-020-01971-w>
- Bacchelli, E., Battaglia, A., Cameli, C., Lomartire, S., Tancredi, R., Thomson, S., Sutcliffe, J. S., & Maestrini, E. (2015). Analysis of CHRNA7 rare variants in autism spectrum disorder susceptibility. *Am J Med Genet A*, 167A(4), 715-723.  
<https://doi.org/10.1002/ajmg.a.36847>
- Barak, B., Zhang, Z., Liu, Y., Nir, A., Trangle, S. S., Ennis, M., Levandowski, K. M., Wang, D., Quast, K., Boulting, G. L., Li, Y., Bayarsaihan, D., He, Z., & Feng, G. (2019). Neuronal deletion of Gtf2i, associated with Williams syndrome, causes behavioral and myelin alterations rescuable by a remyelinating drug. *Nature Neuroscience*, 22(5), 700-708. <https://doi.org/10.1038/s41593-019-0380-9>
- Barber, J. C. K., Rosenfeld, J. A., Foulds, N., Laird, S., Bateman, M. S., Thomas, N. S., Baker, S., Maloney, V. K., Anilkumar, A., Smith, W. E., Banks, V., Ellingwood, S., Kharbutli, Y., Mehta, L., Eddleman, K. A., Marble, M., Zambrano, R., Crolla, J. A., & Lamb, A. N. (2013). 8p23.1 duplication syndrome; common, confirmed, and novel features in six further patients. *American Journal of Medical Genetics Part A*, 161(3), 487-500. <https://doi.org/10.1002/ajmg.a.35767>
- Barretto, N., Zhang, H., Powell, S. K., Fernando, M. B., Zhang, S., Flaherty, E. K., Ho, S. M., Slesinger, P. A., Duan, J., & Brennand, K. J. (2020). ASCL1- and DLX2-induced GABAergic neurons from hiPSC-derived NPCs. *J Neurosci Methods*, 334, 108548. <https://doi.org/10.1016/j.jneumeth.2019.108548>
- Bassett, A. S., Marshall, C. R., Lionel, A. C., Chow, E. W. C., & Scherer, S. W. (2008). Copy number variations and risk for schizophrenia in 22q11.2 deletion syndrome. *Human Molecular Genetics*, 17(24), 4045-4053.  
<https://doi.org/10.1093/hmg/ddn307>
- Basu, S. N., Kollu, R., & Banerjee-Basu, S. (2009). AutDB: a gene reference resource for autism research. *Nucleic Acids Res*, 37(Database issue), D832-836.  
<https://doi.org/10.1093/nar/gkn835>
- Bates, R. C., Stith, B. J., Stevens, K. E., & Adams, C. E. (2014). Reduced CHRNA7 expression in C3H mice is associated with increases in hippocampal parvalbumin and glutamate decarboxylase-67 (GAD67) as well as altered levels of GABA(A) receptor subunits. *Neuroscience*, 273, 52-64.  
<https://doi.org/10.1016/j.neuroscience.2014.05.004>
- Bekpen, C., & Tautz, D. (2019). Human core duplicon gene families: game changers or game players? *Briefings in functional genomics*, 18(6), 402-411.  
<https://doi.org/10.1093/bfgp/elz016>
- Béna, F., Bruno, D. L., Eriksson, M., van Ravenswaaij-Arts, C., Stark, Z., Dijkhuizen, T., Gerkes, E., Gimelli, S., Ganesamoorthy, D., Thuresson, A. C., Labalme, A., Till, M., Bilan, F., Pasquier, L., Kitzis, A., Dubourg, C., Rossi, M., Bottani, A., Gagnebin, M., . . . Schoumans, J. (2013). Molecular and clinical characterization of 25 individuals with exonic deletions of *NRXN1* and comprehensive review of the literature. *American Journal of Medical Genetics Part B*:

- Neuropsychiatric Genetics*, 162(4), 388-403.  
<https://doi.org/10.1002/ajmg.b.32148>
- Benchling. (2023). *Benchling*. In Benítez-Burraco, A., Barcos-Martínez, M., Espejo-Portero, I., Fernández-Urquiza, M., Torres-Ruiz, R., Rodríguez-Perales, S., & Jiménez-Romero, M. S. (2018). Narrowing the Genetic Causes of Language Dysfunction in the 1q21.1 Microduplication Syndrome. *Frontiers in pediatrics*, 6, 163-163.  
<https://doi.org/10.3389/fped.2018.00163>
- Bernier, R., Steinman, K. J., Reilly, B., Wallace, A. S., Sherr, E. H., Pojman, N., Mefford, H. C., Gerdtts, J., Earl, R., Hanson, E., Goin-Kochel, R. P., Berry, L., Kanne, S., Snyder, L. G., Spence, S., Ramocki, M. B., Evans, D. W., Spiro, J. E., Martin, C. L., . . . Simons, V. I. P. c. (2016). Clinical phenotype of the recurrent 1q21.1 copy-number variant. *Genet Med*, 18(4), 341-349. <https://doi.org/10.1038/gim.2015.78>
- Blumenthal, I., Ragavendran, A., Erdin, S., Klei, L., Sugathan, A., Guide, J. R., Manavalan, P., Zhou, J. Q., Wheeler, V. C., Levin, J. Z., Ernst, C., Roeder, K., Devlin, B., Gusella, J. F., & Talkowski, M. E. (2014). Transcriptional consequences of 16p11.2 deletion and duplication in mouse cortex and multiplex autism families. *Am J Hum Genet*, 94(6), 870-883.  
<https://doi.org/10.1016/j.ajhg.2014.05.004>
- Boecking, B., Usuyama, N., Bannur, S., Castro, D. C., Schwaighofer, A., Hyland, S., Wetscherek, M., Naumann, T., Nori, A., & Alvarez-Valle, J. (2022). Making the Most of Text Semantics to Improve Biomedical Vision--Language Processing. *arXiv preprint arXiv:2204.09817*.
- Bolzer, A., Kreth, G., Solovei, I., Koehler, D., Saracoglu, K., Fauth, C., Muller, S., Eils, R., Cremer, C., Speicher, M. R., & Cremer, T. (2005). Three-dimensional maps of all chromosomes in human male fibroblast nuclei and prometaphase rosettes. *PLoS Biol*, 3(5), e157. <https://doi.org/10.1371/journal.pbio.0030157>
- Bourgeron, T. (2015). From the genetic architecture to synaptic plasticity in autism spectrum disorder. *Nat Rev Neurosci*, 16(9), 551-563.  
<https://doi.org/10.1038/nrn3992>
- Breen, M. S., Fan, X., Levy, T., Pollak, R. M., Collins, B., Osman, A., Tocheva, A. S., Sahin, M., Berry-Kravis, E., Soorya, L., Thurm, A., Powell, C. M., Bernstein, J. A., Kolevzon, A., Buxbaum, J. D., & Developmental Synaptopathies, C. (2023). Large 22q13.3 deletions perturb peripheral transcriptomic and metabolomic profiles in Phelan-McDermid syndrome. *HGG Adv*, 4(1), 100145.  
<https://doi.org/10.1016/j.xhgg.2022.100145>
- Burke, E. E., Chenoweth, J. G., Shin, J. H., Collado-Torres, L., Kim, S. K., Micali, N., Wang, Y., Colantuoni, C., Straub, R. E., Hoepfner, D. J., Chen, H. Y., Sellers, A., Shibbani, K., Hamersky, G. R., Diaz Bustamante, M., Phan, B. N., Ulrich, W. S., Valencia, C., Jaishankar, A., . . . Jaffe, A. E. (2020). Dissecting transcriptomic signatures of neuronal differentiation and maturation using iPSCs. *Nat Commun*, 11(1), 462. <https://doi.org/10.1038/s41467-019-14266-z>
- Bushnell, B. (2018, 2018). *BBMap*.
- Butler, M. G., & Thompson, T. (2000). Prader-Willi Syndrome: Clinical and Genetic Findings. *The Endocrinologist*, 10(4 Suppl 1), 3S-16S.  
<https://doi.org/10.1097/00019616-200010041-00002>
- Carlson, C., Sirotkin, H., Pandita, R., Goldberg, R., McKie, J., Wadey, R., Patanjali, S. R., Weissman, S. M., Anyane-Yeboah, K., Warburton, D., Scambler, P.,

- Shprintzen, R., Kucherlapati, R., & Morrow, B. E. (1997). Molecular definition of 22q11 deletions in 151 velo-cardio-facial syndrome patients. *American journal of human genetics*, 61(3), 620-629. <https://doi.org/10.1086/515508>
- Chen, C. C., Xie, X. M., Zhao, X. K., Zuo, S., & Li, H. Y. (2022). Kruppel-like Factor 13 Promotes HCC Progression by Transcriptional Regulation of HMGCS1-mediated Cholesterol Synthesis. *J Clin Transl Hepatol*, 10(6), 1125-1137. <https://doi.org/10.14218/JCTH.2021.00370>
- Chen, J., Calhoun, V. D., Perrone-Bizzozero, N. I., Pearlson, G. D., Sui, J., Du, Y., & Liu, J. (2016). A pilot study on commonality and specificity of copy number variants in schizophrenia and bipolar disorder. *Translational psychiatry*, 6(5), e824-e824. <https://doi.org/10.1038/tp.2016.96>
- Chen, Z., & Cobb, M. H. (2001). Regulation of Stress-responsive Mitogen-activated Protein (MAP) Kinase Pathways by TAO2. *Journal of Biological Chemistry*, 276(19), 16070-16075. <https://doi.org/10.1074/jbc.m100681200>
- Ching, M. S. L., Shen, Y., Tan, W.-H., Jeste, S. S., Morrow, E. M., Chen, X., Mukaddes, N. M., Yoo, S.-Y., Hanson, E., Hundley, R., Austin, C., Becker, R. E., Berry, G. T., Driscoll, K., Engle, E. C., Friedman, S., Gusella, J. F., Hisama, F. M., Irons, M. B., . . . Children's Hospital Boston Genotype Phenotype Study, G. (2010). Deletions of NRXN1 (neurexin-1) predispose to a wide spectrum of developmental disorders. *American journal of medical genetics. Part B, Neuropsychiatric genetics : the official publication of the International Society of Psychiatric Genetics*, 153B(4), 937-947. <https://doi.org/10.1002/ajmg.b.31063>
- Colvert, E., Tick, B., McEwen, F., Stewart, C., Curran, S. R., Woodhouse, E., Gillan, N., Hallett, V., Lietz, S., Garnett, T., Ronald, A., Plomin, R., Rijdsdijk, F., Happe, F., & Bolton, P. (2015). Heritability of Autism Spectrum Disorder in a UK Population-Based Twin Sample. *JAMA Psychiatry*, 72(5), 415-423. <https://doi.org/10.1001/jamapsychiatry.2014.3028>
- Cornelis, T., Rayyan, M., Devriendt, K., & Casteels, I. (2015). Ophthalmological Findings in 6p Deletion Syndrome. *Ophthalmic Genet*, 36(2), 165-167. <https://doi.org/10.3109/13816810.2015.1010735>
- Correction: Corrigendum: The phenotypic spectrum of Schaaf-Yang syndrome: 18 new affected individuals from 14 families. (2016). *Genetics in Medicine*, 18(10), 1066. <https://doi.org/10.1038/gim.2016.114>
- Crespi, B. J., & Hurd, P. L. (2014). Cognitive-behavioral phenotypes of Williams syndrome are associated with genetic variation in the GTF2I gene, in a healthy population. *BMC neuroscience*, 15, 127-127. <https://doi.org/10.1186/s12868-014-0127-1>
- Cubells, J. F., Deoreo, E. H., Harvey, P. D., Garlow, S. J., Garber, K., Adam, M. P., & Martin, C. L. (2011). Pharmaco-genetically guided treatment of recurrent rage outbursts in an adult male with 15q13.3 deletion syndrome. *Am J Med Genet A*, 155A(4), 805-810. <https://doi.org/10.1002/ajmg.a.33917>
- Cuberos, H., Vallée, B., Vourc'h, P., Tastet, J., Andres, C. R., & Bénédicti, H. (2015). Roles of LIM kinases in central nervous system function and dysfunction. *FEBS Letters*, 589(24PartB), 3795-3806. <https://doi.org/10.1016/j.febslet.2015.10.032>
- Dabell, M. P., Rosenfeld, J. A., Bader, P., Escobar, L. F., El-Khechen, D., Vallee, S. E., Dinulos, M. B. P., Curry, C., Fisher, J., Tervo, R., Hannibal, M. C., Siefkas, K., Wyatt, P. R., Hughes, L., Smith, R., Ellingwood, S., Lacassie, Y., Stroud, T., Farrell, S. A., . . . Shaffer, L. G. (2013). Investigation of NRXN1 deletions:

- Clinical and molecular characterization. *American Journal of Medical Genetics Part A*, 161(4), 717-731. <https://doi.org/10.1002/ajmg.a.35780>
- Dai, L., Bellugi, U., Chen, X. N., Pulst-Korenberg, A. M., Järvinen-Pasley, A., Tirosch-Wagner, T., Eis, P. S., Graham, J., Mills, D., Searcy, Y., & Korenberg, J. R. (2009). Is it Williams syndrome? GTF2IRD1 implicated in visual-spatial construction and GTF2I in sociability revealed by high resolution arrays. *American journal of medical genetics. Part A*, 149A(3), 302-314. <https://doi.org/10.1002/ajmg.a.32652>
- Damiano, J. A., Mullen, S. A., Hildebrand, M. S., Bellows, S. T., Lawrence, K. M., Arsov, T., Dibbens, L., Major, H., Dahl, H. H., Mefford, H. C., Darbro, B. W., Scheffer, I. E., & Berkovic, S. F. (2015). Evaluation of multiple putative risk alleles within the 15q13.3 region for genetic generalized epilepsy. *Epilepsy Res*, 117, 70-73. <https://doi.org/10.1016/j.eplepsyres.2015.09.007>
- Davies, A. F., Mirza, G., Sekhon, G., Turnpenny, P., Leroy, F., Speleman, F., Law, C., van Regemorter, N., Vamos, E., Flinter, F., & Ragoussis, J. (1999). Delineation of two distinct 6p deletion syndromes. *Human genetics*, 104(1), 64-72. <https://doi.org/10.1007/s004390050911>
- de Anda, F. C., Rosario, A. L., Durak, O., Tran, T., Gräff, J., Meletis, K., Rei, D., Soda, T., Madabhushi, R., Ginty, D. D., Kolodkin, A. L., & Tsai, L.-H. (2012). Autism spectrum disorder susceptibility gene TAOK2 affects basal dendrite formation in the neocortex. *Nature Neuroscience*, 15(7), 1022-1031. <https://doi.org/10.1038/nn.3141>
- Degenhardt, F., Heinemann, B., Strohmaier, J., Pfohl, M. A., Giegling, I., Hofmann, A., Ludwig, K. U., Witt, S. H., Ludwig, M., Forstner, A. J., Albus, M., Schwab, S. G., Borrmann-Hassenbach, M., Lennertz, L., Wagner, M., Hoffmann, P., Rujescu, D., Maier, W., Cichon, S., . . . Nöthen, M. M. (2016). Identification of rare variants in KCTD13 at the schizophrenia risk locus 16p11.2. *Psychiatric genetics*, 26(6), 293-296. <https://doi.org/10.1097/YPG.0000000000000145>
- Deneault, E., White, S. H., Rodrigues, D. C., Ross, P. J., Faheem, M., Zaslavsky, K., Wang, Z., Alexandrova, R., Pellecchia, G., Wei, W., Piekna, A., Kaur, G., Howe, J. L., Kwan, V., Thiruvahindrapuram, B., Walker, S., Lionel, A. C., Pasceri, P., Merico, D., . . . Scherer, S. W. (2019). Complete Disruption of Autism-Susceptibility Genes by Gene Editing Predominantly Reduces Functional Connectivity of Isogenic Human Neurons. *Stem Cell Reports*, 12(2), 427-429. <https://doi.org/10.1016/j.stemcr.2019.01.008>
- Dennis, M. Y., Harshman, L., Nelson, B. J., Penn, O., Cantsilieris, S., Huddleston, J., Antonacci, F., Penewit, K., Denman, L., Raja, A., Baker, C., Mark, K., Malig, M., Janke, N., Espinoza, C., Stessman, H. A. F., Nuttle, X., Hoekzema, K., Lindsay-Graves, T. A., . . . Eichler, E. E. (2017). The evolution and population diversity of human-specific segmental duplications. *Nature ecology & evolution*, 1(3), 69-69. <https://doi.org/10.1038/s41559-016-0069>
- Dimitrova, Y. N., Li, J., Lee, Y.-T., Rios-Esteves, J., Friedman, D. B., Choi, H.-J., Weis, W. I., Wang, C.-Y., & Chazin, W. J. (2010). Direct ubiquitination of beta-catenin by Siah-1 and regulation by the exchange factor TBL1. *The Journal of biological chemistry*, 285(18), 13507-13516. <https://doi.org/10.1074/jbc.M109.049411>
- Ding, Y., Xu, Y., Fu, Y., Zhang, H., Zhao, L., & Fan, X. (2022). Kruppel-like factor 13 inhibits cell proliferation of gastric cancer by inducing autophagic degradation of

- beta-catenin. *Discov Oncol*, 13(1), 121. <https://doi.org/10.1007/s12672-022-00587-x>
- Doble, B. W., & Woodgett, J. R. (2003). GSK-3: tricks of the trade for a multi-tasking kinase. *J Cell Sci*, 116(Pt 7), 1175-1186. <https://doi.org/10.1242/jcs.00384>
- Dolcetti, A., Silversides, C. K., Marshall, C. R., Lionel, A. C., Stavropoulos, D. J., Scherer, S. W., & Bassett, A. S. (2013). 1q21.1 Microduplication expression in adults. *Genetics in medicine : official journal of the American College of Medical Genetics*, 15(4), 282-289. <https://doi.org/10.1038/gim.2012.129>
- Doyle, J. M., Gao, J., Wang, J., Yang, M., & Potts, P. R. (2010). MAGE-RING protein complexes comprise a family of E3 ubiquitin ligases. *Molecular cell*, 39(6), 963-974. <https://doi.org/10.1016/j.molcel.2010.08.029>
- Driscoll, D. A., Salvin, J., Sellinger, B., Budarf, M. L., McDonald-McGinn, D. M., Zackai, E. H., & Emanuel, B. S. (1993). Prevalence of 22q11 microdeletions in DiGeorge and velocardiofacial syndromes: implications for genetic counselling and prenatal diagnosis. *Journal of Medical Genetics*, 30(10), 813-817. <https://doi.org/10.1136/jmg.30.10.813>
- Driscoll, D. A., Spinner, N. B., Budarf, M. L., McDonald-McGinn, D. M., Zackai, E. H., Goldberg, R. B., Shprintzen, R. J., Saal, H. M., Zonana, J., Jones, M. C., Mascarello, J. T., & Emanuel, B. S. (1992). Deletions and microdeletions of 22q11.2 in velo-cardio-facial syndrome. *American Journal of Medical Genetics*, 44(2), 261-268. <https://doi.org/10.1002/ajmg.1320440237>
- Durak, O., de Anda, F. C., Singh, K. K., Leussis, M. P., Petryshen, T. L., Sklar, P., & Tsai, L. H. (2015). Ankyrin-G regulates neurogenesis and Wnt signaling by altering the subcellular localization of beta-catenin. *Mol Psychiatry*, 20(3), 388-397. <https://doi.org/10.1038/mp.2014.42>
- Dykens, E. M., Lee, E., & Roof, E. (2011). Prader-Willi syndrome and autism spectrum disorders: an evolving story. *Journal of neurodevelopmental disorders*, 3(3), 225-237. <https://doi.org/10.1007/s11689-011-9092-5>
- Endris, V., Hackmann, K., Neuhan, T. M., Grasshoff, U., Bonin, M., Haug, U., Hahn, G., Schallner, J. C., Schrock, E., Tinschert, S., Rappold, G., & Moog, U. (2010). Homozygous loss of CHRNA7 on chromosome 15q13.3 causes severe encephalopathy with seizures and hypotonia. *Am J Med Genet A*, 152A(11), 2908-2911. <https://doi.org/10.1002/ajmg.a.33692>
- Escamilla, C. O., Filonova, I., Walker, A. K., Xuan, Z. X., Holehonnur, R., Espinosa, F., Liu, S., Thyme, S. B., López-García, I. A., Mendoza, D. B., Usui, N., Ellegood, J., Eisch, A. J., Konopka, G., Lerch, J. P., Schier, A. F., Speed, H. E., & Powell, C. M. (2017). Kctd13 deletion reduces synaptic transmission via increased RhoA. *Nature*, 551(7679), 227-231. <https://doi.org/10.1038/nature24470>
- Fejgin, K., Nielsen, J., Birknow, M. R., Bastlund, J. F., Nielsen, V., Lauridsen, J. B., Stefansson, H., Steinberg, S., Sorensen, H. B., Mortensen, T. E., Larsen, P. H., Klewe, I. V., Rasmussen, S. V., Stefansson, K., Werge, T. M., Kallunki, P., Christensen, K. V., & Didriksen, M. (2014). A mouse model that recapitulates cardinal features of the 15q13.3 microdeletion syndrome including schizophrenia- and epilepsy-related alterations. *Biol Psychiatry*, 76(2), 128-137. <https://doi.org/10.1016/j.biopsych.2013.08.014>
- Fénelon, K., Mukai, J., Xu, B., Hsu, P.-K., Drew, L. J., Karayiorgou, M., Fischbach, G. D., Macdermott, A. B., & Gogos, J. A. (2011). Deficiency of Dgcr8, a gene disrupted by the 22q11.2 microdeletion, results in altered short-term plasticity in the

- prefrontal cortex. *Proceedings of the National Academy of Sciences of the United States of America*, 108(11), 4447-4452. <https://doi.org/10.1073/pnas.1101219108>
- Fernandez, B. A., Roberts, W., Chung, B., Weksberg, R., Meyn, S., Szatmari, P., Joseph-George, A. M., MacKay, S., Whitten, K., Noble, B., Vardy, C., Crosbie, V., Luscombe, S., Tucker, E., Turner, L., Marshall, C. R., & Scherer, S. W. (2009). Phenotypic spectrum associated with de novo and inherited deletions and duplications at 16p11.2 in individuals ascertained for diagnosis of autism spectrum disorder. *Journal of Medical Genetics*, 47(3), 195-203. <https://doi.org/10.1136/jmg.2009.069369>
- Ferrero, G. B., Howald, C., Micale, L., Biamino, E., Augello, B., Fusco, C., Turturo, M. G., Forzano, S., Reymond, A., & Merla, G. (2010). An atypical 7q11.23 deletion in a normal IQ Williams-Beuren syndrome patient. *European journal of human genetics : EJHG*, 18(1), 33-38. <https://doi.org/10.1038/ejhg.2009.108>
- Fiddes, I. T., Lodewijk, G. A., Mooring, M., Bosworth, C. M., Ewing, A. D., Mantalas, G. L., Novak, A. M., van den Bout, A., Bishara, A., Rosenkrantz, J. L., Lorig-Roach, R., Field, A. R., Haeussler, M., Russo, L., Bhaduri, A., Nowakowski, T. J., Pollen, A. A., Dougherty, M. L., Nuttle, X., . . . Haussler, D. (2018). Human-Specific NOTCH2NL Genes Affect Notch Signaling and Cortical Neurogenesis. *Cell*, 173(6), 1356-1369.e1322. <https://doi.org/10.1016/j.cell.2018.03.051>
- Fiddes, I. T., Lodewijk, G. A., Mooring, M., Bosworth, C. M., Ewing, A. D., Mantalas, G. L., Novak, A. M., van den Bout, A., Bishara, A., Rosenkrantz, J. L., Lorig-Roach, R., Field, A. R., Haeussler, M., Russo, L., Bhaduri, A., Nowakowski, T. J., Pollen, A. A., Dougherty, M. L., Nuttle, X., . . . Haussler, D. (2018). Human-Specific NOTCH2NL Genes Affect Notch Signaling and Cortical Neurogenesis. *Cell*, 173(6), 1356-1369 e1322. <https://doi.org/10.1016/j.cell.2018.03.051>
- Fine, S. E., Weissman, A., Gerdes, M., Pinto-Martin, J., Zackai, E. H., McDonald-McGinn, D. M., & Emanuel, B. S. (2005). Autism spectrum disorders and symptoms in children with molecularly confirmed 22q11.2 deletion syndrome. *Journal of autism and developmental disorders*, 35(4), 461-470. <https://doi.org/10.1007/s10803-005-5036-9>
- Fink, J. J., Robinson, T. M., Germain, N. D., Sirois, C. L., Bolduc, K. A., Ward, A. J., Rigo, F., Chamberlain, S. J., & Levine, E. S. (2017). Disrupted neuronal maturation in Angelman syndrome-derived induced pluripotent stem cells. *Nature communications*, 8, 15038-15038. <https://doi.org/10.1038/ncomms15038>
- Florio, M., Albert, M., Taverna, E., Namba, T., Brandl, H., Lewitus, E., Haffner, C., Sykes, A., Wong, F. K., Peters, J., Guhr, E., Klemroth, S., Prüfer, K., Kelso, J., Naumann, R., Nüsslein, I., Dahl, A., Lachmann, R., Pääbo, S., & Huttner, W. B. (2015). Human-specific gene *ARHGAP11B* promotes basal progenitor amplification and neocortex expansion. *Science*, 347(6229), 1465-1470. <https://doi.org/10.1126/science.aaa1975>
- Florio, M., Namba, T., Pääbo, S., Hiller, M., & Huttner, W. B. (2016). A single splice site mutation in human-specific *ARHGAP11B* causes basal progenitor amplification. *Science advances*, 2(12), e1601941-e1601941. <https://doi.org/10.1126/sciadv.1601941>
- Forsingdal, A., Fejgin, K., Nielsen, V., Werge, T., & Nielsen, J. (2016). 15q13.3 homozygous knockout mouse model display epilepsy-, autism- and schizophrenia-related phenotypes. *Transl Psychiatry*, 6(7), e860. <https://doi.org/10.1038/tp.2016.125>

- Frangiskakis, J. M., Ewart, A. K., Morris, C. A., Mervis, C. B., Bertrand, J., Robinson, B. F., Klein, B. P., Ensing, G. J., Everett, L. A., Green, E. D., Pröschel, C., Gutowski, N. J., Noble, M., Atkinson, D. L., Odelberg, S. J., & Keating, M. T. (1996). LIM-kinase1 Hemizygoty Implicated in Impaired Visuospatial Constructive Cognition. *Cell*, 86(1), 59-69. [https://doi.org/10.1016/s0092-8674\(00\)80077-x](https://doi.org/10.1016/s0092-8674(00)80077-x)
- Freire, G., Russell, L., & Oskoui, M. (2013). Terminal 6p deletion syndrome mimicking CHARGE syndrome: A case report. *Journal of pediatric genetics*, 2(2), 103-107. <https://doi.org/10.3233/PGE-13055>
- Frendo, M. E., da Silva, A., Phan, K. D., Riche, S., & Butler, S. J. (2019). The Cofilin/Limk1 Pathway Controls the Growth Rate of Both Developing and Regenerating Motor Axons. *The Journal of neuroscience : the official journal of the Society for Neuroscience*, 39(47), 9316-9327. <https://doi.org/10.1523/JNEUROSCI.0648-19.2019>
- Friedman, A. A., Tucker, G., Singh, R., Yan, D., Vinayagam, A., Hu, Y., Binari, R., Hong, P., Sun, X., Porto, M., Pacifico, S., Murali, T., Finley, R. L., Jr., Asara, J. M., Berger, B., & Perrimon, N. (2011). Proteomic and functional genomic landscape of receptor tyrosine kinase and ras to extracellular signal-regulated kinase signaling. *Science signaling*, 4(196), rs10-rs10. <https://doi.org/10.1126/scisignal.2002029>
- Fu, W., Zhang, F., Wang, Y., Gu, X., & Jin, L. (2010). Identification of copy number variation hotspots in human populations. *Am J Hum Genet*, 87(4), 494-504. <https://doi.org/10.1016/j.ajhg.2010.09.006>
- Fujiwara, T., Mishima, T., Kofuji, T., Chiba, T., Tanaka, K., Yamamoto, A., & Akagawa, K. (2006). Analysis of knock-out mice to determine the role of HPC-1/syntaxin 1A in expressing synaptic plasticity. *The Journal of neuroscience : the official journal of the Society for Neuroscience*, 26(21), 5767-5776. <https://doi.org/10.1523/JNEUROSCI.0289-06.2006>
- Gabriele, M., Lopez Tobon, A., D'Agostino, G., & Testa, G. (2018). The chromatin basis of neurodevelopmental disorders: Rethinking dysfunction along the molecular and temporal axes. *Progress in Neuro-Psychopharmacology and Biological Psychiatry*, 84, 306-327. <https://doi.org/10.1016/j.pnpbp.2017.12.013>
- Gao, M. C., Bellugi, U., Dai, L., Mills, D. L., Sobel, E. M., Lange, K., & Korenberg, J. R. (2010). Intelligence in Williams Syndrome is related to STX1A, which encodes a component of the presynaptic SNARE complex. *PloS one*, 5(4), e10292-e10292. <https://doi.org/10.1371/journal.pone.0010292>
- Garret, P., Ebstein, F., Delplancq, G., Dozieres-Puyravel, B., Boughalem, A., Auvin, S., Duffourd, Y., Klafack, S., Zieba, B. A., Mahmoudi, S., Singh, K. K., Duplomb, L., Thauvin-Robinet, C., Costa, J. M., Kruger, E., Trost, D., Verloes, A., Faivre, L., & Vitobello, A. (2020). Report of the first patient with a homozygous OTUD7A variant responsible for epileptic encephalopathy and related proteasome dysfunction. *Clin Genet*, 97(4), 567-575. <https://doi.org/10.1111/cge.13709>
- Garza, J. C., Qi, X., Gjeluci, K., Leussis, M. P., Basu, H., Reis, S. A., Zhao, W. N., Piguel, N. H., Penzes, P., Haggarty, S. J., Martens, G. J., Poelmans, G., & Petryshen, T. L. (2018). Disruption of the psychiatric risk gene Ankyrin 3 enhances microtubule dynamics through GSK3/CRMP2 signaling. *Transl Psychiatry*, 8(1), 135. <https://doi.org/10.1038/s41398-018-0182-y>
- Gauthier, J., Siddiqui, T. J., Huashan, P., Yokomaku, D., Hamdan, F. F., Champagne, N., Lapointe, M., Spiegelman, D., Noreau, A., Lafrenière, R. G., Fathalli, F.,

- Jooper, R., Krebs, M.-O., DeLisi, L. E., Mottron, L., Fombonne, E., Michaud, J. L., Drapeau, P., Carbonetto, S., . . . Rouleau, G. A. (2011). Truncating mutations in NRXN2 and NRXN1 in autism spectrum disorders and schizophrenia. *Human genetics*, 130(4), 563-573. <https://doi.org/10.1007/s00439-011-0975-z>
- Ge, X.-L., Zhang, Y., Wu, Y., Lv, J., Zhang, W., Jin, Z.-B., Qu, J., & Gu, F. (2014). Identification of a novel GJA8 (Cx50) point mutation causes human dominant congenital cataracts. *Scientific Reports*, 4, 4121-4121. <https://doi.org/10.1038/srep04121>
- George, J., Soares, C., Montersino, A., Beique, J.-C., & Thomas, G. M. (2015). Palmitoylation of LIM Kinase-1 ensures spine-specific actin polymerization and morphological plasticity. *eLife*, 4, e06327-e06327. <https://doi.org/10.7554/eLife.06327>
- Germain, N. D., Chen, P.-F., Plocik, A. M., Glatt-Deeley, H., Brown, J., Fink, J. J., Bolduc, K. A., Robinson, T. M., Levine, E. S., Reiter, L. T., Graveley, B. R., Lalande, M., & Chamberlain, S. J. (2014). Gene expression analysis of human induced pluripotent stem cell-derived neurons carrying copy number variants of chromosome 15q11-q13.1. *Molecular autism*, 5, 44-44. <https://doi.org/10.1186/2040-2392-5-44>
- Gillentine, M. A., Lupo, P. J., Stankiewicz, P., & Schaaf, C. P. (2018). An estimation of the prevalence of genomic disorders using chromosomal microarray data. *J Hum Genet*, 63(7), 795-801. <https://doi.org/10.1038/s10038-018-0451-x>
- Gillentine, M. A., & Schaaf, C. P. (2015). The human clinical phenotypes of altered CHRNA7 copy number. *Biochem Pharmacol*, 97(4), 352-362. <https://doi.org/10.1016/j.bcp.2015.06.012>
- Gillentine, M. A., Yin, J., Bajic, A., Zhang, P., Cummock, S., Kim, J. J., & Schaaf, C. P. (2017). Functional Consequences of CHRNA7 Copy-Number Alterations in Induced Pluripotent Stem Cells and Neural Progenitor Cells. *Am J Hum Genet*, 101(6), 874-887. <https://doi.org/10.1016/j.ajhg.2017.09.024>
- Girirajan, S., Vlangos, C. N., Szomju, B. B., Edelman, E., Trevors, C. D., Dupuis, L., Nezarati, M., Bunyan, D. J., & Elsea, S. H. (2006). Genotype–phenotype correlation in Smith-Magenis syndrome: Evidence that multiple genes in 17p11.2 contribute to the clinical spectrum. *Genetics in Medicine*, 8(7), 417-427. <https://doi.org/10.1097/01.gim.0000228215.32110.89>
- Golzio, C., Willer, J., Talkowski, M. E., Oh, E. C., Taniguchi, Y., Jacquemont, S., Reymond, A., Sun, M., Sawa, A., Gusella, J. F., Kamiya, A., Beckmann, J. S., & Katsanis, N. (2012). KCTD13 is a major driver of mirrored neuroanatomical phenotypes of the 16p11.2 copy number variant. *Nature*, 485(7398), 363-367. <https://doi.org/10.1038/nature11091>
- Gomez-Ramos, A., Dominguez, J., Zafra, D., Corominola, H., Gomis, R., Guinovart, J. J., & Avila, J. (2006). Sodium tungstate decreases the phosphorylation of tau through GSK3 inactivation. *J Neurosci Res*, 83(2), 264-273. <https://doi.org/10.1002/jnr.20726>
- Gong, W. (1996). A transcription map of the DiGeorge and velo-cardio-facial syndrome minimal critical region on 22q11. *Human Molecular Genetics*, 5(6), 789-800. <https://doi.org/10.1093/hmg/5.6.789>
- Goold, R., Flower, M., Moss, D. H., Medway, C., Wood-Kaczmar, A., Andre, R., Farshim, P., Bates, G. P., Holmans, P., Jones, L., & Tabrizi, S. J. (2019). FAN1 modifies

- Huntington's disease progression by stabilizing the expanded HTT CAG repeat. *Human Molecular Genetics*, 28(4), 650-661. <https://doi.org/10.1093/hmg/ddy375>
- Gottesman, I. I. (1991). *Schizophrenia genesis: The origins of madness*. W H Freeman/Times Books/ Henry Holt & Co.
- Greer, P. L., Hanayama, R., Bloodgood, B. L., Mardinly, A. R., Lipton, D. M., Flavell, S. W., Kim, T.-K., Griffith, E. C., Waldon, Z., Maehr, R., Ploegh, H. L., Chowdhury, S., Worley, P. F., Steen, J., & Greenberg, M. E. (2010). The Angelman Syndrome protein Ube3A regulates synapse development by ubiquitinating arc. *Cell*, 140(5), 704-716. <https://doi.org/10.1016/j.cell.2010.01.026>
- Gregoric Kumperscak, H., Krgovic, D., Drobnic Radobuljac, M., Senica, N., Zagorac, A., & Kokalj Vokac, N. (2021). CNVs and Chromosomal Aneuploidy in Patients With Early-Onset Schizophrenia and Bipolar Disorder: Genotype-Phenotype Associations. *Frontiers in psychiatry*, 11, 606372-606372. <https://doi.org/10.3389/fpsy.2020.606372>
- Hanson, E., Nasir, R. H., Fong, A., Lian, A., Hundley, R., Shen, Y., Wu, B.-L., Holm, I. A., & Miller, D. T. (2010). Cognitive and Behavioral Characterization of 16p11.2 Deletion Syndrome. *Journal of Developmental & Behavioral Pediatrics*, 31(8), 649-657. <https://doi.org/10.1097/dbp.0b013e3181ea50ed>
- Hao, Y.-H., Doyle, J. M., Ramanathan, S., Gomez, T. S., Jia, D., Xu, M., Chen, Z. J., Billadeau, D. D., Rosen, M. K., & Potts, P. R. (2013). Regulation of WASH-dependent actin polymerization and protein trafficking by ubiquitination. *Cell*, 152(5), 1051-1064. <https://doi.org/10.1016/j.cell.2013.01.051>
- Harwood, A. J., & Agam, G. (2003). Search for a common mechanism of mood stabilizers. *Biochem Pharmacol*, 66(2), 179-189. [https://doi.org/10.1016/s0006-2952\(03\)00187-4](https://doi.org/10.1016/s0006-2952(03)00187-4)
- Heide, M., Haffner, C., Murayama, A., Kurotaki, Y., Shinohara, H., Okano, H., Sasaki, E., & Huttner, W. B. (2020). Human-specific *ARHGAP11B* increases size and folding of primate neocortex in the fetal marmoset. *Science*, 369(6503), 546-550. <https://doi.org/10.1126/science.abb2401>
- Heide, M., & Huttner, W. B. (2021). Human-Specific Genes, Cortical Progenitor Cells, and Microcephaly. *Cells*, 10(5), 1209. <https://doi.org/10.3390/cells10051209>
- Heider, J., Vogel, S., Volkmer, H., & Breitmeyer, R. (2021). Human iPSC-Derived Glia as a Tool for Neuropsychiatric Research and Drug Development. *International journal of molecular sciences*, 22(19). <https://doi.org/10.3390/ijms221910254>
- Hevner, R. F. (2020). What Makes the Human Brain Human? *Neuron*, 105(5), 761-763. <https://doi.org/10.1016/j.neuron.2020.02.007>
- Hill, C. L., & Stephens, G. J. (2021). An Introduction to Patch Clamp Recording. *Methods Mol Biol*, 2188, 1-19. [https://doi.org/10.1007/978-1-0716-0818-0\\_1](https://doi.org/10.1007/978-1-0716-0818-0_1)
- Hiroi, N., Takahashi, T., Hishimoto, A., Izumi, T., Boku, S., & Hiramoto, T. (2013). Copy number variation at 22q11.2: from rare variants to common mechanisms of developmental neuropsychiatric disorders. *Molecular Psychiatry*, 18(11), 1153-1165. <https://doi.org/10.1038/mp.2013.92>
- Hirota, H., Matsuoka, R., Chen, X.-N., Salandanan, L. S., Lincoln, A., Rose, F. E., Sunahara, M., Osawa, M., Bellugi, U., & Korenberg, J. R. (2003). Williams syndrome deficits in visual spatial processing linked to GTF2IRD1 and GTF2I on Chromosome 7q11.23. *Genetics in Medicine*, 5(4), 311-321. <https://doi.org/10.1097/01.gim.0000076975.10224.67>

- Ho, G. P. H., Selvakumar, B., Mukai, J., Hester, L. D., Wang, Y., Gogos, J. A., & Snyder, S. H. (2011). S-nitrosylation and S-palmitoylation reciprocally regulate synaptic targeting of PSD-95. *Neuron*, 71(1), 131-141. <https://doi.org/10.1016/j.neuron.2011.05.033>
- Hong, Y. J., & Do, J. T. (2019). Neural Lineage Differentiation From Pluripotent Stem Cells to Mimic Human Brain Tissues. *Frontiers in bioengineering and biotechnology*, 7, 400-400. <https://doi.org/10.3389/fbioe.2019.00400>
- Hoogenraad, C. C., Akhmanova, A., Galjart, N., & De Zeeuw, C. I. (2004). LIMK1 and CLIP-115: linking cytoskeletal defects to Williams syndrome. *BioEssays*, 26(2), 141-150. <https://doi.org/10.1002/bies.10402>
- Hoppman-Chaney, N., Wain, K., Seger, P. R., Superneau, D. W., & Hodge, J. C. (2013). Identification of single gene deletions at 15q13.3: further evidence that CHRNA7 causes the 15q13.3 microdeletion syndrome phenotype. *Clin Genet*, 83(4), 345-351. <https://doi.org/10.1111/j.1399-0004.2012.01925.x>
- Hori, T., Ikuta, S., Hattori, S., Takao, K., Miyakawa, T., & Koike, C. (2021). Mice with mutations in *Trpm1*, a gene in the locus of 15q13.3 microdeletion syndrome, display pronounced hyperactivity and decreased anxiety-like behavior. *Molecular brain*, 14(1), 61. <https://doi.org/10.1186/s13041-021-00749-y>
- Hu, H., Brittain, G. C., Chang, J. H., Puebla-Osorio, N., Jin, J., Zal, A., Xiao, Y., Cheng, X., Chang, M., Fu, Y. X., Zal, T., Zhu, C., & Sun, S. C. (2013). OTUD7B controls non-canonical NF-kappaB activation through deubiquitination of TRAF3. *Nature*, 494(7437), 371-374. <https://doi.org/10.1038/nature11831>
- Huang, J., Guo, X., Li, W., & Zhang, H. (2017). Activation of Wnt/ $\beta$ -catenin signalling via GSK3 inhibitors direct differentiation of human adipose stem cells into functional hepatocytes. *Scientific Reports*, 7(1), 40716. <https://doi.org/10.1038/srep40716>
- Huang, X., Xiao, X., Jia, X., Li, S., Li, M., Guo, X., Liu, X., & Zhang, Q. (2015). Mutation analysis of the genes associated with anterior segment dysgenesis, microcornea and microphthalmia in 257 patients with glaucoma. *International Journal of Molecular Medicine*, 36(4), 1111-1117. <https://doi.org/10.3892/ijmm.2015.2325>
- Huber, W., Carey, V. J., Gentleman, R., Anders, S., Carlson, M., Carvalho, B. S., Bravo, H. C., Davis, S., Gatto, L., Girke, T., Gottardo, R., Hahne, F., Hansen, K. D., Irizarry, R. A., Lawrence, M., Love, M. I., MacDonald, J., Obenchain, V., Oles, A. K., . . . Morgan, M. (2015). Orchestrating high-throughput genomic analysis with Bioconductor. *Nat Methods*, 12(2), 115-121. <https://doi.org/10.1038/nmeth.3252>
- Huguet, G., Schramm, C., Douard, E., Jiang, L., Labbe, A., Tihy, F., Mathonnet, G., Nizard, S., Lemyre, E., Mathieu, A., Poline, J. B., Loth, E., Toro, R., Schumann, G., Conrod, P., Pausova, Z., Greenwood, C., Paus, T., Bourgeron, T., . . . Consortium, I. (2018). Measuring and Estimating the Effect Sizes of Copy Number Variants on General Intelligence in Community-Based Samples. *JAMA Psychiatry*, 75(5), 447-457. <https://doi.org/10.1001/jamapsychiatry.2018.0039>
- Ionita-Laza, I., Xu, B., Makarov, V., Buxbaum, J. D., Roos, J. L., Gogos, J. A., & Karayiorgou, M. (2014). Scan statistic-based analysis of exome sequencing data identifies FAN1 at 15q13.3 as a susceptibility gene for schizophrenia and autism. *Proc Natl Acad Sci U S A*, 111(1), 343-348. <https://doi.org/10.1073/pnas.1309475110>
- James, T. F., Nenov, M. N., Wildburger, N. C., Lichti, C. F., Luisi, J., Vergara, F., Panova-Electronova, N. I., Nilsson, C. L., Rudra, J. S., Green, T. A., Labate, D.,

- & Laezza, F. (2015). The Nav1.2 channel is regulated by GSK3. *Biochimica et biophysica acta*, 1850(4), 832-844. <https://doi.org/10.1016/j.bbagen.2015.01.011>
- Jenkins, A. K., Paterson, C., Wang, Y., Hyde, T. M., Kleinman, J. E., & Law, A. J. (2016). Neurexin 1 (NRXN1) splice isoform expression during human neocortical development and aging. *Molecular Psychiatry*, 21(5), 701-706. <https://doi.org/10.1038/mp.2015.107>
- Jiang, M., Meng, J., Zeng, F., Qing, H., Hook, G., Hook, V., Wu, Z., & Ni, J. (2020). Cathepsin B inhibition blocks neurite outgrowth in cultured neurons by regulating lysosomal trafficking and remodeling. *J Neurochem*, 155(3), 300-312. <https://doi.org/10.1111/jnc.15032>
- Jiang, Y.-h., Armstrong, D., Albrecht, U., Atkins, C. M., Noebels, J. L., Eichele, G., Sweatt, J. D., & Beaudet, A. L. (1998). Mutation of the Angelman Ubiquitin Ligase in Mice Causes Increased Cytoplasmic p53 and Deficits of Contextual Learning and Long-Term Potentiation. *Neuron*, 21(4), 799-811. [https://doi.org/10.1016/s0896-6273\(00\)80596-6](https://doi.org/10.1016/s0896-6273(00)80596-6)
- Jin, L., Williamson, A., Banerjee, S., Philipp, I., & Rape, M. (2008). Mechanism of ubiquitin-chain formation by the human anaphase-promoting complex. *Cell*, 133(4), 653-665. <https://doi.org/10.1016/j.cell.2008.04.012>
- Kalebic, N., Gilardi, C., Albert, M., Namba, T., Long, K. R., Kostic, M., Langen, B., & Huttner, W. B. (2018). Human-specific ARHGAP11B induces hallmarks of neocortical expansion in developing ferret neocortex. *eLife*, 7, e41241. <https://doi.org/10.7554/eLife.41241>
- Kalsner, L., & Chamberlain, S. J. (2015). Prader-Willi, Angelman, and 15q11-q13 Duplication Syndromes. *Pediatr Clin North Am*, 62(3), 587-606. <https://doi.org/10.1016/j.pcl.2015.03.004>
- Kanai, T., Nemoto, T., Yanagita, T., Maruta, T., Satoh, S., Yoshikawa, N., & Wada, A. (2009). Nav1.7 sodium channel-induced Ca<sup>2+</sup> influx decreases tau phosphorylation via glycogen synthase kinase-3 $\beta$  in adrenal chromaffin cells. *Neurochem Int*, 54(8), 497-505. <https://doi.org/10.1016/j.neuint.2009.02.002>
- Kanber, D., Giltay, J., Wiczorek, D., Zogel, C., Hochstenbach, R., Caliebe, A., Kuechler, A., Horsthemke, B., & Buiting, K. (2009). A paternal deletion of MKRN3, MAGEL2 and NDN does not result in Prader-Willi syndrome. *European journal of human genetics : EJHG*, 17(5), 582-590. <https://doi.org/10.1038/ejhg.2008.232>
- Kandel, E. R. (2013). *Principles of neural science* (5th ed.). McGraw-Hill.
- Karayorgou, M., Morris, M. A., Morrow, B., Shprintzen, R. J., Goldberg, R., Borrow, J., Gos, A., Nestadt, G., Wolyniec, P. S., Lasseter, V. K., & et al. (1995). Schizophrenia susceptibility associated with interstitial deletions of chromosome 22q11. *Proceedings of the National Academy of Sciences of the United States of America*, 92(17), 7612-7616. <https://doi.org/10.1073/pnas.92.17.7612>
- Kasu, Y. A. T., Arva, A., Johnson, J., Sajjan, C., Manzano, J., Hennes, A., Haynes, J., & Brower, C. S. (2022). BAG6 prevents the aggregation of neurodegeneration-associated fragments of TDP43. *iScience*, 25(5), 104273. <https://doi.org/10.1016/j.isci.2022.104273>
- Kirov, G., Rujescu, D., Ingason, A., Collier, D. A., O'Donovan, M. C., & Owen, M. J. (2009). Neurexin 1 (NRXN1) deletions in schizophrenia. *Schizophrenia bulletin*, 35(5), 851-854. <https://doi.org/10.1093/schbul/sbp079>
- Kishino, T., Lalande, M., & Wagstaff, J. (1997). UBE3A/E6-AP mutations cause Angelman syndrome. *Nat Genet*, 15(1), 70-73. <https://doi.org/10.1038/ng0197-70>

- Kizner, V., Naujock, M., Fischer, S., Jäger, S., Reich, S., Schlotthauer, I., Zuckschwerdt, K., Geiger, T., Hildebrandt, T., Lawless, N., Macartney, T., Dorner-Ciossek, C., & Gillardon, F. (2019). CRISPR/Cas9-mediated Knockout of the Neuropsychiatric Risk Gene KCTD13 Causes Developmental Deficits in Human Cortical Neurons Derived from Induced Pluripotent Stem Cells. *Molecular Neurobiology*, *57*(2), 616-634. <https://doi.org/10.1007/s12035-019-01727-1>
- Kluin, R. J. C., Kemper, K., Kuilman, T., de Ruiter, J. R., Iyer, V., Forment, J. V., Cornelissen-Steijger, P., de Rink, I., Ter Brugge, P., Song, J. Y., Klarenbeek, S., McDermott, U., Jonkers, J., Velds, A., Adams, D. J., Peeper, D. S., & Krijgsman, O. (2018). Xenofilter: computational deconvolution of mouse and human reads in tumor xenograft sequence data. *BMC Bioinformatics*, *19*(1), 366. <https://doi.org/10.1186/s12859-018-2353-5>
- Korner, M. B., Velluva, A., Bundalian, L., Radtke, M., Lin, C. C., Zacher, P., Bartolomaeus, T., Kirstein, A. S., Mrestani, A., Scholz, N., Platzer, K., Teichmann, A. C., Hentschel, J., Langenhan, T., Lemke, J. R., Garten, A., Abou Jamra, R., & Le Duc, D. (2022). Altered gene expression profiles impair the nervous system development in individuals with 15q13.3 microdeletion. *Sci Rep*, *12*(1), 13507. <https://doi.org/10.1038/s41598-022-17604-2>
- Krishnan, V., Stoppel, D. C., Nong, Y., Johnson, M. A., Nadler, M. J., Ozkaynak, E., Teng, B. L., Nagakura, I., Mohammad, F., Silva, M. A., Peterson, S., Cruz, T. J., Kasper, E. M., Arnaout, R., & Anderson, M. P. (2017). Autism gene Ube3a and seizures impair sociability by repressing VTA Cbln1. *Nature*, *543*(7646), 507-512. <https://doi.org/10.1038/nature21678>
- Krishnan, V., Stoppel, D. C., Nong, Y., Johnson, M. A., Nadler, M. J. S., Ozkaynak, E., Teng, B. L., Nagakura, I., Mohammad, F., Silva, M. A., Peterson, S., Cruz, T. J., Kasper, E. M., Arnaout, R., & Anderson, M. P. (2017). Autism gene Ube3a and seizures impair sociability by repressing VTA Cbln1. *Nature*, *543*(7646), 507-512. <https://doi.org/10.1038/nature21678>
- Kumar, R. A., KaraMohamed, S., Sudi, J., Conrad, D. F., Brune, C., Badner, J. A., Gilliam, T. C., Nowak, N. J., Cook, E. H., Dobyns, W. B., & Christian, S. L. (2007). Recurrent 16p11.2 microdeletions in autism. *Human Molecular Genetics*, *17*(4), 628-638. <https://doi.org/10.1093/hmg/ddm376>
- Kumar, R. A., Marshall, C. R., Badner, J. A., Babatz, T. D., Mukamel, Z., Aldinger, K. A., Sudi, J., Brune, C. W., Goh, G., Karamohamed, S., Sutcliffe, J. S., Cook, E. H., Geschwind, D. H., Dobyns, W. B., Scherer, S. W., & Christian, S. L. (2009). Association and mutation analyses of 16p11.2 autism candidate genes. *PloS one*, *4*(2), e4582-e4582. <https://doi.org/10.1371/journal.pone.0004582>
- Lancaster, M. A., & Knoblich, J. A. (2014). Organogenesis in a dish: modeling development and disease using organoid technologies. *Science*, *345*(6194), 1247125. <https://doi.org/10.1126/science.1247125>
- Lancaster, M. A., Renner, M., Martin, C.-A., Wenzel, D., Bicknell, L. S., Hurles, M. E., Homfray, T., Penninger, J. M., Jackson, A. P., & Knoblich, J. A. (2013). Cerebral organoids model human brain development and microcephaly. *Nature*, *501*(7467), 373-379. <https://doi.org/10.1038/nature12517>
- Lavallee, G., Andelfinger, G., Nadeau, M., Lefebvre, C., Nemer, G., Horb, M. E., & Nemer, M. (2006). The Kruppel-like transcription factor KLF13 is a novel regulator of heart development. *The EMBO journal*, *25*(21), 5201-5213. <https://doi.org/10.1038/sj.emboj.7601379>

- Lee, H.-M., Clark, E. P., Kuijter, M. B., Cushman, M., Pommier, Y., & Philpot, B. D. (2018). Characterization and structure-activity relationships of indenoisoquinoline-derived topoisomerase I inhibitors in unsilencing the dormant Ube3a gene associated with Angelman syndrome. *Molecular autism*, 9, 45-45. <https://doi.org/10.1186/s13229-018-0228-2>
- Lee, S. (2000). Expression and imprinting of MAGEL2 suggest a role in Prader-Willi syndrome and the homologous murine imprinting phenotype. *Human Molecular Genetics*, 9(12), 1813-1819. <https://doi.org/10.1093/hmg/9.12.1813>
- Lee, S. Y., Chae, M. K., Yoon, J. S., & Kim, C. Y. (2021). The Effect of CHIR 99021, a Glycogen Synthase Kinase-3beta Inhibitor, on Transforming Growth Factor beta-Induced Tenon Fibrosis. *Invest Ophthalmol Vis Sci*, 62(15), 25. <https://doi.org/10.1167/iovs.62.15.25>
- Lepichon, J. B., Bittel, D. C., Graf, W. D., & Yu, S. (2010). A 15q13.3 homozygous microdeletion associated with a severe neurodevelopmental disorder suggests putative functions of the TRPM1, CHRNA7, and other homozygously deleted genes. *Am J Med Genet A*, 152A(5), 1300-1304. <https://doi.org/10.1002/ajmg.a.33374>
- Li, Z., Wang, Y., Li, Y., Yin, W., Mo, L., Qian, X., Zhang, Y., Wang, G., Bu, F., Zhang, Z., Ren, X., Zhu, B., Niu, C., Xiao, W., & Zhang, W. (2018). Ube2s stabilizes beta-Catenin through K11-linked polyubiquitination to promote mesendoderm specification and colorectal cancer development. *Cell Death Dis*, 9(5), 456. <https://doi.org/10.1038/s41419-018-0451-y>
- Liang, X., Feng, Z., Yan, R., Liu, F., Yin, L., Shen, H., Lu, H., & Zhang, L. (2023). Kruppel-like Factors 3 Regulates Migration and Invasion of Gastric Cancer Cells Through NF-kappaB Pathway. *Altern Ther Health Med*, 29(2), 64-69. <https://www.ncbi.nlm.nih.gov/pubmed/36580668>
- Lin, G. N., Corominas, R., Lemmens, I., Yang, X., Tavernier, J., Hill, D. E., Vidal, M., Sebat, J., & Lakoucheva, L. M. (2015). Spatiotemporal 16p11.2 protein network implicates cortical late mid-fetal brain development and KCTD13-Cul3-RhoA pathway in psychiatric diseases. *Neuron*, 85(4), 742-754. <https://doi.org/10.1016/j.neuron.2015.01.010>
- Lin, R. J., Cherry, A. M., Chen, K. C., Lyons, M., Hoyme, H. E., & Hudgins, L. (2005). Terminal deletion of 6p results in a recognizable phenotype. *Am J Med Genet A*, 136(2), 162-168. <https://doi.org/10.1002/ajmg.a.30784>
- Liu, H., Abecasis, G. R., Heath, S. C., Knowles, A., Demars, S., Chen, Y.-J., Roos, J. L., Rapoport, J. L., Gogos, J. A., & Karayiorgou, M. (2002). Genetic variation in the 22q11 locus and susceptibility to schizophrenia. *Proceedings of the National Academy of Sciences of the United States of America*, 99(26), 16859-16864. <https://doi.org/10.1073/pnas.232186099>
- Liu, X., & Klein, P. S. (2018). Glycogen synthase kinase-3 and alternative splicing. *Wiley Interdiscip Rev RNA*, 9(6), e1501. <https://doi.org/10.1002/wrna.1501>
- Liu, X., Zhou, Z.-W., & Wang, Z.-Q. (2016). The DNA damage response molecule MCPH1 in brain development and beyond. *Acta Biochimica et Biophysica Sinica*, 48(7), 678-685. <https://doi.org/10.1093/abbs/gmw048>
- Loomes, R., Hull, L., & Mandy, W. P. L. (2017). What Is the Male-to-Female Ratio in Autism Spectrum Disorder? A Systematic Review and Meta-Analysis. *J Am Acad Child Adolesc Psychiatry*, 56(6), 466-474. <https://doi.org/10.1016/j.jaac.2017.03.013>

- Lou, X., Zhou, X., Li, H., Lu, X., Bao, X., Yang, K., Liao, X., Chen, H., Fang, H., Yang, Y., Lyu, J., & Zheng, H. (2021). Biallelic Mutations in ACACA Cause a Disruption in Lipid Homeostasis That Is Associated With Global Developmental Delay, Microcephaly, and Dysmorphic Facial Features. *Front Cell Dev Biol*, 9, 618492. <https://doi.org/10.3389/fcell.2021.618492>
- Love, M. I., Anders, S., Kim, V., & Huber, W. (2015). RNA-Seq workflow: gene-level exploratory analysis and differential expression. *F1000Res*, 4, 1070. <https://doi.org/10.12688/f1000research.7035.1>
- Love, M. I., Huber, W., & Anders, S. (2014). Moderated estimation of fold change and dispersion for RNA-seq data with DESeq2. *Genome Biol*, 15(12), 550. <https://doi.org/10.1186/s13059-014-0550-8>
- Lowther, C., Costain, G., Stavropoulos, D. J., Melvin, R., Silversides, C. K., Andrade, D. M., So, J., Faghfoury, H., Lionel, A. C., Marshall, C. R., Scherer, S. W., & Bassett, A. S. (2015). Delineating the 15q13.3 microdeletion phenotype: a case series and comprehensive review of the literature. *Genet Med*, 17(2), 149-157. <https://doi.org/10.1038/gim.2014.83>
- Lowther, C., Speevak, M., Armour, C. M., Goh, E. S., Graham, G. E., Li, C., Zeesman, S., Nowaczyk, M. J. M., Schultz, L.-A., Morra, A., Nicolson, R., Bikangaga, P., Samdup, D., Zaazou, M., Boyd, K., Jung, J. H., Siu, V., Rajguru, M., Goobie, S., . . . Bassett, A. S. (2017). Molecular characterization of NRXN1 deletions from 19,263 clinical microarray cases identifies exons important for neurodevelopmental disease expression. *Genetics in medicine : official journal of the American College of Medical Genetics*, 19(1), 53-61. <https://doi.org/10.1038/gim.2016.54>
- Lupski, J. R., & Stankiewicz, P. (2005). Genomic disorders: molecular mechanisms for rearrangements and conveyed phenotypes. *PLoS Genet*, 1(6), e49. <https://doi.org/10.1371/journal.pgen.0010049>
- Ma, S., Abou-Khalil, B., Sutcliffe, J. S., Haines, J. L., & Hedera, P. (2005). The GABBR1 locus and the G1465A variant is not associated with temporal lobe epilepsy preceded by febrile seizures. *BMC Med Genet*, 6, 13. <https://doi.org/10.1186/1471-2350-6-13>
- Mao, R., Deng, R., Wei, Y., Han, L., Meng, Y., Xie, W., & Jia, Z. (2019). LIMK1 and LIMK2 regulate cortical development through affecting neural progenitor cell proliferation and migration. *Molecular brain*, 12(1), 67-67. <https://doi.org/10.1186/s13041-019-0487-7>
- Marosi, M., Arman, P., Aceto, G., D'Ascenzo, M., & Laezza, F. (2022). Glycogen Synthase Kinase 3: Ion Channels, Plasticity, and Diseases. *International journal of molecular sciences*, 23(8). <https://doi.org/10.3390/ijms23084413>
- Marton, R. M., & Pasca, S. P. (2020). Organoid and Assembloid Technologies for Investigating Cellular Crosstalk in Human Brain Development and Disease. *Trends Cell Biol*, 30(2), 133-143. <https://doi.org/10.1016/j.tcb.2019.11.004>
- Mayhew, C. N., & Singhania, R. (2022). A review of protocols for brain organoids and applications for disease modeling. *STAR Protoc*, 4(1), 101860. <https://doi.org/10.1016/j.xpro.2022.101860>
- Mbikay, M., Seidah, N. G., & Chretien, M. (2001). Neuroendocrine secretory protein 7B2: structure, expression and functions. *The Biochemical journal*, 357(Pt 2), 329-342. <https://doi.org/10.1042/0264-6021:3570329>

- Meijer, M., Rebach, K., Brunner, J. W., Classen, J. A., Lammertse, H. C. A., van Linge, L. A., Schut, D., Krutenko, T., Hebisch, M., Cornelisse, L. N., Sullivan, P. F., Peitz, M., Toonen, R. F., Brustle, O., & Verhage, M. (2019). A Single-Cell Model for Synaptic Transmission and Plasticity in Human iPSC-Derived Neurons. *Cell Rep*, 27(7), 2199-2211 e2196. <https://doi.org/10.1016/j.celrep.2019.04.058>
- Mercer, R. E., Michaelson, S. D., Chee, M. J. S., Atallah, T. A., Wevrick, R., & Colmers, W. F. (2013). Magel2 is required for leptin-mediated depolarization of POMC neurons in the hypothalamic arcuate nucleus in mice. *PLoS genetics*, 9(1), e1003207-e1003207. <https://doi.org/10.1371/journal.pgen.1003207>
- Mergener, R., Furtado, G. V., de Mattos, E. P., Leotti, V. B., Jardim, L. B., & Saraiva-Pereira, M. L. (2019). Variation in DNA Repair System Gene as an Additional Modifier of Age at Onset in Spinocerebellar Ataxia Type 3/Machado–Joseph Disease. *NeuroMolecular Medicine*, 22(1), 133-138. <https://doi.org/10.1007/s12017-019-08572-4>
- Mevissen, T. E., Hospenthal, M. K., Geurink, P. P., Elliott, P. R., Akutsu, M., Arnaudo, N., Ekkebus, R., Kulathu, Y., Wauer, T., El Oualid, F., Freund, S. M., Ovaa, H., & Komander, D. (2013). OTU deubiquitinases reveal mechanisms of linkage specificity and enable ubiquitin chain restriction analysis. *Cell*, 154(1), 169-184. <https://doi.org/10.1016/j.cell.2013.05.046>
- Mevissen, T. E. T., Kulathu, Y., Mulder, M. P. C., Geurink, P. P., Maslen, S. L., Gersch, M., Elliott, P. R., Burke, J. E., van Tol, B. D. M., Akutsu, M., Oualid, F. E., Kawasaki, M., Freund, S. M. V., Ovaa, H., & Komander, D. (2016). Molecular basis of Lys11-polyubiquitin specificity in the deubiquitinase Cezanne. *Nature*, 538(7625), 402-405. <https://doi.org/10.1038/nature19836>
- Meziane, H., Schaller, F., Bauer, S., Villard, C., Matarazzo, V., Riet, F., Guillon, G., Lafitte, D., Desarmenien, M. G., Tauber, M., & Muscatelli, F. (2015). An Early Postnatal Oxytocin Treatment Prevents Social and Learning Deficits in Adult Mice Deficient for Magel2, a Gene Involved in Prader-Willi Syndrome and Autism. *Biological Psychiatry*, 78(2), 85-94. <https://doi.org/10.1016/j.biopsych.2014.11.010>
- Miller, D. T., Shen, Y., Weiss, L. A., Korn, J., Anselm, I., Bridgemohan, C., Cox, G. F., Dickinson, H., Gentile, J., Harris, D. J., Hegde, V., Hundley, R., Khwaja, O., Kothare, S., Luedke, C., Nasir, R., Poduri, A., Prasad, K., Raffalli, P., . . . Wu, B. L. (2009). Microdeletion/duplication at 15q13.2q13.3 among individuals with features of autism and other neuropsychiatric disorders. *J Med Genet*, 46(4), 242-248. <https://doi.org/10.1136/jmg.2008.059907>
- Mitz, A. R., Philyaw, T. J., Boccuto, L., Shcheglovitov, A., Sarasua, S. M., Kaufmann, W. E., & Thurm, A. (2018). Identification of 22q13 genes most likely to contribute to Phelan McDermid syndrome. *European journal of human genetics : EJHG*, 26(3), 293-302. <https://doi.org/10.1038/s41431-017-0042-x>
- Miyazaki, T., Hashimoto, K., Uda, A., Sakagami, H., Nakamura, Y., Saito, S.-y., Nishi, M., Kume, H., Tohgo, A., Kaneko, I., Kondo, H., Fukunaga, K., Kano, M., Watanabe, M., & Takeshima, H. (2006). Disturbance of cerebellar synaptic maturation in mutant mice lacking BSRPs, a novel brain-specific receptor-like protein family. *FEBS Letters*, 580(17), 4057-4064. <https://doi.org/10.1016/j.febslet.2006.06.043>

- Moore, D. L., Blackmore, M. G., Hu, Y., Kaestner, K. H., Bixby, J. L., Lemmon, V. P., & Goldberg, J. L. (2009). KLF family members regulate intrinsic axon regeneration ability. *Science*, 326(5950), 298-301. <https://doi.org/10.1126/science.1175737>
- Morris, C. A., Mervis, C. B., Hobart, H. H., Gregg, R. G., Bertrand, J., Ensing, G. J., Sommer, A., Moore, C. A., Hopkin, R. J., Spallone, P. A., Keating, M. T., Osborne, L., Kimberley, K. W., & Stock, A. D. (2003). GTF2I hemizyosity implicated in mental retardation in Williams syndrome: Genotype-phenotype analysis of five families with deletions in the Williams syndrome region. *American Journal of Medical Genetics*, 123A(1), 45-59. <https://doi.org/10.1002/ajmg.a.20496>
- Mukai, J., Dhillia, A., Drew, L. J., Stark, K. L., Cao, L., MacDermott, A. B., Karayiorgou, M., & Gogos, J. A. (2008). Palmitoylation-dependent neurodevelopmental deficits in a mouse model of 22q11 microdeletion. *Nature Neuroscience*, 11(11), 1302-1310. <https://doi.org/10.1038/nn.2204>
- Mukai, J., Liu, H., Burt, R. A., Swor, D. E., Lai, W.-S., Karayiorgou, M., & Gogos, J. A. (2004). Evidence that the gene encoding ZDHHC8 contributes to the risk of schizophrenia. *Nature Genetics*, 36(7), 725-731. <https://doi.org/10.1038/ng1375>
- Mukai, J., Tamura, M., Fénelon, K., Rosen, A. M., Spellman, T. J., Kang, R., MacDermott, A. B., Karayiorgou, M., Gordon, J. A., & Gogos, J. A. (2015). Molecular substrates of altered axonal growth and brain connectivity in a mouse model of schizophrenia. *Neuron*, 86(3), 680-695. <https://doi.org/10.1016/j.neuron.2015.04.003>
- Munro, S. (2011). The golgin coiled-coil proteins of the Golgi apparatus. *Cold Spring Harbor perspectives in biology*, 3(6), a005256. <https://doi.org/10.1101/cshperspect.a005256>
- Nakamura, K., Anitha, A., Yamada, K., Tsujii, M., Iwayama, Y., Hattori, E., Toyota, T., Suda, S., Takei, N., Iwata, Y., Suzuki, K., Matsuzaki, H., Kawai, M., Sekine, Y., Tsuchiya, K. J., Sugihara, G.-i., Ouchi, Y., Sugiyama, T., Yoshikawa, T., & Mori, N. (2008). Genetic and expression analyses reveal elevated expression of syntaxin 1A (STX1A) in high functioning autism. *The International Journal of Neuropsychopharmacology*, 11(08), 1073. <https://doi.org/10.1017/s1461145708009036>
- Nakane, T., Kousuke, N., Sonoko, H., Yuko, K., Sato, H., Kubota, T., & Sugita, K. (2013). 6p subtelomere deletion with congenital glaucoma, severe mental retardation, and growth impairment. *Pediatr Int*, 55(3), 376-381. <https://doi.org/10.1111/j.1442-200X.2012.03729.x>
- Namba, T., Doczi, J., Pinson, A., Xing, L., Kalebic, N., Wilsch-Brauninger, M., Long, K. R., Vaid, S., Lauer, J., Bogdanova, A., Borgonovo, B., Shevchenko, A., Keller, P., Drechsel, D., Kurzchalia, T., Wimberger, P., Chinopoulos, C., & Huttner, W. B. (2020). Human-Specific ARHGAP11B Acts in Mitochondria to Expand Neocortical Progenitors by Glutaminolysis. *Neuron*, 105(5), 867-881 e869. <https://doi.org/10.1016/j.neuron.2019.11.027>
- Nguyen, T. A., Wu, K., Pandey, S., Lehr, A. W., Li, Y., Bemben, M. A., Badger, J. D., 2nd, Lauzon, J. L., Wang, T., Zaghloul, K. A., Thurm, A., Jain, M., Lu, W., & Roche, K. W. (2020). A Cluster of Autism-Associated Variants on X-Linked NLGN4X Functionally Resemble NLGN4Y. *Neuron*, 106(5), 759-768 e757. <https://doi.org/10.1016/j.neuron.2020.03.008>

- Niki, T., Imamura, K., Enami, T., Kinoshita, M., & Inoue, H. (2019). Establishment of human induced pluripotent stem cell line from a patient with Angelman syndrome carrying the deletion of maternal chromosome 15q11.2-q13. *Stem Cell Research*, 34, 101363. <https://doi.org/10.1016/j.scr.2018.101363>
- Nilsson, S. R. O., Celada, P., Fejgin, K., Thelin, J., Nielsen, J., Santana, N., Heath, C. J., Larsen, P. H., Nielsen, V., Kent, B. A., Saksida, L. M., Stensbol, T. B., Robbins, T. W., Bastlund, J. F., Bussey, T. J., Artigas, F., & Didriksen, M. (2016). A mouse model of the 15q13.3 microdeletion syndrome shows prefrontal neurophysiological dysfunctions and attentional impairment. *Psychopharmacology (Berl)*, 233(11), 2151-2163. <https://doi.org/10.1007/s00213-016-4265-2>
- Nilsson, S. R. O., Celada, P., Fejgin, K., Thelin, J., Nielsen, J., Santana, N., Heath, C. J., Larsen, P. H., Nielsen, V., Kent, B. A., Saksida, L. M., Stensbøl, T. B., Robbins, T. W., Bastlund, J. F., Bussey, T. J., Artigas, F., & Didriksen, M. (2016). A mouse model of the 15q13.3 microdeletion syndrome shows prefrontal neurophysiological dysfunctions and attentional impairment. *Psychopharmacology*, 233(11), 2151-2163. <https://doi.org/10.1007/s00213-016-4265-2>
- Obien, M. E., Deligkaris, K., Bullmann, T., Bakkum, D. J., & Frey, U. (2014). Revealing neuronal function through microelectrode array recordings. *Front Neurosci*, 8, 423. <https://doi.org/10.3389/fnins.2014.00423>
- Pak, C., Danko, T., Zhang, Y., Aoto, J., Anderson, G., Maxeiner, S., Yi, F., Wernig, M., & Südhof, T. C. (2015). Human Neuropsychiatric Disease Modeling using Conditional Deletion Reveals Synaptic Transmission Defects Caused by Heterozygous Mutations in NRXN1. *Cell stem cell*, 17(3), 316-328. <https://doi.org/10.1016/j.stem.2015.07.017>
- Park, S. M., Park, H. R., & Lee, J. H. (2017). MAPK3 at the Autism-Linked Human 16p11.2 Locus Influences Precise Synaptic Target Selection at Drosophila Larval Neuromuscular Junctions. *Molecules and cells*, 40(2), 151-161. <https://doi.org/10.14348/molcells.2017.2307>
- Pazos Obregón, F., Soto, P., Lavín, J. L., Cortázar, A. R., Barrio, R., Aransay, A. M., & Cantera, R. (2018). Cluster Locator, online analysis and visualization of gene clustering. *Bioinformatics*, 34(19), 3377-3379. <https://doi.org/10.1093/bioinformatics/bty336>
- Penisson, M., Ladewig, J., Belvindrah, R., & Francis, F. (2019). Genes and Mechanisms Involved in the Generation and Amplification of Basal Radial Glial Cells. *Frontiers in cellular neuroscience*, 13, 381-381. <https://doi.org/10.3389/fncel.2019.00381>
- Pleseac, T., Brown, K., Allen, C., C, A. B., Church, J., Kalady, M., LaGuardia, L., O'Malley, M., & Heald, B. (2017). Clinicopathological features of a kindred with SCG5-GREM1-associated hereditary mixed polyposis syndrome. *Hum Pathol*, 60, 75-81. <https://doi.org/10.1016/j.humpath.2016.10.002>
- Pober, B. R. (2010). Williams–Beuren Syndrome. *New England Journal of Medicine*, 362(3), 239-252. <https://doi.org/10.1056/nejmra0903074>
- Pólvora-Brandão, D., Joaquim, M., Godinho, I., Aprile, D., Álvaro, A. R., Onofre, I., Raposo, A. C., Pereira de Almeida, L., Duarte, S. T., & da Rocha, S. T. (2018). Loss of hierarchical imprinting regulation at the Prader-Willi/Angelman syndrome locus in human iPSCs. *Human Molecular Genetics*, 27(23), 3999-4011. <https://doi.org/10.1093/hmg/ddy274>

- Pravdivyi, I., Ballanyi, K., Colmers, W. F., & Wevrick, R. (2015). Progressive postnatal decline in leptin sensitivity of arcuate hypothalamic neurons in the *Magel2*-null mouse model of Prader–Willi syndrome. *Human Molecular Genetics*, 24(15), 4276-4283. <https://doi.org/10.1093/hmg/ddv159>
- Raman, M., Earnest, S., Zhang, K., Zhao, Y., & Cobb, M. H. (2007). TAO kinases mediate activation of p38 in response to DNA damage. *The EMBO journal*, 26(8), 2005-2014. <https://doi.org/10.1038/sj.emboj.7601668>
- Rasband, M. N. (2010). The axon initial segment and the maintenance of neuronal polarity. *Nat Rev Neurosci*, 11(8), 552-562. <https://doi.org/10.1038/nrn2852>
- Raudvere, U., Kolberg, L., Kuzmin, I., Arak, T., Adler, P., Peterson, H., & Vilo, J. (2019). g:Profiler: a web server for functional enrichment analysis and conversions of gene lists (2019 update). *Nucleic Acids Res*, 47(W1), W191-W198. <https://doi.org/10.1093/nar/gkz369>
- Relaix, F., Wei, X. J., Wu, X., & Sassoon, D. A. (1998). Peg3/Pw1 is an imprinted gene involved in the TNF-NFkappaB signal transduction pathway. *Nat Genet*, 18(3), 287-291. <https://doi.org/10.1038/ng0398-287>
- Rhee, H. J., Shaib, A. H., Rehbach, K., Lee, C., Seif, P., Thomas, C., Gideons, E., Guenther, A., Krutenko, T., Hebisch, M., Peitz, M., Brose, N., Brustle, O., & Rhee, J. S. (2019). An Autaptic Culture System for Standardized Analyses of iPSC-Derived Human Neurons. *Cell Rep*, 27(7), 2212-2228 e2217. <https://doi.org/10.1016/j.celrep.2019.04.059>
- Richter, M., Murtaza, N., Scharrenberg, R., White, S. H., Johanns, O., Walker, S., Yuen, R. K. C., Schwanke, B., Bedürftig, B., Henis, M., Scharf, S., Kraus, V., Dörk, R., Hellmann, J., Lindenmaier, Z., Ellegood, J., Hartung, H., Kwan, V., Sedlacik, J., . . . Calderon de Anda, F. (2019). Altered TAOK2 activity causes autism-related neurodevelopmental and cognitive abnormalities through RhoA signaling. *Molecular Psychiatry*, 24(9), 1329-1350. <https://doi.org/10.1038/s41380-018-0025-5>
- Ring, D. B., Johnson, K. W., Henriksen, E. J., Nuss, J. M., Goff, D., Kinnick, T. R., Ma, S. T., Reeder, J. W., Samuels, I., Slabiak, T., Wagman, A. S., Hammond, M. E., & Harrison, S. D. (2003). Selective glycogen synthase kinase 3 inhibitors potentiate insulin activation of glucose transport and utilization in vitro and in vivo. *Diabetes*, 52(3), 588-595. <https://doi.org/10.2337/diabetes.52.3.588>
- Robinson-Agramonte, M. L. A., Noris Garcia, E., Fraga Guerra, J., Vega Hurtado, Y., Antonucci, N., Semprun-Hernandez, N., Schultz, S., & Siniscalco, D. (2022). Immune Dysregulation in Autism Spectrum Disorder: What Do We Know about It? *International journal of molecular sciences*, 23(6). <https://doi.org/10.3390/ijms23063033>
- Rosen, T. E., Mazefsky, C. A., Vasa, R. A., & Lerner, M. D. (2018). Co-occurring psychiatric conditions in autism spectrum disorder. *Int Rev Psychiatry*, 30(1), 40-61. <https://doi.org/10.1080/09540261.2018.1450229>
- Rosenfeld, J. A., Coe, B. P., Eichler, E. E., Cuckle, H., & Shaffer, L. G. (2013). Estimates of penetrance for recurrent pathogenic copy-number variations. *Genetics in medicine : official journal of the American College of Medical Genetics*, 15(6), 478-481. <https://doi.org/10.1038/gim.2012.164>
- Rosenfeld, J. A., Traylor, R. N., Schaefer, G. B., McPherson, E. W., Ballif, B. C., Klopocki, E., Mundlos, S., Shaffer, L. G., Aylsworth, A. S., & q21.1 Study, G. (2012). Proximal microdeletions and microduplications of 1q21.1 contribute to

- variable abnormal phenotypes. *European journal of human genetics : EJHG*, 20(7), 754-761. <https://doi.org/10.1038/ejhg.2012.6>
- Roskoski, R. (2012). ERK1/2 MAP kinases: Structure, function, and regulation. *Pharmacological Research*, 66(2), 105-143. <https://doi.org/10.1016/j.phrs.2012.04.005>
- Rougeulle, C., Glatt, H., & Lalande, M. (1997). The Angelman syndrome candidate gene, UBE3A/E6-AP, is imprinted in brain. *Nat Genet*, 17(1), 14-15. <https://doi.org/10.1038/ng0997-14>
- Sahoo, T., Peters, S. U., Madduri, N. S., Glaze, D. G., German, J. R., Bird, L. M., Barbieri-Welge, R., Bichell, T. J., Beaudet, A. L., & Bacino, C. A. (2006). Microarray based comparative genomic hybridization testing in deletion bearing patients with Angelman syndrome: genotype-phenotype correlations. *J Med Genet*, 43(6), 512-516. <https://doi.org/10.1136/jmg.2005.036913>
- Sakurai, T., Dorr, N. P., Takahashi, N., McInnes, L. A., Elder, G. A., & Buxbaum, J. D. (2010). Haploinsufficiency of Gtf2i, a gene deleted in Williams Syndrome, leads to increases in social interactions. *Autism Research*, 4(1), 28-39. <https://doi.org/10.1002/aur.169>
- Sanders, S. J., Sahin, M., Hostyk, J., Thurm, A., Jacquemont, S., Avillach, P., Douard, E., Martin, C. L., Modi, M. E., Moreno-De-Luca, A., Raznahan, A., Anticevic, A., Dolmetsch, R., Feng, G., Geschwind, D. H., Glahn, D. C., Goldstein, D. B., Ledbetter, D. H., Mulle, J. G., . . . Bearden, C. E. (2019). A framework for the investigation of rare genetic disorders in neuropsychiatry. *Nat Med*, 25(10), 1477-1487. <https://doi.org/10.1038/s41591-019-0581-5>
- Saw, J., Yang, M. L., Trinder, M., Tcheandjieu, C., Xu, C., Starovoytov, A., Birt, I., Mathis, M. R., Hunker, K. L., Schmidt, E. M., Jackson, L., Fendrikova-Mahlay, N., Zawistowski, M., Brummett, C. M., Zoellner, S., Katz, A., Coleman, D. M., Swan, K., O'Donnell, C. J., . . . Ganesh, S. K. (2020). Chromosome 1q21.2 and additional loci influence risk of spontaneous coronary artery dissection and myocardial infarction. *Nat Commun*, 11(1), 4432. <https://doi.org/10.1038/s41467-020-17558-x>
- Scala, F., Nenov, M. N., Crofton, E. J., Singh, A. K., Folorunso, O., Zhang, Y., Chesson, B. C., Wildburger, N. C., James, T. F., Alshammari, M. A., Alshammari, T. K., Elfrink, H., Grassi, C., Kasper, J. M., Smith, A. E., Hommel, J. D., Lichti, C. F., Rudra, J. S., D'Ascenzo, M., . . . Laezza, F. (2018). Environmental Enrichment and Social Isolation Mediate Neuroplasticity of Medium Spiny Neurons through the GSK3 Pathway. *Cell Rep*, 23(2), 555-567. <https://doi.org/10.1016/j.celrep.2018.03.062>
- Scambler, P. J., Kelly, D., Lindsay, E., Williamson, R., Goldberg, R., Shprintzen, R., Wilson, D. I., Goodship, J. A., Cross, I. E., & Burn, J. (1992). Velo-cardio-facial syndrome associated with chromosome 22 deletions encompassing the DiGeorge locus. *The Lancet*, 339(8802), 1138-1139. [https://doi.org/10.1016/0140-6736\(92\)90734-k](https://doi.org/10.1016/0140-6736(92)90734-k)
- Schaaf, C. P., Boone, P. M., Sampath, S., Williams, C., Bader, P. I., Mueller, J. M., Shchelochkov, O. A., Brown, C. W., Crawford, H. P., Phalen, J. A., Tartaglia, N. R., Evans, P., Campbell, W. M., Tsai, A. C.-H., Parsley, L., Grayson, S. W., Scheuerle, A., Luzzi, C. D., Thomas, S. K., . . . Cheung, S. W. (2012). Phenotypic spectrum and genotype-phenotype correlations of NRXN1 exon deletions.

- European journal of human genetics* : *EJHG*, 20(12), 1240-1247.  
<https://doi.org/10.1038/ejhg.2012.95>
- Schaaf, C. P., Gonzalez-Garay, M. L., Xia, F., Potocki, L., Gripp, K. W., Zhang, B., Peters, B. A., McElwain, M. A., Drmanac, R., Beaudet, A. L., Caskey, C. T., & Yang, Y. (2013). Truncating mutations of MAGEL2 cause Prader-Willi phenotypes and autism. *Nature Genetics*, 45(11), 1405-1408.  
<https://doi.org/10.1038/ng.2776>
- Schaaf, C. P., Sabo, A., Sakai, Y., Crosby, J., Muzny, D., Hawes, A., Lewis, L., Akbar, H., Varghese, R., Boerwinkle, E., Gibbs, R. A., & Zoghbi, H. Y. (2011). Oligogenic heterozygosity in individuals with high-functioning autism spectrum disorders. *Human Molecular Genetics*, 20(17), 3366-3375.  
<https://doi.org/10.1093/hmg/ddr243>
- Schaller, F., Watrin, F., Sturny, R., Massacrier, A., Szepetowski, P., & Muscatelli, F. (2010). A single postnatal injection of oxytocin rescues the lethal feeding behaviour in mouse newborns deficient for the imprinted Magel2 gene. *Human Molecular Genetics*, 19(24), 4895-4905. <https://doi.org/10.1093/hmg/ddq424>
- Sharp, A. J., Mefford, H. C., Li, K., Baker, C., Skinner, C., Stevenson, R. E., Schroer, R. J., Novara, F., De Gregori, M., Ciccone, R., Broomer, A., Casuga, I., Wang, Y., Xiao, C., Barbacioru, C., Gimelli, G., Bernardina, B. D., Torniero, C., Giorda, R., . . . Eichler, E. E. (2008). A recurrent 15q13.3 microdeletion syndrome associated with mental retardation and seizures. *Nat Genet*, 40(3), 322-328.  
<https://doi.org/10.1038/ng.93>
- Shi, H.-F., Yang, J.-F., Wang, Q., Li, R.-G., Xu, Y.-J., Qu, X.-K., Fang, W.-Y., Liu, X. U., & Yang, Y.-Q. (2012). Prevalence and spectrum of GJA5 mutations associated with lone atrial fibrillation. *Molecular Medicine Reports*, 7(3), 767-774.  
<https://doi.org/10.3892/mmr.2012.1252>
- Shinawi, M., Schaaf, C. P., Bhatt, S. S., Xia, Z., Patel, A., Cheung, S. W., Lanpher, B., Nagl, S., Herding, H. S., Nevinny-Stickel, C., Immken, L. L., Patel, G. S., German, J. R., Beaudet, A. L., & Stankiewicz, P. (2009). A small recurrent deletion within 15q13.3 is associated with a range of neurodevelopmental phenotypes. *Nat Genet*, 41(12), 1269-1271. <https://doi.org/10.1038/ng.481>
- Shirai, Y., Li, W., & Suzuki, T. (2017). Role of Splice Variants of Gtf2i, a Transcription Factor Localizing at Postsynaptic Sites, and Its Relation to Neuropsychiatric Diseases. *International journal of molecular sciences*, 18(2), 411.  
<https://doi.org/10.3390/ijms18020411>
- Sjolin, K., Kultima, K., Larsson, A., Freyhult, E., Zjukovskaja, C., Alkass, K., & Burman, J. (2022). Distribution of five clinically important neuroglial proteins in the human brain. *Molecular brain*, 15(1), 52. <https://doi.org/10.1186/s13041-022-00935-6>
- Smith, S. E. P., Zhou, Y.-D., Zhang, G., Jin, Z., Stoppel, D. C., & Anderson, M. P. (2011). Increased gene dosage of Ube3a results in autism traits and decreased glutamate synaptic transmission in mice. *Science translational medicine*, 3(103), 103ra197-103ra197. <https://doi.org/10.1126/scitranslmed.3002627>
- Soemedi, R., Topf, A., Wilson, I. J., Darlay, R., Rahman, T., Glen, E., Hall, D., Huang, N., Bentham, J., Bhattacharya, S., Cosgrove, C., Brook, J. D., Granados-Riveron, J., Setchfield, K., Bu'lock, F., Thornborough, C., Devriendt, K., Breckpot, J., Hofbeck, M., . . . Keavney, B. D. (2012). Phenotype-specific effect of chromosome 1q21.1 rearrangements and GJA5 duplications in 2436 congenital

- heart disease patients and 6760 controls. *Human Molecular Genetics*, 21(7), 1513-1520. <https://doi.org/10.1093/hmg/ddr589>
- Soutar, M. P., Kim, W. Y., Williamson, R., Peggie, M., Hastie, C. J., McLauchlan, H., Snider, W. D., Gordon-Weeks, P. R., & Sutherland, C. (2010). Evidence that glycogen synthase kinase-3 isoforms have distinct substrate preference in the brain. *J Neurochem*, 115(4), 974-983. <https://doi.org/10.1111/j.1471-4159.2010.06988.x>
- Spielmann, M., Reichelt, G., Hertzberg, C., Trimborn, M., Mundlos, S., Horn, D., & Klopocki, E. (2011). Homozygous deletion of chromosome 15q13.3 including CHRNA7 causes severe mental retardation, seizures, muscular hypotonia, and the loss of KLF13 and TRPM1 potentially cause macrocytosis and congenital retinal dysfunction in sibs. *Eur J Med Genet*, 54(4), e441-445. <https://doi.org/10.1016/j.ejmg.2011.04.004>
- Stanurova, J., Neureiter, A., Hiber, M., de Oliveira Kessler, H., Stolp, K., Goetzke, R., Klein, D., Bankfalvi, A., Klump, H., & Steenpass, L. (2016). Angelman syndrome-derived neurons display late onset of paternal UBE3A silencing. *Scientific Reports*, 6, 30792-30792. <https://doi.org/10.1038/srep30792>
- Stoppel, L. J., Kazdoba, T. M., Schaffler, M. D., Preza, A. R., Heynen, A., Crawley, J. N., & Bear, M. F. (2018). R-Baclofen Reverses Cognitive Deficits and Improves Social Interactions in Two Lines of 16p11.2 Deletion Mice. *Neuropsychopharmacology : official publication of the American College of Neuropsychopharmacology*, 43(3), 513-524. <https://doi.org/10.1038/npp.2017.236>
- Strang, K. H., Golde, T. E., & Giasson, B. I. (2019). MAPT mutations, tauopathy, and mechanisms of neurodegeneration. *Lab Invest*, 99(7), 912-928. <https://doi.org/10.1038/s41374-019-0197-x>
- Subramanian, A., Tamayo, P., Mootha, V. K., Mukherjee, S., Ebert, B. L., Gillette, M. A., Paulovich, A., Pomeroy, S. L., Golub, T. R., Lander, E. S., & Mesirov, J. P. (2005). Gene set enrichment analysis: a knowledge-based approach for interpreting genome-wide expression profiles. *Proc Natl Acad Sci U S A*, 102(43), 15545-15550. <https://doi.org/10.1073/pnas.0506580102>
- Sundberg, M., Pinson, H., Smith, R. S., Winden, K. D., Venugopal, P., Tai, D. J. C., Gusella, J. F., Talkowski, M. E., Walsh, C. A., Tegmark, M., & Sahin, M. (2021). 16p11.2 deletion is associated with hyperactivation of human iPSC-derived dopaminergic neuron networks and is rescued by RHOA inhibition in vitro. *Nat Commun*, 12(1), 2897. <https://doi.org/10.1038/s41467-021-23113-z>
- Szafranski, P., Schaaf, C. P., Person, R. E., Gibson, I. B., Xia, Z., Mahadevan, S., Wiszniewska, J., Bacino, C. A., Lalani, S., Potocki, L., Kang, S. H., Patel, A., Cheung, S. W., Probst, F. J., Graham, B. H., Shinawi, M., Beaudet, A. L., & Stankiewicz, P. (2010). Structures and molecular mechanisms for common 15q13.3 microduplications involving CHRNA7: benign or pathological? *Hum Mutat*, 31(7), 840-850. <https://doi.org/10.1002/humu.21284>
- Tacer, K. F., & Potts, P. R. (2017). Cellular and disease functions of the Prader-Willi Syndrome gene MAGEL2. *The Biochemical journal*, 474(13), 2177-2190. <https://doi.org/10.1042/BCJ20160616>
- Takahashi, K., Tanabe, K., Ohnuki, M., Narita, M., Ichisaka, T., Tomoda, K., & Yamanaka, S. (2007). Induction of pluripotent stem cells from adult human

- fibroblasts by defined factors. *Cell*, 131(5), 861-872.  
<https://doi.org/10.1016/j.cell.2007.11.019>
- Talkowski, M. E., Mullegama, S. V., Rosenfeld, J. A., van Bon, B. W., Shen, Y., Repnikova, E. A., Gastier-Foster, J., Thrush, D. L., Kathiresan, S., Ruderfer, D. M., Chiang, C., Hanscom, C., Ernst, C., Lindgren, A. M., Morton, C. C., An, Y., Astbury, C., Brueton, L. A., Lichtenbelt, K. D., . . . Elsea, S. H. (2011). Assessment of 2q23.1 microdeletion syndrome implicates MBD5 as a single causal locus of intellectual disability, epilepsy, and autism spectrum disorder. *Am J Hum Genet*, 89(4), 551-563. <https://doi.org/10.1016/j.ajhg.2011.09.011>
- Tamura, M., Mukai, J., Gordon, J. A., & Gogos, J. A. (2016). Developmental Inhibition of Gsk3 Rescues Behavioral and Neurophysiological Deficits in a Mouse Model of Schizophrenia Predisposition. *Neuron*, 89(5), 1100-1109.  
<https://doi.org/10.1016/j.neuron.2016.01.025>
- Tapia, M., Del Puerto, A., Puime, A., Sanchez-Ponce, D., Fronzaroli-Molinieres, L., Pallas-Bazarrá, N., Carlier, E., Giraud, P., Debanne, D., Wandosell, F., & Garrido, J. J. (2013). GSK3 and beta-catenin determines functional expression of sodium channels at the axon initial segment. *Cell Mol Life Sci*, 70(1), 105-120.  
<https://doi.org/10.1007/s00018-012-1059-5>
- Tassabehji, M., Hammond, P., Karmiloff-Smith, A., Thompson, P., Thorgeirsson, S. S., Durkin, M. E., Popescu, N. C., Hutton, T., Metcalfe, K., Rucka, A., Stewart, H., Read, A. P., Maconochie, M., & Donnai, D. (2005). GTF2IRD1 in Craniofacial Development of Humans and Mice. *Science*, 310(5751), 1184-1187.  
<https://doi.org/10.1126/science.1116142>
- Thiaville, M. M., Huang, J. M., Kim, H., Ekram, M. B., Roh, T. Y., & Kim, J. (2013). DNA-binding motif and target genes of the imprinted transcription factor PEG3. *Gene*, 512(2), 314-320. <https://doi.org/10.1016/j.gene.2012.10.005>
- Tick, B., Bolton, P., Happe, F., Rutter, M., & Rijdsdijk, F. (2016). Heritability of autism spectrum disorders: a meta-analysis of twin studies. *J Child Psychol Psychiatry*, 57(5), 585-595. <https://doi.org/10.1111/jcpp.12499>
- Todarello, G., Feng, N., Kolachana, B. S., Li, C., Vakkalanka, R., Bertolino, A., Weinberger, D. R., & Straub, R. E. (2014). Incomplete penetrance of NRXN1 deletions in families with schizophrenia. *Schizophrenia Research*, 155(1-3), 1-7.  
<https://doi.org/10.1016/j.schres.2014.02.023>
- Torres, A. R., Westover, J. B., & Rosenspire, A. J. (2012). HLA Immune Function Genes in Autism. *Autism Res Treat*, 2012, 959073. <https://doi.org/10.1155/2012/959073>
- Trimborn, M., Bell, S. M., Felix, C., Rashid, Y., Jafri, H., Griffiths, P. D., Neumann, L. M., Krebs, A., Reis, A., Sperling, K., Neitzel, H., & Jackson, A. P. (2004). Mutations in microcephalin cause aberrant regulation of chromosome condensation. *American journal of human genetics*, 75(2), 261-266. <https://doi.org/10.1086/422855>
- Trotter, J. H., Hao, J., Maxeiner, S., Tsetsenis, T., Liu, Z., Zhuang, X., & Südhof, T. C. (2019). Synaptic neurexin-1 assembles into dynamically regulated active zone nanoclusters. *The Journal of cell biology*, 218(8), 2677-2698.  
<https://doi.org/10.1083/jcb.201812076>
- Uddin, M., Unda, B. K., Kwan, V., Holzapfel, N. T., White, S. H., Chalil, L., Woodbury-Smith, M., Ho, K. S., Harward, E., Murtaza, N., Dave, B., Pellecchia, G., D'Abate, L., Nalpathamkalam, T., Lamoureux, S., Wei, J., Speevak, M., Stavropoulos, J., Hope, K. J., . . . Singh, K. K. (2018). OTUD7A Regulates Neurodevelopmental

- Phenotypes in the 15q13.3 Microdeletion Syndrome. *Am J Hum Genet*, 102(2), 278-295. <https://doi.org/10.1016/j.ajhg.2018.01.006>
- Unda, B. K., Chalil, L., Yoon, S., Kilpatrick, S., Irwin, C., Xing, S., Murtaza, N., Cheng, A., Brown, C., Afonso, A., McCready, E., Ronen, G. M., Howe, J., Caye-Eude, A., Verloes, A., Doble, B. W., Faivre, L., Vitobello, A., Scherer, S. W., . . . Singh, K. K. (2023). Impaired OTUD7A-dependent Ankyrin regulation mediates neuronal dysfunction in mouse and human models of the 15q13.3 microdeletion syndrome. *Molecular Psychiatry*. <https://doi.org/10.1038/s41380-022-01937-5>
- Vadgama, N., Pittman, A., Simpson, M., Nirmalanathan, N., Murray, R., Yoshikawa, T., De Rijk, P., Rees, E., Kirov, G., Hughes, D., Fitzgerald, T., Kristiansen, M., Pearce, K., Cerveira, E., Zhu, Q., Zhang, C., Lee, C., Hardy, J., & Nasir, J. (2019). De novo single-nucleotide and copy number variation in discordant monozygotic twins reveals disease-related genes. *European journal of human genetics : EJHG*, 27(7), 1121-1133. <https://doi.org/10.1038/s41431-019-0376-7>
- Vandeweyer, G., Van der Aa, N., Reyniers, E., & Kooy, R. F. (2012). The contribution of CLIP2 haploinsufficiency to the clinical manifestations of the Williams-Beuren syndrome. *American journal of human genetics*, 90(6), 1071-1078. <https://doi.org/10.1016/j.ajhg.2012.04.020>
- Voineagu, I., & Eapen, V. (2013). Converging Pathways in Autism Spectrum Disorders: Interplay between Synaptic Dysfunction and Immune Responses. *Front Hum Neurosci*, 7, 738. <https://doi.org/10.3389/fnhum.2013.00738>
- Vorstman, J. A. S., Morcus, M. E. J., Duijff, S. N., Klaassen, P. W. J., Heineman-de Boer, J. A., Beemer, F. A., Swaab, H., Kahn, R. S., & van Engeland, H. (2006). The 22q11.2 Deletion in Children. *Journal of the American Academy of Child & Adolescent Psychiatry*, 45(9), 1104-1113. <https://doi.org/10.1097/01.chi.0000228131.56956.c1>
- Vu, T. H., & Hoffman, A. R. (1997). Imprinting of the Angelman syndrome gene, UBE3A, is restricted to brain. *Nature Genetics*, 17(1), 12-13. <https://doi.org/10.1038/ng0997-12>
- Wang, S. S., Wang, T. M., Qiao, X. H., Huang, R. T., Xue, S., Dong, B. B., Xu, Y. J., Liu, X. Y., & Yang, Y. Q. (2020). KLF13 loss-of-function variation contributes to familial congenital heart defects. *Eur Rev Med Pharmacol Sci*, 24(21), 11273-11285. [https://doi.org/10.26355/eurrev\\_202011\\_23617](https://doi.org/10.26355/eurrev_202011_23617)
- Wang, Z., Li, Y., Ahmad, A., Azmi, A. S., Banerjee, S., Kong, D., & Sarkar, F. H. (2010). Targeting Notch signaling pathway to overcome drug resistance for cancer therapy. *Biochimica et biophysica acta*, 1806(2), 258-267. <https://doi.org/10.1016/j.bbcan.2010.06.001>
- Warren, R. P., Margaretten, N. C., Pace, N. C., & Foster, A. (1986). Immune abnormalities in patients with autism. *Journal of autism and developmental disorders*, 16(2), 189-197. <https://doi.org/10.1007/BF01531729>
- Whitney, R., Nair, A., McCready, E., Keller, A. E., Adil, I. S., Aziz, A. S., Borys, O., Siu, K., Shah, C., Meaney, B. F., Jones, K., & RamachandranNair, R. (2021). The spectrum of epilepsy in children with 15q13.3 microdeletion syndrome. *Seizure*, 92, 221-229. <https://doi.org/10.1016/j.seizure.2021.09.016>
- Xing, L., Kubik-Zahorodna, A., Namba, T., Pinson, A., Florio, M., Prochazka, J., Sarov, M., Sedlacek, R., & Huttner, W. B. (2021). Expression of human-specific ARHGAP11B in mice leads to neocortex expansion and increased memory

- flexibility. *The EMBO journal*, 40(13), e107093-e107093.  
<https://doi.org/10.15252/embj.2020107093>
- Xu, B., Hsu, P.-K., Stark, K. L., Karayiorgou, M., & Gogos, J. A. (2013). Derepression of a neuronal inhibitor due to miRNA dysregulation in a schizophrenia-related microdeletion. *Cell*, 152(1-2), 262-275. <https://doi.org/10.1016/j.cell.2012.11.052>
- Xu, J. S., Liao, K. L., Wang, X., He, J., & Wang, X. Z. (2020). Combining bioinformatics techniques to explore the molecular mechanisms involved in pancreatic cancer metastasis and prognosis. *J Cell Mol Med*, 24(24), 14128-14138.  
<https://doi.org/10.1111/jcmm.16023>
- Xu, P., Duong, D. M., Seyfried, N. T., Cheng, D., Xie, Y., Robert, J., Rush, J., Hochstrasser, M., Finley, D., & Peng, J. (2009). Quantitative proteomics reveals the function of unconventional ubiquitin chains in proteasomal degradation. *Cell*, 137(1), 133-145. <https://doi.org/10.1016/j.cell.2009.01.041>
- Yadav, S., Oses-Prieto, J. A., Peters, C. J., Zhou, J., Pleasure, S. J., Burlingame, A. L., Jan, L. Y., & Jan, Y.-N. (2017). TAOK2 Kinase Mediates PSD95 Stability and Dendritic Spine Maturation through Septin7 Phosphorylation. *Neuron*, 93(2), 379-393. <https://doi.org/10.1016/j.neuron.2016.12.006>
- Yang, N., Chanda, S., Marro, S., Ng, Y.-H., Janas, J. A., Haag, D., Ang, C. E., Tang, Y., Flores, Q., Mall, M., Wapinski, O., Li, M., Ahlenius, H., Rubenstein, J. L., Chang, H. Y., Buylia, A. A., Südhof, T. C., & Wernig, M. (2017). Generation of pure GABAergic neurons by transcription factor programming. *Nature methods*, 14(6), 621-628. <https://doi.org/10.1038/nmeth.4291>
- Yang, Q., Zheng, F., Hu, Y., Yang, Y., Li, Y., Chen, G., Wang, W., He, M., Zhou, R., Ma, Y., Xu, D., Tian, X., Gao, X., Wang, Q., & Wang, X. (2018). ZDHHC8 critically regulates seizure susceptibility in epilepsy. *Cell death & disease*, 9(8), 795-795. <https://doi.org/10.1038/s41419-018-0842-0>
- Yang, S. D., Song, J. S., Yu, J. S., & Shiah, S. G. (1993). Protein kinase FA/GSK-3 phosphorylates tau on Ser235-Pro and Ser404-Pro that are abnormally phosphorylated in Alzheimer's disease brain. *J Neurochem*, 61(5), 1742-1747. <https://doi.org/10.1111/j.1471-4159.1993.tb09811.x>
- Yang, S. D., Yu, J. S., Shiah, S. G., & Huang, J. J. (1994). Protein kinase FA/glycogen synthase kinase-3 alpha after heparin potentiation phosphorylates tau on sites abnormally phosphorylated in Alzheimer's disease brain. *J Neurochem*, 63(4), 1416-1425. <https://doi.org/10.1046/j.1471-4159.1994.63041416.x>
- Yin, J., Chen, W., Chao, E. S., Soriano, S., Wang, L., Wang, W., Cummock, S. E., Tao, H., Pang, K., Liu, Z., Pereira, F. A., Samaco, R. C., Zoghbi, H. Y., Xue, M., & Schaaf, C. P. (2018). Otud7a Knockout Mice Recapitulate Many Neurological Features of 15q13.3 Microdeletion Syndrome. *Am J Hum Genet*, 102(2), 296-308. <https://doi.org/10.1016/j.ajhg.2018.01.005>
- Yin, J., Chen, W., Yang, H., Xue, M., & Schaaf, C. P. (2017). Chrna7 deficient mice manifest no consistent neuropsychiatric and behavioral phenotypes. *Sci Rep*, 7, 39941. <https://doi.org/10.1038/srep39941>
- Young, A. L., Bocchetta, M., Russell, L. L., Convery, R. S., Peakman, G., Todd, E., Cash, D. M., Greaves, C. V., van Swieten, J., Jiskoot, L., Seelaar, H., Moreno, F., Sanchez-Valle, R., Borroni, B., Laforce, R., Jr., Masellis, M., Tartaglia, M. C., Graff, C., Galimberti, D., . . . Genetic, F. T. D. I. (2021). Characterizing the Clinical Features and Atrophy Patterns of MAPT-Related Frontotemporal

- Dementia With Disease Progression Modeling. *Neurology*, 97(9), e941-e952. <https://doi.org/10.1212/WNL.00000000000012410>
- Yuan, X., Wu, H., Xu, H., Xiong, H., Chu, Q., Yu, S., Wu, G. S., & Wu, K. (2015). Notch signaling: An emerging therapeutic target for cancer treatment. *Cancer Letters*, 369(1), 20-27. <https://doi.org/10.1016/j.canlet.2015.07.048>
- Zhang, F., Potocki, L., Sampson, J. B., Liu, P., Sanchez-Valle, A., Robbins-Furman, P., Navarro, A. D., Wheeler, P. G., Spence, J. E., Brasington, C. K., Withers, M. A., & Lupski, J. R. (2010). Identification of uncommon recurrent Potocki-Lupski syndrome-associated duplications and the distribution of rearrangement types and mechanisms in PTLs. *American journal of human genetics*, 86(3), 462-470. <https://doi.org/10.1016/j.ajhg.2010.02.001>
- Zhang, S., Zhang, X., Ma, S., Purmann, C., Davis, K., Wong, W. H., Bernstein, J., Hallmayer, J., & Urban, A. E. (2019). Network effects of the neuropsychiatric 15q13.3 microdeletion on the transcriptome and epigenome in human induced neurons. In: Cold Spring Harbor Laboratory.
- Zhang, S., Zhang, X., Purmann, C., Ma, S., Shrestha, A., Davis, K. N., Ho, M., Huang, Y., Pattni, R., Wong, W. H., Bernstein, J. A., Hallmayer, J., & Urban, A. E. (2021). Network Effects of the 15q13.3 Microdeletion on the Transcriptome and Epigenome in Human-Induced Neurons. *Biol Psychiatry*, 89(5), 497-509. <https://doi.org/10.1016/j.biopsych.2020.06.021>
- Zhang, Y., Pak, C., Han, Y., Ahlenius, H., Zhang, Z., Chanda, S., Marro, S., Patzke, C., Acuna, C., Covy, J., Xu, W., Yang, N., Danko, T., Chen, L., Wernig, M., & Sudhof, T. C. (2013). Rapid single-step induction of functional neurons from human pluripotent stem cells. *Neuron*, 78(5), 785-798. <https://doi.org/10.1016/j.neuron.2013.05.029>
- Zhang, Y., Pak, C., Han, Y., Ahlenius, H., Zhang, Z., Chanda, S., Marro, S., Patzke, C., Acuna, C., Covy, J., Xu, W., Yang, N., Danko, T., Chen, L., Wernig, M., & Südhof, T. C. (2013). Rapid single-step induction of functional neurons from human pluripotent stem cells. *Neuron*, 78(5), 785-798. <https://doi.org/10.1016/j.neuron.2013.05.029>
- Zhao, X.-N., & Usdin, K. (2018). FAN1 protects against repeat expansions in a Fragile X mouse model. *DNA repair*, 69, 1-5. <https://doi.org/10.1016/j.dnarep.2018.07.001>
- Ziats, M. N., Goin-Kochel, R. P., Berry, L. N., Ali, M., Ge, J., Guffey, D., Rosenfeld, J. A., Bader, P., Gambello, M. J., Wolf, V., Penney, L. S., Miller, R., Lebel, R. R., Kane, J., Bachman, K., Troxell, R., Clark, G., Minard, C. G., Stankiewicz, P., . . . Schaaf, C. P. (2016). The complex behavioral phenotype of 15q13.3 microdeletion syndrome. *Genet Med*, 18(11), 1111-1118. <https://doi.org/10.1038/gim.2016.9>
- Zufferey, F., Sherr, E. H., Beckmann, N. D., Hanson, E., Maillard, A. M., Hippolyte, L., Macé, A., Ferrari, C., Kutalik, Z., Andrieux, J., Aylward, E., Barker, M., Bernier, R., Bouquillon, S., Conus, P., Delobel, B., Faucett, W. A., Goin-Kochel, R. P., Grant, E., . . . p11.2 European, C. (2012). A 600 kb deletion syndrome at 16p11.2 leads to energy imbalance and neuropsychiatric disorders. *Journal of Medical Genetics*, 49(10), 660-668. <https://doi.org/10.1136/jmedgenet-2012-101203>